

Isohexide and Plant Oil Based Renewable and Degradable Polymers

Thesis Submitted to AcSIR for the Award of
the Degree of

DOCTOR OF PHILOSOPHY

In

Chemical Sciences

By

BHAUSAHEB S. RAJPUT

(Registration Number: 10CC16A26007)

Under the Guidance of

Dr. SAMIR H. CHIKKALI

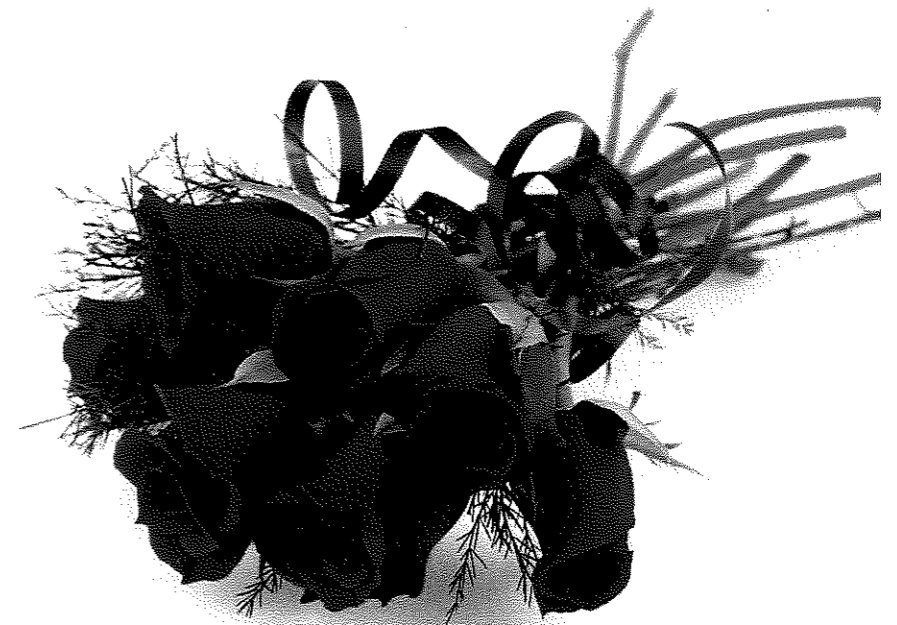


Polymer Science and Engineering Division

CSIR-NATIONAL CHEMICAL LABORATORY

PUNE – 411008, INDIA

May 2019



Dedicated to
My Family and Teachers


Date: 08th May 2019

Declaration by the Candidate

I hereby declare that the original research work embodied in this thesis entitled "**Isohexide and Plant Oil Based Renewable and Degradable Polymers**" submitted to Academy of Scientific and Innovative Research (AcSIR) for the award of degree of the Doctor of Philosophy (Ph. D.). This is the outcome of experimental investigations carried out by me under the supervision of **Dr. Samir H. Chikkali**, Principal Scientist, Polymer Science and Engineering Division, CSIR-National Chemical Laboratory, Pune. I affirm that the work incorporated is original and has not been submitted to any other academy or institute for the award of any degree or diploma.

May 2019

Polymer Science and Engineering Division
CSIR-National Chemical Laboratory
Pune-411008


Bhausaheb S. Rajput
(Research Fellow)



सीएसआयआर-राष्ट्रीय रासायनिक प्रयोगशाला
(विज्ञानिक तथा औद्योगिक अनुसंधान परिषद)
डॉ. होमी भाभा मार्ग, पुणे - 411 008 भारत
CSIR-NATIONAL CHEMICAL LABORATORY
(Council of Scientific & Industrial Research)
Dr. Homi Bhabha Road, Pune - 411 008, India.



08th May 2019

Dr. Samir H. Chikkali
Principal Scientist and Associate Professor
Polymer Science and Engineering Division
CSIR-National Chemical Laboratory
Dr. Homi Bhabha Road, Pune-411008
Maharashtra, India. Tel.: 020-2590-3145
E-mail: s.chikkali@ncl.res.in

Ph.D. Thesis Certificate

This is to certify that the work incorporated in this Ph. D. thesis entitled "Isohexide and Plant Oil Based Renewable and Degradable Polymers" submitted by Mr. Bhausaheb S. Rajput (Registration No. 10CC16A26007) to Academy of Scientific and Innovative Research (AcSIR) in fulfilment of the requirements for the award of the Degree of the Doctor of Philosophy, embodies original research work under my supervision. I further certify that this work has not been submitted to any other University or Institution in part or full for the award of any degree or diploma. Research material obtained from other sources has been duly acknowledged in the thesis. Any text, illustration, table etc., used in the thesis from other sources, have been duly cited and acknowledged.

It is also certified that this work done by the student, under my supervision, is plagiarism free.

B.S.R.
Mr. Bhausaheb S. Rajput
(Research Student)

S.H.C.
Dr. Samir H. Chikkali
(Research Supervisor)

Place: Pune

Communication Channels		FAX	WEBSITE	
NCL Layer DID	2590	Director's Office	+91-20-25902901	www.ncl.res.in
NCL Board No.	+91-20-25902000	COA's Office	+91-20-25902660	
EPABX	+91-20-25993300	CS&P's Office	+91-20-25902564	
	+91-20-25993400			

ACKNOWLEDGEMENT

The process of earning a doctorate and writing a dissertation is long and arduous and it is certainly not done singlehandedly. So, I am using this opportunity to express my gratitude to everyone who helped and supported me throughout the course of my research.

*Firstly, I would like to express my special appreciation and thanks to my research supervisor **Dr. Samir Chikkali** for his valuable guidance and scholarly inputs. I have enjoyed the opportunity to watch and learn from his knowledge and experience. His enthusiasm, encouragement and faith in me throughout have been extremely helpful. He is the one who moulded me into a good researcher. I am thankful to the god almighty for giving me such a wonderful and humble personality as my mentor. He has given me full freedom in my research and I could not imagine to have a better mentor than him.*

I wish to express my sincere thanks to the Doctoral Advisory Committee members, Dr. Suresh Bhat, Dr. Kadiravan Shanmuganathan and Dr. Ashootosh Ambade whose contribution in stimulating suggestions and encouragement helped me to coordinate my work.

I am grateful to Prof. A. K. Nangia, Director, NCL, Dr. V. K. Pillai and Prof. S. Pal (Former Director, NCL), Dr. Ulhas Kharul, Head, PSE Division, and Dr. Ashish Lele (Former Head, PSE Division) for giving me this opportunity and providing all necessary infrastructure and facilities. I also acknowledge the financial support of CSIR, New Delhi for senior research fellowship.

I extend my thanks to our collaborators Dr. Kadiravan Shanmuganathan and Farsa Ram for Dynamic Mechanical Analysis. I would also like to thank Mr. Shamal K. Menon for timely GPC analysis. My sincere thanks to the people in various parts of the institute and SAC office staff for their cooperation. I would also like to acknowledge all the staff members of IR, NMR, Mass spectroscopy, Microanalysis, Library, Administration and technical divisions of NCL for their assistance during the course of my work.

A special thanks goes to my lab mates Dr. Vijay Koshti and Mr. Shahaji Gaikwad for their valuable chemistry guidance and encouragements to enroll in Ph. D programme which I greatly acknowledge and other lab colleagues Satej, Dr. Swechcha, Dattatraya, Nilesh, Dr. Ketan, Anirban, Dynaneshwar, Ravi, Dr. Dipa, Rohit, Dr. Sandip, Amol, Tanuja, Rajkumar, Kishor, Shailaja, Uday and Manish for the lively lab atmosphere and fruitful discussions. Also, I am thankful to Dr. Punji's lab members Dr. Shrikant, Dr. Hanuman, Dr. Vineeta, Dr. Ulhas, Dilip, Rahul, Dipesh, Siddheshwar, Vijay, Suryadev, Anand, Sadhana and Sandip for their help. A

ACKNOWLEDGEMENT

special thanks goes to the summer trainees Kailash, Umesh, Lekshmy, Julia, Deepak and Manod for their help.

A special thanks goes to Dr. Prakash Wadgaonkar group members Yogesh, Samadhan, Dipak, Dr. Bhausahab and Dr. Sachin also Dr. Asha's lab members Dr. Swapnil, Dr. Nagesh, Dr. Shekhar and Dr. Prajita for their endless support during my initial days at NCL.

No words will be sufficient to express my thanks to my friends Balasaheb, Manik, Shridhar, Arun, Pravin, Bhagyashree, Megha, Sagar, Vishal, Tushar, Bhushan, Rohit, Brijesh, Srinivas and Bhupendra for the cherished friendships and creating such wonderful atmosphere around me with their support outside the lab. I also extend my gratitude to all my friends of Mi-Marathi group of CSIR-NCL for their help and exquisite moments.

My family is always source of inspiration and great moral support for me in perceiving my education, I am thankful to God for having me such a supportive family. The words are insufficient to express my gratitude towards my family. I take this opportunity to express gratitude to my parents, Shobhabai and Shivaji Rajput and my wife Mohini for their tons of love, sacrifice, blessings, unconditional support and encouragement. I express my deep and paramount gratitude to my sister Ranu and cousin brother Dinesh and his wife Sonal without their constant support and encouragement, I could not stand with this dissertation. I am lucky to have lovely sun Abhimanyu, nephew Krushna and Durgesh I always enjoy their company even at short stays at home.

At last but not the least, I thank wholeheartedly, the omnipotent God, the illimitable superior spirit, for the strength and determination to put my chin up when faced with hardships in life.

Bhausahab S. Rajput

TABLE OF CONTENTS

	Abbreviations	
	Preface	
Chapter 1	Introduction	1-19
1.1	Sugar to Isohexides	2
1.2	Polymers from Sugar Based Isohexides	5
1.3	Polymers from Plant Oil Derived Long Chain Diols	7
1.4	Renewable and Degradable Polymers	11
1.5	Setting the Goals	14
1.6	References	16
Chapter 2	Sustainable Polyacetals from Isohexides	20-70
2.1	Abstract	21
2.2	Introduction	21
2.3	Results and Discussion	23
2.3.1	Synthesis of Acetals	23
2.3.2	Acetal Metathesis Polymerization (AMP)	25
2.3.2	Polyacetal Degradation	29
2.4	Experimental Section	31
2.4.1	Materials and Methods	31
2.4.2	Synthesis of Acetals	32
2.4.2.1	Synthesis of Isomannide-Diacetal (2a)	32
2.4.2.2	Synthesis of Isosorbide-Diacetal (2b)	35
2.4.2.3	Synthesis of Isoidide (1c)	39
2.4.2.4	Synthesis of Isoidide-Diacetal (2c)	43
2.4.3	Polycondensation of Isohexides 2a-c	46
2.4.3.1	Polycondensation of Isomannide-Diacetal to P2a-1	47
2.4.3.2	Polycondensation of Isosorbide-Diacetal to P2b-2	52
2.4.3.3	Polycondensation of Isoidide-Diacetal to P2c-1	57
2.4.4	Molecular Weight Determination by End Group Analysis (NMR)	62
2.4.5	Degradation of P2b	65

TABLE OF CONTENTS

2.4.5.1	Hydrolytic Degradation	65
2.4.5.2	Degradation in Organic Media	67
2.4.5.3	Monitoring the Acid Induced Degradation by GPC	67
2.5	Conclusions	68
2.6	References	68
Chapter 3	<i>Synthesis of Renewable Copolyacetals with Tunable Degradation</i>	71-
		133
3.1	Abstract	72
3.2	Introduction	72
3.3	Results and Discussion	74
3.3.1	Diacetal and Copolyacetal Synthesis	74
3.3.2	Copolyacetal of Isomannide-Diacetal (2a) and Linear Diacetals (3a-e)	75
3.3.3	Copolyacetal of Isosorbide/Isoidide-Diacetal (2b/2c) and Linear Diacetals (3a-e)	80
3.3.4	Degradation of Copolyacetals	81
3.3.4.1	Monitoring Acid Induced Degradation by GPC	81
3.3.4.2	Solid-State Hydrolytic Degradation of Copolyacetal	82
3.3.4.3	Monitoring Acid Induced Degradation by NMR and Isolation of Degradation Products	84
3.4	Experimental Section	86
3.4.1	General Methods and Materials	86
3.4.2	Acid Catalyzed Synthesis of Diacetals	87
3.4.2.1	Synthesis of 1, 6-Hexanediactal (3a)	87
3.4.2.2	Synthesis of 1, 8-Octanediactal (3b)	89
3.4.3	Acetal Metathesis Copolymerization (AMCP)	91
3.4.3.1	Copolymerization of Isomannide-Diacetal (2a) with Linear Diacetals (3a-e) to [P3(2a-3a)-P7(2a-3e)]	93
3.4.3.2	Copolymerization of Isosorbide-Diacetal (2b) with Linear Diacetals (3a-e) to [P8(2b-3a)-P12(2b-3e)]	102

TABLE OF CONTENTS

3.4.3.3	Copolymerization of Isoidide-Diacetal (2c) with Linear Diacetals (3a-e) to P13(2c-3a)-P17(2c-3e)	112
3.4.4	Degradation of Copolyacetals	121
3.4.4.1	Monitoring the Acid Induced Degradation by GPC	121
3.4.4.2	Hydrolytic Degradation of Copolyacetal	123
3.4.4.3	Monitoring Acid Induced Degradation by NMR and Isolation of Degradation Products	123
3.5	Conclusions	129
3.6	References	130
Chapter 4	<i>Cross-Metathesis of Biorenewable Dioxalates and Diols to Film Forming Degradable Polyoxalates</i>	134-
		205
4.1	Abstract	135
4.2	Introduction	135
4.3	Results and discussion	136
4.3.1	Synthesis of Isohexide-Dioxalates	136
4.3.2	Polymerization Mechanism and Poly(isohexide-co-alkane)oxalates.	138
4.3.3	Polyoxalate Film	142
4.3.4	Degradation of Polyoxalates	142
4.4	Experimental Section	144
4.4.1	General Methods and Materials	144
4.4.2	Syntheses of Isohexide-Dioxalates	145
4.4.2.1	Synthesis of <i>O, O'</i> -((3 <i>R, 6R</i>)-Hexahydrofuro [3,2- <i>b</i>]furan-3,6-diyl) dimethyl dioxalates [Isomannide-Dioxalate] (4a)	145
4.4.2.2	Synthesis of <i>O, O'</i> -((3 <i>R, 6S</i>)-Hexahydrofuro [3,2- <i>b</i>]furan-3,6-diyl) dimethyl dioxalates [Isosorbide-Dioxalate] (4b)	148
4.4.2.3	Synthesis of <i>O, O'</i> -((3 <i>S, 6S</i>)-Hexahydrofuro[3,2- <i>b</i>]furan-3,6-diyl) dimethyl dioxalates[Isoidide-Dioxalate] (4c)	150
4.4.3	Investigating the Reactivity and Control Experiments	153
4.4.3.1	Direct Polymerization of Isomannide with Dimethyl Oxalate	153

TABLE OF CONTENTS

4.4.3.2	Investigating the Reactivity of Isomannide-Dioxalate with 1, 6-Hexane Diol	155
4.4.3.3	Polymerization of Isomannide-Monoxalate (4a') with 1, 6-Hexane Monoxalate (5a'):	158
4.4.3.3.1	Synthesis of Isomannide-Monoxalate (4a')	158
4.4.3.3.2	Synthesis of 1, 6-Hexane Monoxalate (5a')	161
4.4.3.3.3	Polymerization of (4a') and (5a') to P18(4a-5a)'	163
4.4.4	General Procedure for Polymer Synthesis	165
4.4.4.1	Polycondensation of Isomannide-Dioxalate (4a)	167
4.4.4.2	Polycondensation of Isosorbide-Dioxalate (4b)	176
4.4.4.3	Polycondensation of Isoidide-Dioxalate (4c)	185
4.4.5	Polyoxalate Film and their Mechanical Properties	193
4.4.6	Degradation of Polyoxalates	195
4.4.6.1	Monitoring Acid Induced Degradation by GPC	195
4.4.6.2	Solid-State Hydrolytic Degradation of Polyoxalate P20(4a-5c)	197
4.4.6.3	Tracking Acid Induced Degradation by NMR	197
4.5	Conclusions	201
4.6	References	202
Chapter 5	Synthesis of Isohexide-di(ether-ene)s and ADMET Polymerization	206-
		249
5.1	Abstract	207
5.2	Introduction	207
5.3	Results and Discussion	210
5.3.1	Monomer Synthesis	210
5.3.2	Acyclic Diene Metathesis (ADMET) Polymerization of Isohexide-di(ether-ene)s to Polyether-enes	213
5.4	Experimental Section	218

TABLE OF CONTENTS

5.4.1	General Methods and Materials	218
5.4.2	Synthesis of Isomannide-di(ether-ene) 6a	218
5.4.3	Synthesis of Isosorbide-di(ether-ene) 6b	220
5.4.4	Synthesis of Isoidide-di(ether-ene) 6c	223
5.4.5	ADMET Polymerization of Isomannide-di(ether-ene) to P27a-1-P27a-2	226
5.4.6	ADMET Polymerization of Isosorbide-di(ether-ene) to P27b-1-P27b-2	232
5.4.7	ADMET Polymerization of Isoidide-di(ether-ene) to P27c-1-P27c-2	242
5.5	Molecular Weight Determination by NMR Spectroscopy	246
5.6	Conclusions	246
5.7	References	247
Chapter 6	Summary and Outlook	250-
		259
6.1	Summary	251
6.2	Outlook	258

ABBREVIATIONS

AMP	Acetal Metathesis Polymerization
ADMET	Acyclic Diene Metathesis Polymerization
AMCP	Acetal Metathesis Copolymerization
CDCl ₃	Deuterated chloroform
Da	Dalton
DCI	Deuterium chloride
DCM	Dichloromethane
DSC	Differential Scanning Calorimetry
DMA	Dynamic Mechanical Analysis
ESI-MS	Electrospray Ionization Mass Spectroscopy
FT-IR	Fourier-Transform Infrared Spectroscopy
Grubbs Catalyst 1 st Generation	Benzylidene-bis(tricyclohexylphosphine)dichlororuthenium
Grubbs Catalyst 2 nd Generation	(1,3-Bis(2,4,6-trimethylphenyl)-2-imidazolidinylidene)dichloro (phenylmethylene)(tricyclohexylphosphine)ruthenium
HDPE	High-Density Polyethylene
HMBC	Heteronuclear Multiple Bond Coherence
HSQC	Heteronuclear Single Quantum Coherence
HCl	Hydrochloric acid
IIDMC	Isoidide Dimethyl Carboxylate
IIDML	Isoidide Dimethanol
IIDCA	Isoidide Dicarboxylic Acid
LDPE	Low-Density Polyethylene
LLDPE	Linear Low-Density Polyethylene
LiAlH ₄	Lithium Aluminium Hydride
MPa	Megapascal
MSA	Methanesulfonic acid
MgSO ₄	Magnesium Sulphate
MALDI-ToF-MS	Matrix Assisted Laser Desorption/Ionization Time of Flight Mass Spectroscopy

ABBREVIATIONS

M_n	Number Average Molecular Weight
M_w	Weight Average Molecular Weight
NOESY	Nuclear Overhauser Effect Spectroscopy
OMP	Oxalate Metathesis Polymerization
OCMP	Oxalate Cross-Metathesis Polymerization.
PE	Polyethylene
PLA	Poly(lactic acid)
<i>p</i> -TSA	Para Toluene Sulfonic Acid
PDI	Polydispersity Index
PS	Polystyrene Standard
ppm	Parts-Per Million
RT	Room Temperature
Ti(O <i>i</i> Pr) ₄	Titanium Isopropoxide
THF	Tetrahydrofuran
TMS	Tetramethyl Silane
T_g	Glass Transition Temperature
T_m	Melting Temperature
T_c	Crystallization Temperature
TBD	Triazabicyclodecene
TGA	Thermal Gravimetric Analysis
VLDPE	Very Low-Density Polyethylene
WAXD	Wide-Angle X-ray Diffraction

PREFACE



Synopsis of the Thesis to be Submitted to the Academy of Scientific and Innovative Research for Award of the Degree of Doctor of Philosophy in Chemical Sciences

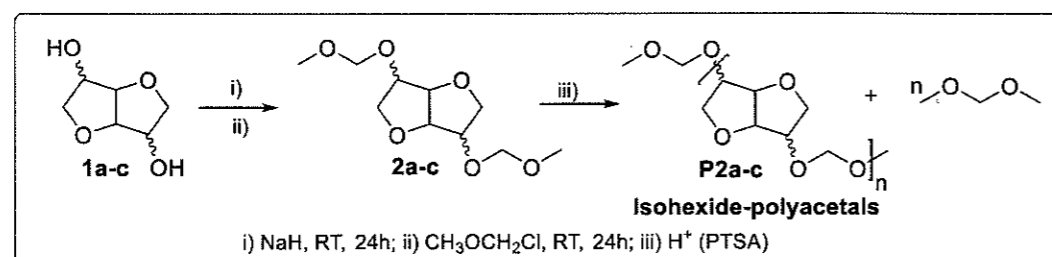
Name of the Candidate	Bhausahab S. Rajput
Degree Enrolment No. & Date	Ph. D in Chemical Sciences (10CC16A26007); August-2016
Title of the Thesis	Isohexide and Plant Oil Based Renewable and Degradable Polymers
Research Supervisor	Dr. Samir H. Chikkali

The thesis titled "Isohexide and Plant Oil Based Renewable and Degradable Polymers" is divided into six chapters. **Chapter-1** deals with the detailed literature survey on the use of sugar based isohexides (isomannide **1a**, isosorbide **1b** and isoidide **1c**) and plant oil based diols for the synthesis of various renewable and degradable polymers.¹ **Chapter-2** describes the synthesis of sugar based isohexide-diacetals and their polymerization to corresponding degradable polyacetals. **Chapter-3** deals with the synthesis of renewable copolyacetals from sugar based isohexide-diacetals and plant oil based long chain diacetals with tunable degradation. **Chapter-4** presents the synthesis of sugar based isohexide-dioxalates and their polymerization with linear diols to corresponding film forming high molecular weight polyoxalates. **Chapter-5** highlights the synthesis of isohexide-di(ether-ene)s and their ADMET polymerization to polyethers. **Chapter-6** concludes the work and provides the future direction.

Chapter 2: Sustainable Polyacetals from Isohexides

Last decade has seen a resurgence in renewable resource-based polymeric materials. Among the various renewable resources, sugars and plant oils provide direct entry to chemical modification and functionalization. Hence, sugars and plant oils are the most competitive candidates for further utilization in platform chemicals and polymerization. Degradability is another material requirement for clean and sustainable future. In this chapter we demonstrate preparation of sugar-derived renewable isohexide-diacetals (**2a-c**) in good to excellent yields by accessing a single step synthetic protocol (**Scheme 1**).² The resultant chiral isohexide-diacetals are valuable building blocks in pharmaceuticals and materials science. To demonstrate their synthetic competence, isohexide-diacetals (**2a-c**) were subjected to Acetal Metathesis Polymerization (AMP) and the corresponding polymers (**P2a-c**) were isolated with

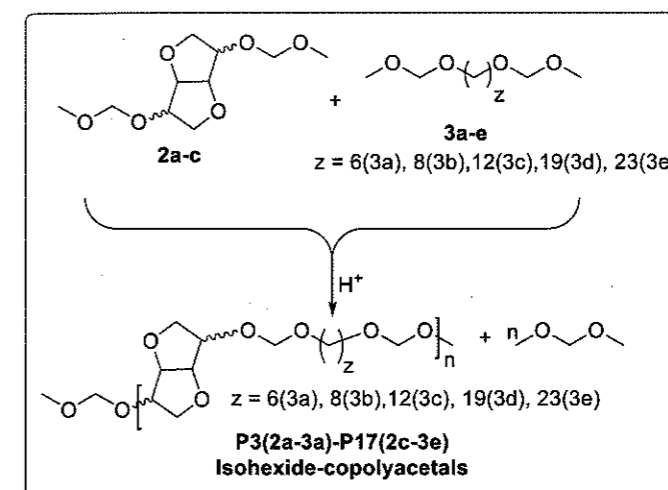
molecular weights in the range 3200-27600 (g/mol). Apart from their renewable origin, degradability will be a decisive parameter for the next generation of sustainable materials. In this context, degradation was investigated and GPC and NMR investigations indicate that the polyacetals degrade in slightly acidic media.



Scheme 1: Synthesis of isohexide-diacetals (**2a-c**) and Acetal Metathesis Polymerization to polyacetals (**P2a-c**).

Chapter 3: Synthesis of Renewable Copolyacetals with Tunable Degradation

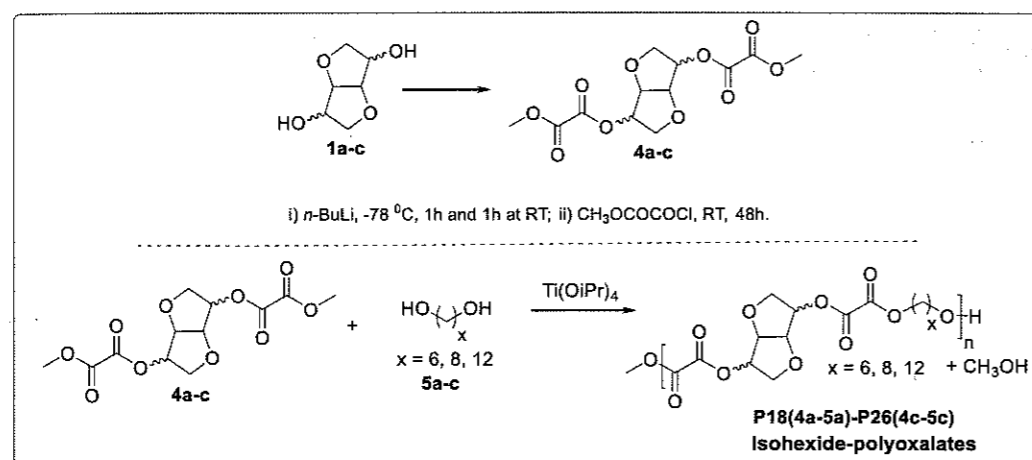
In our previous investigations in chapter 2, the rate of degradation was found to be very fast in case of isohexide-polyacetals.² This is due to the hydrophilic nature of isohexide-polyacetals. To address this issue we synthesized renewable copolyacetals by incorporating the long chain diacetals (hydrophobic) into the isohexide-diacetals (hydrophilic). In this chapter we report the first synthesis of isohexide-based (**2a-c**) and plant oil-based diacetal monomers (**3a-e**), leading to fully bio-based copolyacetals **P3(2a-3a)-P17(2c-3e)** by Acetal Metathesis Copolymerization (AMCP) (**Scheme 2**).³ The existence of copolymeric structures was confirmed with the help of various analytical tools and techniques. In a stark contrast to the earlier reported isohexide-polyacetals, the current copolyacetals revealed very slow degradation. GPC investigations revealed that with increasing chain-length, the rate of degradation reduces, whereas copolyacetals with short-chain aliphatic segments displayed faster degradation profile. The reduced rate of degradation can be attributed to the hydrophobic nature of long-chain acetal segments. In-situ NMR spectroscopy revealed existence of formates, hemiacetals and diols as degradation products. Thus, rate of degradation can be tuned by the judicious choice of isohexide-diacetals and linear-diacetals in a copolyacetal.



Scheme 2. Synthesis of copolyacetals **P3(2a-3a)-P17(2c-3e)** via AMCP.

Chapter 4: Cross-Metathesis of Biorenewable Dioxalates and Diols to Film Forming Degradable Polyoxalates

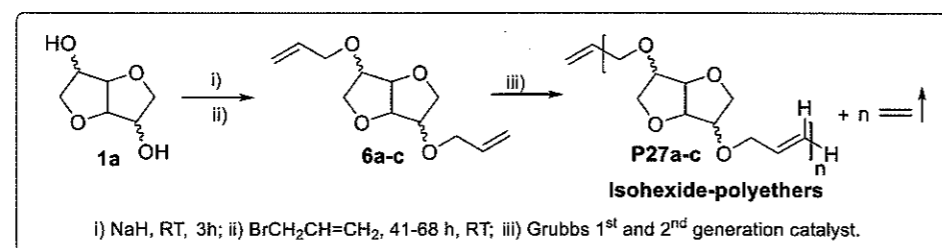
Polyoxalates are a well-known class of polymers containing -O(CO)₂O- linkage and undergo facile degradation in aqueous media.⁴ Considering this advantage, we synthesized sugar-derived isohexide-dioxalates (**4a-c**) in excellent yields using a single step synthetic protocol (**Scheme 3**).⁵ The synthetic utility of these sugar-derived dioxalates was examined in condensation polymerization. Condensing isohexide-dioxalates (**4a-c**) with aliphatic renewable diols (**5a-c**) in presence of Lewis acid catalyst leads to the production of poly(isohexide-co-alkane)oxalates. Surprisingly, the proton NMR of the polyoxalate **P18(4a-5a)** revealed a 2:1 ratio of 1,6-hexanediol (**5a**) and isomannide-dioxalate (**4a**) in the polymer backbone. This intriguing reactivity was found to be an outcome of cross metathesis between the two monomers **4a** and **5a**. Based on direct and indirect evidence, and control experiments, an alternative polymerization mechanism is proposed. Thereafter, polymerization conditions were optimized to obtain high molecular weight polyoxalates **P18(4a-5a)-P26(4c-5c)**. In an attempt to demonstrate direct application of these polymers, transparent films were casted and their mechanical properties indicated formation of soft film. Solid and solution state degradation investigations established that polyoxalates are amenable to degradation over an extended period of time. Thus, utilization of renewable feed-stocks to prepare chiral build blocks and commercially attractive sustainable polyoxalates has been demonstrated for the first time.



Scheme 3: Synthesis of isohexide-dioxalates and Oxalate Metathesis Polymerization with linear diols to polyoxalates **P18(4a-5a)-P26(4c-5c)**.

Chapter 5: Synthesis of Isohexide-di(ether-ene)s and ADMET Polymerization

Over the years acyclic diene metathesis polymerization has evolved as a very powerful technique for the preparation of a wide range of polymeric architectures, including linear polymers, polymers with a defined branching density and block-copolymers from telechelics. Along the same line sugar-based isohexides can be modified to prepare a library of isohexide-diene monomers for polymerization. Such isohexide-diene monomers can be subjected to acyclic diene metathesis polymerization to obtain green materials. In this chapter we report a single step synthetic protocol to produce small family of isohexide-di(ether-ene)s.⁶ These obtained monomers **6a-c** are subjected to ADMET polymerization using Grubbs 1st and 2nd generation catalysts. ADMET polymers was confirmed by ¹H NMR and MALDI-ToF-MS analysis (**Scheme 4**).⁶ The resultant polyethers **P27a-c** show low molecular weight polymers under the optimized experimental conditions. Afterwards, slight improvement in the molecular weight was observed when benzoquinone was added or when the catalyst was added in two stages.



Scheme 4. Synthesis of isohexide-di(ether-ene)s (**7a-c**) and ADMET polymerization to polyethers (**P27a-c**).

Chapter 6: Conclusions and Outlook

This chapter summarizes the synthesis of sugar based isohexide-diacetals and their corresponding degradable polyacetals. The rate of degradation is found to be very fast in case of isohexide-polyacetals due to the hydrophilic nature of these polyacetals. To overcome the problem of fast degradation we have developed new copolyacetals from isohexide-diacetals (hydrophilic) and plant oil based diacetals (hydrophobic). We could also be able to tune the rate of degradation of copolyacetals by varying the chain length of long chain diacetals. We have developed sugar based isohexide-dioxalate following the single step synthetic protocol. These dioxalates are polymerized with linear diols to afford the film forming high molecular weight polyoxalates. Degradation study revealed that polyoxalates are found to be degrading over an extended period of time. Furthermore we demonstrated the synthesis of isohexide-di(ether-ene)s and their subsequent ADMET polymerization to corresponding low molecular weight polyethers.

References:

1. For recent reviews on renewable to chemical are: (a) Hufendiek, A.; Lingier, S.; Du Prez, F. E. *Polym. Chem.* **2019**, *10*, 9-33. (b) Stempfle, F.; Ortmann, P.; Mecking, S. *Chem. Rev.* **2016**, *116*, 4597-4641. (c) Galbis, J. A.; GraciaGarcía-Martín, M. de.; Violante de Paz, M.; Galbis, E. *Chem. Rev.* **2016**, *116*, 1600- 1636. (d) Meier, M. A. R.; Metzger, J. O.; Schubert, U. S. *Chem. Soc. Rev.* **2007**, *36*, 1788-1802.
2. Rajput, B. S.; Gaikwad, S. R.; Menon, S. K. Chikkali, S. H. *Green Chem.* **2014**, *16*, 3810-3818.
3. Rajput, B. S.; Chander, U.; Arole, K.; Stempfle, F.; Menon, S.; Mecking, S.; Chikkali, S. H. *Macromol. Chem. Phys.* **2016**, *217*, 1396-1410.
4. Gracia, J. J.; Miller, S. A.; *Polym. Chem.* **2014**, *5*, 955-961.
5. Rajput, B. S.; Ram, F.; Menon, S. K.; Shanmuganathan, K. Chikkali, S. H. *J. Polym. Sci. Part A: Polym. Chem.* **2018**, *56*, 1584-1592.
6. Rajput, B. S.; Lekshmy, K. G.; Menon, S. K.; Chikkali, S. H. *Green Materials* **2017**, *5*, 63-73.

Chapter 1

Introduction

1.1. Sugar to Isohexides:

With diminishing fossil reserves and growing emission of greenhouse gases, it is clear that the use of renewable raw materials is going to be a sustainable solution for the future.¹⁻³ Fossil feedstocks are being used for both, energy production and plastic manufacturing.^{2, 4} Considering the huge requirement of fossil feedstocks, it was evident that the price of petroleum and petroleum-derived products is going to increase. The increasing emission of greenhouse gases and finite fossil feedstocks has triggered researchers to find sustainable alternatives.⁵ Not only depletion of fossil resources is of great concern but also disposal of non-degradable materials has led to severe environmental pollution.⁵ Considering those issues, there is a need to develop renewable and biodegradable plastic (derived from renewable feedstocks). The most extensively used renewable raw materials are polysaccharides, vegetable oils, proteins, lignin, etc.⁶ Among these renewable resources, plant oils and sugars provide direct access to the chemical modification and functionalization.⁷⁻⁸ Sugar-derived isohexides can be possible alternatives to fossil feedstocks. Carbohydrates and starch are the richest and readily available biomass feedstocks (these can be obtained from various renewable resources such as wheat, maize, potato, rice, etc.) and they have found several applications in polycondensates.⁸ Sorbitol and mannitol can be produced from the hydrogenation of carbohydrate i.e., glucose and mannose (**Figure 1.1** top). Consequent double dehydration of mannitol and sorbitol leads to isohexides (**1a-c**, **Figure 1.1** bottom). The 1,4:3,6-dianhydrohexitols (isohexides) are chiral, rigid and non-toxic.

Isohexides (**1a-c**) are very promising precursors and exist in three different isomeric forms such as isomannide (**1a**), isosorbide (**1b**) and isoidide (**1c**). The five-membered bicyclic framework induces improved rigidity, which makes isohexides (**1a-c**) a proficient substitute for fossil fuel-derived various diols. Among these three isomers, isosorbide is easily accessible from polysaccharides.⁸

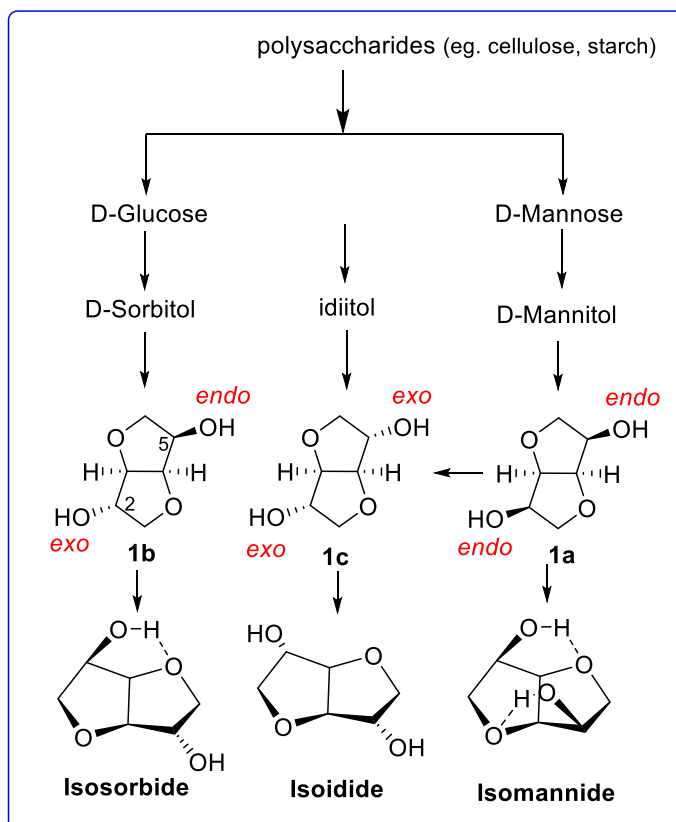
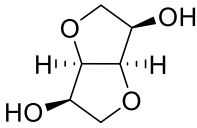
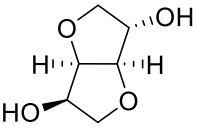
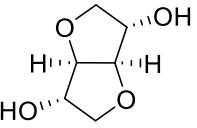


Figure 1.1. Production of isohexides (**1a-c**) from a biogenic polysaccharide and their stereo-isomeric forms.

Isosorbide, also recognized as 1,4:3,6-dianhydro-D-glucitol or 1,4:3,6-dianhydro-D-sorbitol, is a V-shaped molecule of two *cis* connected tetrahydrofuran rings with an opening angle of 120° and secondary hydroxyl groups in the C2 and C5-positions (**Figure 1.1**, bottom-left) and it was first reported in 1927. The crystalline isosorbide was prepared a few years later, and the evidence of its structure was demonstrated in late 1946.⁹ The only difference between isosorbide in contrast to its two isomers isomannide and isoidide is the configuration of the two hydroxyl (-OH) groups. Isoidide (**1c**) exhibits *exo-exo* and isomannide (**1a**) shows *endo-endo* configuration for both hydroxyl groups, while in isosorbide the hydroxyl group in the C2-position has *exo* and that in the C5-position *endo* configuration. Due to this difference in configuration it shows the variable melting temperatures as well as diverse reactivity of hydroxyl groups (see **Table 1.1**).

Table 1.1. Structure and properties of 1,4:3,6-dianhydrohexitols.

Chemical Name	Isomannide 1,4:3,6-dianhydro-D-mannitol	Isosorbide 1,4:3,6-dianhydro-D-glucitol	Isoidide 1,4:3,6-dianhydro-L-iditol
Molecular Structure			
Molecular Weight	146.14 gmol ⁻¹	146.14 gmol ⁻¹	146.14 gmol ⁻¹
Melting Temperature	81-85 °C	61-62 °C	64 °C

In case of isosorbide, the *exo* hydroxyl group does not form hydrogen bonding, whereas *endo* hydroxyl group forms intramolecular hydrogen bonds to the oxygen atoms of the opposite furan ring (see **Figure 1.1**, bottom-left). This different behaviour of *exo-endo* configuration in the case of isosorbide has been established by two different bands in the corresponding IR absorption spectra. The IR absorption for free -OH group appears at 3624 cm⁻¹, whereas the absorption of hydrogen-bonded -OH occurs at 3540 cm⁻¹.¹⁰ These IR bands can be used to describe the isomers and substitution behaviour upon reaction of only one hydroxyl (-OH) group.⁹ However, this dissimilarity in the reactivity of the two hydroxyl groups (*exo-endo*) renders isosorbide a highly attractive platform chemical for functionalizations and transformations. The global market size for isosorbide was reached to 300 million USD in 2015.¹¹

The increasing demand for replacing fossil feedstock based derivatives with isosorbide has some potential industrial applications¹²⁻¹³ such as;

- Isosorbide nitrates is used in vascular and cardiac diseases.⁸
- The alkyl derivatives are used in solvents in cosmetic compositions and pharmaceuticals.^{8,9}
- The major application is in the copolymerization of polyethylene terephthalate (PET) to increase the strength of polymers. Isosorbide modified PET that is polyethylene isosorbide terephthalate (PEIT) finds applications in beverages and food packaging.¹¹
- It is used in synthesis of other polymers such as polycarbonate, polyurethane, polyester polyisosorbide, isosorbide diesters etc.¹¹

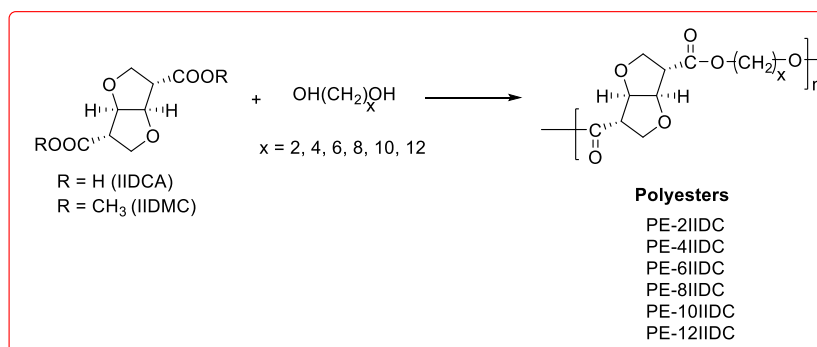
- e) An interesting application for isosorbide is a replacement for the controversial compound such as BPA (Bisphenol A) which is the key monomer in polycarbonate and epoxy resins synthesis.¹⁴

The major chemical companies such as SK Chemicals and Mitsubishi Chemicals are increasingly using polymers based on isosorbide. The demand for isosorbide is basically fueled by ongoing capacity expansion of bioplastic industries in the world.¹¹ The second isomer, isomannide (**1a**), is less attractive for large scale industrial applications for two reasons: i) The two hydroxyl (-OH) groups show a considerably lower reactivity because of their *endo* stereochemistry and the hydrogen bonding, ii) Its production is more costly as starting materials such as fructose or mannitol are less readily accessible than glucose or sorbitol (in isosorbide). The third isomer, isoidide (**1c**), shows a considerably higher reactivity, but its starting material L-idose, cannot be obtained from plant biomass source.⁹ Other way to synthesize two isomers is isomerization of isosorbide but this process is currently not economically viable. Thus, isosorbide has gained appreciably higher interest as a platform chemicals or monomers than its two other isomers.⁹

1.2. Polymers from Sugar Based Isohexides:

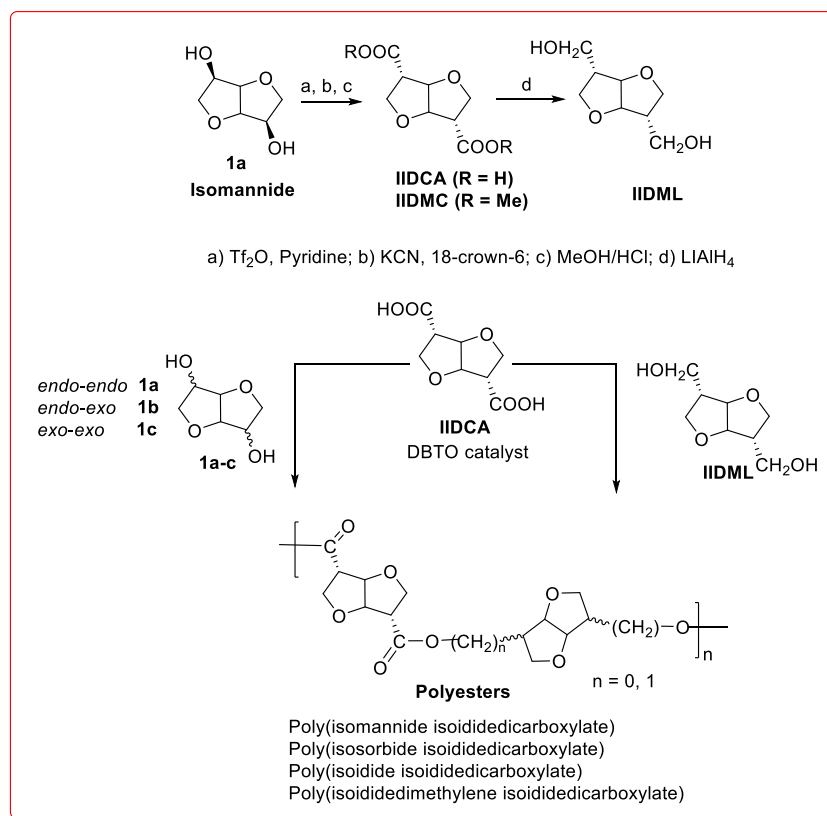
It was observed that direct use of isohexides usually requires harsh polymerization conditions and produces a dark, tar-like material with reduced molecular weights.⁸ This is most likely because of poor reactivity of sterically hindered secondary -OH groups. Secondly, the hydrogen bonding of these secondary -OH groups with ring oxygen is also responsible for the reduced reactivity. Considering the above challenges associated with the direct use of isohexides in polymerization, Daan and co-workers synthesized various derivatives of isohexides employing a “1-carbon extension” strategy.¹⁵ Furthermore, these modified monomers with enhanced reactivity were successfully polymerized to polyesters,¹⁶ polyamides,¹⁷ polyurethanes¹⁸ and copolyesters with diols¹⁹. These obtained polymers were found to be less colored and showed increased glass transition temperature (T_g) compared to their linear fossil feedstock derived analogues.^{17, 18} With the aim to increase reactivity of isohexide while at the same time retain rigidity, Daan and co-workers¹⁹ synthesized a new isoididedicarboxylic acid (IIDCA) by transforming the secondary hydroxyls group into carboxylate functionalities. In this report, they synthesized the aliphatic semicrystalline polyesters by polycondensation of isoididedicarboxylic acid (IIDCA) or isoididedimethyl carboxylate (IIDMC) with α, ω -diols (**Scheme 1.1**). Synthesized polyesters were obtained via melt polymerization technique and exhibited weight-average

molecular weight (M_w) in the range of 13000-34000 g mol^{-1} and polydispersities (PDI) close to 2.0. Semicrystallinity of resultant IIDCA polyester was determined with the help of differential scanning calorimetry and wide-angle X-ray diffractions. Comparison with corresponding polyadipates²⁰ (polyadipates were synthesized from polycondensation of adipic acid with α , ω -diols) this IIDCA increases the glass transition temperatures (T_g) by approximately 50-70 $^\circ\text{C}$ due to the rigidity of bicyclic ring.



Scheme 1.1. Polymerization of IIDCA/IIDMC and α , ω -diols yielding aliphatic polyesters.

Further, the scope of isoidide dicarboxylic acid (IIDCA) was extended to synthesize fully sugar based renewable polyesters (**Scheme 1.2**).¹⁶ Synthesized isoidide dicarboxylic acid (IIDCA) was polymerized with rigid isohexide diols (isomannide **1a**, isosorbide **1b**, isoidide **1c**) and the novel 2, 5-methylene-extended isoidide dimethanol (IIDML). Novel 2, 5-methylene-extended isoididedimethanol (IIDML) was synthesized from the (IIDCA). IIDML were developed to enhance the reactivity of the isohexides, while at the same time to retain the rigidity and therefore the beneficial effect on glass transition temperature (T_g). However, it was observed that compared to the parent isohexides, IIDML showed a noticeably higher reactivity, resulting in three to four times higher weight-average molecular weight (M_w , 10400 g mol^{-1}) for resulting polyesters (**Scheme 1.2**). The isoidide/isosorbide based polyesters have high T_g values (70 and 85 $^\circ\text{C}$, respectively), while the IIDML-based polyester has a lower T_g of approximately 48 $^\circ\text{C}$. The incorporation of IIDML (having the $-\text{CH}_2-$ linkage) into the backbone of the IIDCA-based polyesters leads to polymers having higher degrees of crystallinity (symmetrical/regular structural arrangement) compared to the polyesters based on the parent isohexides (unsymmetrical/irregular structural arrangement). The sugar based isohexides were also used in synthesis of various polymers such as polyamides,^{17, 21-23} polyimides,²⁴⁻²⁵ polycarbonates,²⁶⁻²⁹ polyurathanes,³⁰⁻³³ and polymethylacrylates³⁴⁻³⁵.



Scheme 1.2. Synthesis of isoididedicarboxylic acid (**IIDCA**), isoidide dimethyl dicarboxylate (**IIDMC**), and isoididedimethanol (**IIDML**) from isomannide (top) and synthesis of polyesters from isohexide-based monomers (bottom).

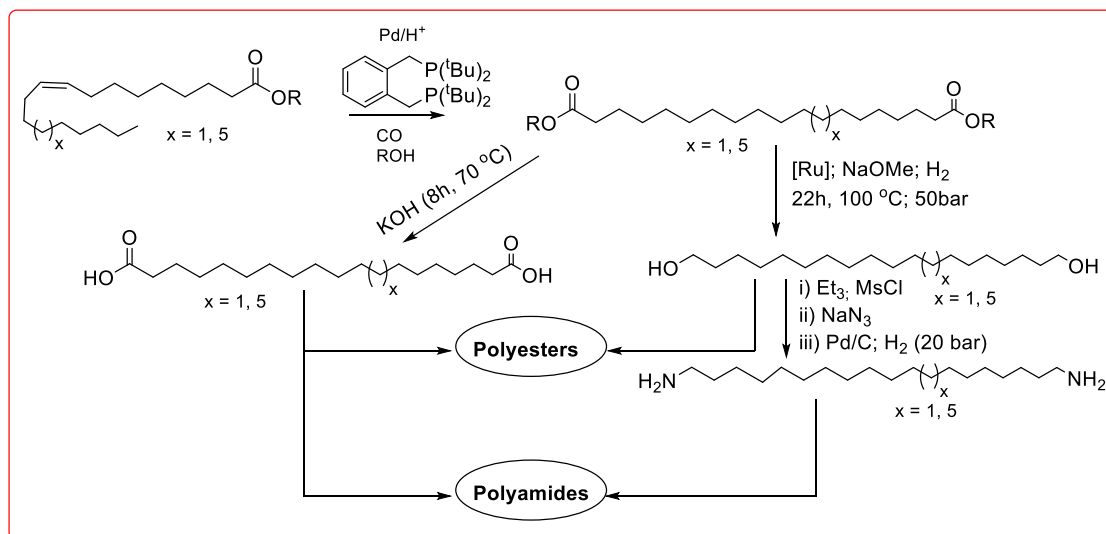
1.3. Polymers from Plant Oil Derived Long Chain Diols:

The second and readily available resource is plant oils. Plant oils and their derivatives are being used because of the worldwide accessibility and applications in the polymerization.³⁶ The plant-derived oils and fats provide a potential replacement for the presently used fossil feedstocks in a straightforward fashion. Plant oils are tri-ester of long chain-fatty acids with varying composition of fatty acids depending on the plant type or category.¹ Plant oil derivatives were proved to be helpful in the synthesis of range of monomers as well as linear and cross-linked polymers such as polyesters,³⁷⁻⁴⁰ polyurethane,⁴¹⁻⁴² polyamides,³⁷⁻⁴³ polyethers⁴⁴ and epoxy resin.⁴⁵⁻⁴⁶

Plant oil derived long-chain diols are very interesting candidates for the synthesis of long-chain aliphatic polymers.⁷ Polyamides and polyesters were synthesized using appropriate ratio of linear long-chain diols.³⁷ Initially, these linear long-chain difunctional compounds were

synthesized by tedious and time consuming organic transformations via sequential synthesis starting from shorter-chain congeners. To overcome this challenge a new method has been introduced. In this method, selective terminal functionalization of fatty acid long chain derivatives is achieved through a catalytic process. With this strategy, the polymerization grades linear α , ω -difunctional monomers were synthesized. This catalytic process brings out the possible replacement for petroleum-derived analogues.

In 2011, Mecking and co-workers³⁷ utilized the isomerizing alkoxyacylation strategy to prepare α , ω -functionalized long chain linear compounds (**Scheme 1.3**). In these studies two readily available substrates, methyl oleate and ethyl erucate were used as starting materials for the isomerizing alkoxyacylation. The resultant C19 and C23 α , ω -diesters were synthesized for the first time in a practicable approach which provided an access to a range of novel long-chain α , ω -difunctional compounds or monomers. Polymerization grade α , ω -dicarboxylic acids and α , ω -diols were also synthesized in high purity and high yield. C19 and C23 derived polyesters display the melting temperature which falls under thermoplastic materials. Similarly, the nonadecane-1, 19-diamine and tricosane 1, 23-diamine were prepared from the corresponding alcohols. The polyamides were synthesized from the polycondensation of novel long-chain α , ω -diamine with C19 and C23 based α , ω -dicarboxylic acid. It is well known that due to the presence of H-bonding in polyamides the melting (T_m) and crystallization temperature (T_c) decreases with increasing chain length.⁴⁷ Polyamides C23-C19 and C23-C23, based on 1, 23-tricosanediamine, exhibited a melting temperature (T_m) of 156 °C and 152 °C respectively. On the other hand, polymerization of 1, 11-diaminoundecane with 1, 23-tricosanedicarboxylic acid produce a polyamide which shows the expected higher T_m of 167 °C.



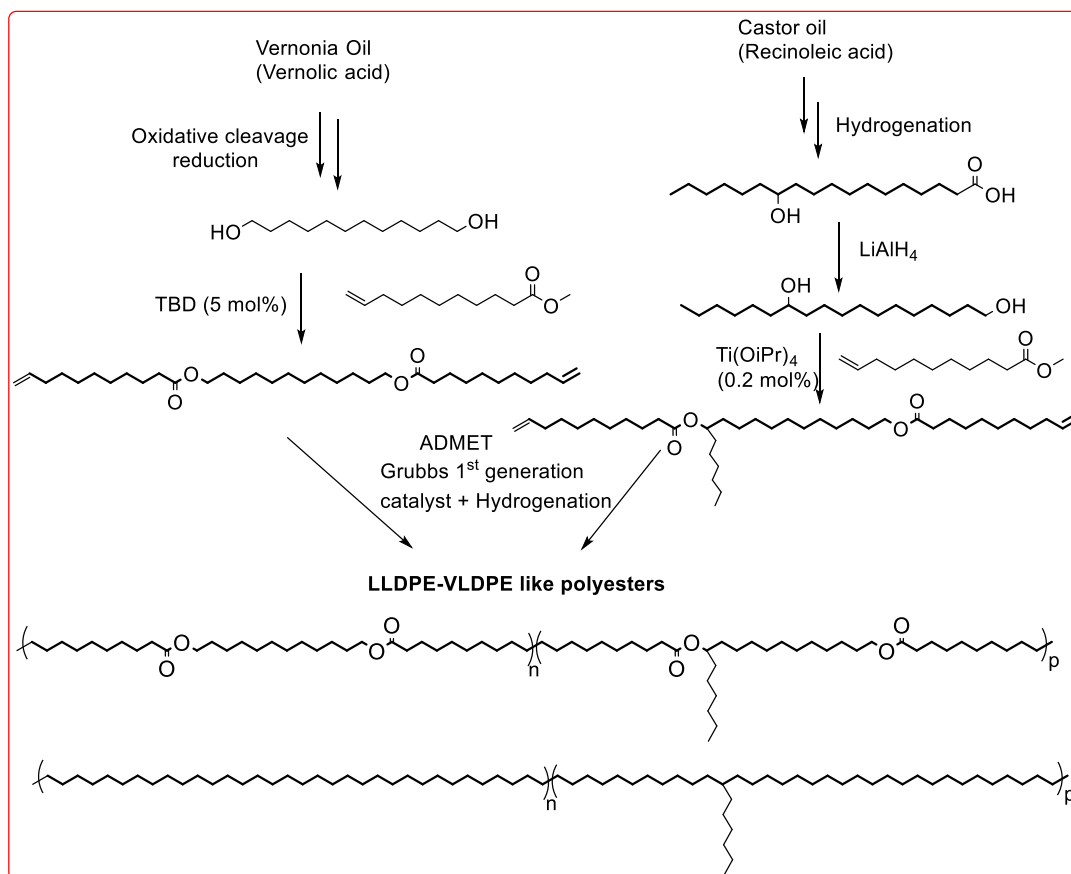
Scheme 1.3. Synthesis of polyesters and polyamides from long chain α, ω -difunctional compounds.

Then the same group⁴⁸ developed polycondensation grade dimethyl-1,19-nonadecanedioate and dimethyl-1,23-tricosanedioate monomers. The C19 and C23 diester were obtained on a 100 g scale with 99% purity. Long-chain α, ω -diols were generated by the reduction of diesters which polymerized with long chain α, ω -diesters to afford the linear aliphatic polyesters. They include both long crystallizable polyethylene-like hydrocarbon chain as well as ester moieties in the main backbone. Dumbbell test specimen was obtained from polyesters **PE-19.19** (derived from polycondensation between C19-diol and C19-diester) and **PE-23.23** (derived from polycondensation between C23-diol and C23-diester). The obtained polyesters clearly show distinctive polymer properties instead of brittle wax-like behavior and these both polymers show the Young moduli around 400 MPa and elongation at break is 600%. Later on in 2015, same group⁴⁹ synthesized the thermoplastic polyester elastomers. In this, plant oil derived α, ω -diester (C23) and the corresponding α, ω -diol (C23) give a completely hard segment and poly(tetramethylene glycol, PTMG) or carbohydrate-based poly(trimethylene glycol) supply the soft segment.

In literature, efforts have been made to synthesize biobased and degradable polyethylene like polyesters. Various synthetic routes such as thiol-ene addition, metathesis and isomerizing alkoxy-carbonylation etc. of fatty acids produced long chain aliphatic monomers possessing hydroxyl acid ($-\text{OH}$) or ester group have been studied.⁵⁰⁻⁵¹ Most of the studies were focused on developing PE like polyesters from long chain fatty acids and resulted in materials that mimic the

structure of neat HDPE. In contrast, there are very few reports on the synthesis of LDPE, LLDPE and VLDPE-like long chain polyesters from plant oils. Considering the above limitations, Cramail group⁵² developed LLDPE and VLDPE-like polyester using acyclic diene metathesis (ADMET) copolymerization of two long-chain fatty acid based α, ω -diene monomers (**Scheme 1.4**).

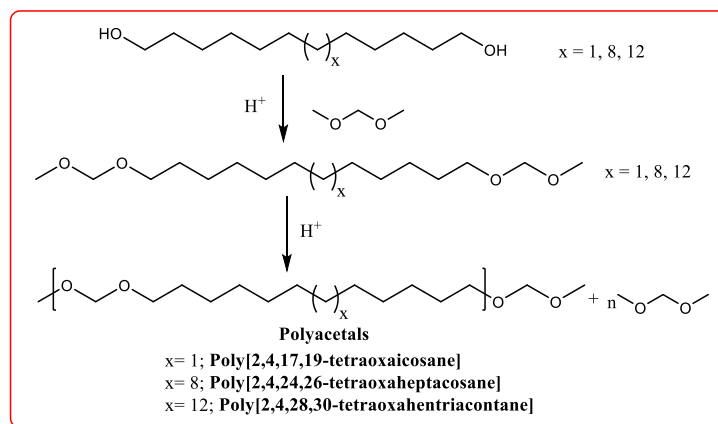
Bulk copolymerization of α, ω -diene monomers was carried out to afford copolyesters having various degree of branching, and moreover, their subsequent hydrogenation yielded the corresponding saturated analogues mimicking the structure of LDPE as well as VLDPE. Afterward, thermomechanical properties of the obtained copolyesters were investigated and compared to the petrochemical-based polymers. After hydrogenation, resulting copolyesters showed thermo-mechanical properties in agreement with those of LLDPE and VLDPE with variable melting temperatures (T_m) between 50 °C and 90 °C. Apart from the renewable origin of resultant polymers, degradability is one of the important parameters for a sustainable future. Therefore, polymer degradation has become a key challenge for current research.



Scheme 1.4. Synthetic strategy to prepare LLDPE-VLDPE like polyesters.

1.4. Renewable and Degradable Polymers:

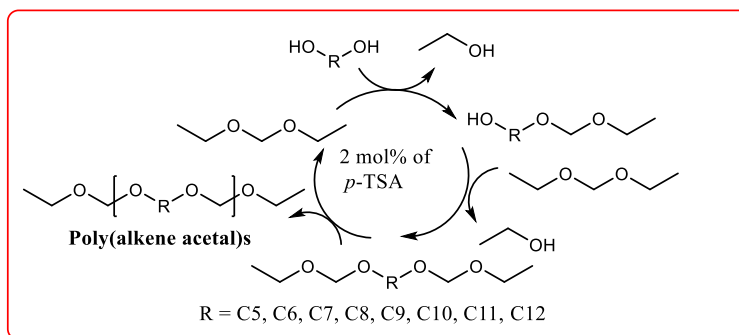
Besides the renewable origin of the monomer, the choice of functional group is also an important parameter which decides the polymer degradation. The research on synthesis of renewable and degradable polymers has already begun, but to date there are very few reports which emphasized on use of renewable resources to make degradable polymers. In 2012 Mecking and co-workers⁵³ synthesized a small library of long-chain diacetals and the corresponding degradable polyacetals (**Scheme 1.5**). Polyacetals are known to degrade in acidic conditions due to the presence of acetal linkage. The starting diols (C19) and (C23) were produced by the catalytic isomerizing alkoxy-carbonylation of unsaturated fatty acid esters and subsequent catalytic reduction to corresponding diols. Commercially available C12-diol and in-house prepared C19 and C23-diols were treated with an excess of dimethoxymethane to afford the corresponding diacetals. Self-condensation of difunctional acetals monomers in presence of 2-4 mol% of catalyst afforded the corresponding polyacetals. The rate of hydrolytic degradation for long-chain polyacetals was noticeably lower compared to their shorter chain (C12) analogue.



Scheme 1.5. Synthesis of linear long chain diacetals and the corresponding polyacetals.

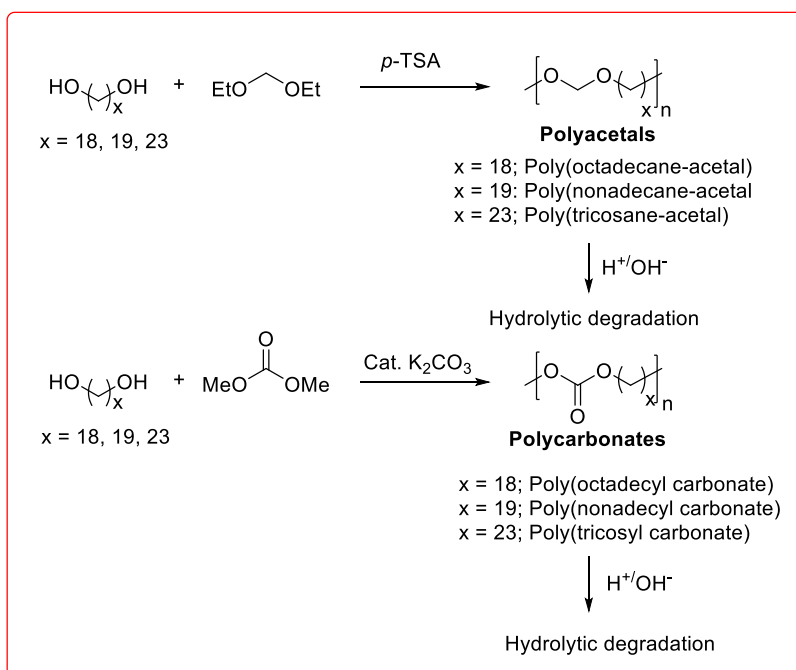
Later on Miller and co-workers⁵⁴ developed one-pot protocol for direct conversion of diols to polyalkylene acetals via a novel technique involving interchange of acetal functional groups by Acetal Metathesis Polymerization (AMP) (**Scheme 1.6**). Initially, the term AMP was proposed by Miller due to the resemblance between metal catalyzed ADMET polymerization and acid catalyzed acetal interchange chemistry (AMP). Direct conversion of commercially available diols (C5, C6, C7, C8, C9, C10, C11, C12) in presence of excess of diethoxymethane to poly(alkylene acetal)s was carried out. These polyacetals showed the number average molecular weight M_n of

8800-38700 g mol⁻¹. Polyacetals obtained from the shorter chain diols showed lower melting temperatures compared to the earlier reported long chain diols (higher melting temperature).⁵³ This observation suggests that the thermal stability of polyacetals increased with increasing chain length.



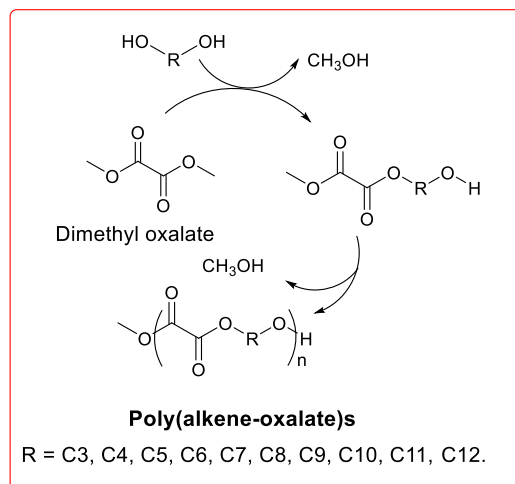
Scheme 1.6. Direct conversion of a diol to a poly(alkylene acetal)s via Acetal Metathesis Polymerization (AMP).

Afterward, Mecking group⁵⁵ improved the synthetic procedure and developed one-pot synthetic protocol for the synthesis of thermoplastic long chain polyacetals (**Scheme 1.7**, top). Synthesis of long chain polyacetals was carried out by reaction of long chain diols (C18, C19, and C23) with an excess of diethoxymethane in the presence of catalytic amount of *p*-toluene sulfonic acid. Hydrolytic degradation of polyacetals was also carried out by making the solid pellets and maximum weight loss was observed under acidic conditions compared to the basic environment. In contrast with ester group, carbonate functionality is more amenable to hydrolysis. Polycarbonates are non-toxic⁵⁶ and biocompatible, and they are susceptible towards basic as well as acidic aqueous environments.⁵⁷ Considering these advantages, thermoplastic long chain polycarbonates⁵⁵ were synthesized from α , ω -diols (C18, C19, C23) and dimethyl carbonate in a single step (**Scheme 1.7**, bottom). These obtained polycarbonates showed hydrolytic degradation in both acidic as well as basic conditions. Hydrolytic degradation of solid pellets for long-chain polycarbonates and polyacetals shows better stability compared to their shorter chain analogues.



Scheme 1.7. One pot synthesis of long chain polyacetals (top) and polycarbonates (bottom) with possible hydrolytic degradation pathway.

Like Acetal Metathesis Polymerization (AMP), the Oxalate Metathesis Polymerization (OMP) was reported by Miller and co-workers in 2014.⁵⁸ Various types of diols (C3, C4, C5, C6, C7, C8, C9, C10, C11, C12) were used for this study. The mechanism involves the acid catalyzed interchange of dimethyl oxalate and diols in the presence of *p*-toluene sulfonic acid (**Scheme 1.8**). In DSC analysis different thermal behavior was noted depending on the odd or even carbon atoms. Polyoxalates having the odd methylene groups showed lower melting temperatures compared to even number counterparts. The highest melting temperature was attributed to the proper packing of the chain in case of even methylene groups. Furthermore, to increase the thermal properties, the biobased aromatic diols were incorporated. Degradation result of copolyoxalate poly(decylene-*co*-RBHE) (derived from the resorcinol bis(2-hydroxyethyl) ether and decanediol (C10)) showed the facile hydrolysis in humid air and conversion of high molecular weight to low molecular weight polymers was observed after thirteen months.



Scheme 1.8. Oxalate Metathesis Polymerization (OMP) of dimethyl oxalate and diol to form poly(alkene-oxalate)s *via* acid catalyzed ester interchange.

1.5. Setting the Goals:

As presented in section 1.2, 1.3 and 1.4 significant advancement in the field of renewable and degradable polymers such as polyacetals, polycarbonates, and polyoxalates has been reported. Although these polymers are sustainable, their thermal and mechanical properties fall short of any real life application. Most of the fossil feedstock derived polymers are aromatic due to which they induce the rigidity in the resultant polymers and offer high T_g and high T_m . Whereas, plant oil derived polymers contains flexible long chain methylene segments which ultimately affect the T_g and T_m of corresponding polymers. Considering these challenges associated with plant oil derived polymers, there is a need for alternative renewable material which can bridge the gap between the plant oil and petroleum feedstock derived polymers. In the past decades, considerable research has been carried out to utilize sugar based isohexides for the synthesis of various polymers. It has been found that thermal and mechanical properties of obtained polymer are improved due to incorporation of rigid sugar based isohexides. Apart from that, very few reports emphasized on degradation of isohexide-based polymers.^{8, 27, 30, 59-60} In those reports, isohexides were used as one of the comonomer for enhanced rate of degradation of resultant polymers (since isohexides are hydrophilic in nature). Direct modification of sugar-based isohexides with suitable functionality for synthesis of degradation grade monomer is largely missing in the literature. If we take a closer view, we have a lot of opportunities to play around with isohexide moiety (**Figure 1.2**). Considering their importances, our primary aim is make use of sugar-based isohexides (i.e. isomannide, isosorbide and isoidide) for the synthesis of renewable and degradable polymers.

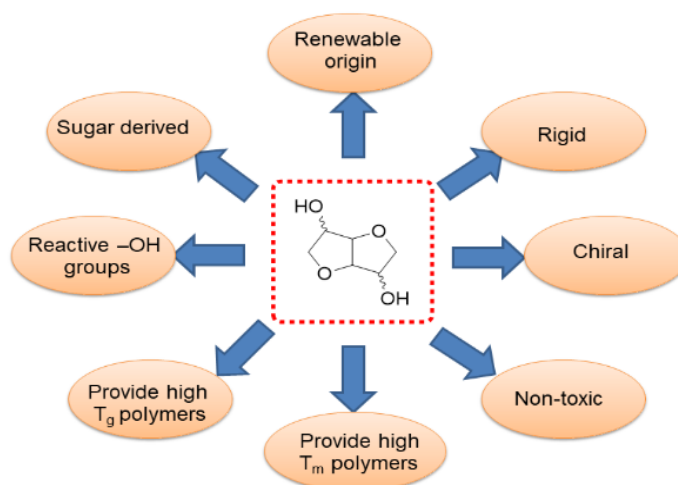


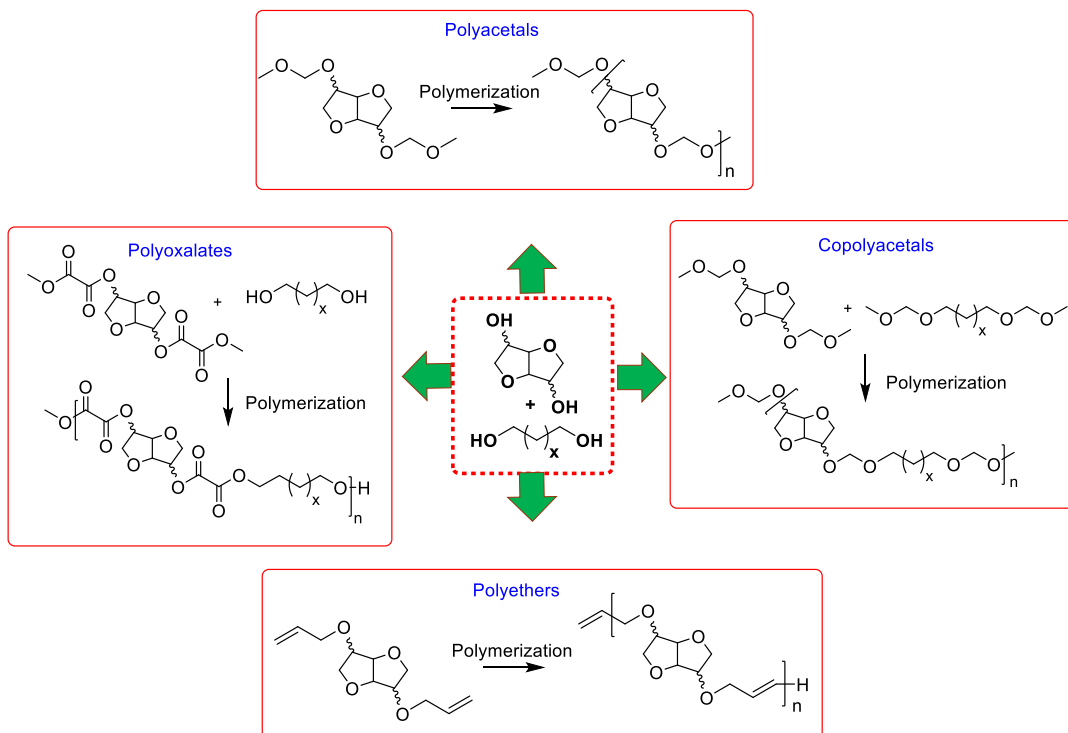
Figure 1.2. Characteristics of isohexides.

It was observed that sugar derived isohexide carry more oxygen atoms (O/C ratio) and plant oils typically have higher carbon content than oxygen. It would be great if one can utilize these resources and prepare feedstock chemicals, monomers, and polymers with balanced O/C ratio to imbibe desired properties. Having this balanced O/C ratio in the resultant polymers, one can tune the properties of polymers depending on the end-use application and also tailor the rate of degradation of polymers.

The overall goal of this thesis work is to utilize easily available sugars and plant oils for the synthesis of renewable and degradable polymers. Also, demonstrate the new strategy for the synthesis of monomers and polymers. The specific goal of present study is:

- Synthesis of sugar derived renewable and degradable isohexide-polyacetals. The rationale behind is that the acetal linkage is known to degrade in mildly acidic conditions (**Scheme 1.9-top**).
- Synthesis of sugar and plant oil based copolyacetals. These resultant copolyacetals will offer both hydrophilic and hydrophobic segments, and these will be beneficial for end use application (**Scheme 1.9-right**).
- Preparation of isohexide based polyoxalates (**Scheme 1.9-left**).

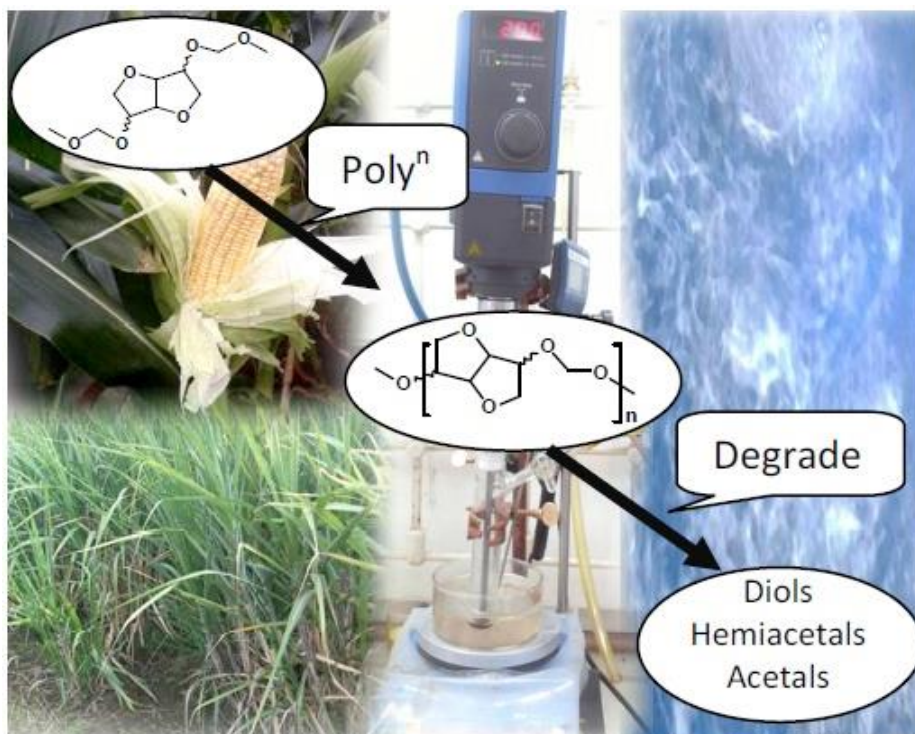
- d) Another objective is to synthesize isohexide based polyethers by using Acyclic Diene Metathesis (ADMET) Polymerization method (**Scheme 1.9**-bottom).



Scheme 1.9. Synthesis of isohexide and plant oil based monomers and corresponding polymers.

Chapter 2

Sustainable Polyacetals from Isohexides



This chapter has been adapted from following publication

Rajput, B. S.; Gaikwad, S. R.; Menon, S. K.; Chikkali, S. H. *Green Chem.* **2014**, *16*, 3810-3818.

2.1. Abstract:

A single step synthetic protocol to access a small family of renewable diacetals was established. The resultant chiral diacetals are valuable building blocks for pharmaceuticals and materials science. To demonstrate their synthetic competence, isohexide-diacetals (**2a-c**) were subjected to acetal metathesis polymerization and the corresponding polymers (**P2a-c**) were isolated as white solids with molecular weights in the range 3200-27600 (g mol^{-1}). The semi-crystalline polymers displayed glass transition temperatures between 38-65 °C and melting temperatures in the range of 103-156 °C. The isohexide derived polyacetals are stable under practical washing and rinsing conditions but degrade in slightly acidic media.

2.2. Introduction:

The majority of current thermoplastic polymers are produced using monomers derived from fossil feedstocks.^{1a-b} However, depleting crude oil reserves and growing environmental constraints have posed a new challenge and a quest to discover a sustainable alternative has already begun.¹ Due to this, the last decade has witnessed a resurgence in platform chemicals² and polymeric materials³ derived from renewables. Among the various renewable resources, plant oils and sugar are considered as an attractive alternative, as they provide direct entry to chemical modification. The green drive has resulted in recent commercialization of renewable polymers such as poly-lactic acid (PLA), polyhydroxyalkanoates and sugar cane based polyethylene on an industrial scale.⁴ Degradability is another material requirement for a clean and sustainable future. PLA⁴ and plant oil based polyacetals⁵ seem to meet these two criteria that are anticipated to be very important for the next generation of sustainable materials.

Among renewable resources, starch and carbohydrates are the most abundant and easily accessible biomass feed stocks (these can be obtained from various renewable resources such as potato, maize, rice, wheat, etc.) and they have found numerous applications. A monomeric unit of carbohydrate (that is glucose or mannose) can be hydrogenated to produce sorbitol (annually 1 million tons of sorbitol is commercially produced)⁶ and mannitol. Subsequent double dehydration of sorbitol and mannitol leads to isohexides (**Figure 2.1**).⁷ Thus, isohexides are very promising non-toxic, biobased precursors that exist in three distinct isomeric forms namely, isomannide (**1a**), isosorbide (**1b**) and isoidide (**1c**). The five membered bicyclic skeleton induces enhanced rigidity, which makes isohexides a promising surrogate for fossil fuel derived diols. The *exo-endo* configuration of the hydroxyl groups further boosts the versatility of isosorbide

leading to several applications in renewable chemicals, solvents, fuel, biopolymers and as a chiral auxiliary and plasticizer.⁸

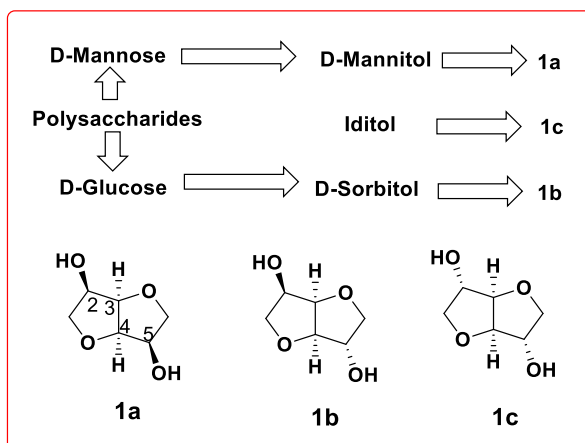


Figure 2.1. Representative synthesis of isohexides (top) and stereo-isomeric forms of isohexides (bottom), isomannide (**1a**), isosorbide (**1b**) and isoidide (**1c**).

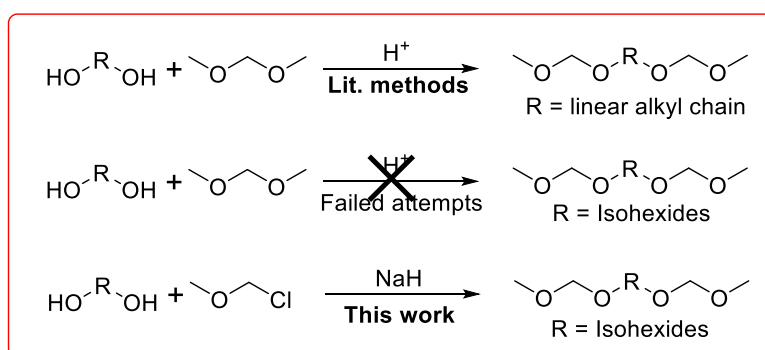
The *endo-endo* compound **1a** is commercially available but the *exo-exo* compound **1c** is quite scarce. Commercially available isohexides have found multiple applications in polycondensates.⁹ However, direct utilization of isohexides usually requires harsh polymerization conditions (high temperatures) and leads to dark, tar like polymers with lower molecular weights.⁹ This is in part due to the limited reactivity of sterically hindered secondary hydroxyl groups (anchored on the C2 and C5 carbons, **Figure 2.1**). Additionally, the hydrogen bonding of these secondary hydroxyl groups is also believed to be responsible for the reduced reactivity. In their pursuit to overcome these limitations Daan and coworkers synthesized various derivatives of isohexides employing a “1-carbon extension” strategy.¹⁰ These fully biobased monomers with enhanced reactivity were tested in various polymerization reactions and polyamides,¹¹ polyesters,¹² co-polyesters with diols¹³ and polyurethanes¹⁴ were prepared. The resultant polymers were found to be less colored and displayed enhanced T_g values compared to their linear petroleum based analogues.¹¹⁻¹⁴ Although convincing progress has been made in synthesizing these polymers, degradation of these materials remains elusive and unattempted. This would be a perfect complement to the renewable-origin of these polymers. We speculate that isohexide based polyacetals would meet both criteria (renewable and degradable) for the next generation of sustainable materials.

This chapter aims to synthesize isohexide-based diacetals. We further demonstrate that, the thus prepared chiral molecules serve as monomers, leading to fully bio-based polycondensates. The renewable polycondensates have been fully investigated and their facile degradation is discussed.

2.3. Results and Discussion:

2.3.1. Synthesis of Acetals:

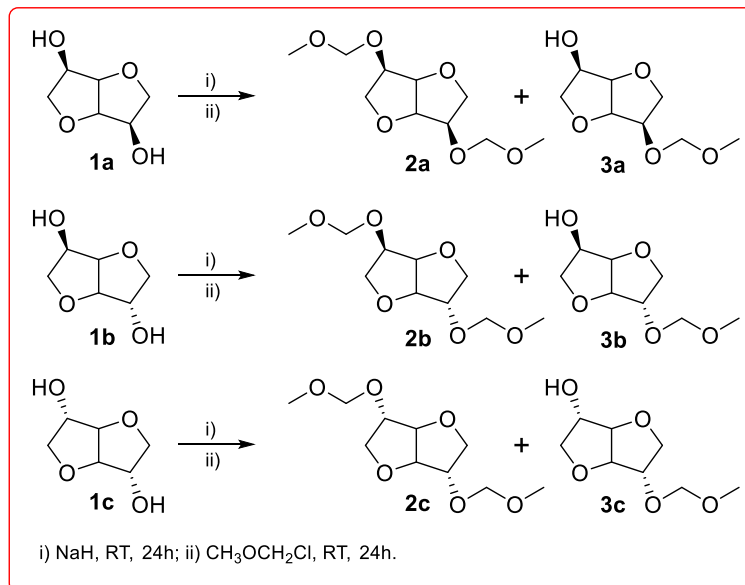
Our initial attempts to prepare diacetals using methoxymethane in the presence of an acid catalyst such as methane sulfonic acid or trifluoromethane-sulfonic acid failed to give the desired product (**Scheme 2.1**-middle). Even use of greater than the stoichiometric amount of methane sulfonic acid gave a very poor yield (23%) of the anticipated diacetal. Although this strategy works well and has been a standard method for acetylating linear aliphatic diols,⁵ the poor performance with isohexides most likely stems from the lower reactivity of the sterically encumbered secondary hydroxyl groups. In our pursuit to access isohexide based diacetal monomers we developed a single step synthetic protocol as depicted in **Scheme 2.1** (bottom). Treatment of **1a** and **1b** with sodium hydride followed by the addition of chloromethyl methyl ether readily produced crude **2a** and **2b**. Aqueous work-up and purification by column chromatography (pet ether-ethyl acetate 3:1) gave the desired diacetals **2a** and **2b** in excellent isolated yields (67% and 74%) (see experimental section for more details).



Scheme 2.1. Classical methods (top) and our approach (bottom) for acetylating terminal hydroxyl groups to diacetals.

Traces of the monoacetal side products **3a** and **3b**, were also isolated (2-3% yield) (**Scheme 2.2**). The isoidide **1c** was synthesized by a modified literature procedure, in an excellent yield and was utilized for diacetal synthesis.¹⁵ Isohide-diacetal **2c** was prepared following a similar protocol as that for **2a** and **2b**, although excess sodium hydride was required

to obtain good yields (83%).¹⁶ The individual reactions were routinely carried out in THF, which turned out to provide optimum solubility for all of the isohexide-diacetal **2c** was prepared following a similar protocol as that for all of the reaction component.

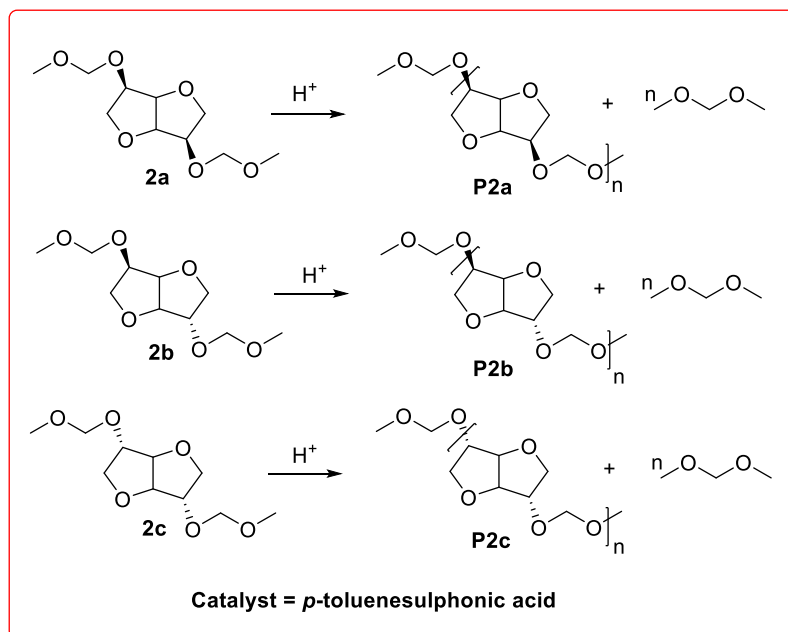


Scheme 2.2. Synthesis of isohexide-diacetals (**2a-c**).

The isolated diacetals **2a-c** are air stable, colourless, oily liquids. The existence of isolated monomers was unambiguously ascertained from spectroscopic and analytical data. Typically, ¹H NMR spectra of **2a-c** displayed characteristic signal around 4.6-4.7 ppm [arising from the methylene protons (OCH₂O)]; 4.1 ppm [from the acetal linked C-H [CH(OCH₂OCH₃)] and a singlet at about 3.3 ppm from the methoxy protons (experimental section **Figure 2.4, 2.9** and **2.18**). ¹³C NMR spectra of diacetals **2a-c** displayed a very characteristic peak at 96 ppm which could be assigned to a methylene (OCH₂O) carbon, and resonance at 55 ppm was ascribed to a terminal methoxy (OCH₃) carbon (**Figure 2.5, 2.10, 2.19**). The chemical shift of the acetal fragment is similar to those reported previously.⁵ The existence of **2a-c** was further corroborated by electrospray ionization mass spectroscopy (ESI-MS). The spectra of a methanol solution of **2a-c** displayed a pseudo-molecular ion peak corresponding to a [M+Na]⁺ ion (where M = **2a-c**) at m/z = 257.1 (**Figure 2.8, 2.14, 2.26**). Various 1D-2D NMR experiments were performed to establish the stereo-specificity of the -OCH₂- fragment connected to the C2 and C5 carbons (**Figure 2.1**). The obtained spectroscopic data confirmed that there is no inversion of configuration and that **2a-c** exist in the same configuration as their parent diols **1a-c**.

2.3.2. Acetal Metathesis Polymerization (AMP):

Having established a convincing protocol for the synthesis of isohexide-diacetals, we set out to evaluate monomers **2a-c** in an Acetal Metathesis Polymerization (AMP) reaction. The term AMP was recently coined by Miller *et al.*, due to the similarity between a metal catalyzed Acyclic Diene Metathesis (ADMET) Polymerization and the acid catalyzed diacetal polymerization.^{5, 17} Conceptually, both ADMET and AMP can be treated as a type of condensation polymerization. The major driving force in these polymerization reactions is the loss of small molecules with low boiling points (ADMET-ethylene; AMP-dimethoxymethane) and a high degree of polymerization is usually achieved by continuous removal of the volatile byproduct. Initial polymerizations were carried out on a 500 mg scale to optimize reaction conditions such as temperature, time and catalyst loading. The isohexide-diacetals were polymerized using 2-5 mol% of para-toluenesulfonic acid (*p*-TSA) as a catalyst in a Schlenk tube that was equipped with a high torque air-tight overhead mechanical stirrer. Two polymerization methods (see experimental section, method A and method B) were developed. Typically, the polymerizations started at 60 °C and the temperature of the reaction vessel was slowly raised to 80/90 °C over a defined period of time. In the first step the monomer was stirred at 60 °C with a regular argon-vacuum purge cycle (3 minutes) to remove dimethoxymethane (by-product). At the same time monomer evaporation must be taken into account and should be minimized. The polymerization continued for a desired amount of time under reduced pressure (0.01 mbar) (**Scheme 2.3**). The resultant highly viscous material was cooled and dissolved in chloroform, and was precipitated from methanol to give the desired polymers **P2a-c** as white solids in excellent yields (58-71%). The polymers were rigorously characterized and **Table 2.1** summarizes the most significant data.



Scheme 2.3. Acetal metathesis polymerization of the isohexide-diacetals to **P2a-c**.

The first line of evidence supporting the formation of **P2a-c** came from proton and 13-carbon NMR spectroscopy. ^1H NMR spectra of the polymers revealed a decrease in the intensity of a peak at 3.37-3.36 ppm (corresponding to the OCH_3 group) and resonance at 4.83-4.82 ppm (OCH_2O), which supports the formation of the anticipated polyacetals (**Figure 2.23, 2.31** and **2.40**). Likewise, the methoxy (OCH_3) and methylene (OCH_2) carbons almost disappeared from the ^{13}C NMR spectra of the polymers (**Figure 2.24, 2.32** and **2.41**). In the proton NMR spectra, the ratio between the 8 backbone protons of **2a** (i.e. 2:2:2:2) is retained in **P2a-1** (101:105:102:103; **Figure 2.23**). Similarly, **2b** displayed a backbone proton ratio of 1:3:2:1:1 and **P2b-2** followed (176:527: 347:173:185; **Figure 2.31**). Although the splitting patterns could not be clearly distinguished in **P2a-c**, the above observations indicate that the stereochemistry of the monomer is most likely retained during the polymerization. The molecular structure of the novel polyacetals was unambiguously established using various spectroscopic and analytical tools. Furthermore, end-group analysis by ^1H NMR spectroscopy revealed a number average molecular weight of 3200 to 27600 g mol^{-1} (**Figure 2.23, 2.31, 2.40**).¹⁸ The NMR molecular weights were corroborated by Gel Permeation Chromatography (GPC) in chloroform at room temperature (**Figure 2.25, 2.35** and **2.42**).

Table 2.1. The molecular weight, thermal properties and isolated yields of the isohexide-polyacetals^a

Run	$M_n \times 10^{3b}$	$M_w \times 10^{3c}$	PDI ^c	T _g (°C)	T _m (°C)	T _c (°C)	Yield in g (theoretical)	Yield in g (isolated)
P2a-1	7.9	2.1	1.4	53.9	126.2	92.4	1.45	1.0
P2a-2 ^d	8.4	3.8	1.6	65.5	130.4	86.9	0.67	0.46
P2a-3 ^d	4.4	3.6	1.5	-	-	-	1.35	1.16
P2b-1 ^d	4.9	5.0	1.6	-	-	-	1.36	0.53
P2b-2	27.6	8.9	2.0	52.1	117.3	49.5	2.70	1.92
P2b-3 ^d	16.9	7.5	2.0	58.5	103.2	56.2	0.95	0.20
P2c-1	5.0	2.9	1.7	37.9	147.9	108.1	0.62	0.36
P2c-2 ^d	3.2	2.8	1.5	-	-	-	1.01	0.64
P2c-3 ^d	16.0	3.7	1.7	51.8	156.4	121.5	0.89	0.56

^aFor detailed polymerization conditions see the experimental section. ^b M_n determined by NMR in g mol⁻¹. ^c M_n , M_w and the polydispersity index (PDI) were obtained from GPC in chloroform solvent at room temperature with respect to polystyrene standards. ^dSee experimental section **Table 2.2** for detailed polymerization conditions.

The GPC molecular weights displayed the same trend as the NMR molecular weights, although the observed molecular weights by GPC were lower.¹⁸ The reactivity of the monomers is directly reflected in the degree of polymerization. The *endo-endo* configured compound **2a** resulted in low molecular weight polymers. Polymerization of **2a** under variable polymerization conditions produced polyacetals **P2a** (**Table 2.1**, run **P2a-1** to **P2a-3**) with molecular weights (M_w) in the range 2000-3800 g mol⁻¹. Increased molecular weights (3800 by GPC and 8400 by NMR) were obtained when **2a** was polymerized at an elevated temperature (**Table 2.1**, **P2a-2** and experimental section (**Table 2.2**)). The *endo-exo* structured compound **2b** after 3 hours at 60-90 °C gave the comparatively higher molecular weight polyacetal **P2b-1** (**Table 2.1**). In our pursuit to further enhance the molecular weight, polymerization of **2b** was carried out under identical conditions for 7 hours. The highest molecular weight (8900 by GPC and 27 600 by NMR) poly(isosorbide-acetal) was obtained under these conditions (**Table 2.1**, run **P2b-2**). However, extended polymerization of **2b** for 12 hours led to a decrease in the molecular weights (7500 by GPC and 16900 by NMR, run **P2b-3**); suggesting the likely degradation/decomposition of the polyacetals. The *exo-exo* configured compound **2c** was polymerized to the corresponding polyacetal **P2c-1** at 60-90 °C in the presence of *p*-TSA (**Table 2.1**). Further temperature and time

screening led to better molecular weights (3700 by GPC and 16000 by NMR), for example, at elevated polymerization temperatures (**Table 2.1**, run **P2c-3**). Thus, the molecular weights of isolated polymers suggest a reactivity trend in the order **P2b** > **P2a** > **P2c**. These trends have been commonly observed in isohexide/modified isohexide polymerization reactions.¹² Thus, formation of color free (white) high molecular weight polyacetal polymers at rather low polymerization temperatures and short reaction times indicate the enhanced reactivity of the monomers **2a-c** compared to the parent isohexides **1a-c**.

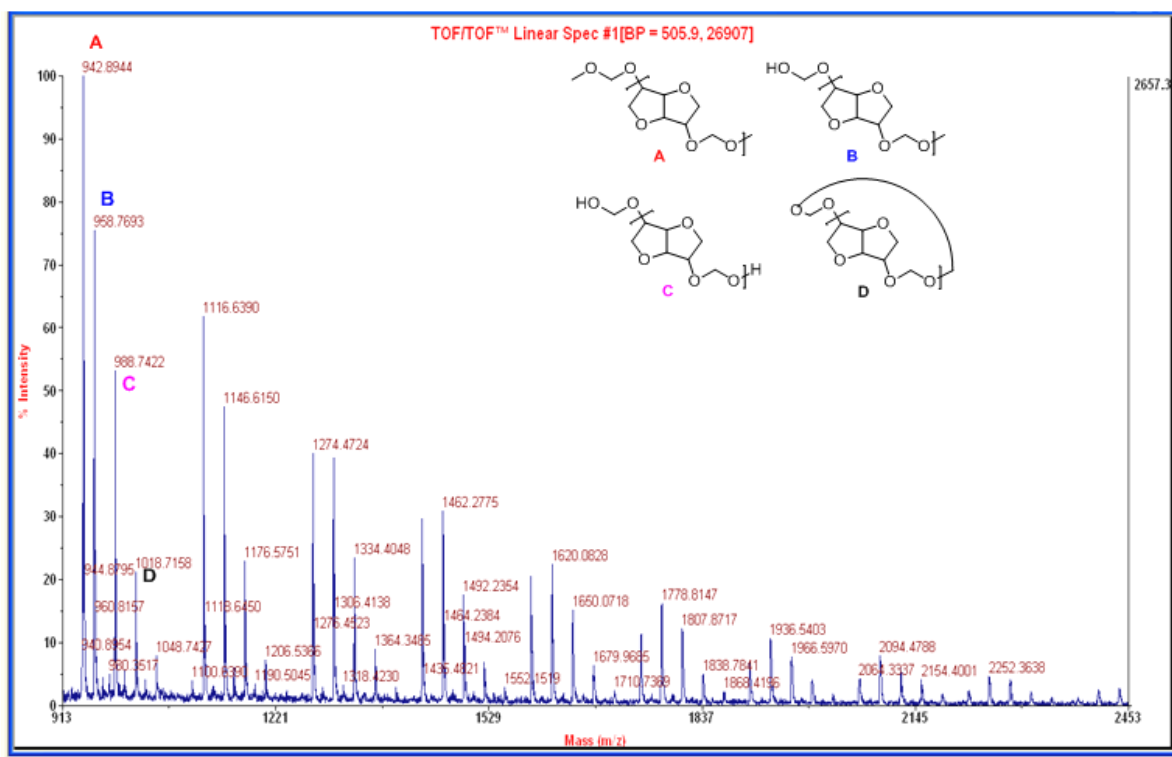


Figure 2.2. MALDI-ToF-MS results for **P2b-1** recorded in chloroform.

The polyacetals **P2a-c** were subjected to MALDI-ToF-MS analysis in order to determine the molar mass of the polymer repeat unit. A representative spectrum of **P2b-2** is displayed in **Figure 2.2**. A typical MALDI-ToF-MS spectrum revealed four sets of MS signals, each with a mass interval of 158 Da, which exactly coincides with the molar mass of the polymer repeat unit. The four MS signals in the MALDI-ToF-MS spectrum can be attributed to the four most probable polymeric structures **A**, **B**, **C** and **D** (**Figure 2.2**). Although MALDI-ToF-MS is a qualitative method, it may be reasonable to assume that structure **A** is the most abundant species followed by **B** and **C**. The cyclic structure **D** was found to be much less abundant (>20%).

The MALDI-ToF-MS observations were corroborated by proton NMR spectroscopy of the polymers. The polyacetals at lower molecular weights displayed at least two types of $-OCH_3$ signals, which most likely originate from the structures **A** and **B** (Figure 2.49; bottom spectrum). The observation of FT-IR bands between $3400-3850\text{ cm}^{-1}$ further supports the existence of hydroxy-terminated polymer chain-ends in structures **B** and **C** (Figure 2.33 for **P2b-2**). The thermal behavior of the polyacetals was investigated by differential scanning calorimetry (DSC) and thermogravimetric analysis (TGA) (see experimental section). The highest molecular weight poly(isomannide-acetal) **P2a-2** and poly(isoidide-acetal) **P2c-3** displayed glass transition temperatures (T_g) of $65.5\text{ }^\circ\text{C}$ and $51.8\text{ }^\circ\text{C}$ respectively. The DSC investigations revealed that **P2a-2** and **P2c-3** melt at relatively high melting temperatures (T_m) ($130\text{ }^\circ\text{C}$ and $156\text{ }^\circ\text{C}$ respectively) compared to the highest molecular weight poly(isosorbide-acetal) **P2b-2** ($T_m = 117\text{ }^\circ\text{C}$). Remarkably, the T_m values of **P2a-c** are almost double than those of the corresponding linear C5-C6- polyacetals.¹⁹ Although the molecular weights of **P2a-c** are lower than the analogous linear C5-C6 polyacetals, the bicyclic backbone in these polymers induces enhanced rigidity and leads to higher melting temperatures. The polyacetals **P2a-2** and **P2c-3** displayed sharp crystallization peaks (at $87\text{ }^\circ\text{C}$ & $121\text{ }^\circ\text{C}$), whereas **P2b-2** exhibits a broad peak (at $49.5\text{ }^\circ\text{C}$). These observations suggest a low degree of crystallinity or a lower rate of crystallization in **P2b-2**. The *endo-exo* orientation of the functionality in **2b** most likely results in stereo-irregular polyacetals (**P2b**); as a consequence the polymers display lower T_g and T_m values. The thermal stability of the polyacetals was determined by TGA between 0 and $600\text{ }^\circ\text{C}$ in a nitrogen atmosphere. Among the three polymers, **P2a-1** starts decomposing at around $100\text{ }^\circ\text{C}$, whereas **P2b-2** and **P2c-1** were found to be stable up to $175\text{ }^\circ\text{C}$ with only 10% weight loss. The maximum decomposition of **P2b-2** and **P2c-1** (about 73% weight loss) was observed between $210-250\text{ }^\circ\text{C}$. The DSC findings were further corroborated by wide angle X-ray diffraction (WAXD) measurements (Figure 2.30, 2.39 and 2.47). The X-ray diffraction profiles of **P2a-1** and **P2c-1** revealed relatively sharp peaks indicating the semi-crystalline nature of the polymers. However, **P2b-2** displayed a rather broad diffraction signal, suggesting decreased crystallinity of the *exo-endo*, stereo-irregular polymer.²⁰

2.3.3. Polyacetal Degradation:

Apart from their renewable origin, degradability will be a decisive parameter for the next generation of sustainable materials. For example, acid-labile polymers with acetal moieties in the

main chain are being increasingly used in controlled drug release and other medical applications.^{5, 21} Having known that polyacetals are sensitive to acid catalyzed hydrolytic cleavage we set out to evaluate the rate of degradation of **P2a-c** in mild acidic media. The highest molecular weight polyacetal (**P2b-2**) was chosen as the most relevant representative for degradation investigations. **P2b-2** was stable towards practical washing (D₂O) and rinsing conditions, as the proton NMR spectrum of the washing displayed only a solvent signal and no peaks corresponding to polyacetal could be detected (**Figure 2.51**). However, a proton NMR spectrum of a **P2b-2** in D₂O after 24 hours displayed **P2b-2** signals; although the intensity of the signals was very poor and the solid polymer could be seen in the NMR tube (**Figure 2.52**, bottom). The degradation was accelerated by adding 0.1 ml of DCI (35% DCI in D₂O) to the above NMR tube; however, the solid polymer was still visible. To enhance the degradation further, an additional 0.1 ml of DCI was added to the above NMR tube and a spectrum was recorded after 12 hours. The proton NMR spectrum of the clear solution revealed sharp signals corresponding to the bicyclic skeleton and decreased intensity of the acetal (-OCH₂O-) fragment, indicating partial degradation of the polymer. The degradation was investigated also in organic media (CDCl₃) by acidifying the **P2b-2** solution with dilute hydrochloric acid (2M HCl in Et₂O) (see experimental section for more details). A time resolved proton NMR spectrum of this solution displayed a new signal at 5.4–5.5 ppm which grows in intensity over time (**Figure 2.54**). As anticipated, the above experiments (in aqueous and organic media) suggest that the polyacetal degrades in slightly acidic media. Time resolved GPC analysis of the acid treated polymer revealed a decrease in the molecular weight of the polymer with time (**Figure 2.3**), further supporting the NMR findings.

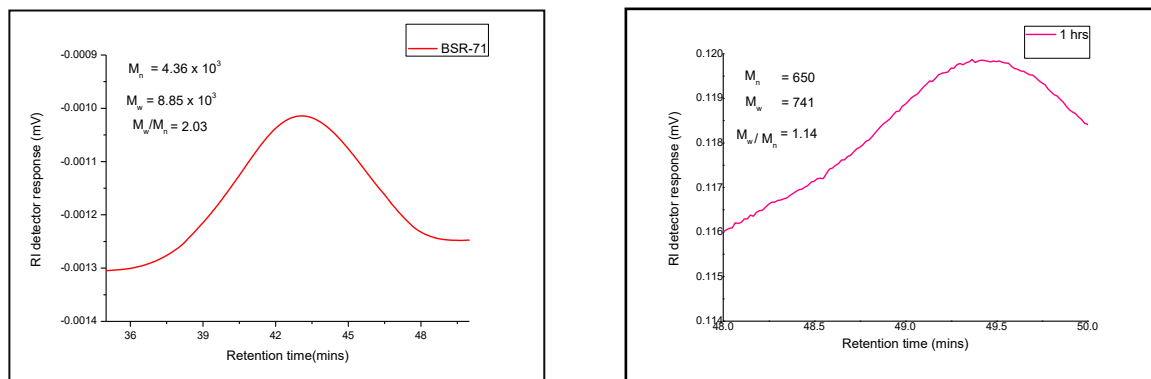


Figure 2.3. Time resolved GPC curve of **P2b-1** (left) and GPC curve after acidic degradation (right), in chloroform, against a PS standard.

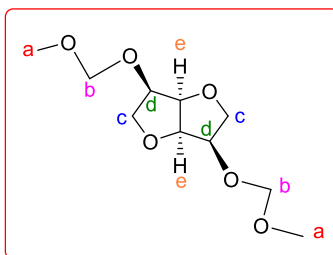
2.4. Experimental Section:

2.4.1. Materials and Methods:

All manipulations involving moisture sensitive compounds were carried out in an inert gas atmosphere using standard Schlenk or glove box techniques. Tetrahydrofuran was distilled from sodium/benzophenone under inert conditions. All other solvents were used as received without further purification. Isomannide, sodium hydride, sodium methoxide, deuterated chloroform, deuterium oxide, deuterium chloride (DCI 35 wt% in D₂O) were purchased from Sigma Aldrich and used without further purification. Chloromethylmethyl ether, methane sulfonic acid, *p*-toluene sulfonic acid monohydrate, trifluoromethane sulfonic acid, dimethoxymethane, diethyl azodicarboxylate, triphenylphosphine and benzoic acid were purchased from Spectrochem Pvt Ltd and used without further purification. NMR spectra were recorded using Bruker Avance 200, 400, 500 instruments. Chemical shifts are referenced to the external reference TMS (¹H and ¹³C). Coupling constants are given as absolute values. FT-IR spectra were recorded using a Bruker α -T spectrophotometer in the range 4000-400 cm⁻¹. Mass spectra were recorded using a Thermo scientific Q-Exactive mass spectrometer, with a Hypersil gold C18 column (150 x 4.6 mm, 8 μ m particle size, 90% methanol-10% water-0.1% formic acid). Differential scanning calorimetry (DSC) was carried out using a DSC Q-10 from TA instruments with a heating and cooling rate of 10 K min⁻¹. Thermogravimetric analysis (TGA) was carried out using a PerkinElmer STA 6000 simultaneous thermal analyzer. Elemental analysis results were recorded using a Flash EA 1112 series instrument. MALDI-TOF was performed using a AB SCIEX TOF/TOF™ 5800 system in a dithranol matrix. GPC measurements were carried out using a Thermo Quest (TQ) GPC at 25 °C using chloroform (Merck, Lichrosolv) as the mobile phase. The analysis was carried out at a flow rate of 1 ml min⁻¹ using a set of five μ -styragel HT columns (HT-2 to HT-6) and a refractive index (RI) detector. Wide angle X-ray data was collected using a Rigaku Micromax-007 HF with a high intensity micro focus rotating anode.

2.4.2. Synthesis of Acetals:

2.4.2.1. Synthesis of Isomannide-Diacetal (2a):



0.98 g (41.04 mmol) of sodium hydride was suspended in 20 ml dry tetrahydrofuran. A THF solution of isomannide (2 g, 13.68 mmol in 30 ml THF) was slowly added to the sodium hydride suspension over a period of 2 hours and the mixture was stirred for 24 hours at room temperature. To this mixture was added chloromethyl methyl ether (3.12 ml, 41.04 mmol) over 4-5 hours and the resultant reaction mixture was stirred for 24 hours. Excess sodium hydride was quenched and the reaction mixture was washed with saturated sodium chloride solution. The aqueous phase was extracted with ethyl acetate (3 × 20 ml). The combined organic phase was dried over MgSO₄, filtered and the filtrate was evaporated in a vacuum to obtain a pale yellow oily liquid. Purification by column chromatography (pet ether-ethyl acetate 75:25) yielded 2.129 g (9.1 mmol) of the desired diacetal (67%).

¹H NMR (200 MHz, CDCl₃, 298 K) δ = 4.71-4.61 (dd, J_{H-H} = 6.68 Hz, 4H_b), 4.50-4.45 (m, 2H_e), 4.20-4.10 (m, 2H_d), 4.06-3.98 (m, 2H_c), 3.69-3.60 (m, 2H_c), 3.33 (s, 6 H_a); **¹³C NMR** (100 MHz, CDCl₃, 298 K) δ = 96.64 (s, C_b), 80.80 (s, C_e), 78.25 (s, C_d), 70.91 (s, C_c), 55.72 (s, C_a). **ESI-MS** (+ve mode) Cal. m/z = 257.10 [M+Na]⁺; Obs. m/z = 257.09 [M+Na]⁺; **Elemental analysis** (%) calculated for C₁₀H₁₈O₆: C-51.23%, H-7.69%; Found : C- 51.01%, H- 7.92%, **IR** (C₁₀H₁₈O₆) cm⁻¹ =1128, 1080 (C-H/C-O stretching).

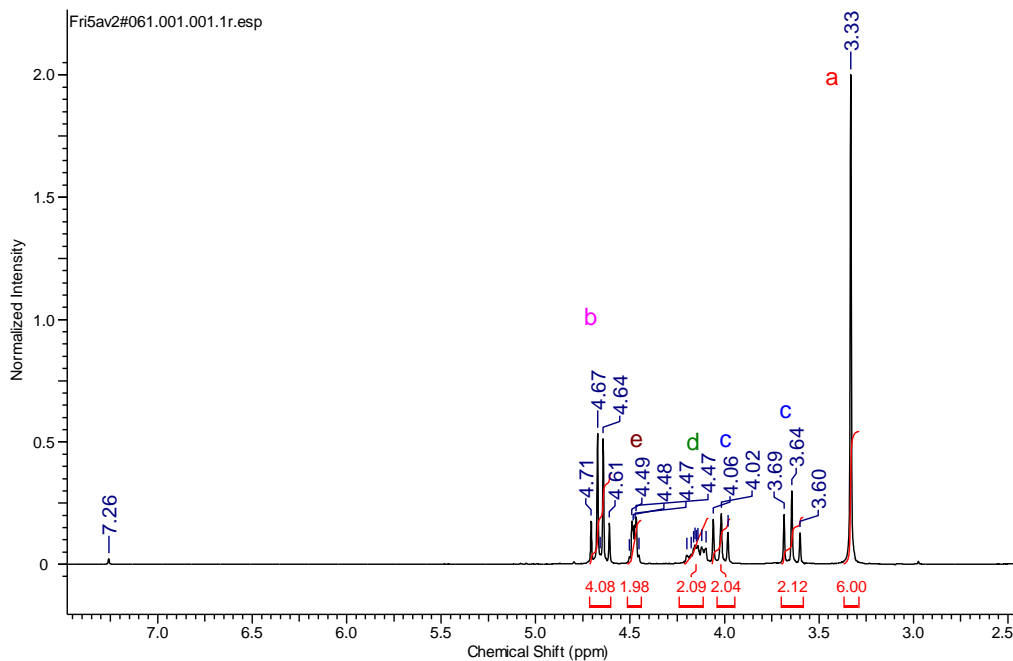


Figure 2.4. ^1H NMR spectrum of compound **2a** in CDCl_3 (200 MHz at 298 K).

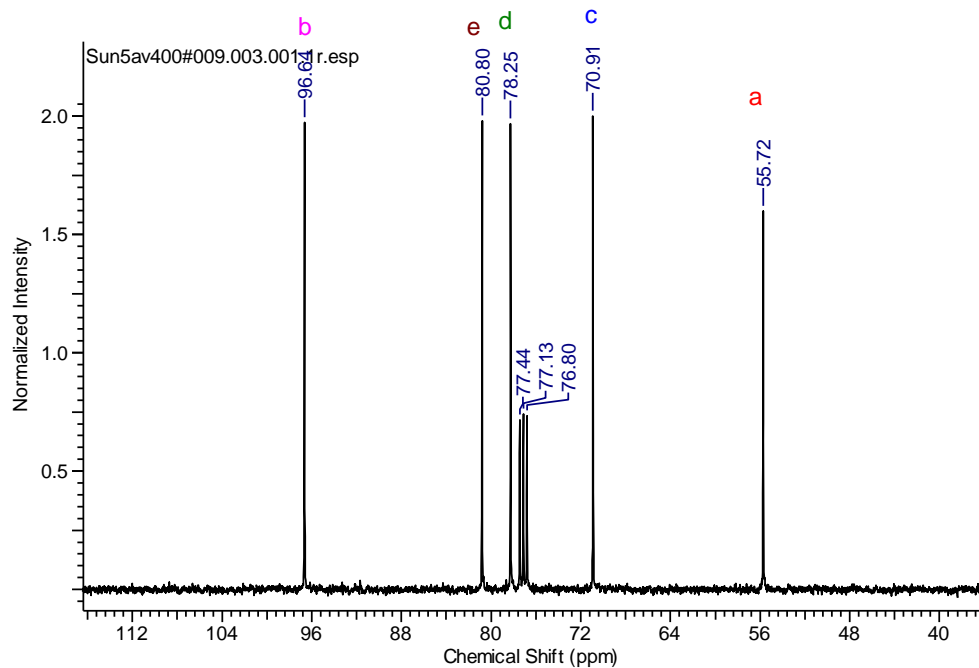


Figure 2.5. ^{13}C NMR spectrum of compound **2a** in CDCl_3 (100 MHz at 298 K).

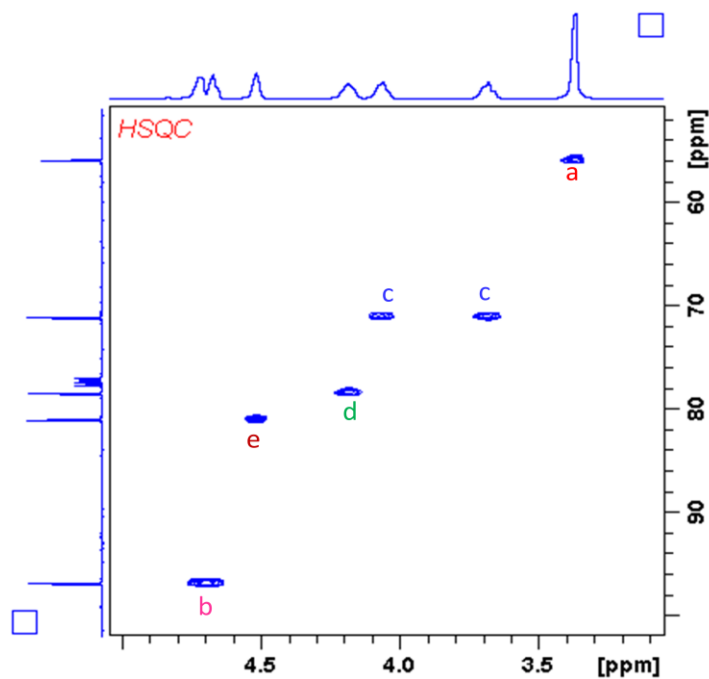
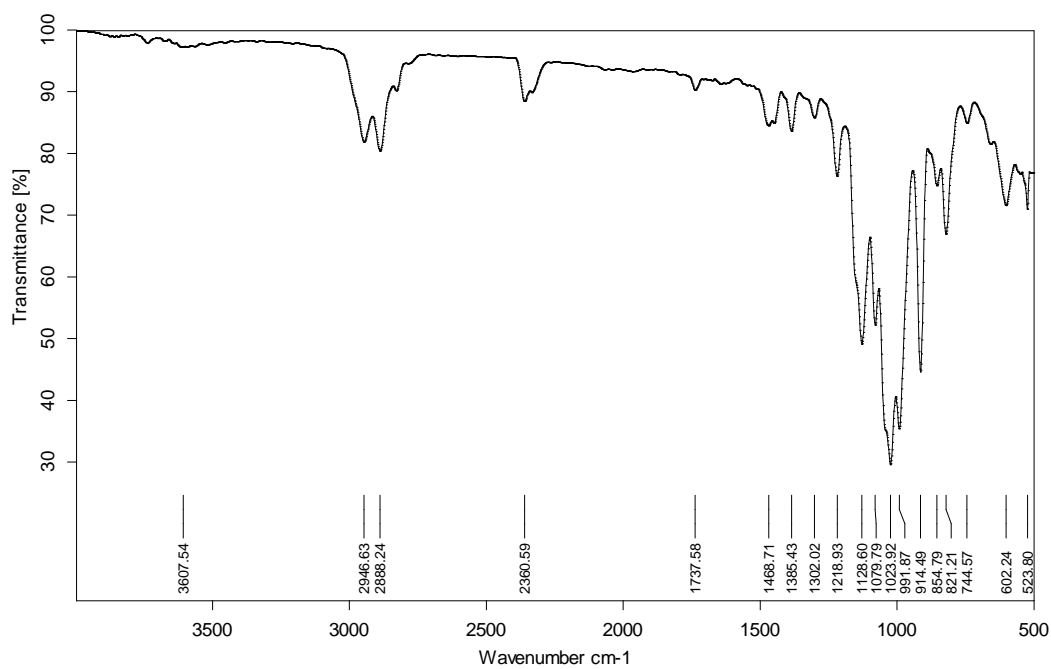


Figure 2.6. HSQC (C-H correlation) NMR spectrum of compound **2a** in CDCl_3 (400 MHz at 298 K).



D:\De Samir Chikal\Bhausaha\15 Jan-14\MEAS\Isomannide-Di.0	Isomannide-Di	Instrument type and / or accessory	15/01/2014
--	---------------	------------------------------------	------------

Figure 2.7. IR spectrum of compound **2a**.

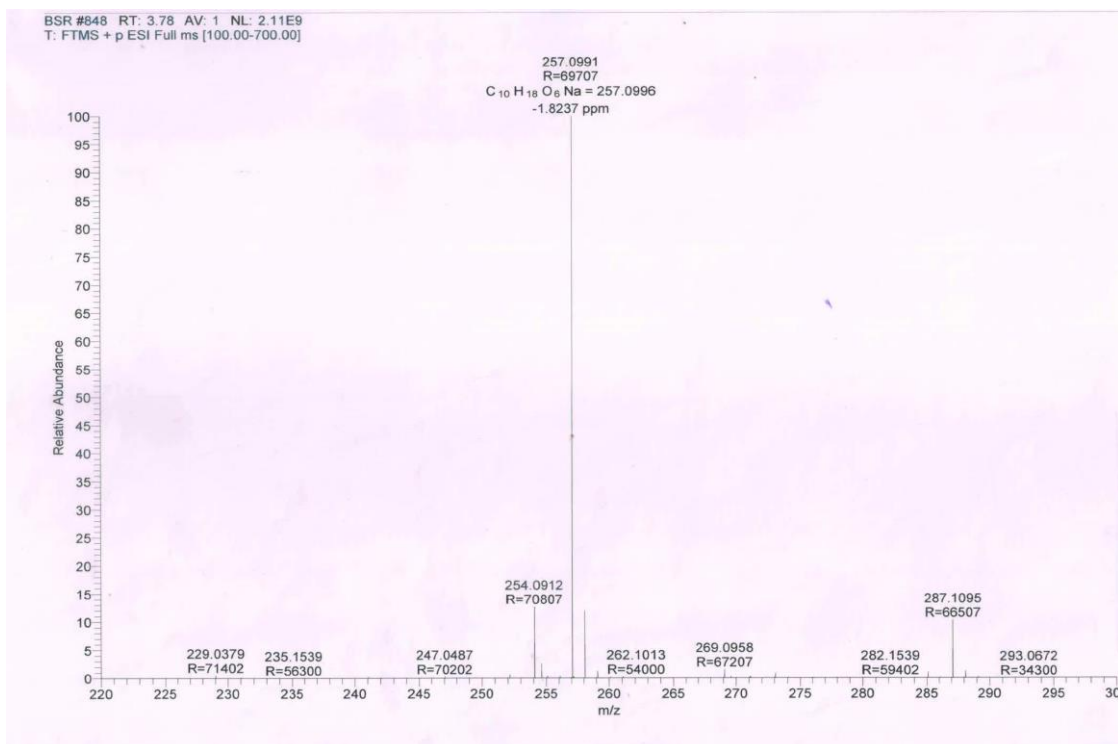
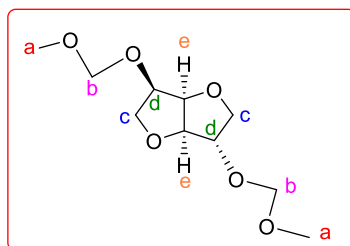


Figure 2.8. ESI-MS (+) spectrum of compound **2a** with a molecular ion peak $[M+Na]^+ = 257.1$ (100%) and 258.1 (10%).

2.4.2.2. Synthesis of Isosorbide-Diacetal (**2b**):



2.462 g (102.63 mmol) of sodium hydride was suspended in 50 ml dry tetrahydrofuran. A THF solution of isosorbide (5 g, 34.21 mmol in 50 ml THF) was slowly added to the sodium hydride suspension over a period of 2 hours and the mixture was stirred for 24 hours at room temperature. To this mixture was added chloromethyl methyl ether (7.80 ml, 102.63 mmol) over 4–5 hours and the resultant reaction mixture was stirred for 24 hours. Excess sodium hydride was quenched, the reaction mixture was washed with saturated sodium chloride solution and the aqueous phase was extracted with ethyl acetate (3 × 30 ml). The combined organic phase was dried over $MgSO_4$, filtered and the filtrate was evaporated in vacuum to obtain a pale yellow oily liquid. Purification by column chromatography (pet ether-ethyl acetate 75:25) yielded 5.9 g (25.22 mmol) of the desired diacetal (74%).

^1H NMR (500 MHz, CDCl_3 , 298 K) δ = 4.74 - 4.63 (dd, $J_{\text{H-H}} = 6.94$ Hz, 4H_b), 4.61-4.60 (m, H_e), 4.50 (m, 1H_d), 4.18-4.16 (m, 1H_e), 4.16-4.14 (m, 1H_d), 3.96-3.92 (m, 3H_c), 3.57-3.53 (m, 1H_c), 3.37 (s, 3H_a), 3.34 (s, 3H_a); ^{13}C NMR (125 MHz, CDCl_3 , 298 K) δ = 96.6 (s, C_b), 95.6 (s, C_b), 86.2 (s, C_e), 81.6 (s, C_d), 80.8 (s, C_e), 77.9 (s, C_d), 73.7 (s, C_c), 69.6 (s, C_c), 55.7 (s, C_a), 55.5 (s, C_a); ESI-MS (+ve mode) Cal. $m/z = 257.10$ [$\text{M}+\text{Na}$]⁺; Obs. $m/z = 257.09$ [$\text{M}+\text{Na}$]⁺; Elemental analysis (%) calculated for $\text{C}_{10}\text{H}_{18}\text{O}_6$: C- 51.23 %, H-7.69%; Found: C- 50.95 %, H- 7.84 %, IR ($\text{C}_{10}\text{H}_{18}\text{O}_6$) cm^{-1} : 1146, 1104 (C-H/C-O stretching).

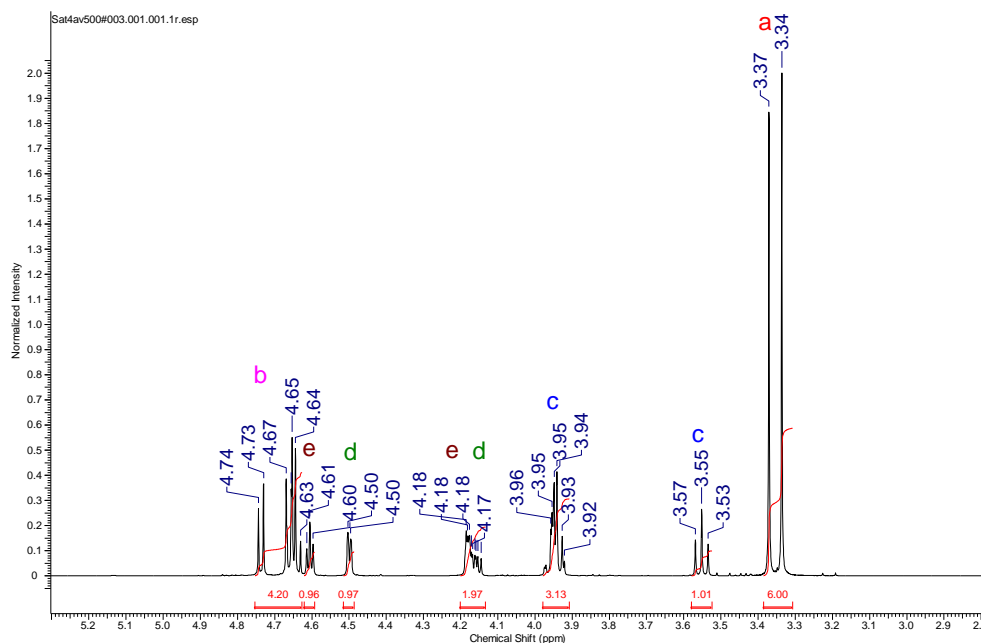


Figure 2.9. ^1H NMR spectrum of **2b** in CDCl_3 (500 MHz at 298 K).

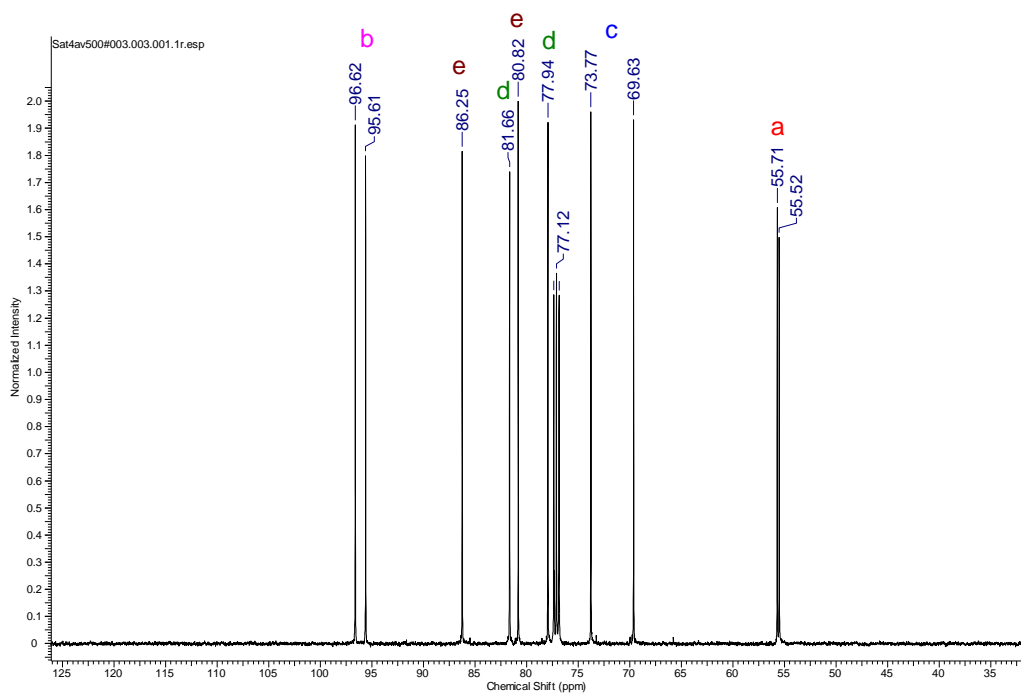


Figure 2.10. ^{13}C NMR spectrum of **2b** in CDCl_3 (125 MHz at 298 K).

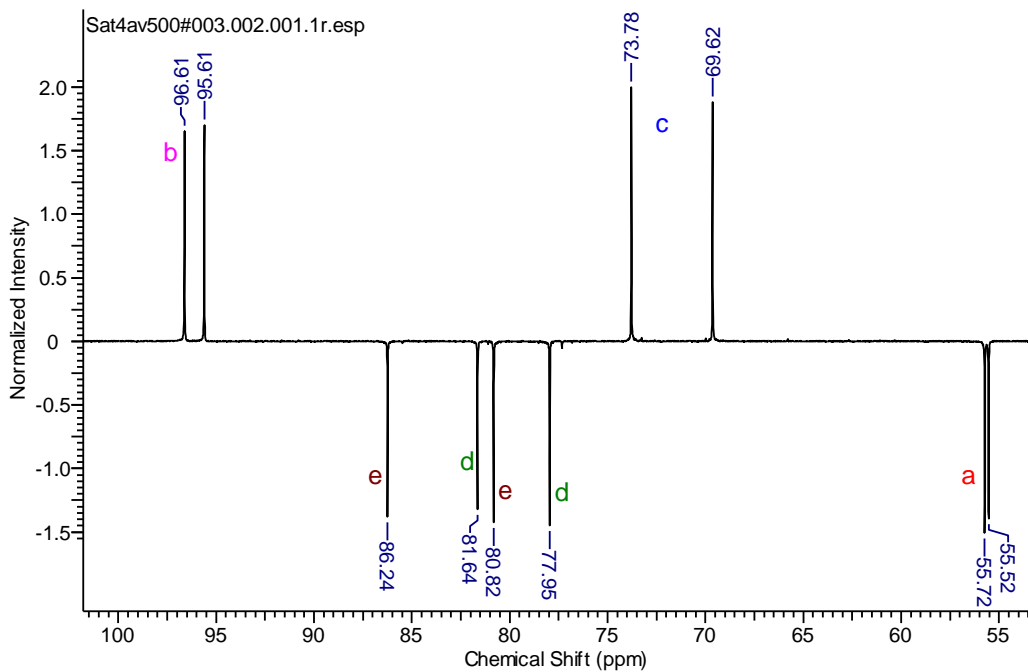


Figure 2.11. $^{135}\text{-DEPT}$ NMR of compound **2b** in CDCl_3 (125 MHz at 298 K).

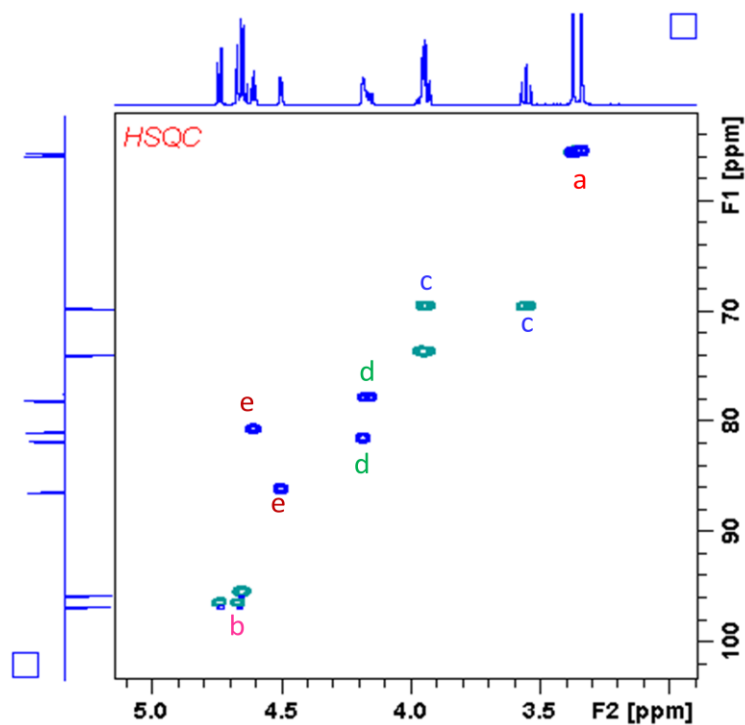
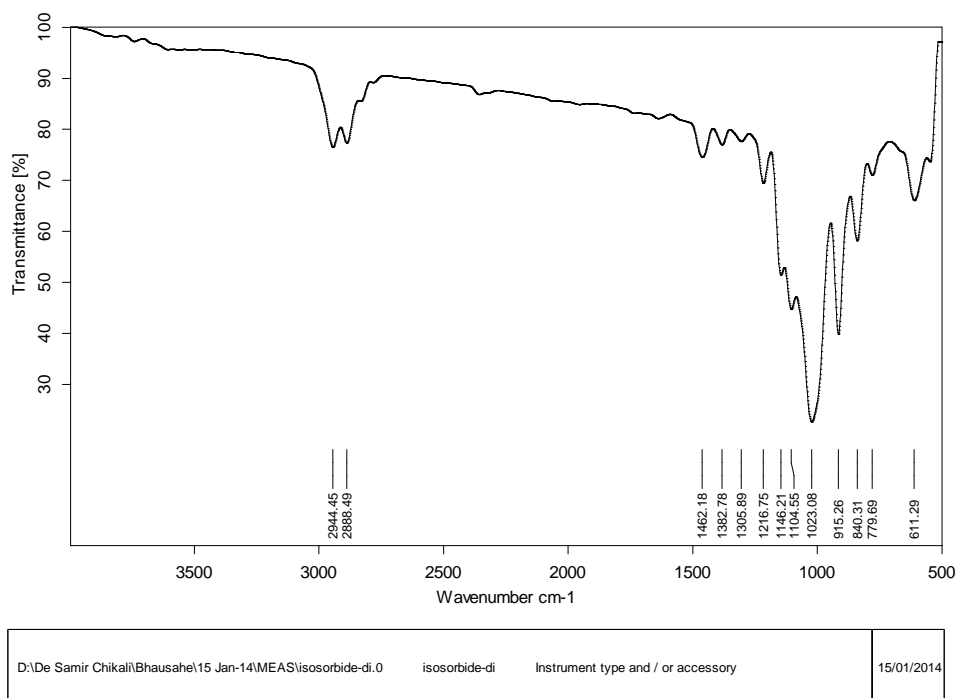


Figure 2.12. HSQC (C-H correlation) NMR spectrum of compound **2b** in CDCl_3 (500 MHz at 298 K).



Page 1/1

Figure 2.13. IR spectrum of compound **2b**.

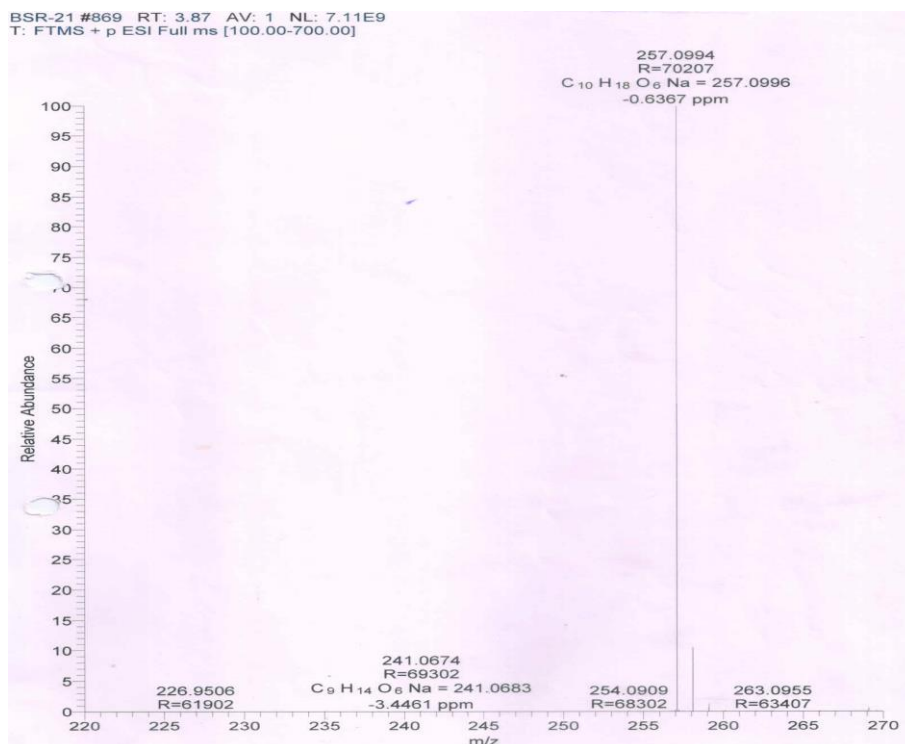


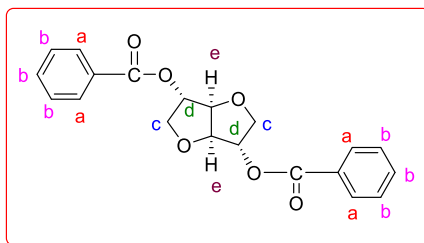
Figure 2.14. ESI-MS (+) spectrum of **2b** with a molecular ion peak $[M+Na]^+ = 257.1$ (100%) and 258.1 (10%).

2.4.2.3. Synthesis of Isoidide (**1c**):

a) Synthesis of (3*S*, 3*aR*, 6*S*, 6*aR*)-Hexahydrofuro[3,2-*b*]-furan-3,6-diyl dibenzoate:

The title compound was synthesized following an earlier report with slight modifications.¹⁵ Isomannide (4 g, 27.37 mmol) and triphenylphosphine (14.35 g, 54.74 mmol) were dissolved in tetrahydrofuran (80 ml). To this solution was added benzoic acid (6.68 g, 54.74 mmol) and diethyl azodicarboxylate (8.58 ml, 54.74 mmol) in tetrahydrofuran (80 ml) over a period of 3 hours at ambient temperature. Water bath was used to maintain the temperature of the reaction mixture during the addition. The reaction mixture was stirred for 15 hours and then additional benzoic acid (0.66 g, 5.474 mmol), triphenylphosphine (1.435 g, 5.474 mmol), diethyl azodicarboxylate (0.85 mL, 5.474 mmol) were added and the mixture was stirred for 3 hours. After completion of the reaction, volatiles were evaporated in vacuo and the residue was subjected to column chromatography (pet ether: ethyl acetate 80:20). This procedure resulted

into a white solid of (3*S*, 3*aR*, 6*S*, 6*aR*)-hexahydrofuro[3,2-*b*]-furan-3,6-diyl dibenzoate (8.5 g, 88 %).



$^1\text{H NMR}$ (200 MHz, CDCl_3 , 298 K): $\delta = 8.06\text{--}8.01$ (m, 4 H_a), 7.63–7.41 (m, 6 H_b), 5.52–5.51 (m, 2 H_e), 4.94–4.88 (m, 2 H_d), 4.13–4.12 (m, 4 H_c). $^{13}\text{C NMR}$ (100 MHz, CDCl_3 , 298 K): 165.3 (s, C_a), 133.2 (s, C_b), 130.0 (s, C_c), 129.5 (s, C_d), 128.3 (s, C_e), 85.4 (s, C_f), 77.8 (s, C_g), 72.5 (s, C_h).

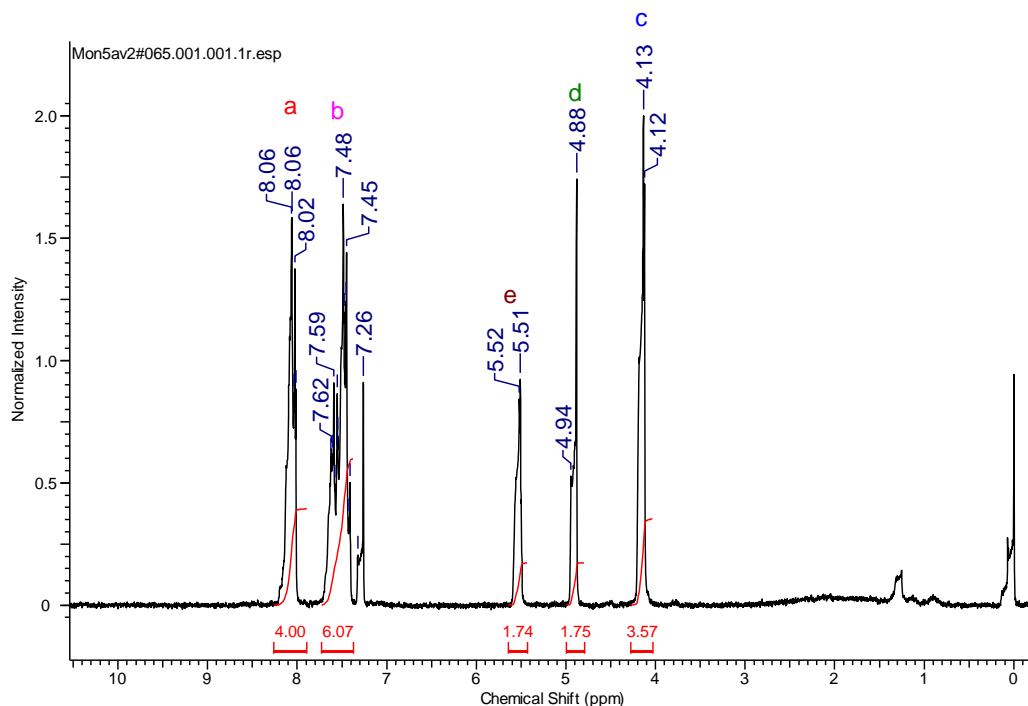
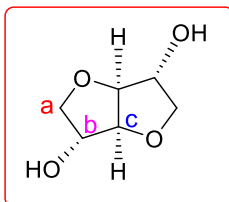


Figure 2.15. $^1\text{H NMR}$ of (3*S*, 3*aR*, 6*S*, 6*aR*)-hexahydrofuro[3,2-*b*]-furan-3,6-diyl dibenzoate in CDCl_3 (200 MHz at 298 K).

b) Synthesis of Isoidide {(3*S*, 3*aR*, 6*S*, 6*aR*)-Hexahydrofuro[3,2-*b*] furon-3-6 diol} from the *exo*-Dibenzoate:

A methanol (200 ml) suspension of 3*S*, 3*aR*, 6*S*, 6*aR*)-hexahydrofuro[3,2-*b*]-furan-3,6-diyl dibenzoate (4 g; 11.30 mmol) was gently heated (50-60 °C for 2 h) and was allowed to cool to room temperature with constant stirring. Sodium methoxide (200 mg; 3.70 mmol) was added to the above solution and the reaction mixture was stirred for 22 hours at room temperature. The clear solution was neutralized with DOWEX (50 x 2) and filtered through a celite bed. The filtrate was diluted with dichloromethane (100 ml) and the organic phase was extracted with distilled water (3 x 50 ml). The combined methanol-water phase was concentrated in vacuo and the residue was subjected to column chromatography (dichloromethane/methanol 9:1) leading to semisolid product (1.3 g; 8.90mmol) 78 %.

¹H NMR (400 MHz, D₂O, 298 K): δ = 4.57 (s, 2H_b), 4.28 (m, 2H_c), 3.84-3.74 (dd, 9.96 Hz, 4H_a). ¹³C NMR (100 MHz, D₂O, 298 K): δ = 86.37 (s, C_b), 74.67 (s, C_c), 73.75 (s, C_a).

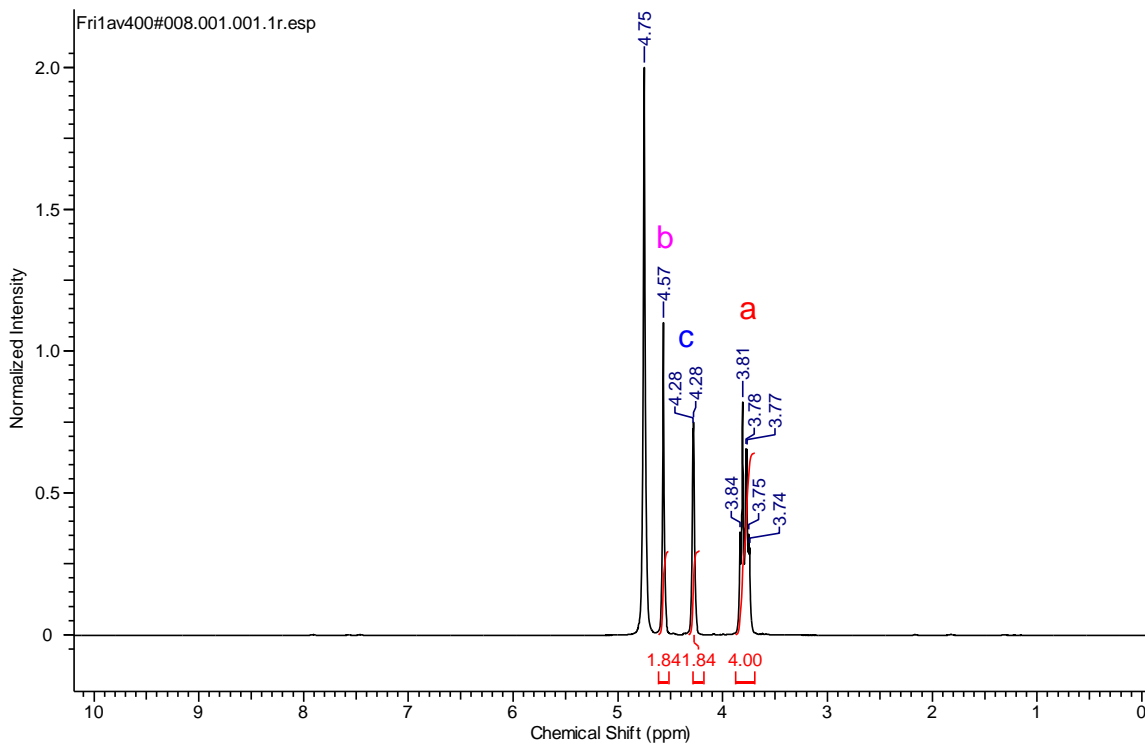


Figure 2.16. ^1H NMR of compound **1c** in D_2O (400 MHz at 298 K).

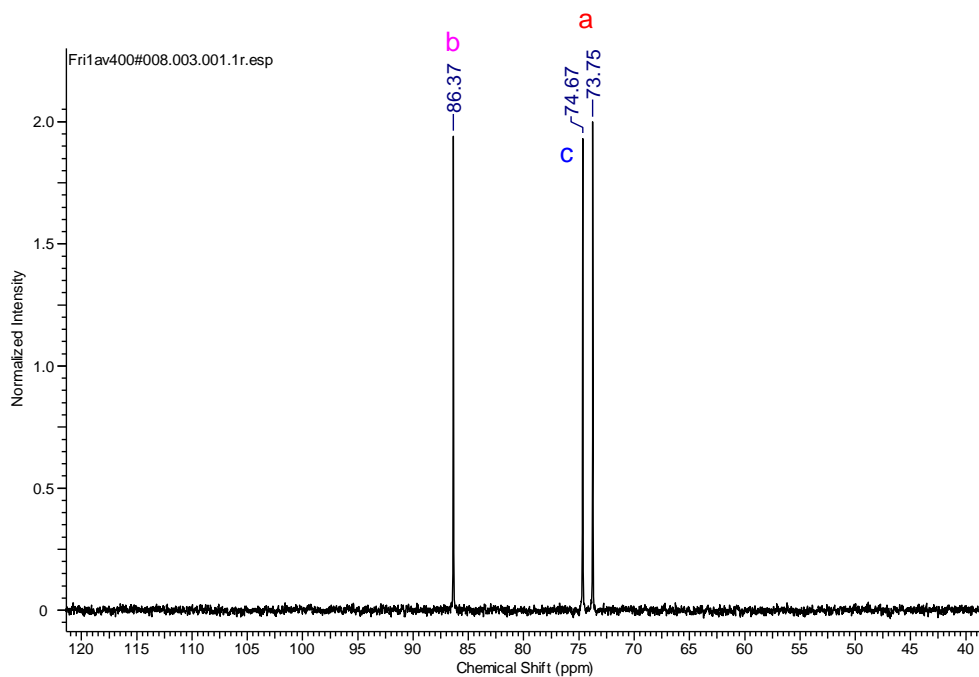
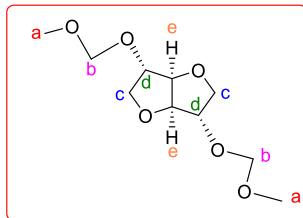


Figure 2.17. ^{13}C NMR of compound **1c** in D_2O (100 MHz at 298 K).

2.4.2.4. Synthesis of Isoidide-Diacetal (2c):

1.92 g (80.16 mmol) of sodium hydride was suspended in 30 ml dry tetrahydrofuran. A THF solution of isoidide (2.34 g, 16.03 mmol in 30 mL THF) was slowly added to the sodium hydride suspension over a period of 2 hours and the mixture was stirred for another 24 hours at room temperature. To this mixture was added chloromethyl methyl ether (6.08 ml, 80.16 mmol) over 4-5 hours and the resultant reaction mixture was stirred for 24 hours. Excess sodium hydride was quenched with the minimum amount of distilled water (approx. 1 ml) and the reaction mixture was filtered, dried over MgSO_4 and the volatiles were evaporated. The resultant residue (greenish oily liquid) was purified by column chromatography (pet ether-ethyl acetate 75:25), which produced 3.10 g (13.23 mmol) of the desired diacetal **2c** (83%).

$^1\text{H NMR}$ (400 MHz, CDCl_3 , 298 K) δ = 4.71-4.65 (dd, 4 H_b), 4.62 (m, 2 H_e), 4.20 (m, 2 H_d), 3.90-3.79 (m, 4 H_c), 3.36 (s, 6 H_a); $^{13}\text{C NMR}$ (100 MHz, CDCl_3 , 298 K) δ = 95.6 (s, C_b), 85.9 (s, C_e), 80.8 (s, C_d), 72.5 (s, C_c), 55.5 (s, C_a). **ESI-MS** (+ve mode) Cal. m/z = 257.10 [$\text{M}+\text{Na}$] $^+$; Obs. m/z = 257.10 [$\text{M}+\text{Na}$] $^+$; **Elemental analysis** (%) calculated for $\text{C}_{10}\text{H}_{18}\text{O}_6$: C- 51.23, H-7.69; Found: C-51.51, H-8.35, **IR** ($\text{C}_{10}\text{H}_{18}\text{O}_6$) cm^{-1} 1150, 1078.

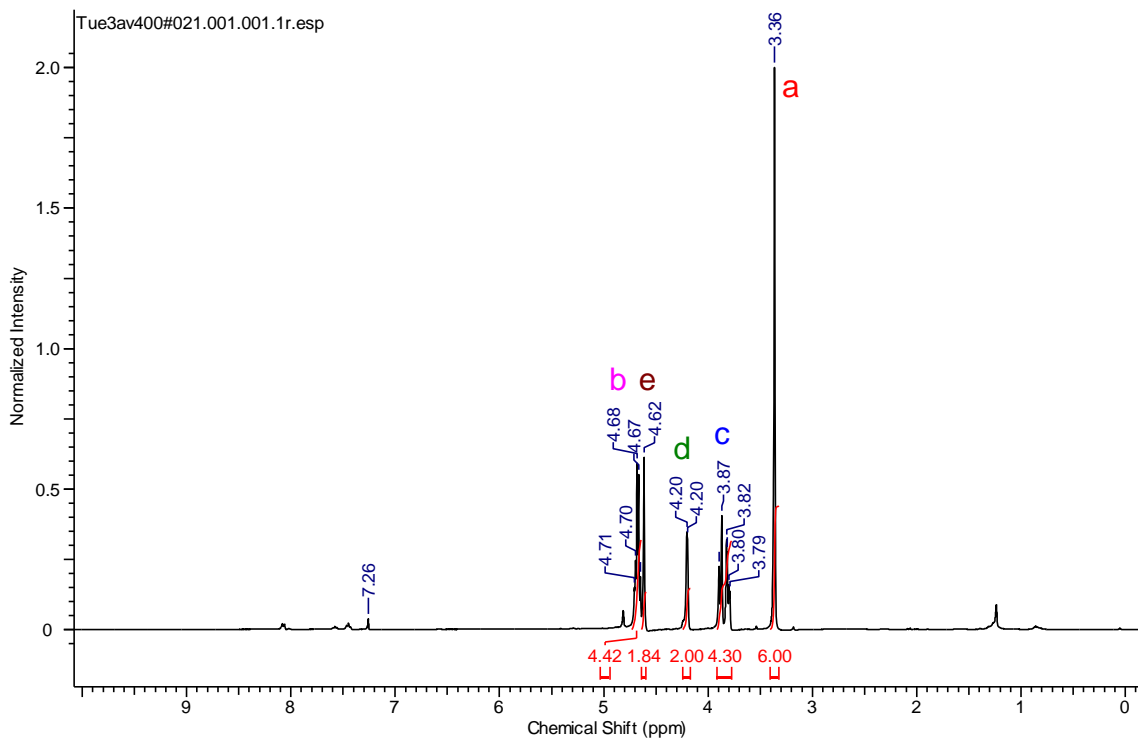


Figure 2.18. ^1H NMR spectrum of compound **2c** in CDCl_3 (400 MHz at 298 K).

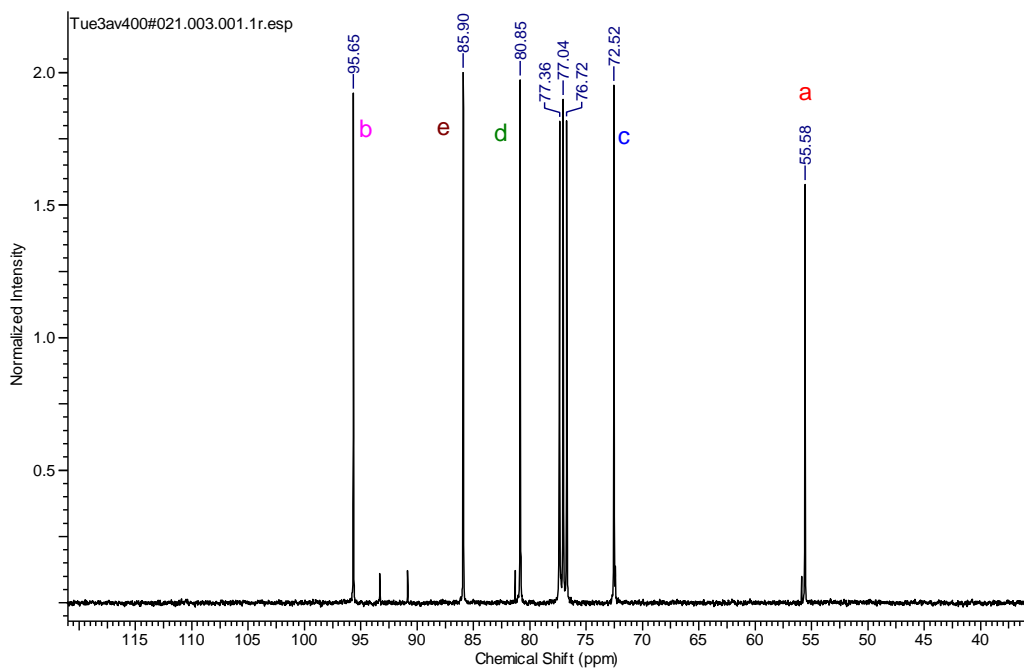


Figure 2.19. ^{13}C NMR spectrum of compound **2c** in CDCl_3 (100 MHz at 298 K).

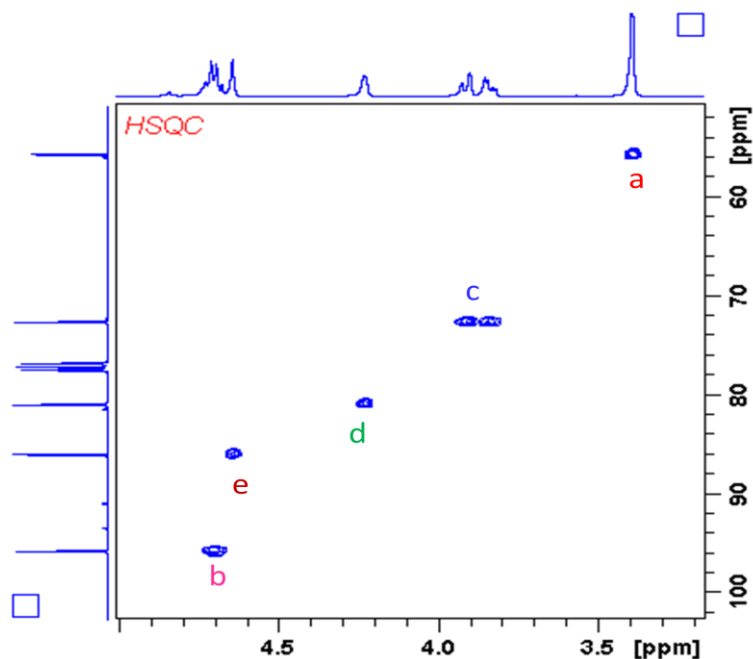
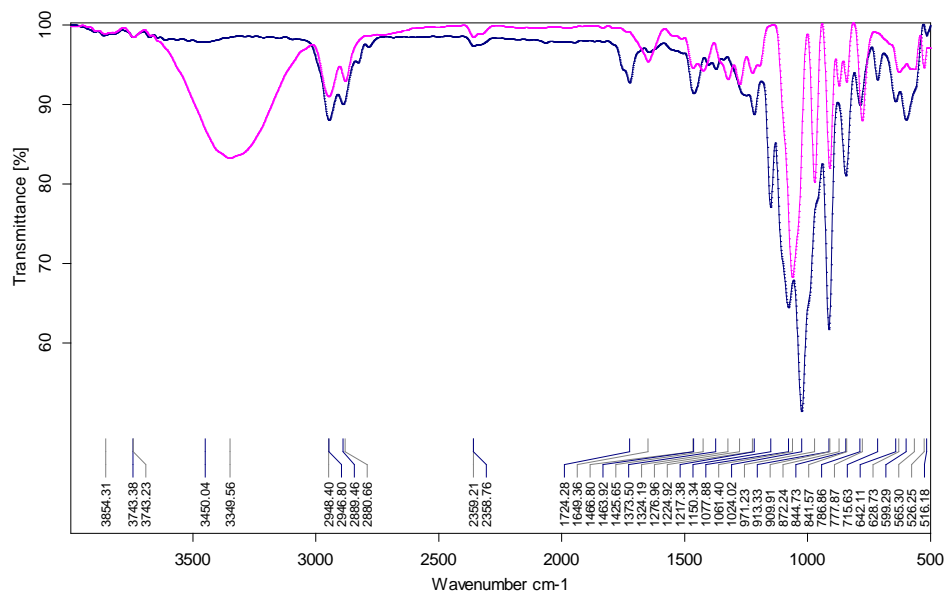


Figure 2.20. HSQC (C-H correlation) NMR spectrum of compound **2c** in CDCl_3 (400 MHz at 298 K).



D:\De Samir Chikali\Bhausahel15 Jan-14\MEAS\isoidide.1	isoidide	Instrument type and / or accessory	15/01/2014
D:\De Samir Chikali\Bhausahel15 Jan-14\MEAS\isoidide-di.0	Isoidide-di	Instrument type and / or accessory	15/01/2014

Page 1/1

Figure 2.21. Overlap of IR spectrum of **2c** (black) with the isoidide **1c** (pink).

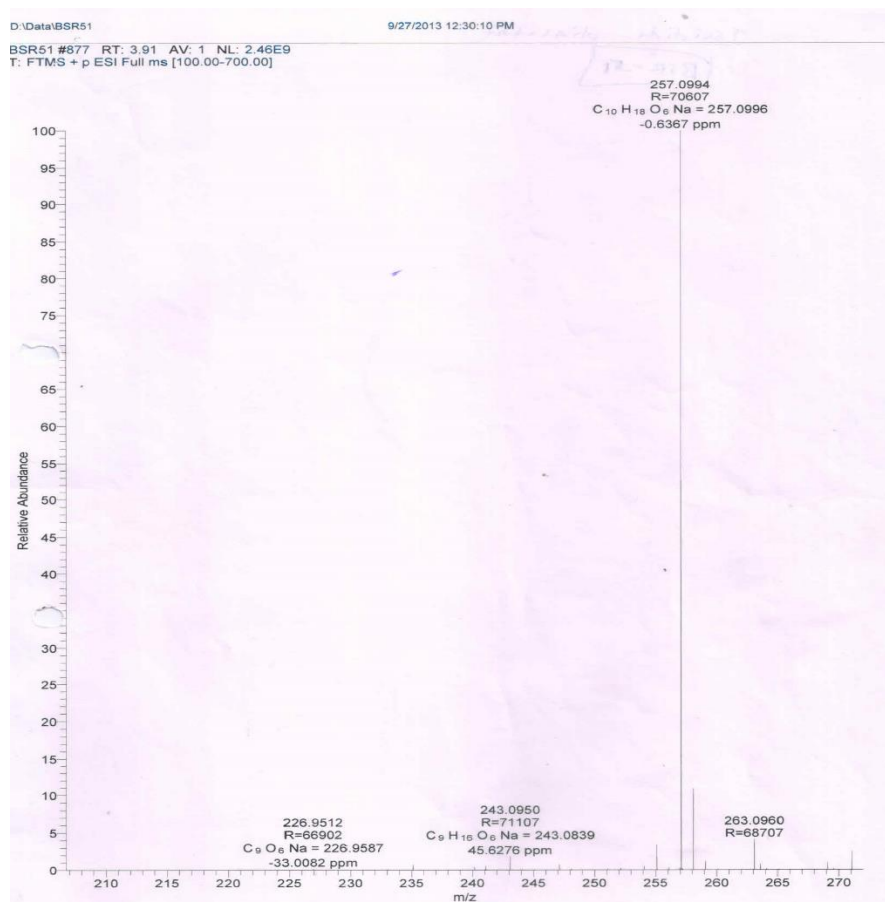


Figure 2.22. ESI-MS (+) spectrum of **2c** with a molecular ion peak $[M+Na]^+ = 257.1$ (100%) and 258.1 (10%).

2.4.3. Polycondensation of Isohexides **2a-c**:

Polycondensation Method A:

The polymerization was run in a 70 ml Schlenk tube equipped with air-tight high torque overhead mechanical stirrer. The **P2a-c** was prepared by heating neat **2a-c** with *P*-TSA at 60 °C which was raised to 90/120/140 °C over a defined period. The byproduct (dimethoxymethane) was continuously removed on vacuum. The polymerization was terminated after desired time, the vessel was cooled down and the solid polymer was dissolved in minimum amount of chloroform. Precipitation from methanol produced desired polymers as white solid materials. See the following **Table 2.2** for polymerization details.

Polycondensation Method B:

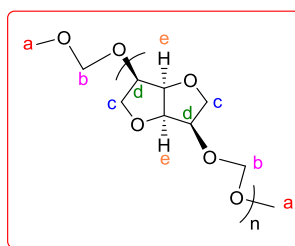
The polymerization was run in a 50 ml round bottom flask which was connected to rotary evaporator under argon. The polymer was prepared by heating neat **2a-c** with *P*-TSA at 60 °C

under argon flush, followed by increased temperature (70-140 °C) over desired time under 0.01 mbar vacuum. The byproduct (dimethoxymethane) was continuously removed on vacuum. The polymerization was terminated after desired time, the vessel was cooled down and the solid polymer was dissolved in minimum amount of chloroform. Precipitation from methanol produced desired polymers as white solid materials. See the following **Table 2.2** for polymerization details.

Table 2.2. Polymerization of isohexide diacetals under different polymerization conditions.

Run	Polymerization Conditions
P2a-2 Method B	Temperature was increased from 60-70 °C over 25 mins. with a vacuum-argon purge cycles. This was followed by increase in temperature from 70-140 °C with 0.01 mbar vacuum for next 35 mins to give solid polymer.
P2a-3 Method A	Temperature was raised from 60-80 °C for 15 min with regular vacuum-argon purge cycles. This was followed by increase in temperature from 80-130 °C with 0.01 mbar vacuum for next 25 min resulting into solid mass.
P2b-1 Method A	Temperature was raised from 60-90 °C for 1 h with regular vacuum-argon purge cycles. This was followed by 0.01 mbar vacuum for next 2 h. Solid polymer was observed after cooling.
P2b-3 Method A	Temperature was raised from 60-90 °C for 1 h with regular vacuum-argon purge cycles. This was followed by 0.01 mbar vacuum for next 11 h. Solid polymer was observed after cooling.
P2c-2 Method A	Temperature was raised from 60-80 °C for 30 min with regular vacuum-argon purge cycles. This was followed by heating from 80-138 °C under 0.01 mbar vacuum for next 30 mins. leading to solid polymer material.
P2c-3 Method A	Polymerization was started at 60 °C under argon atmosphere. In the first step the reaction vessel was heated from 60-80 °C for 30 min with regular vacuum-argon purge cycles. This was followed by heating from 80-117 °C under 0.01 mbar vacuum for next 30 mins. Finally the polymer was obtained as solid material.

2.4.3.1. Polycondensation of Isomannide-Diacetal to P2a-1:



The polymerization was carried out in a 70 ml Schlenk tube equipped with an air-tight high torque overhead mechanical stirrer. **P2a-1** was prepared by heating neat 2a (2.15 g 9.18 mmol) with 2 mol% p-TSA (0.034 g, 0.18 mmol) at 60 °C, which was raised to 90 °C over a period of one hour. The byproduct (dimethoxymethane) was continuously removed under vacuum. After 2 hours a solid mass was observed. The polymerization was terminated after 3 hours, the vessel was cooled down and the solid polymer was dissolved in the minimum amount of chloroform (approx. 2 ml). Re-precipitation from methanol produced 1 g (6.32 mmol) of a white solid material (69% yield).

$^1\text{H NMR}$ (400 MHz, CDCl_3 , 298 K) δ = 4.84-4.83 (m, 94H_b), 4.54-4.51 (m, 103H_e), 4.28-4.25 (m, 102H_d), 4.05-3.93 (m, 105H_c), 3.67-3.61 (m, 101H_c), 3.37 (s, 6H_a). $^{13}\text{C NMR}$ (100 MHz, CDCl_3 , 298 K) δ = 96.0-95.0 (s, C_b), 81.6-80.7 (s, C_e), 78.1-77.9 (s, C_d), 74.6 (s, C_c), 72.3 (s, C_d) 70.9 (s, C_c), 55.7 (s, C_a).

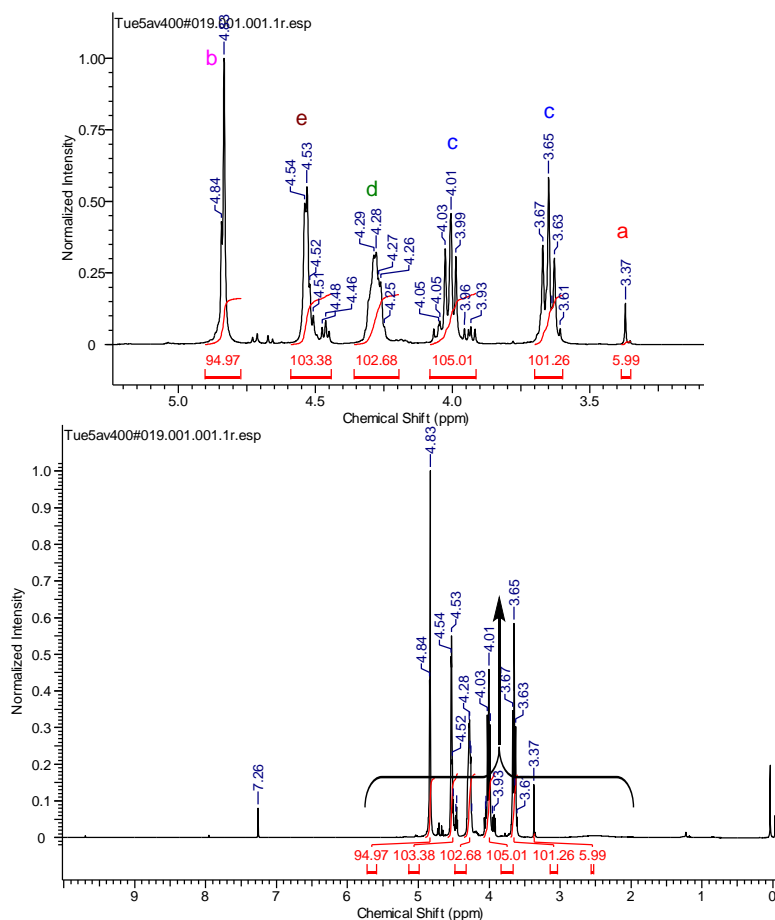


Figure 2.23. $^1\text{H NMR}$ spectrum of **P2a-1** in CDCl_3 (400 MHz at 298 K).

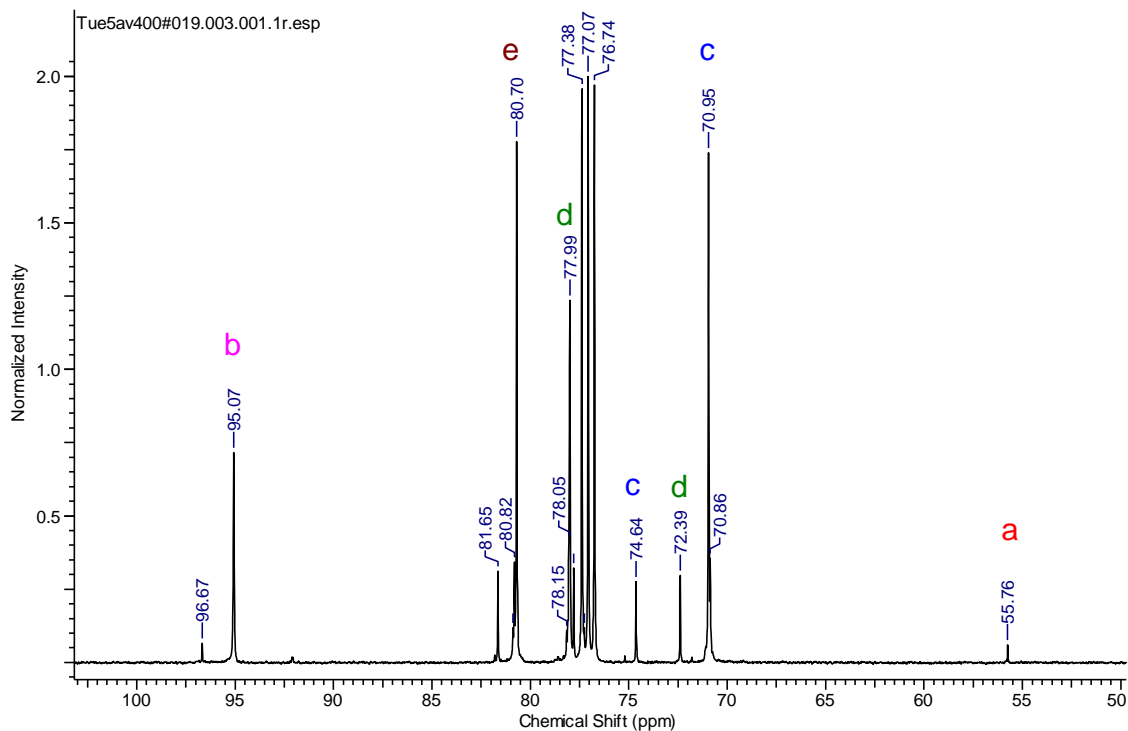


Figure 2.24. ^{13}C NMR spectrum of **P2a-1** in CDCl_3 (100 MHz at 298 K).

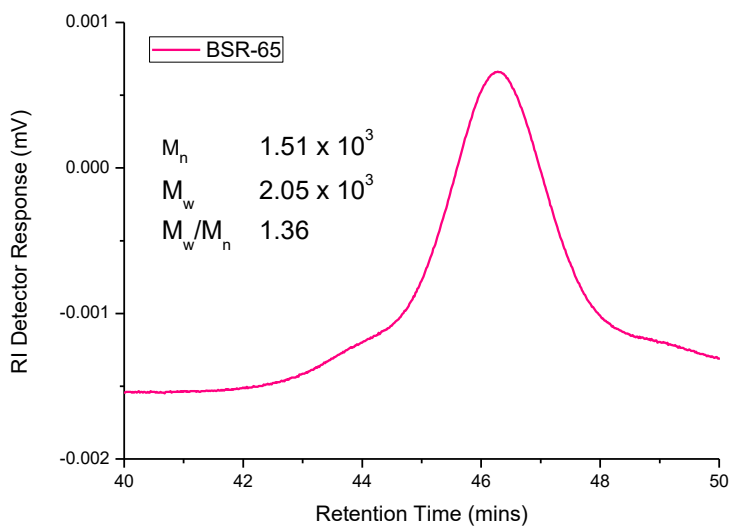


Figure 2.25. GPC chromatogram of **P2a-1** (in chloroform at room temperature).

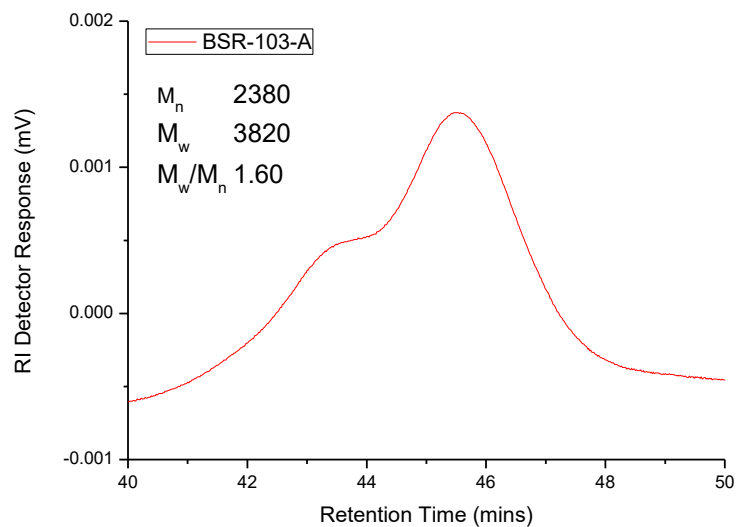


Figure 2.26. GPC chromatogram of **P2a-2** (in chloroform at room temperature).

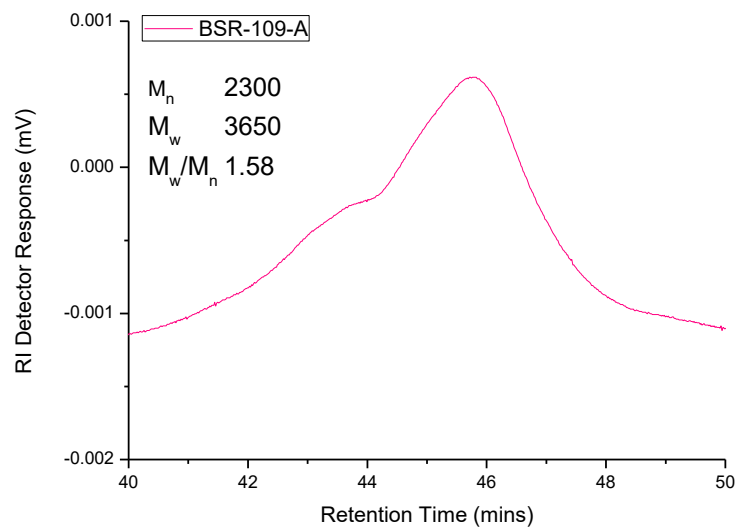


Figure 2.27. GPC chromatogram of **P2a-3** (in chloroform at room temperature).

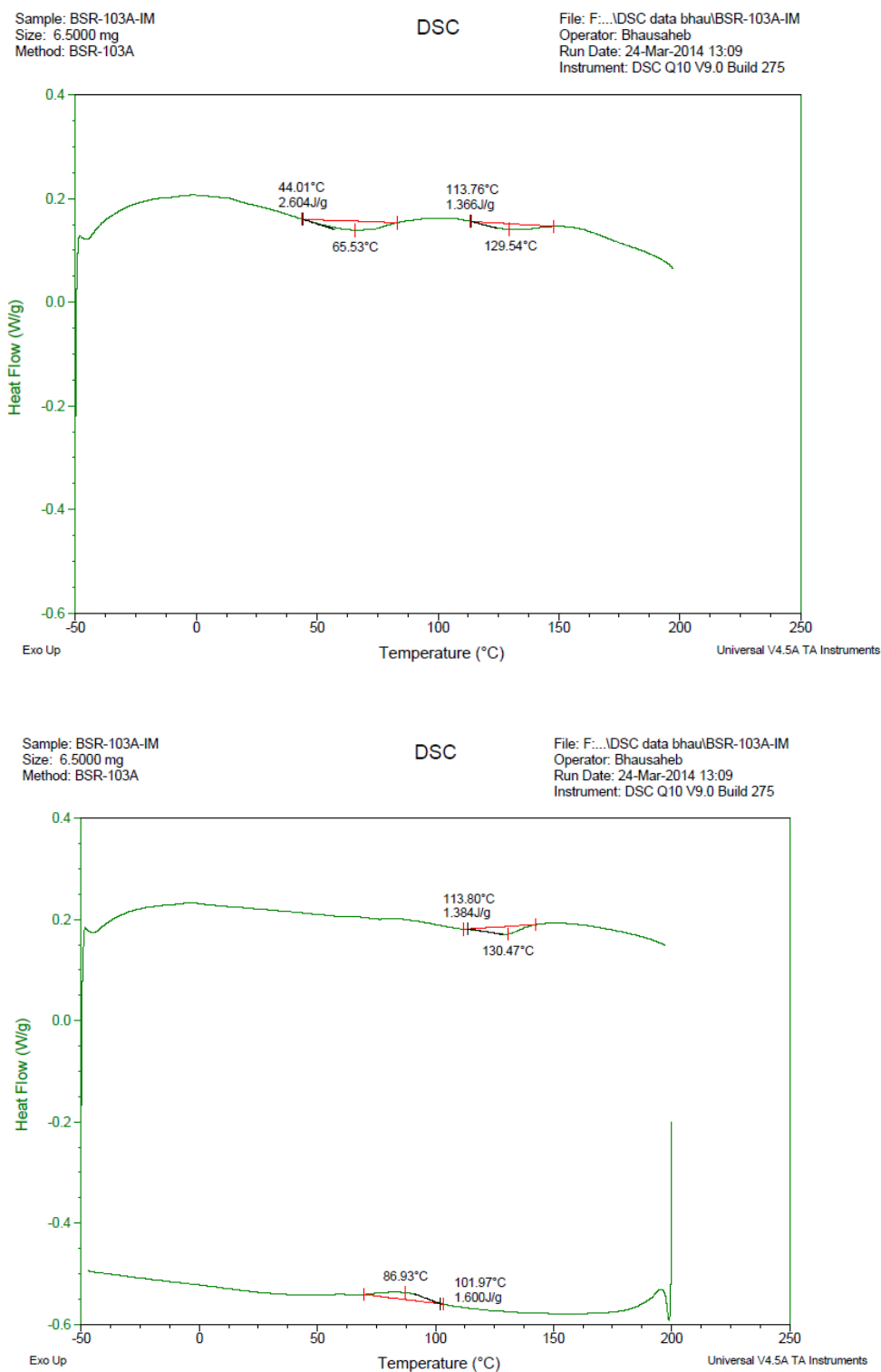


Figure 2.28. DSC heating and cooling curves of **P2a-2**; first heating (top), cooling and second heating (bottom).

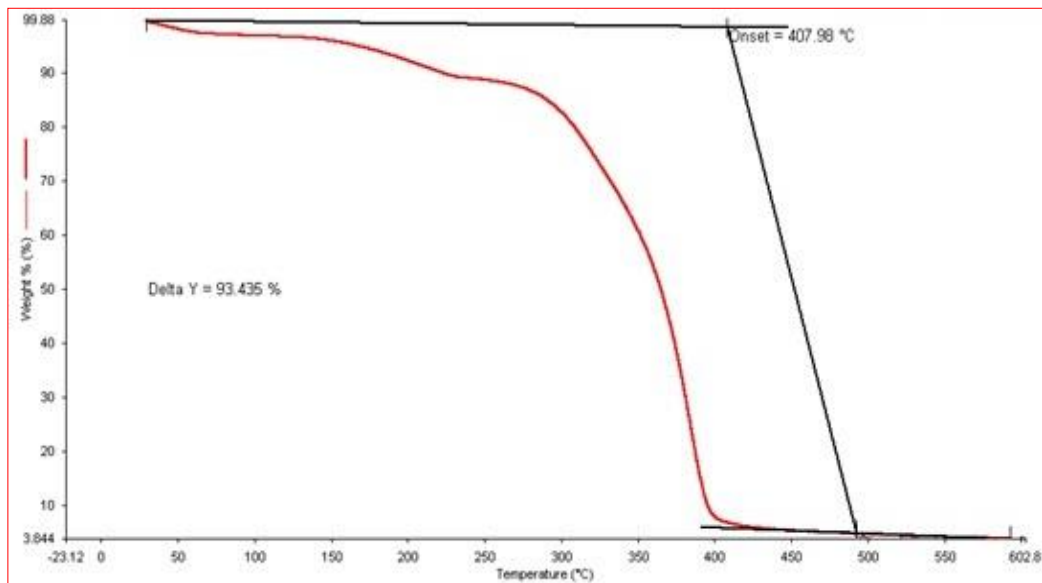


Figure 2.29. TGA trace of **P2a-1** recorded between 0-600 °C in N₂ atmosphere.

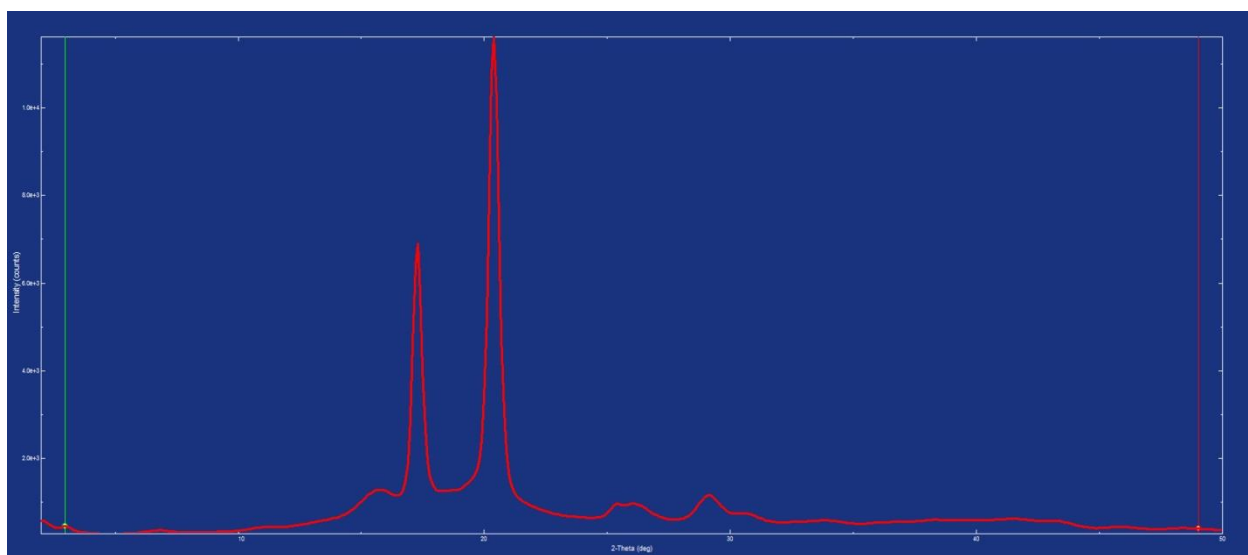
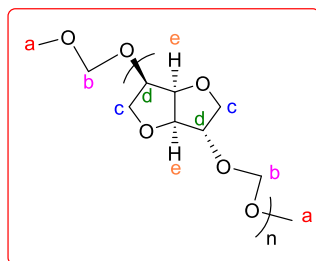


Figure 2.30. X-ray powder diffraction profile of **P2a-1**.

2.4.3.2. Polycondensation of Isosorbide-Diacetal to **P2b-2**:



The polymerization was carried out in a 70 ml Schlenk tube equipped with an air-tight high torque overhead mechanical stirrer. **P2b-2** was prepared by heating neat **2b** (4 g, 17.07 mmol) with 5 mol% *p*-TSA (0.16 g, 0.85 mmol) at 60 °C, which was raised to 90 °C over a period of an hour. The byproduct (dimethoxymethane) was continuously removed under vacuum. The polymerization was terminated after 6 hours, the vessel was cooled down and the solid polymer was dissolved in the minimum amount of chloroform (approx. 2 ml). Reprecipitation from methanol produced 1.92 g (12.15 mmol) of a white solid material (71% yield).

¹H NMR (400 MHz, CDCl₃, 298 K) δ = 4.85-4.75 (m, 342H_b), 4.62-4.59 (m, 185H_c), 4.46 (m, 173H_d), 4.30-4.17 (m, 347H_{e, d}), 3.95-3.92 (m, 527H_c), 3.60-3.52 (m, 176H_c), 3.38-3.34 (s, 6H_a).
¹³C NMR (100 MHz, CDCl₃, 298 K) δ = 94.9-93.3 (s, C_b), 88.0 (s, C_c), 86.2-86.1 (s, C_d), 81.9-80.7 (s, C_e), 78.2-78.0 (s, C_d), 73.4 (s, C_c), 69.8 (s, C_c).

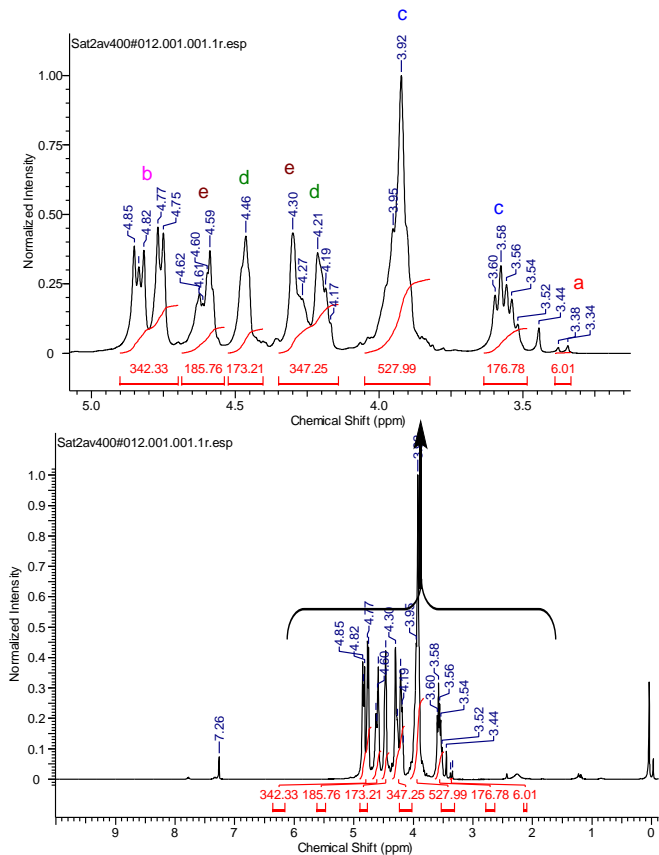


Figure 2.31. ¹H NMR spectrum of **P2b-2** in CDCl₃ (400 MHz at 298 K).

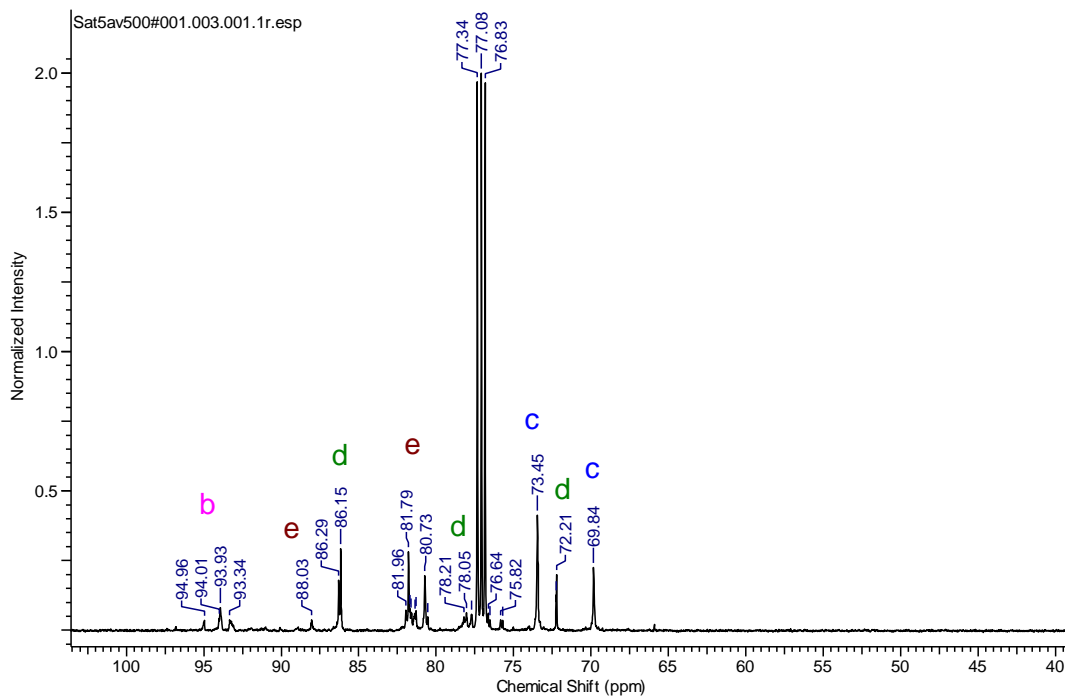
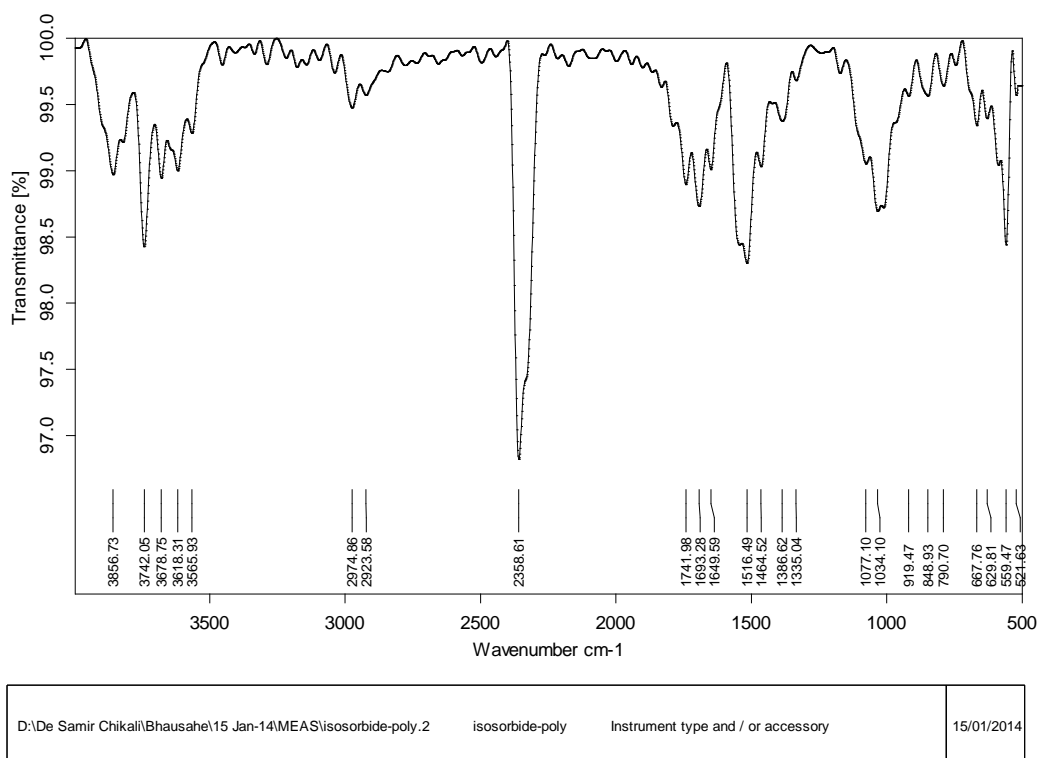


Figure 2.32. ^{13}C NMR spectrum of **P2b-2** in CDCl_3 (100 MHz at 298 K).



Page 1/1

Figure 2.33. IR spectrum of **P2b-2**.

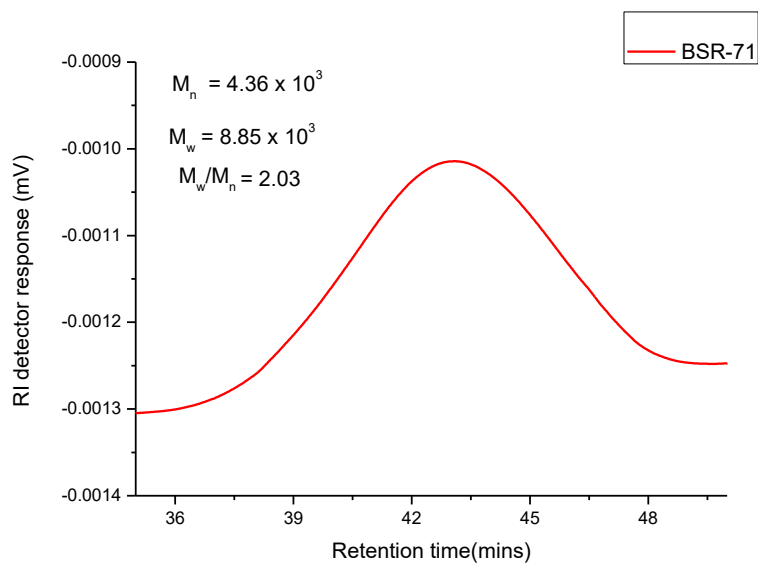


Figure 2.34. GPC chromatogram of **P2b-2** (in chloroform at room temperature).

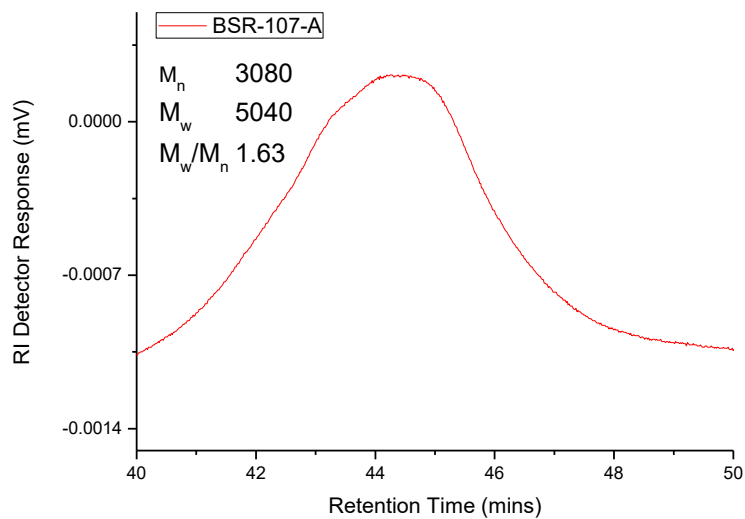


Figure 2.35. GPC chromatogram of **P2b-1** (in chloroform at room temperature).

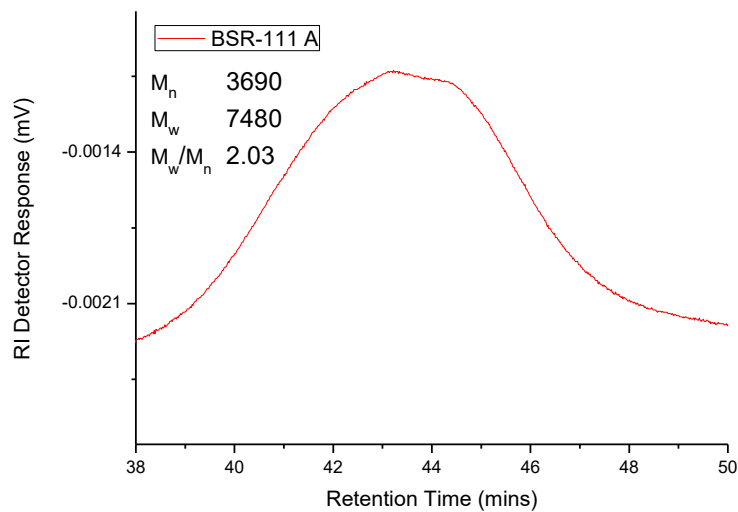


Figure 2.36. GPC chromatogram of **P2b-3** (in chloroform at room temperature).

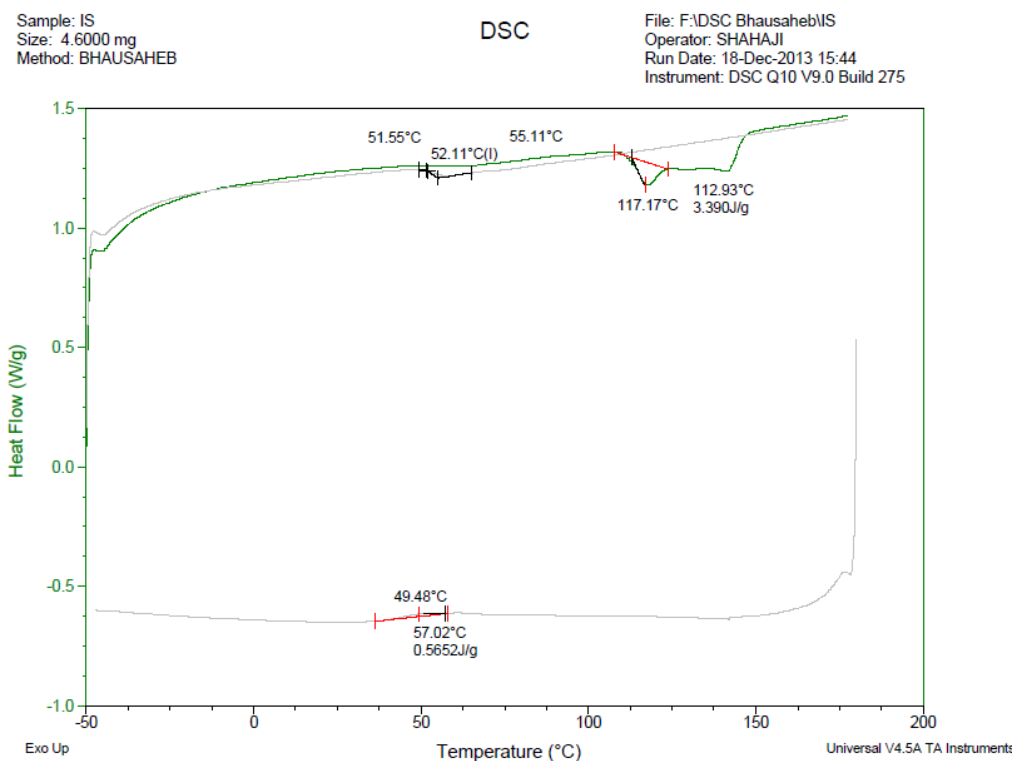


Figure 2.37. DSC heating (1st heating green, 2nd heating black) and cooling curves of **P2b-2**.

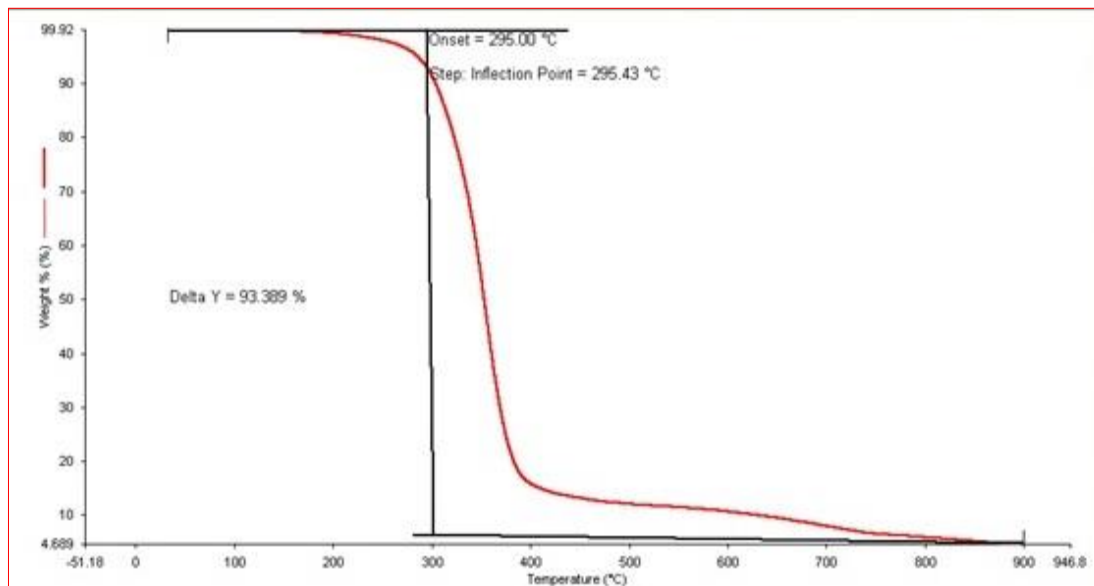


Figure 2.38. TGA trace of **P2b-2** recorded between 0-600 °C in N₂ atmosphere.

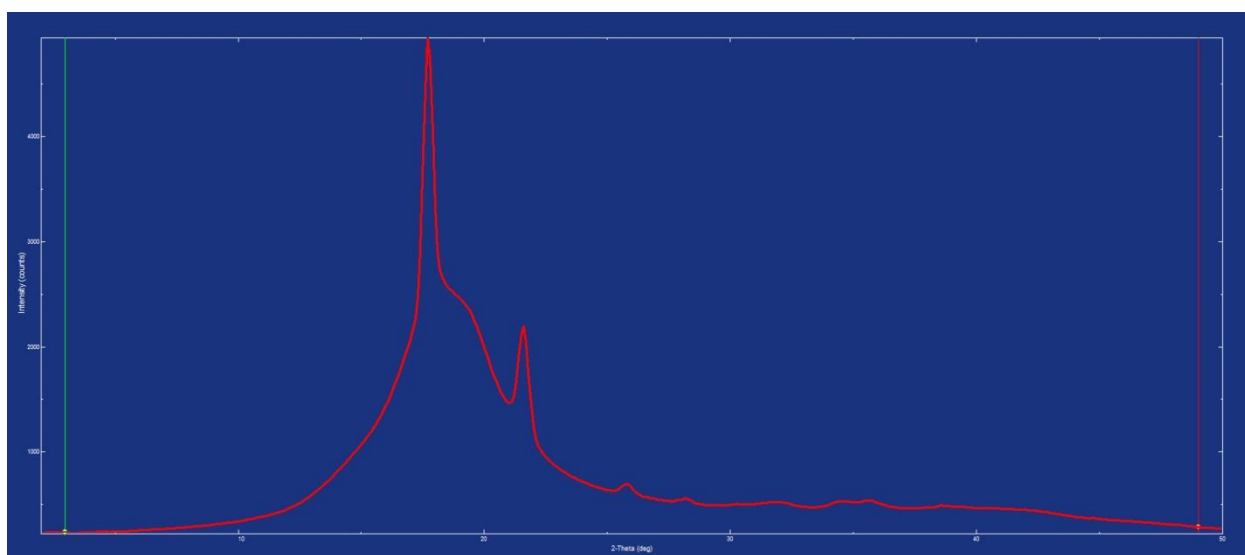
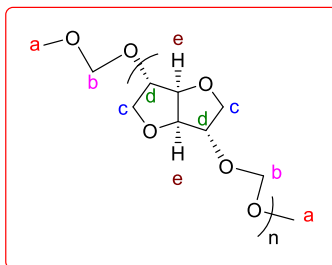


Figure 2.39. X-ray powder diffraction profile of **P2b-2**.

2.4.3.3. Polycondensation of Isoidide-Diacetal to P2c-1:



The polymerization was carried out in a 70 ml Schlenk tube equipped with an air-tight high torque overhead mechanical stirrer. **P2c-1** was prepared by heating neat **2c** (0.91 g, 3.88 mmol) with 5 mol% *p*-TSA (0.037 g, 0.194 mmol) at 60 °C, which was raised to 90 °C over a period of one hour. The byproduct (dimethoxymethane) was continuously removed under vacuum. After 2 hours a solid mass was observed. The polymerization was terminated after 3 hours, the vessel was cooled down and the solid polymer was dissolved in minimum amount of chloroform (approx. 1 ml). Re-precipitation from methanol produced 0.35 g (2.2 mmol) of a white solid material (58% yield).

$^1\text{H NMR}$ (500 MHz, CDCl_3 , 298 K) δ = 4.80 - 4.57 (m, 130H_{b, e}), 4.28-4.21 (m, 61H_d), 3.87-3.80 (m, 127H_c), 3.36 (s, 6H_a). $^{13}\text{C NMR}$ (125 MHz, CDCl_3 , 298 K) δ = 95.6-93.1 (s, C_b), 87.6-85.7 (s, C_e), 80.9 (s, C_d), 74.4 (s, C_c), 72.37 (s, C_d), 72.30 (s, C_c), 55.6 (s, C_a).

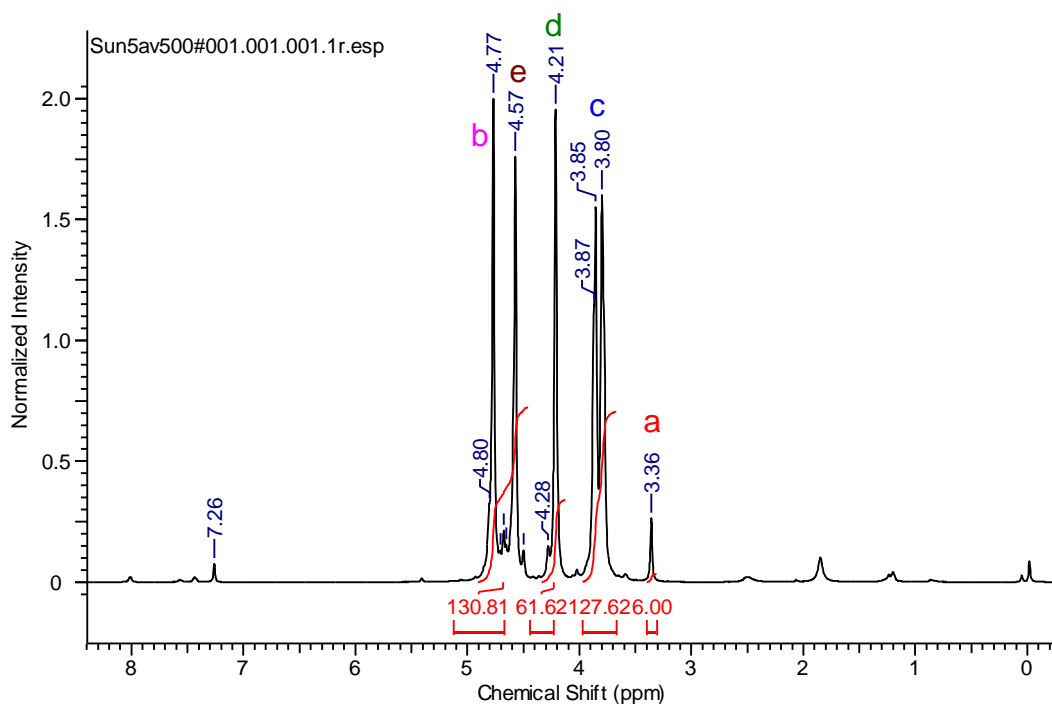


Figure 2.40. $^1\text{H NMR}$ spectrum of **P2c-1** in CDCl_3 (500 MHz at 298 K).

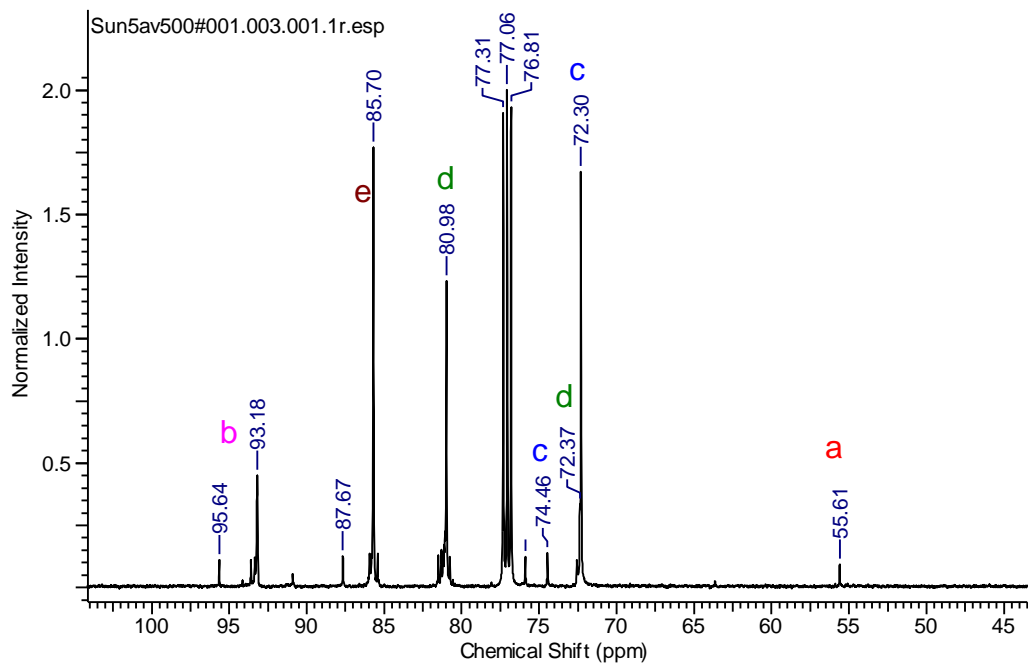


Figure 2.41. ^{13}C NMR spectrum of **P2c-1** in CDCl_3 (125 MHz at 298 K).

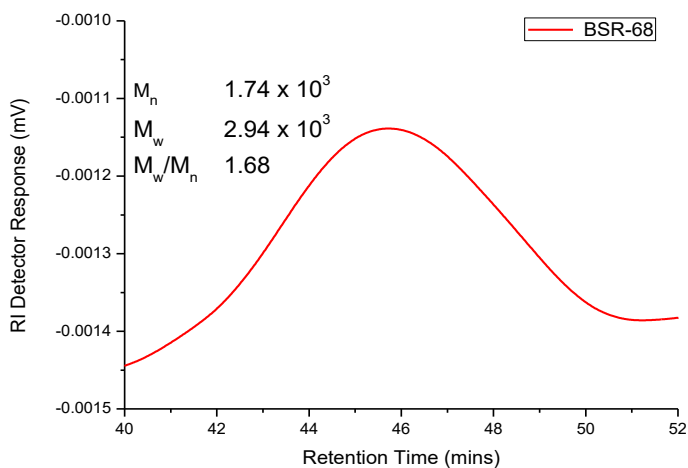


Figure 2.42. GPC chromatogram of **P2c-1** (in chloroform at room temperature).

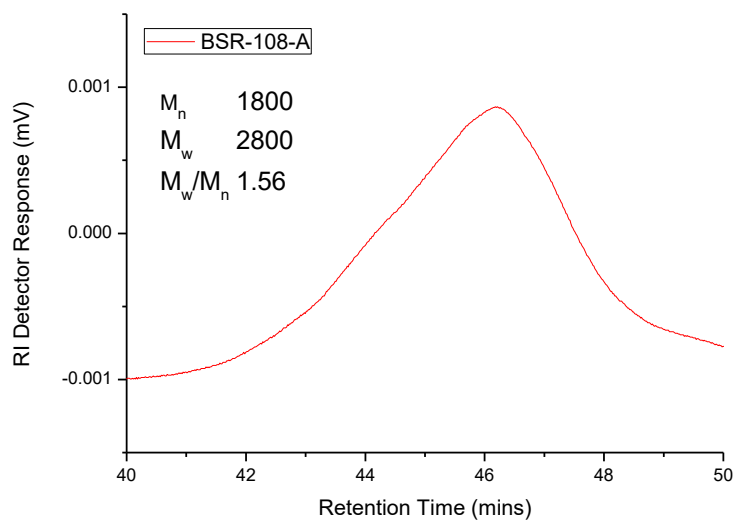


Figure 2.43. GPC chromatogram of **P2c-2** (in chloroform at room temperature).

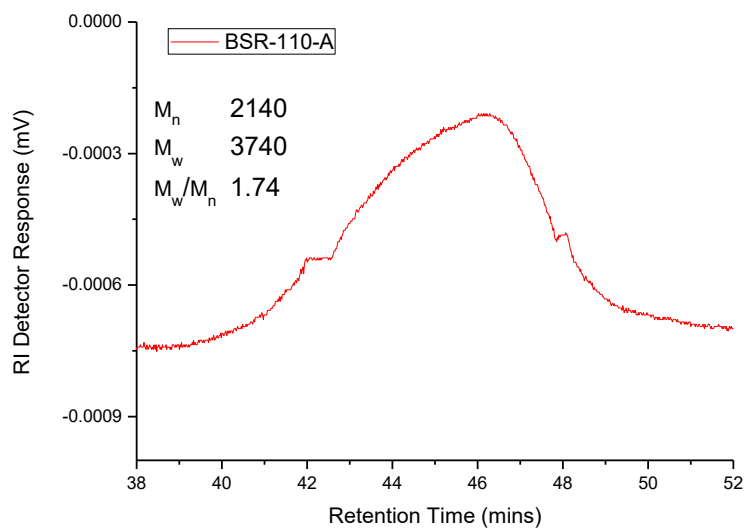


Figure 2.44. GPC chromatogram of **P2c-3** (in chloroform at room temperature).

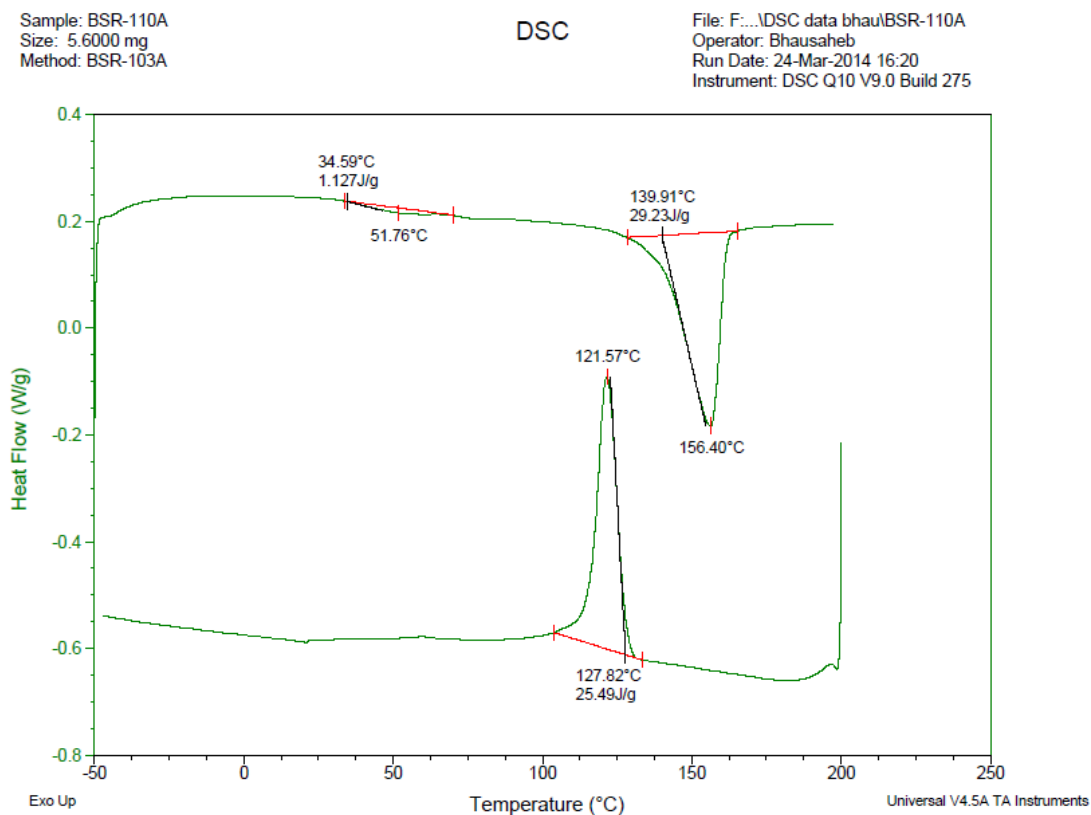


Figure 2.45. DSC heating and cooling curves of P2c-3.

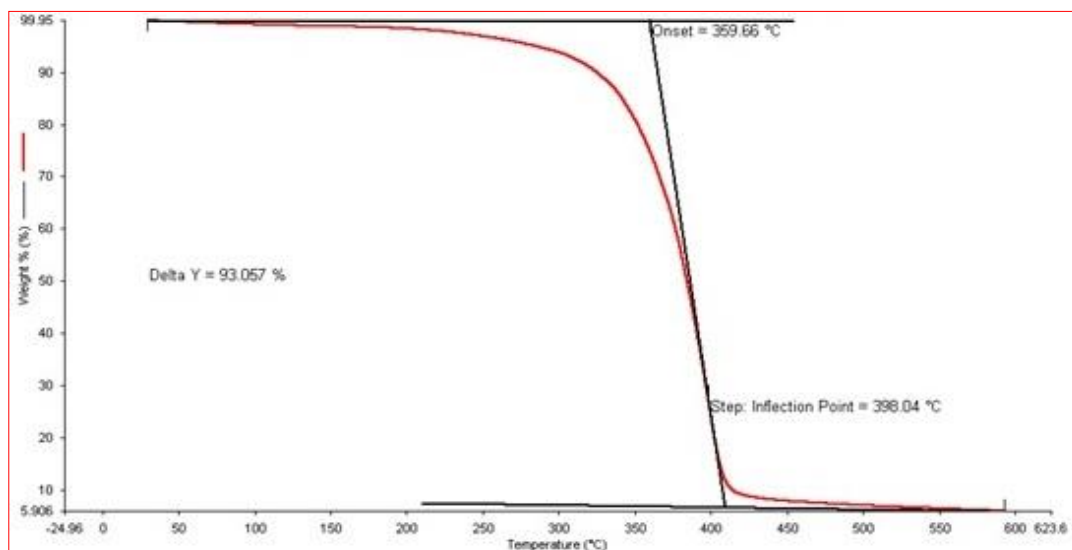


Figure 2.46. TGA trace of P2c-3 recorded between 0-600 °C in N₂ atmosphere.

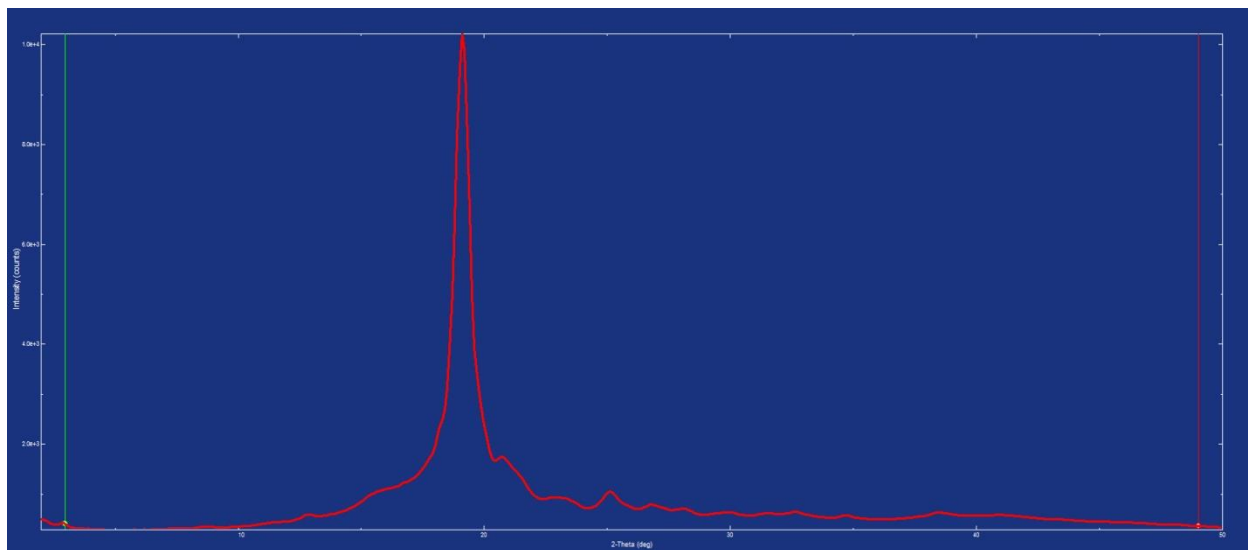


Figure 2.47. X-ray powder diffraction profile of **P2c-3**.

2.4.4. Molecular Weight Determination by End Group Analysis (NMR):

Polymerization experiments were performed at different time intervals to establish the exact chemical shift of the end groups (in this case the $-\text{OCH}_3$ groups). Thus, it was established that the methoxy end groups appear at 3.35 ppm (**Figure 2.48** bottom) and the signal disappears if the polymerization is run for 24 hours, indicating high molecular weight polymers with negligible amount of end-groups (**Figure 2.48** top). An exemplary molecular weight calculation is given below. Addition of total number of backbone protons = 1750, then divide total number of backbone protons by the number of protons in single repeat unit of the polymer (i.e. 10). So $1750/10 = 175$. The number of repeat units (175) is multiplied by 158 (where 158 is the molecular weight of repeating unit). Hence, $175 \times 158 = 27600$ (see **Figure 2.48, P2b-2**).

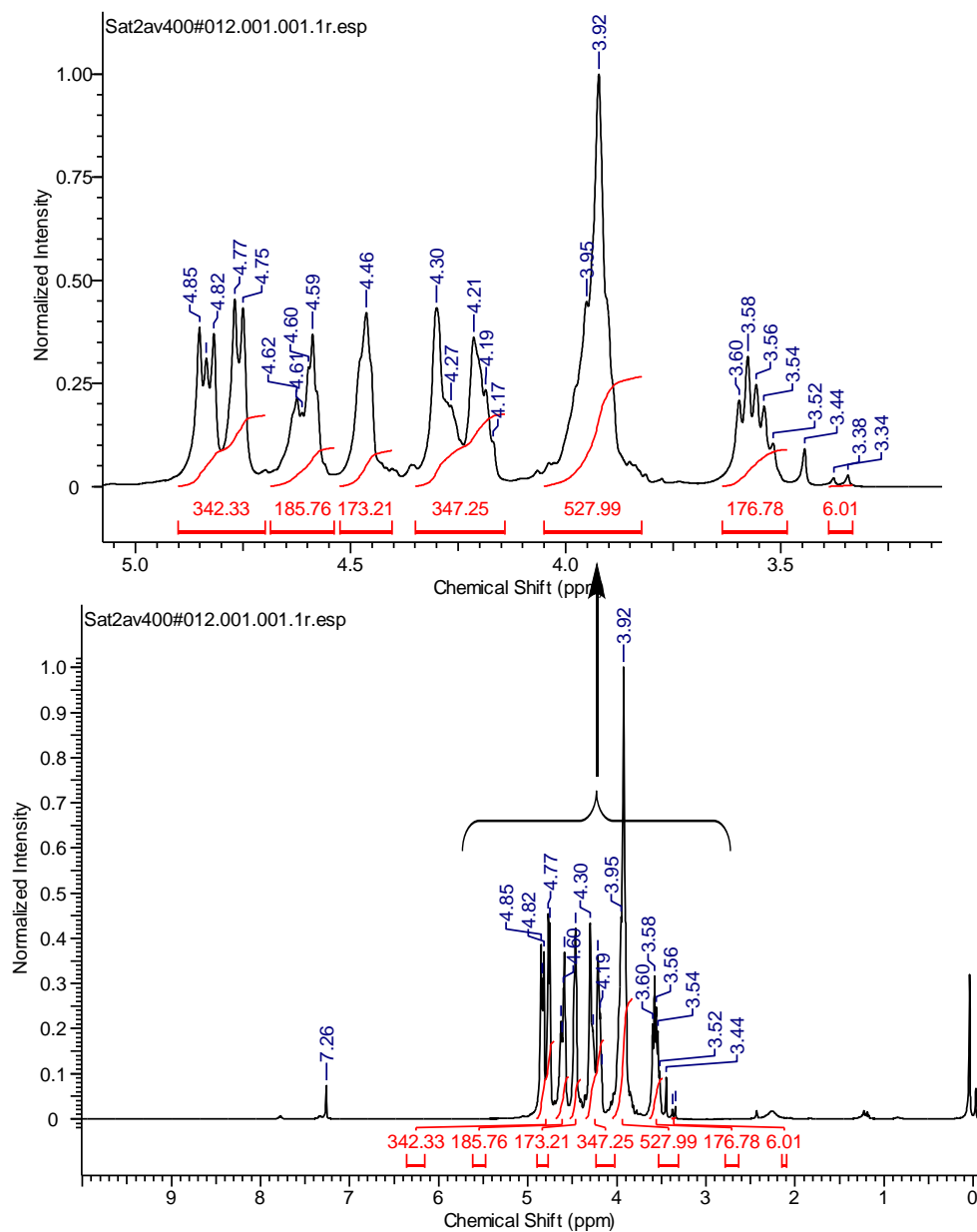


Figure 2.48. ^1H NMR of **P2b-2** in CDCl_3 (400 MHz at 298 K).

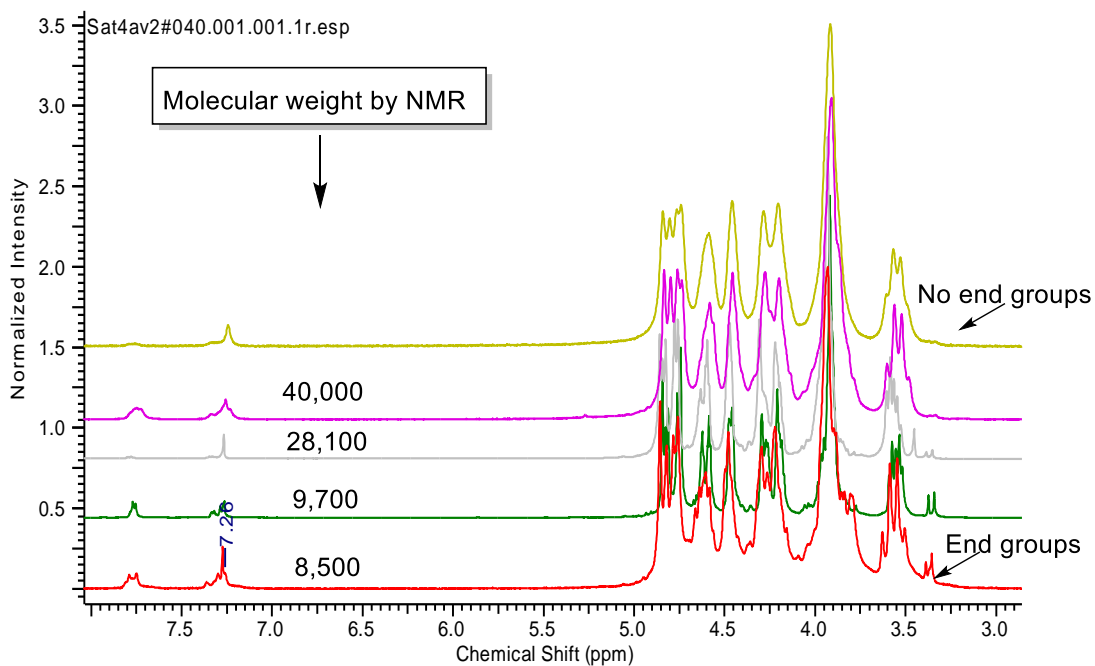


Figure 2.49. ^1H NMR of P2b at different time intervals.



Figure 2.50. Isolated polyacetals IS (P2b), IM (P2a) and II (P2c).

2.4.5. Degradation of P2b:

2.4.5.1. Hydrolytic Degradation:

The polyacetal **P2b-2** was selected as the most relevant representative of the three polymers for degradation studies. 40 mg of **P2b-2** was taken in a frit and was washed with 0.8 ml of D₂O. Proton NMR of the washing displayed only solvent (D₂O) signal (see **Figure 2.51**), indicating that the polyacetal is stable under washing conditions. However, a clear solution was obtained when the same polymer was transferred to a round bottom flask and stirred with D₂O (total 0.2 ml; 35% DCl in D₂O solution) over a period of 54 hours. ¹H NMR of initial mixture (solid polymer was visible) displayed a spectrum similar to neat **P2b-2** (see **Figure 2.52** bottom). Whereas, after acid treatment a clear solution was obtained; with sharp proton signal corresponding to the bicyclic skeleton (see **Figure 2.52**; 5, 20, 33 and 54 hours). These findings were further supported by the ¹³C NMR (**Figure 2.53**); suggesting that the polymer breaks down to the isosorbide backbone.

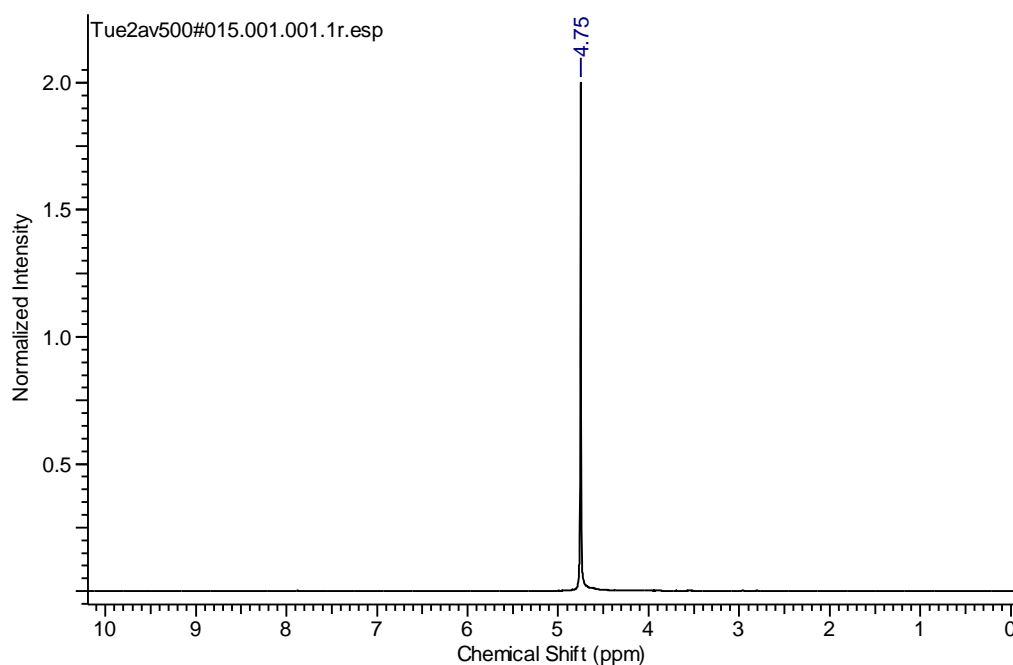


Figure 2.51. ¹H NMR of **P2b-2** after rinsing with D₂O (500 MHz, 298 K).

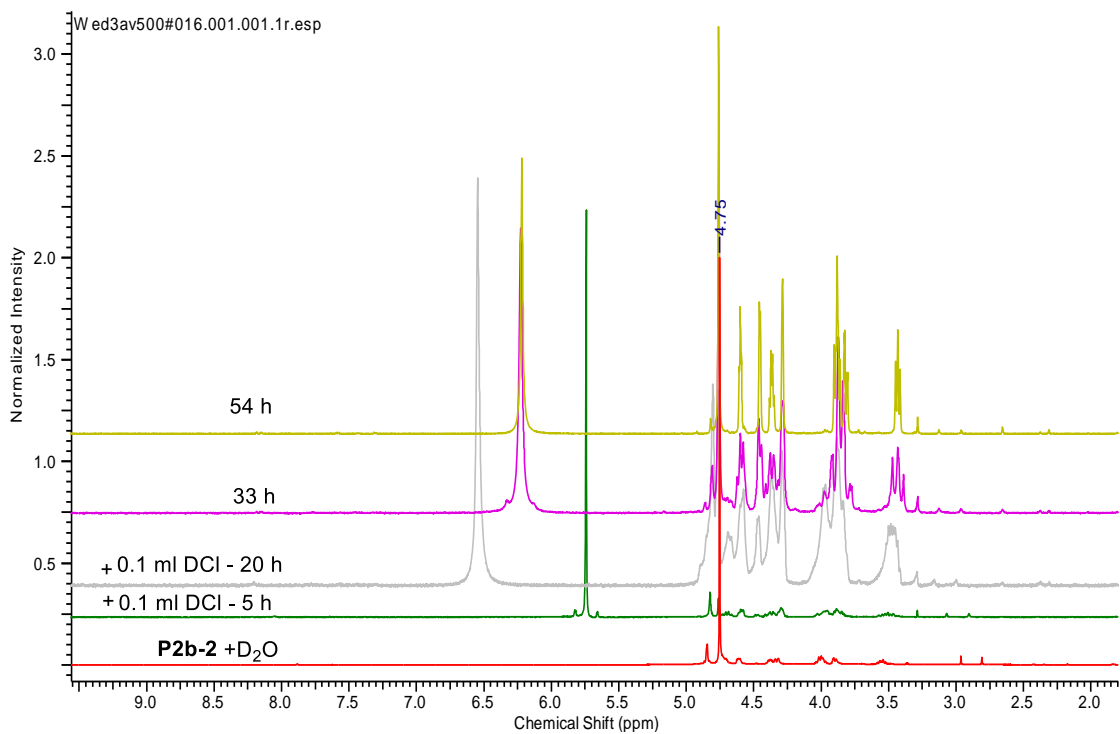


Figure 2.52. Time dependent ^1H NMR of **P2b-2** in acidic media (in D_2O).

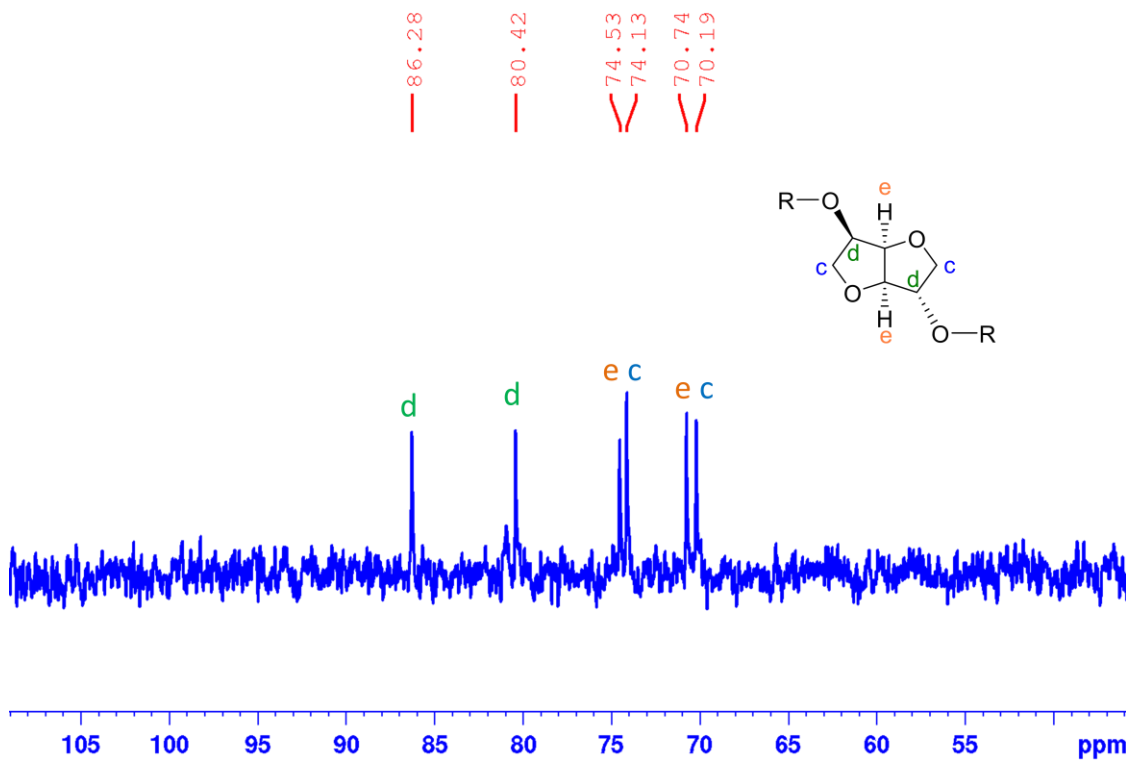


Figure 2.53. ^{13}C NMR of **P2b-2** in acidic media after 112 h (50 MHz in D_2O at 298 K).

2.4.5.2. Degradation in Organic Media:

P2b-2 (40 mg) was dissolved in 0.6 ml CDCl_3 and initial spectrum was recorded (**Figure 2.54** bottom). Hydrochloric acid (0.05 ml, 2M HCl in diethylether) was added to the above NMR tube and spectra were recorded after 0, 4, 58 and 80 hours (**Figure 2.54**). A new proton signal at 5.5-5.4 ppm, indicating degradation of the polyacetal was observed. Furthermore, the intensity of this peak grows over time.

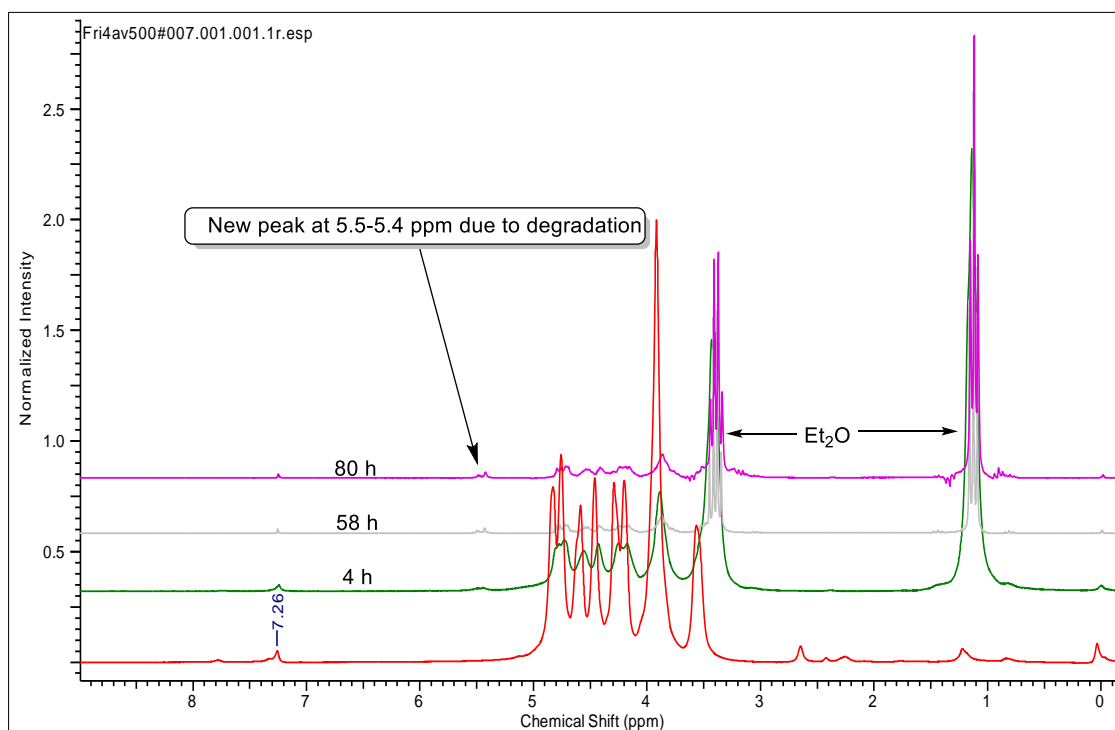


Figure 2.54. Variable time ^1H NMR (stacked) of **P2b-2** in acidic media (in CDCl_3).

2.4.5.3. Monitoring the Acid Induced Degradation by GPC:

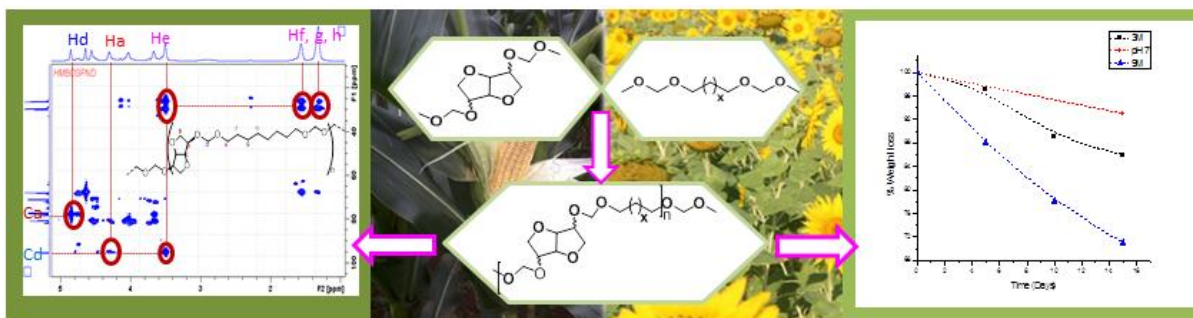
P2b-2 (20 mg) was dissolved in 4 ml chloroform and 0.2 ml HCl (2M in diethylether) was added. The solution was allowed to stand for 1 hour and was filtered through a bed of basic alumina. The filtrate was collected and the GPC was recorded (see **Figure 2.3** right in section 2.3.3). The parent polyacetal with a M_w of 8900 g mol^{-1} (**P2b**; **Figure 2.3** left) degrades to low molecular weight fragments of about 741 g mol^{-1} (**Figure 2.3** right). Although such low molecular weights from GPC measurement are unreliable (lower detection limits of GPC), these observations indicate that the polymer chain degrades to low molecular weight fragments.

2.5. Conclusions:

In summary, a single step synthetic protocol to access a small family of isohexide-diacetals (**2a-c**) derived from renewable isohexides (**1a-c**) was developed. The methodology can be extended to synthesize renewable chiral building blocks for pharmaceuticals and medicinal applications. In our pursuit to demonstrate the synthetic utility of these renewable building blocks, the diacetals **2a-c** were subjected to condensation polymerization. Acid catalyzed polycondensation of **2a-c** under mild conditions produced the corresponding polyacetals (**P2a-c**) as white solids (with molecular weights in the range of 3200 to 27600 g mol⁻¹) in good yields. Mild polymerization conditions and color-free polymers suggest enhanced reactivity (due to one atom extension) of the new monomers compared to their parent isohexides. The identity of the resultant polymers was established after rigorous characterization. MALDI-ToF-MS revealed a repeat unit of 158 Da which exactly matches with the polyacetal repeat unit molecular weight, whereas 1D and 2D NMR experiments suggest that the stereochemistry of the monomer is retained in the polymer. The rigid polyacetals displayed higher melting temperatures compared to their linear analogues C5-C6-polyacetals.²⁰ GPC and NMR investigations indicate that the polyacetals degrade in slightly acidic media. Thus, polyacetals **P2a-c** represent a class of renewable and degradable polymers that can meet both the criteria of sustainable materials.

Chapter 3

Synthesis of Renewable Copolyacetals with Tunable Degradation



This chapter has been adapted from following publication

Rajput, B. S.; Chander, U.; Arole, K.; Stempfle, F.; Menon, S. K.; Mecking, S.; Chikkali, S. H.

Macromol. Chem. Phys. **2016**, *217*, 1396-1410.

3.1. Abstract:

Acetal Metathesis Copolymerization (AMCP) of renewable isohexide diacetals and aliphatic long-chain diacetals is reported and access to a small family of copolyacetals has been established. Crucial 1-2D NMR and MALDI-ToF-MS findings unambiguously confirm the existence of copolymeric structure. In a stark contrast to the earlier reported isohexide-polyacetals, the current copolyacetals revealed very slow degradation. Hydrolytic degradation of copolyacetal pellets displayed extremely slow degradation at pH 7, whereas, only 30% degradation over a period of 15 days was observed in 9M hydrochloric acid solution. GPC investigations revealed that with increasing chain-length, the rate of degradation reduces, whereas copolyacetals with short-chain aliphatic segments displayed faster degradation profile. The reduced rate of degradation can be attributed to the hydrophobic nature of long-chain acetal-segments. In-situ NMR spectroscopy revealed existence of formates, hemiacetals and diols as degradation products. Thus, rate of degradation can be tuned by the judicious choice of isohexide-diacetal and linear-diacetals in a copolyacetal.

3.2. Introduction:

Polymer industry heavily relies on monomers derived from non-renewable fossil feed-stock's.¹ The ever growing demand of fossil feed-stocks and the consequent depletion of crude oil reserves is driving the scientific community to find better alternatives.² It has been unanimously agreed that, use of renewable feed-stocks could be one of the better alternatives. Thus, last decade has witnessed a renewed interest in renewable feed-stocks.³ Conversion of plant derived sugars and oil to chemicals by various chemical transformations has been intensively investigated.⁴ Although the chemical industry is dominated by non-renewable fossil feed-stocks; the renewable resource based products such as poly-lactic acid (PLA), polyhydroxyalkanoates and sugar cane based polyethylene have been recently commercialized.⁵ Apart from the renewable origin, decomposition of the polymeric products without adversely affecting the surrounding is another demanding requirement for the next generation of materials. Recent reports indicate that renewable polyacetals meet both these criteria that are pivotal to the development of futuristic ecofriendly materials (**Figure 3.1**).⁶⁻⁷ Among renewable resources, starch and carbohydrates are the most abundant and easily accessible biomass feed-stocks and have found numerous applications.⁸ These polysaccharides (starch and cellulose) can be readily converted to rigid bicyclic-diols called isohexides.⁹⁻¹¹ Depending on the arrangement of the two hydroxyl groups the isohexides are named

as, isomannide, isosorbide and isoidide. In isomannide (1,4:3,6-dianhydromannitol) the two hydroxyl groups on C2 and C5 carbon are in the *endo-endo* positions, while the unsymmetrical *endo-exo* isomer is known as isosorbide (1,4: 3,6-dianhydrosorbitol), and the *exo-exo* isomer as isoidide (1,4:3,6-dianhydroiditol).¹²⁻¹³ Isomannide and isosorbide are commercially available and have found various applications in polymer science.¹⁴ Owing to their chirality and intrinsic rigidity, isohexides have been the subject of exhaustive research in various fields ranging from catalysis,¹⁵ pharmaceuticals,¹⁶⁻¹⁸ liquid crystalline materials,⁷ chiral auxiliary/plasticizers¹⁹ and polymers.¹⁴

These isohexides are rigid, chiral, and nontoxic molecules that are known to dramatically increase the glass transition temperature (T_g) when incorporated into a polymer chain.²⁰ However, direct utilization of isohexides in polymerization requires extreme polymerization conditions and produces dark tar like polymers.¹⁴

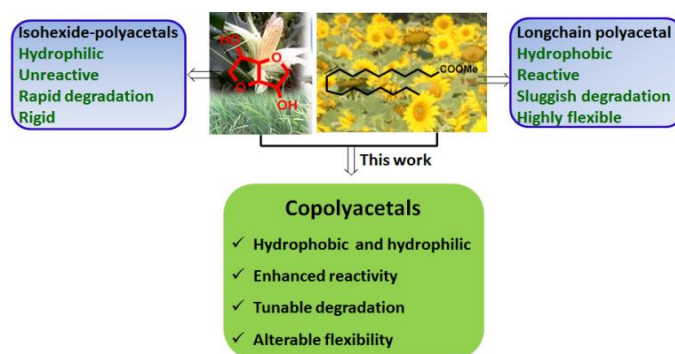


Figure 3.1. Sate-of-the-art in renewable polyacetals and present work.

The reduced reactivity of the isohexides can be attributed to two structural features, namely: a) compromised reactivity of the sterically encumbered secondary hydroxyl groups, and b) the inter-intra molecular hydrogen bonding in these motifs. These limitations have been partly addressed by Daan and coworkers who introduced a “1-carbon extension” strategy.²¹ These monomers with 1-carbon extension were found to be highly reactive compared to the parent isohexides and various polymers such as polyamides,²² polyurethanes,²³ polyesters²⁴ and copolyesters²⁵ have been reported. Thus, significant progress has been made in the synthesis of polymers derived from isohexides; however degradation of these polymers remains unattempted. In our pursuit to address these two issues of a) reactivity of the isohexides and, b) degradation of the resultant polymers; in chapter 2 we discussed about the syntheses of isohexide-diacetals and the corresponding polyacetals.²⁶ We could also demonstrate that the isohexide derived polyacetals degrade under slightly acidic conditions. However, it was found that the isohexide-polyacetals

degrade at a much faster rate than required for most anticipated applications of these materials. Hence, there is a need of new strategy, that will provide an additional handle to reduce the rate of degradation of these materials or that will allow to tune the rate of degradation.

In this chapter we report the synthesis of a small library of 15 copolyacetals derived from hydrophilic isohexide repeat units and hydrophobic plant oil based long-chain segments (**Figure 3.1**). We demonstrate the impact of varying the number of methylene repeat units (chain-length) on the rate of degradation and how the degradation rate can be tuned.

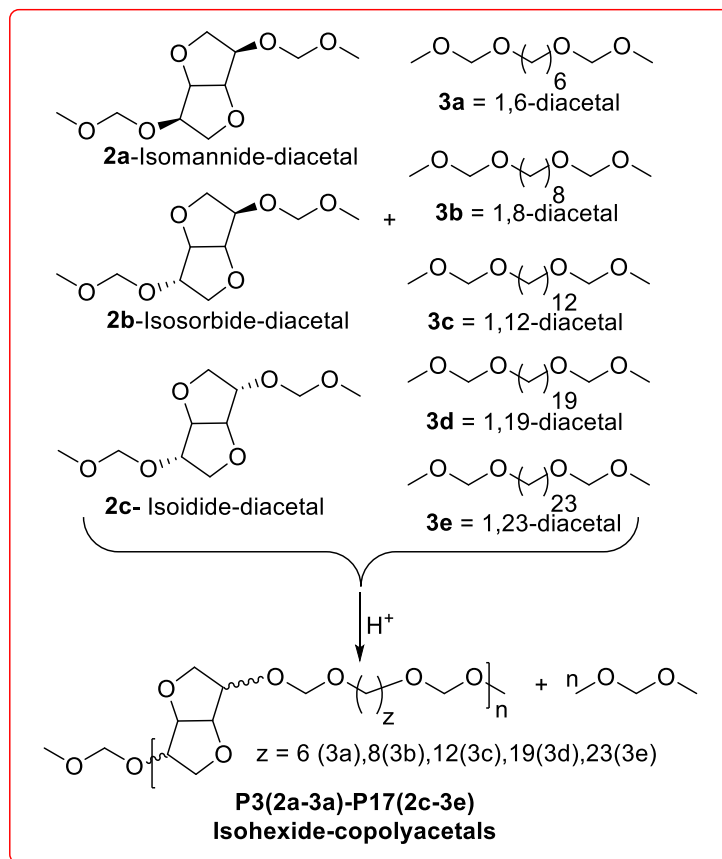
3.3. Results and Discussion:

3.3.1. Diacetal and Copolyacetal Synthesis:

The isohexide-diacetals (**2a-c**) and the long chain diacetals (**3a-e**) were prepared in moderate yields in a single step synthetic protocol.²⁷ Treatment of 1,6-hexanediol and 1, 8-octanediol with dimethoxymethane in presence of methanesulfonic acid produced the diacetals **3a** and **3b** in a good yield (**Scheme 3.1**). The existence of isolated monomers **3a** and **3b** was unambiguously ascertained from spectroscopic and analytical data (see experimental section). Typically, ¹H NMR spectra of **3a, b** displayed a characteristic signal around 4.6 ppm arising from the methylene protons (OCH₂O) and a singlet at 3.3 ppm for the methoxy protons (**Figure 3.10 & 3.13**). The ¹³C NMR resonance at 96 ppm (OCH₂O) further confirmed the formation of acetal moiety and resonance at 55 ppm can be ascribed to the terminal methoxy (OCH₃) carbon (**Figure 3.11 & 3.14**). The existence of the diacetals **3a, b** was further corroborated by a characteristic electrospray ionization mass-spectrum (+ve) signal at m/z = 229.14 [M+Na]⁺ for **3a** and m/z = 257.17 [M+Na]⁺ for **3b** (**Figure 3.12 & 3.15**). The isohexide-diacetals **2a-c** and long chain diacetals **3a-e** were subjected to the Acetal Metathesis CoPolymerization (AMCP) (the term AMCP is similar to the ADMET polymerization). A small library of 15-copolyacetals was prepared by varying isohexide-diacetals (**2a-c**) and the methylene sequence of the linear-diacetals (**3a-e**). Typical copolymerization conditions include heating the monomers from 60 °C to 90 °C in a 50 ml Schlenk tube equipped with overhead stirrer and vacuum connection.

The copolymerization was initiated by adding suitable amount of catalyst (*p*-Toluenesulfonic acid) and the by-product (dimethoxymethane) was continuously expelled by vacuum-argon-purge cycles. Here, the evaporation of short-chain diacetal monomers must be taken in to account while applying vacuum and should be minimized. After polymerization, the resultant highly viscous material was cooled to room temperature. The thus obtained solid was

dissolved in chloroform, and was precipitated from methanol to give the desired copolyacetals **P3(2a-3a)-P17(2c-3e)** as white solids in low to excellent yields (20-80%). However, some copolyacetals (isohexide-diacetals with short-chain 1,6-diacetal and 1,8-diacetal; see the table 1) could not be



Scheme 3.1. Synthesis of copolyacetals **P3(2a-3a)-P17(2c-3e)** by AMCP. precipitated out as they were found to be present in liquid state. The low yields for **P3(2a-3a)** indicate monomer evaporation or stoichiometric imbalance in the reaction system. The copolyacetals were rigorously characterized and **Table 3.1** summarizes the most significant findings.

3.3.2. Copolyacetal of Isomannide-Diacetal (2a) and Linear Diacetals (3a-e):

AMCP was carried out as described above and the resultant copolyacetals were characterized using a combination of spectroscopic and analytical methods. The formation of copolyacetal **P4(2a-3b)** was attested by the reduced intensity of a proton resonance at 3.3 and 4.6-4.7 ppm and absence of a ^{13}C peak at 55 ppm (corresponding to terminal $-\text{OCH}_3$ group **Figure 3.18** & **3.19**). The ratio between the eight backbone protons of **2a** (2:2:2:2) and the sixteen backbone

protons of **3b** was retained in **P4(2a-3b)**. The splitting pattern of the polymer backbone protons is similar to that of **2a** protons; suggesting that the stereochemistry of the monomer **2a** is most likely preserved during the polymerization. These typical features were associated with all other copolyacetals derived from isosorbide and isoidide. These assignments were further corroborated by 2D NMR findings. In a decisive long-range through bond C-H correlation experiment (HMBC), an acetal carbon (**Figure 3.2**, “d” carbon) at 95 ppm revealed through bond correlation to protons at 4.2 (“a” proton that originates from the isomannide backbone)

Table 3.1. Isohexide derived copolyacetals and their properties^{a)}.

Run	Monomers	Polymers	M _n ^b	M _w ^c	PDI ^c	T _m	Yield
1	2a:3a	P3(2a-3a)	ND	10.7	1.7	NO	20
2	2a:3b	P4(2a-3b)	ND	4.9	1.9	45, 118	41
3 ^d	2a-3c	P5(2a-3c)	12.3	8.0	1.8	49, 61	48
4	2a:3d	P6(2a-3d)	ND	3.4	1.8	53, 77	50
5	2a:3e	P7(2a-3e)	ND	6.5	2.8	52, 75	64
6	2b:3a	P8(2b-3a)	ND	3.9	2.2	ND	59
7	2b:3b	P9(2b-3b)	ND	4.5	2.5	ND	43
8	2b:3c	P10(2b-3c)	11.9	4.2	2.2	57	65
9	2b:3d	P11(2b-3d)	ND	5.1	2.5	53, 75	73
10	2b:3e	P12(2b-3e)	ND	3.9	2.4	54, 75	66
11	2c:3a	P13(2c-3a)	9.5	2.0	1.9	ND	80
12	2c:3b	P14(2c-3b)	8.0	3.8	2.1	ND	57
13	2c:3c	P15(2c-3c)	ND	4.8	3.1	55	64
14	2c:3d	P16(2c-3d)	ND	4.9	2.0	68	66
15	2c:3e	P17(2c-3e)	ND	9.7	3.0	92	64

^{a)}Refer to experimental section for detailed polymerization conditions; ND = end groups could not be detected, hence absolute molecular weight could not be determined. NO = Not observed due to liquid samples; ^{b)}M_n (into 10³) determined by NMR in g mol⁻¹; ^{c)}M_w (into 10³) and the polydispersity index (PDI) were obtained from GPC in chloroform solvent at room temperature with respect to polystyrene standards; ^{d)}Polymerization was carried out at 60-110 °C under vacuum.

and 3.5 ppm (“e” protons from the long-chain aliphatic segment). The 3.5 ppm “e” protons further displayed cross peaks to methylene carbons (f, g, h, etc.) in the range of 25-30 ppm. The HMBC experimental findings were further strengthened by a NOESY experiment. In a typical NOESY

experiment, the 4.7-4.6 ppm (d-protons) protons displayed cross peaks to 4.2 and 3.5 ppm protons (see **Figure 3.20**). Thus, the above NMR experiments unambiguously prove the existence of anticipated copolyacetal and demonstrate through bond correlation between “a-d-e” type protons and carbons. End group analysis of **P5(2a-3c)** by ^1H NMR spectroscopy revealed a number average molecular weight (M_n) of 12300 gmol^{-1} . However, detection of end groups by NMR was difficult in the majority of the copolyacetals and hampered absolute molecular weight determination. Gel permeation chromatography (GPC) investigation of the copolyacetals revealed on an average, increased molecular weight as compared to previously reported parent isohexide-diacetal homopolymers. The enhancement in molecular weight can be ascribed to the increased reactivity of linear diacetals (see **Table 3.1**). Note that GPC data is recorded with polystyrene standards (to calculate M_w), which is apparently not a very suitable standard for this type of polymers.

The copolyacetal **P4(2a-3b)** was subjected to MALDI-ToF-MS analysis in order to determine the molar mass and repeat unit mass. It should be noted that different copolymers such as alternating, random, block or graft, can potentially generate different and probably more complex fragmentation patterns which cannot be clearly distinguished. A representative spectrum

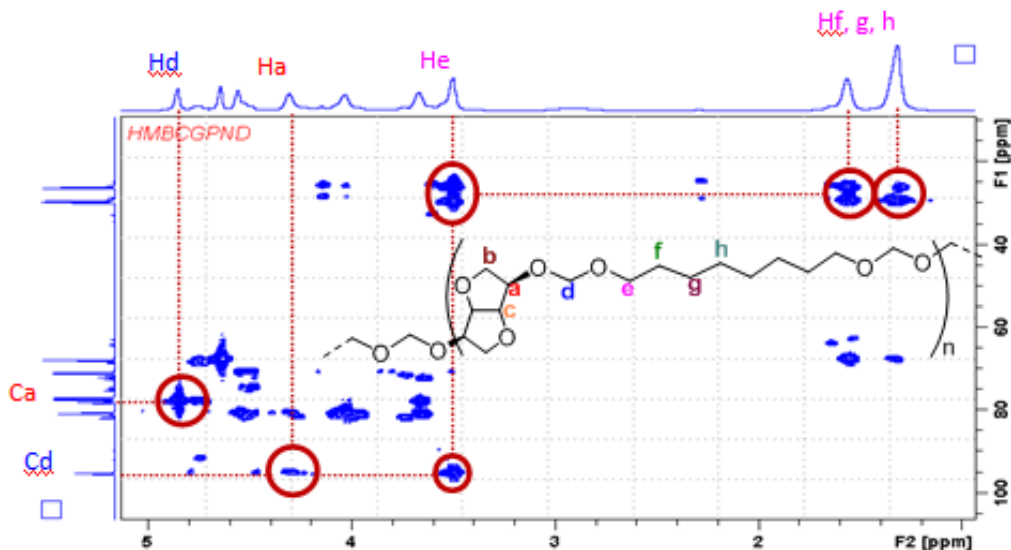


Figure 3.2. ^1H - ^{13}C (HMBC) spectrum of **P4(2a-3b)** in CDCl_3 (500 MHz at 298 K).

of the **P4(2a-3b)** is displayed in **Figure 3.3**. A typical MALDI-ToF-MS spectrum revealed a set of MS signals, each with a mass interval of 316 Da which exactly matches with the molar mass of copolymer repeat unit (along with repeat unit mass for **2a** = 158 Da and **3b** = 158Da). However,

since both the repeat units in this copolymer have same molar mass (158 Da), we collected MALDI-ToF-MS data for **P5(2a-3c)**. As anticipated, a repeat unit mass of 372 Da was observed, confirming the molar mass of the repeat unit (**Figure 3.24**), though the end-groups could not be accurately determined. After having fully established the structural characteristics of the copolyacetals, we turned our attention towards the thermal behaviour of the copolyacetals.

Thermal behaviour of the copolyacetals was investigated by differential scanning calorimetry (DSC) and thermogravimetric analysis (TGA). Majority of the copolyacetals displayed at least two melting transitions, suggesting formation different types of copolyacetals (see **Figure 3.4**). As compared to the parent isohexide polyacetals; the copolyacetals were found to melt at lower temperatures. The reduction in melting temperature (T_m) of the copolyacetal can be attributed to the incorporation of flexible segment in the form of linear-diacetals. Typically, the melting temperature of copolyacetals was found to increase with increasing chain-length of the linear-diacetals. For instance, **P5(2a-3c)** with 12-carbon chain length displayed a T_{m2} of 61 °C; whereas **P6(2a-3d)** with 19-carbon chain length displayed a T_{m2} of 77 °C. However, no significant difference could be observed for **P6(2a-3d)** and **P7(2a-3e)**. The thermal stability of copolyacetals was determined by the TGA between 0 to 600 °C in nitrogen atmosphere (see **Figure 3.5**). The copolyacetals **P4(2a-3b)** and **P5(2a-3c)** started decomposing around 150 °C and maximum decomposition (>50%) was observed around 300 °C. By comparison, the long-chain derived copolyacetals **P6(2a-3d)** and **P7(2a-3e)** were found to be thermally stable up to 325 °C with only less than 15% weight loss. Furthermore, the maximum weight loss (about 80%) in these cases [**P6(2a-3d)** and **P7(2a-3e)**] was observed at 400 °C. Thus, above observation suggest that the stability of the copolyacetals increases with increasing chain-length of the aliphatic long-chain diacetal monomers.

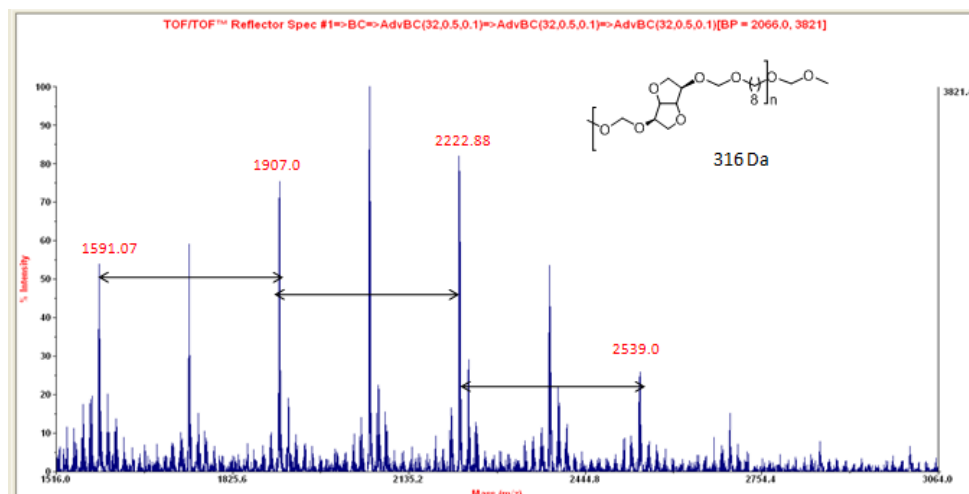


Figure 3.3. MALDI-ToF-MS spectrum of **P4(2a-3b)** recorded in dithranol.

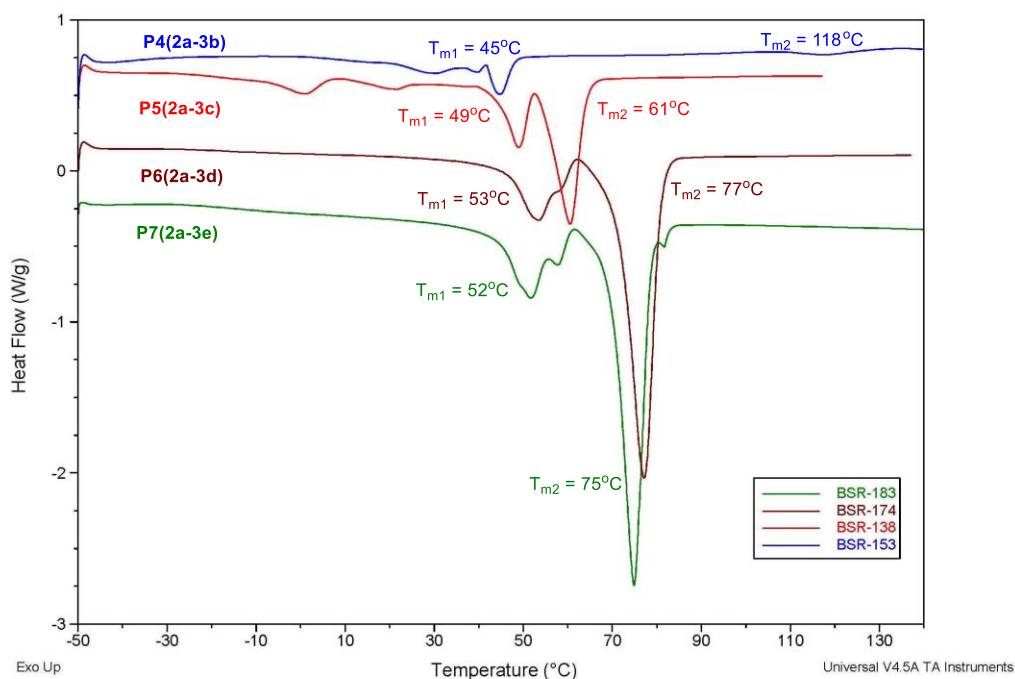


Figure 3.4. DSC heating curves of isomannide-copolyacetals under N_2 atmosphere (data from second heating except **P4(2a-3b)** [1st heating]).

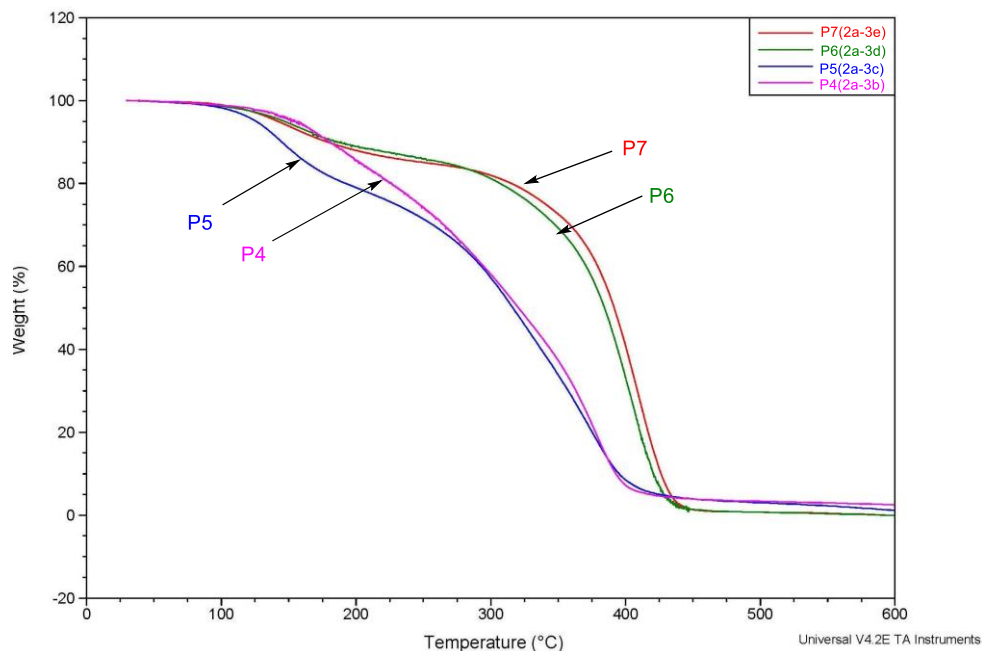


Figure 3.5. TGA traces of isomannide-copolyacetals **P4(2a-3b)** to **P7(2a-3e)** recorded between 0-600 °C in N₂ atmosphere.

3.3.3. Copolyacetal of Isosorbide/Isoidide-Diacetal (2b/2c) and Linear Diacetals (3a-e):

The isosorbide (**2b**) and isoidide (**2c**) derived copolyacetals were prepared as reported in the general copolymerization section and **Table 3.1** summarizes the significant properties of resultant copolyacetals [**P8(2b-3a)**-**P17(2c-3e)**]. The proton and carbon NMR investigations revealed formation of anticipated copolyacetals. Appearance of isosorbide backbone protons in the ratio of 1:3:2:1:1 (**Figure 3.32**) suggested that the stereochemistry of the monomer **4b** is most likely retained during the polymerization (**Figure 3.34, 3.37, 3.41** and **3.45**). ¹³C NMR revealed absence of 55 ppm signals confirming the formation of high molecular weight copolyacetal **P9(2b-3b)** (**Figure 3.35**). The isosorbide derived copolyacetals were further analysed by MALDI-ToF-MS. A typical MALDI-ToF-MS spectrum of copolyacetal **P11(2b-3d)** (run 9) revealed three sets of MS signals with molar mass of 470 Da; which exactly coincides with the theoretical molar mass of the repeat unit of [**P11(2b-3d)**] (**Figure 3.43**). The 3 sets of signals might originate from copolyacetals with different chain-ends. The thermal transitions for the above copolyacetals were recorded by DSC and thermal stability was evaluated using TGA. The short-chain copolyacetals **P8(2b-3a)** and **P9(2b-3b)** were found to be in the liquid state at room temperature, indicating that the T_m is lower than room temperature. Differently, the long-chain derived copolyacetal [**P10(2b-3c)**-**P12(2b-3e)**] were isolated as solids with similar T_m (**Table 3.1**, run 8, 9, 10; see **Figure 3.48**).

The short chain copolyacetals [P10(2b-3c)] displayed about 60% weight loss below 300 °C; whereas, only 20% weight loss was observed in case of long chain copolyacetals [P11(2b-3d)] and [P12(2b-3e)] (see Figure 3.49).

Similarly, isoidide-diacetal derived copolyacetals and their properties are listed in Table 3.1. The resultant copolyacetals were precipitated from chloroform:methanol mixture to obtain desired copolyacetals in excellent isolated yields. The detailed polymerization conditions are reported in Table 3.2 (See experimental section). The copolyacetals P13(2c-3a) to P17(2c-3e) were analysed using a combination of spectroscopic and analytical methods. 1-2D NMR studies revealed formation of high molecular weight copolyacetals, with retention of configuration at the isoidide-diacetals repeat unit (see Figure 3.50, 3.53, 3.56, 3.59 and 3.61). The NMR observations were further confirmed by GPC measurements that displayed weight average molecular weight in the range of 2000-10700 g/mol.²⁸ MALDI-ToF-MS analysis of the copolyacetals P13(2c-3a) displayed a repeat unit mass of 288 Da, which is consistent with the theoretical molar mass of the copolyacetal repeat unit (Figure 3.51). However, the spectrum is more complex due to the likely presence of various types of copolymers (block, random, alternating, graft etc.) and chain-ends. The thermal behaviour of these copolyacetals was monitored by DSC and TGA. Copolyacetals with 1:1 comonomer ratio displayed single melting transition (run 13, 14, 15) that lies in between the T_m of the two homopolymers (Figure 3.63). The isoidide-C12 derived copolyacetal [P15(2c-3c)] displayed about 50% weight loss around 300 °C; whereas, only 15% weight loss was observed in case of long chain copolyacetals [P16(2c-3d)] and [P17(2c-3e)] (see Figure 3.64).

3.3.4. Degradation of Copolyacetals:

The fate of next generation of polymeric materials for some niche applications will heavily rely on two decisive parameters; a) the origin (renewable or non-renewable) of the material and b) environmental-compatibility. Although significant progress has been made in terms of renewable monomers and polymers, very little information exists on the degradation of majority of polymeric materials. In this context, the acetal (-OCH₂O-) link is found to be very sensitive to acidic environments and is primarily responsible for degradation of polyacetals in acidic media.²⁹⁻³⁰ In the previous chapter we reported that the long chain polyacetals degrade very slowly, while isohexide-polyacetals were found to degrade rapidly within minutes.²⁶ Given these findings, we anticipated that varying the chain-length of linear long-chain diacetal monomers will allow us to tune the degradation rate of the resultant copolyacetals. The copolyacetals were subjected to acidic

induced degradation and their degradation behaviour was investigated by: 1) GPC, 2) solid-state degradation, 3) NMR investigations and column chromatographic isolation of degradation products.

3.3.4.1. Monitoring Acid Induced Degradation by GPC:

The acid induced degradation of copolyacetal [P10(2b-3c)] was monitored by gel permeation chromatography (GPC). Suitable amount of isosorbide derived-copolyacetal [P10(2b-3c)] was dissolved in chloroform, 1M HCl (in dioxane) was added and the resultant mixture was stored for 20, 40 and 60 minutes. The volatiles were evaporated to obtain solid material, which was

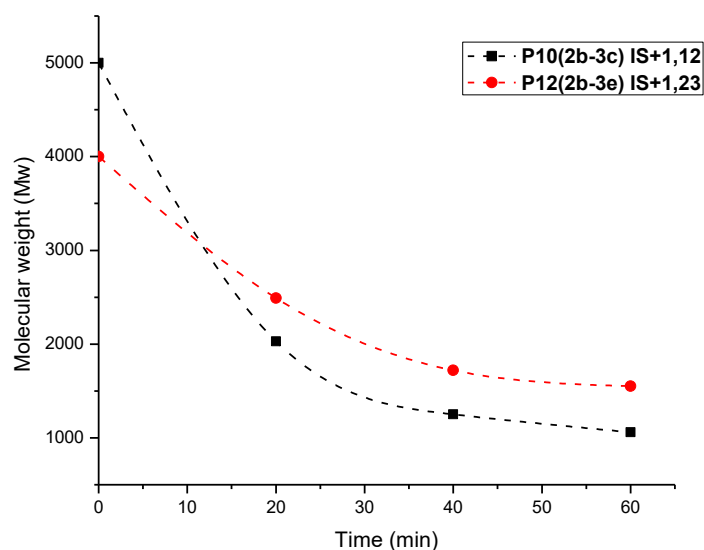


Figure 3.6. Monitoring the degradation of copolyacetals P10(2b-3c) and P12(2b-3e) using the GPC.

dissolved in chloroform and GPC was recorded. Similar protocol was followed for P5(2a-3c), P7(2a-3e), P12(2b-3e), P15(2c-3c) and P17(2c-3e). The relatively short chain (C12) copolyacetal [P10(2b-3c)] was found to degrade to low molecular weight fragments within 20 minutes, whereas the long-chain diacetal (C23) derived copolyacetal [P12(2b-3e)] required at least an hour to degrade to similar low molecular weight fragments (Figure 3.6). Similar protocol was followed to investigate the degradation of isomannide and isoidide derived copolyacetals. The short chain isoidide based copolyacetal P15(2c-3c) degrades with much faster rates (slope of the line) than the

corresponding long-chain copolyacetal **P17(2c-3e)** (Figure 3.66). Almost same trend was observed for the isomannide-short (C12) chain copolyacetal **P5(2a-3c)** and **P7(2a-3e)** (Figure 3.65), although slight deviation was noted in case of **P7(2a-3e)**. These observations clearly demonstrate that incorporation of long-chain diacetals into the copolyacetals significantly retarded the rate of degradation compared to the previously reported parent isohexide-polyacetals.

3.3.4.2. Solid-State Hydrolytic Degradation of Copolyacetal:

Above GPC investigations dealt with liquid samples and degradation behaviour of copolyacetals in solution state. In our efforts to investigate the solid-state behaviour of the copolyacetals, solid samples were prepared and subjected to hydrolytic degradation.³¹ The isoidide derived long-chain copolyacetal **P17(2c-3e)** was chosen as a representative copolyacetal for these investigations. Compact pellets (see Figure 3.7) of identical dimensions were prepared from the polymer melt.

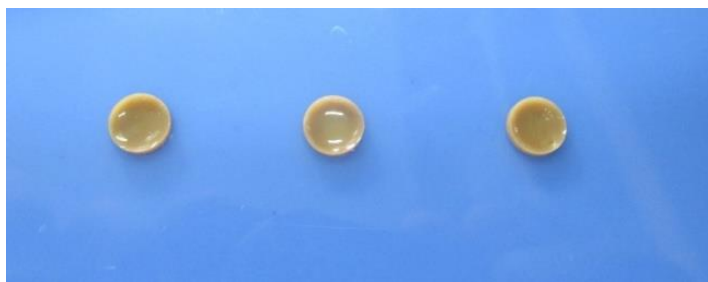


Figure 3.7. Pellets obtained from copolyacetal **P17(2c-3e)**.

Typically, the pellets were suspended in solution for defined period of time, the solution was decanted after the specific interval, and pellet was dried under vacuum until constant weight is obtained. Next, the same pellet was suspended in a fresh solution for a defined time and above procedure was repeated for desired number of times or as in Table 3.4. Suspending the pellet in pH 7 solution for 15 days led to minor (only 7%; average of two experiments) weight loss (see Figure 3.8). The lethargic weight loss can be attributed to the presence of hydrophobic long-chain diacetals (**2e** 1, 23-diacetal) segment in the copolyacetal **P17(2c-3e)**. Unlike the physiological pH, considerable weight loss was observed when pellets were exposed to acidic solutions (3M and 9M HCl) for the period of 5, 10 and 15 days (see Figure 3.8). Thus, exposure of **P17(2c-3e)** to 3M HCl for 5 days led to 3% weight loss, while higher weight loss (12%) was observed in 9M hydrochloric acid solutions. Monitoring the weight loss over 15 days revealed a total weight loss of 15% in 3M HCl, while almost double weight loss (30%) was observed in 9M HCl solution.

Also, the rate of weight loss was higher for the first 10 days, while the next 5 days revealed reduced rate of weight loss. This is most likely due to the deposition of degraded material over the pellet surface which is now (after 10 days) not directly exposed to the acidic media and therefore no longer available for further degradation. These observations clearly demonstrate that incorporation of hydrophobic long-chain diacetals (such as 1, 23-diacetal) significantly decrease the degradation rate and the rate of degradation can be tuned by varying the composition of the two monomers. Thus, the present strategy provides an additional handle to tune the rate of degradation that is very crucial for end use applications.³²

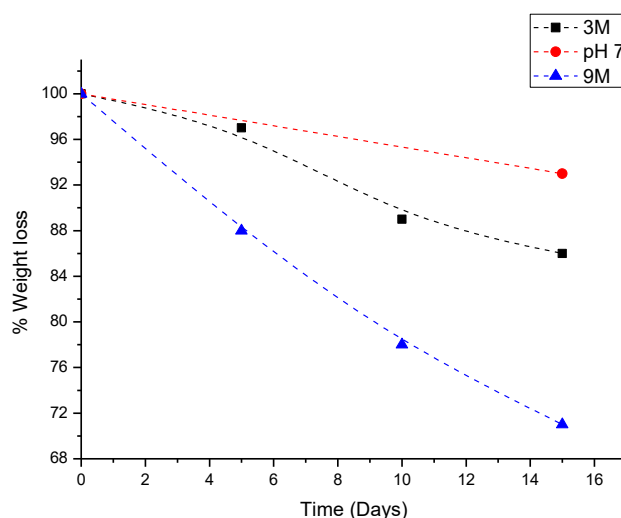


Figure 3.8. Hydrolytic degradation of pellets derived from the **P17(2c-3e)**.

3.3.4.3. Monitoring Acid Induced Degradation by NMR and Isolation of Degradation Products:

The GPC and solid state (hydrolytic degradation) studies allow to conclude that the copolyacetals degrade in acidic media. However, the nature of degradation products remains unclear at this point. In our attempt to shed light on this issue; we tracked the degradation behaviour using NMR spectroscopy and attempted isolation of degradation products. In an NMR tube experiment, 55 mg of **P5(2a-3c)** was dissolved in 0.6 ml CDCl_3 and 0.1 ml methanesulfonic acid (MSA) was added to this solution. A time resolved proton NMR spectrum of **P5(2a-3c)** after addition of MSA is depicted in **Figure 3.67**. The intensity of a $-\text{OCH}_2\text{O}-$ proton resonance at 4.6 & 4.8 ppm decreases suggesting that the acetal moiety is breaking or the copolyacetal is degrading to smaller fragments. Almost simultaneously, new peaks at 4.7, 4.9 and 5.1 ppm start appearing,

which can be assigned to various methylene protons originating from $-\text{ROCH}_2\text{OH}$ type fragments (see **Figure 3.68**). Along the same line, the resonance at 3.5 ppm disappears and a new signal at 3.6 ppm appears. The 3.6 ppm resonance can be tentatively ascribed to a $-\text{RCH}_2\text{OH}$ fragment (**Figure 3.69**). Interestingly, a peak at 8.1 ppm was observed, which can be assigned to formate (see chart 1: A/D) type fragments. The proton NMR findings were further supplemented by ^{13}C NMR, which revealed decreasing intensity of resonances at 67.8 and 95.1-95.2 ppm (**Figure 3.70 & 3.71**) and consequent appearance of peaks at 64.9, 65.8, 94.9 & 96.7 ppm.

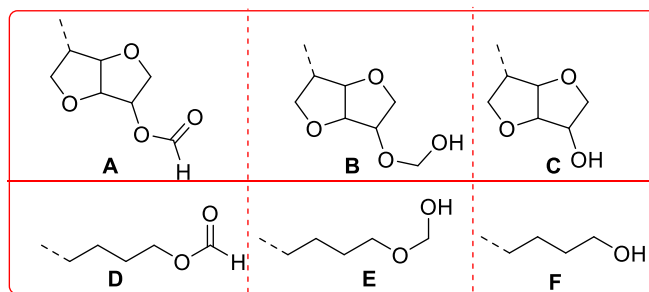


Chart 1. Proposed degradation products based on NMR investigation.

The former resonances between 64-66 ppm can be assigned to the carbons in $-\text{RCH}_x\text{OH}$ fragments (see chart 1, C/F), whereas the later methylenic-carbon resonances (94.9 & 96.7) can be assigned to hemiacetal-type fragments **B** and **E** (chart 1). These findings were further corroborated by various 2D NMR measurements. In a direct C-H correlation (HSQC) spectroscopy, the carbon at 163 ppm displayed a cross peak to protons at 8.1 ppm, confirming the existence of formate group (see **Figure 3.72**). Furthermore, a C-H cross-peak between protons at 4.9-5.2 and carbons at 94.9 and 96.7 ppm suggested existence of hemiacetals of type **B** and **E** (chart 1). The HSQC findings were corroborated by long-range C-H correlation (HMBC) experiment which revealed cross-peak between a proton at 4.1 ppm (Hm) and a carbon at 163 ppm (Ck) (see **Figure 3.9**) that can be ascribed fragment **D** (chart 1). Thus, above NMR investigations indicate that the copolyacetal degrades down to parent isohexides or linear-diols. The above hypothesis was further supported by chromatographic separation of the degradation products. About 200 mg of **P5(2a-3c)** was dissolved in 20 ml chloroform and acidified by adding 1ml of hydrochloric acid (1M in dioxane). After 24 hours, volatiles were evaporated to obtain the residue, which displayed presence of acetal resonances. In order to further degrade the polyacetals, 0.5 ml of hydrochloric acid (1M in dioxane) was added and the copolymer was allowed to degrade for next 24 hours. Volatiles were

evaporated and the residue was subjected to column chromatography. The first fraction (ethyl acetate: pet-ether, 40:60) revealed presence of 1, 12-dodecanediol (**Figure 3.73, 3.74**) whereas, change of polarity (dichloromethane:methanol, 80:20) was necessary to flush out the second fraction. The proton NMR of this fraction suggested presence of isomannide. The existence of isomannide was confirmed by comparing the ^1H NMR spectrum of commercially available isomannide and the one obtained after column chromatographic separation (**Figure 3.75, 3.76**). However, the formates, acetal/hemiacetals could not be isolated. It is most likely that these meta-stable fragments degrade to low boiling entities that evaporate along with solvent before loading on the column.

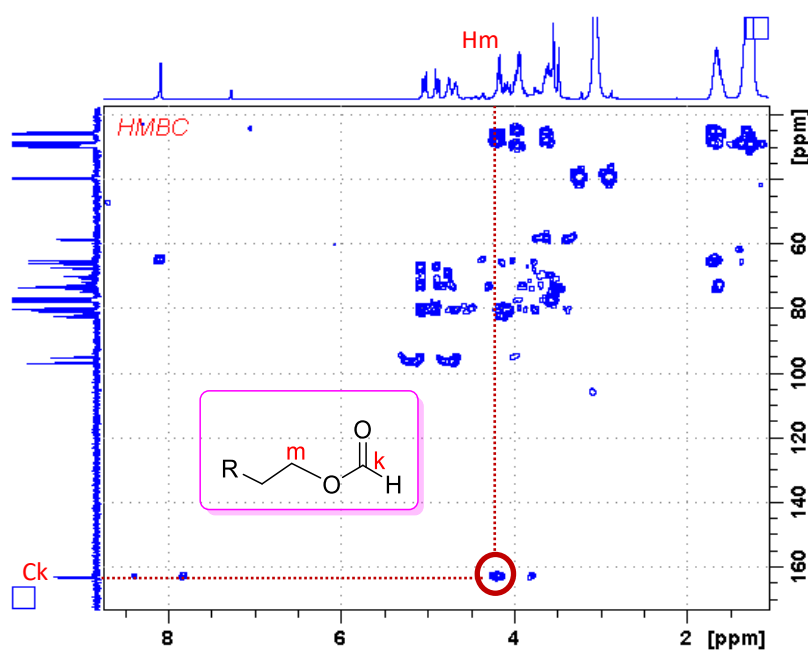


Figure 3.9. Long-range C-H correlation (HMBC) NMR spectrum of acid (MSA) induced degradation of **P5(2a-3c)** in CDCl_3 (500 MHz at 298 K).

3.4. Experimental Section:

3.4.1. General Methods and Material:

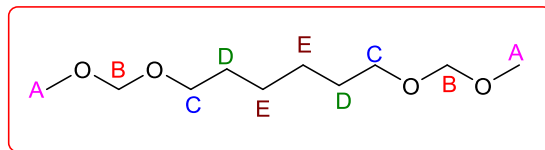
Manipulation involving moisture sensitive compounds were carried out under inert gas atmosphere using standard Schlenk techniques or glove box. Tetrahydrofuran was distilled from sodium/benzophenone under inert conditions. All other solvents were used as received without further purification. Isomannide, Isosorbide, 1,12-dodecanediol, sodium hydride, sodium methoxide, deuterated chloroform, were purchased from Sigma Aldrich and used without further purification. 1,6-hexanediol, 1, 8-octanediol were purchased from Alfa Aesar and used without

further purification. Chloromethyl methyl ether, methanesulfonic acid, p-Toluenesulfonic acid monohydrate, dimethoxymethane, diethyl azodicarboxylate, triphenyl phosphine, benzoic acid, hydrochloric acid (4M in dioxane) were purchased from Spectrochem Pvt. Ltd. and used without further purification. Isoidide was prepared from isomannide using a reported procedure.³³ NMR spectra were recorded on a Bruker Avance 200, 400, 500 instruments. Chemical shifts are referenced to external reference TMS (¹H and ¹³C). Coupling constants are given as absolute values. Mass spectra were recorded on Thermo scientific Q-Exactive mass spectrometer, with a Hypersil gold C18 column 150 x 4.6 mm diameter 8 μm particle size. The mobile phase used is 90% methanol + 10 % water + 0.1 % formic acid. Differential scanning calorimetric (DSC) analysis was carried out on DSC Q-100 from TA instruments with a heating and cooling rate of 10K min⁻¹. Thermo-gravimetric analysis (TGA) was carried out on TA instrument TGA Q5000 under nitrogen atmosphere. Elemental analysis was recorded on Flash EA 1112 series. MALDI-ToF-MS was performed on AB SCIEX TOF/TOF™ 5800 and matrix used is dithranol. GPC measurement was carried out on a Thermo Quest (TQ) GPC at 25 °C using chloroform (Merck, Lichrosolv) as the mobile phase. The analysis were carried out at a flow rate 1 mL/min using a set of five μ-styragel HT columns (HT-2 to HT-6) and a refractive index (RI) detector. This column set enabled the determination of wide range of molecular weight from 10² to 10⁶. Columns were calibrated with polystyrene standard and the molecular weights reported were with respect to polystyrene standard.

3.4.2. Acid Catalyzed Synthesis of Diacetals:

3.4.2.1. Synthesis of 1, 6-Hexanediactal (3a):

To a dichloromethane solution (100 mL) of 1, 6-hexanediol (5 g; 42.37 mmol) was added dimethoxymethane (20 mL; 223.1 mmol) and methanesulfonic acid (0.55 mL; 8.47 mmol; 20 mol%), and the mixture was stirred for 24 hours at room temperature. Subsequently, the reaction was quenched by adding ammonium hydroxide solution (0.55 mL, 25% solution), followed by washing with saturated sodium chloride solution (50 mL). The aqueous phase was extracted with ethyl acetate (3 × 50 mL) and the combined organic phase was dried over MgSO₄, filtered and the filtrate evaporated to obtain a colourless oily liquid. Purification by column chromatography (pet ether: ethyl acetate 90:10) yielded 4.0 g (46%) of colourless oily liquid.



$^1\text{H NMR}$ (400 MHz, CDCl_3 , 298 K) δ = 4.59 (s, 4H_B), 3.50 (t, $J_{\text{H-H}}$ = 6.6 Hz, 4H_C), 3.34 (s, 6H_A), 1.64-1.53 (m, 4H_D), 1.43-1.33 (m, 4H_E). $^{13}\text{C NMR}$ (100 MHz, CDCl_3 , 298 K) δ = 96.6 (s, C_B), 67.9 (s, C_C), 55.3 (s, C_A), 29.9 (s, C_D), 26.2 (s, C_E). **ESI-MS** (+ve mode) m/z : calculated for $\text{C}_{10}\text{H}_{22}\text{O}_4$, 206.15; found 229.14 $[\text{M}+\text{Na}]^+$. **Elemental analysis** (%) calculated for $\text{C}_{10}\text{H}_{22}\text{O}_4$: C 58.23, H 10.75; Found: C 58.61, H 10.93.

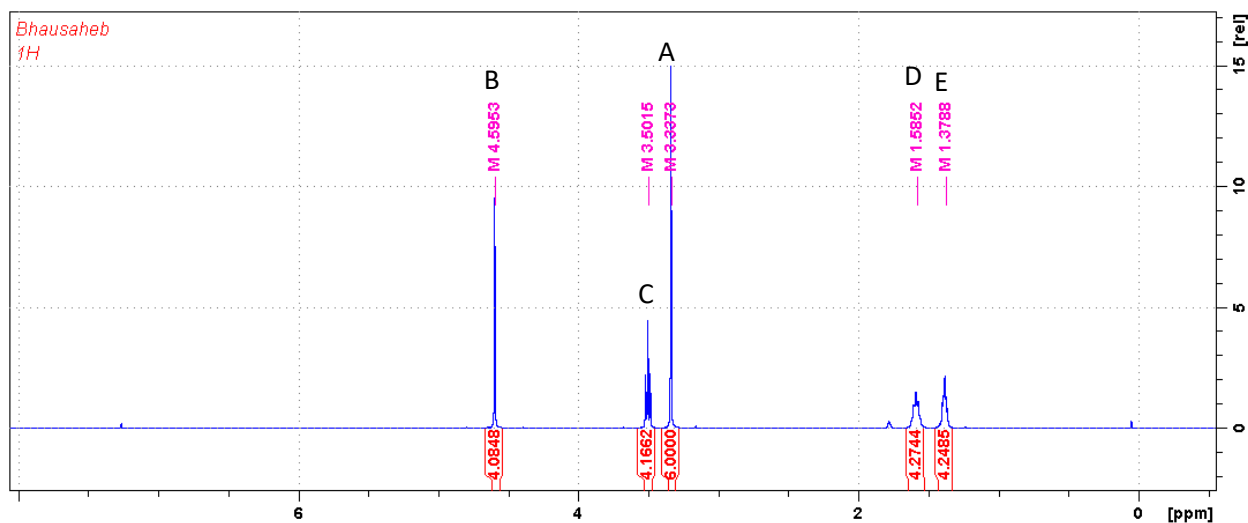


Figure 3.10. $^1\text{H NMR}$ spectrum of **3a** in CDCl_3 (400 MHz at 298 K).

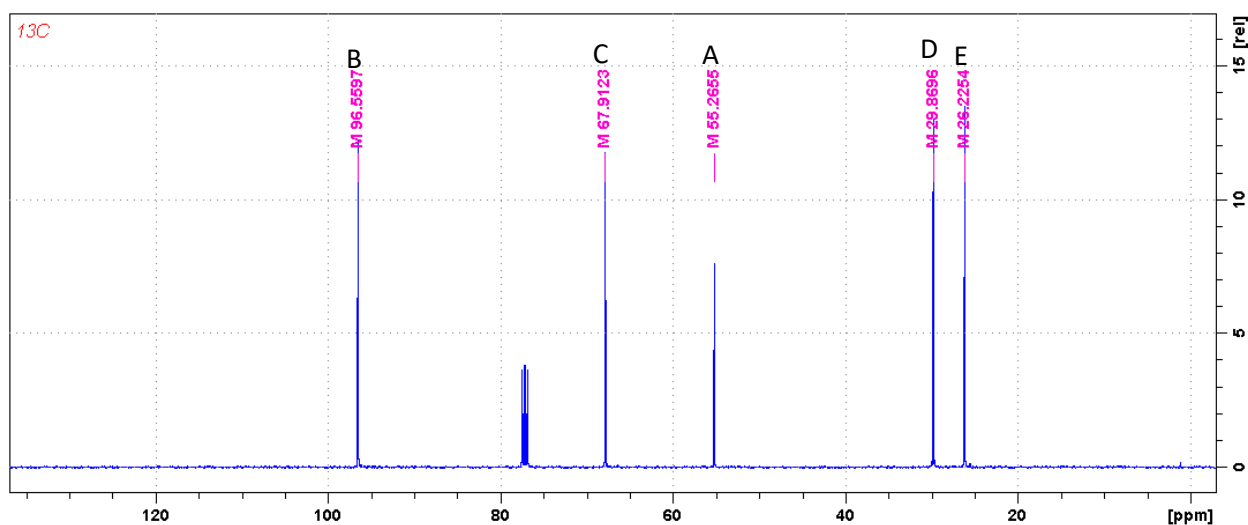


Figure 3.11. $^{13}\text{C NMR}$ spectrum of **3a** in CDCl_3 (100 MHz at 298 K).

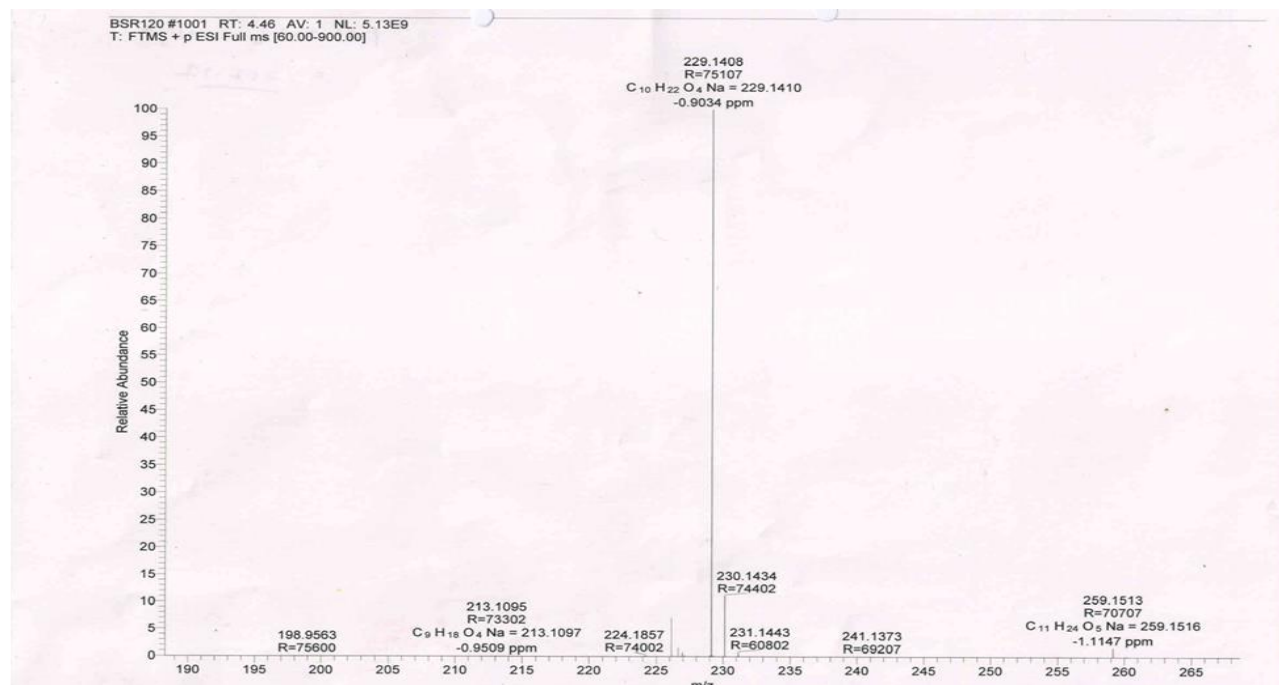
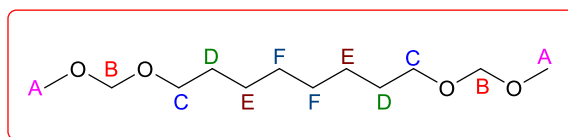


Figure 3.12. ESI-MS (+ve) spectrum of **3a** 229.14 [M +Na]⁺.

3.4.2.2. Synthesis of 1, 8-Octanediactal (3b):

Dimethoxymethane (20 mL; 223.1 mmol) and methanesulfonic acid (0.44 mL; 6.84 mmol; 20 mol %) were added to a dichloromethane solution (100 mL) of 1, 8-octanediol (5 g; 34.19 mmol) and the mixture was stirred for 24 hours at room temperature to give a clear solution. Subsequently, the reaction was quenched by adding ammonium hydroxide solution (0.44 mL, 25 % solution) followed by washing with saturated sodium chloride solution (50 mL). The aqueous phase was extracted with ethyl acetate (3 × 50 mL) and the combined organic phase was dried over MgSO₄, filtered and the filtrate evaporated to obtain a colourless oily liquid. Purification by column chromatography (pet ether: ethyl acetate 90:10) yielded 4.6 g (57%) of liquid oily product.



¹H NMR (500 MHz, CDCl₃, 298 K) δ = 4.54 (s, 4H_B), 3.44 (t, *J*_{H-H} = 6.5 Hz, 4H_C), 3.28 (s, 6H_A), 1.59-1.45 (m, 4H_D), 1.36-1.23 (m, 8H_{E+F}). ¹³C NMR (125 MHz, CDCl₃, 298K) δ = 96.5 (s, C_B), 67.9 (s, C_C), 55.1 (s, C_A), 29.8 (s, C_D), 29.5 (s, C_E), 26.3 (s, C_F). **ESI-MS** (+ve mode) m/z: calculated for C₁₂H₂₆O₄, 234.18; found 257.17 [M+Na]⁺. **Elemental analysis** (%) calculated for C₁₂H₂₆O₄: C 61.51, H 11.18; Found: C 61.99, H 11.51.

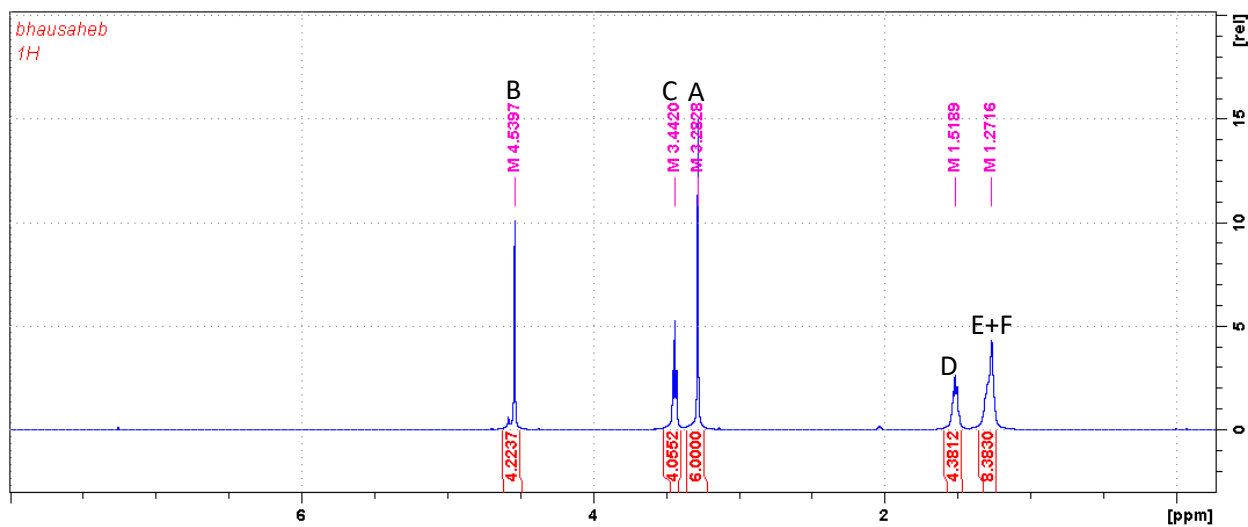


Figure 3.13. ^1H NMR spectrum of **3b** in CDCl_3 (500 MHz at 298 K).

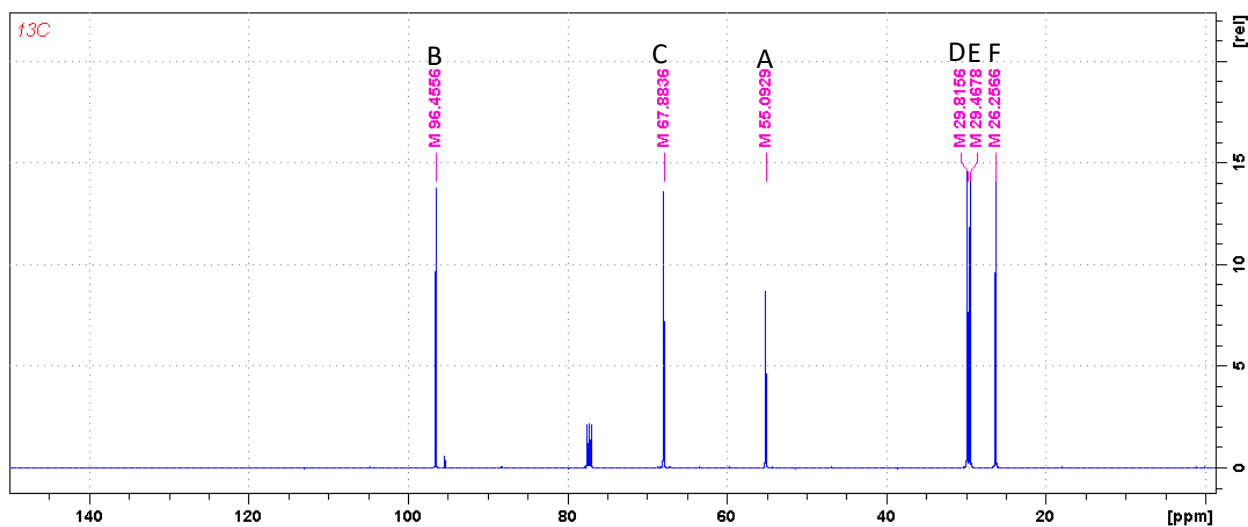


Figure 3.14. ^{13}C NMR spectrum of **3b** in CDCl_3 (125 MHz at 298 K).

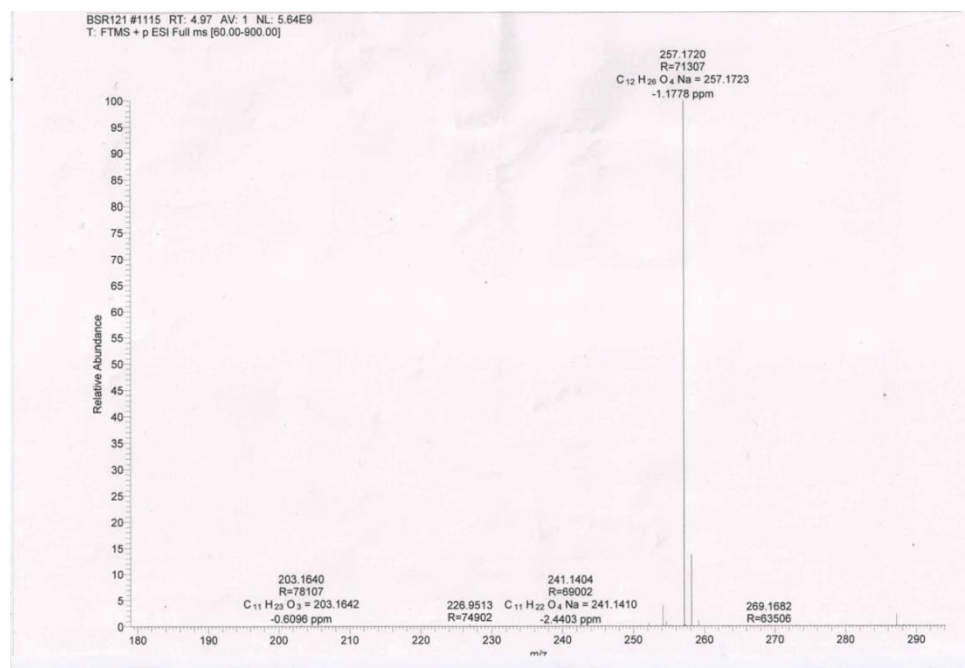


Figure 3.15. ESI-MS spectrum of **3b** $m/z = 257.17$ $[M+Na]^+$.

3.4.3. Acetal Metathesis Copolymerization (AMCP):

The copolyacetals were prepared in a 50 ml Schlenk tube equipped with an overhead mechanical stirrer, heating arrangement and vacuum line. Isohexide-diacetals and linear-diacetals were transferred to the Schlenk tube and *p*-Toluenesulfonic acid was added under positive argon flow. The copolymerization was started by heating the monomer mixture (neat monomers) at 60 °C which was raised to 90 °C over a period of an hour. During the initial 30 minutes the reaction vessels was shortly evacuated after every 3 minute to remove dimethoxymethane. Note that; over evacuation might lead to the loss of short-chain diacetals such as **3a**, **3b** and might create stoichiometric imbalance in the system. Finally, the copolymer melt was stirred for 6 to 12 hours under reduced pressure (0.01 mbar), and the copolymer was recovered. The thus obtained copolymer was dissolved in chloroform and precipitated by pouring in methanol. The resultant solid/semisolid material was dried in vacuum. The quantitative details and reaction parameters are summarized in **Table 3.2** and **Table 3.3** respectively. Representative analytical data and detail spectra for the herein synthesized copolyacetals is supplied in the following sections.

Table 3.2. Copolymerization of isohexide-diacetals (**2a-c**) with linear diacetals (**3a-e**).

Polymers	2a-c (mmol)	3a-e g(mmol)	<i>p</i> -TSA (mmol)	Time (h)
P3(2a-3a)	1.0(4.27)	0.88(4.27)	0.42	12
P4(2a-3b)	1.0(4.27)	0.99(4.27)	0.42	6
P5(2a-3c)	1.0(4.27)	1.24(4.27)	0.42	12
P6(2a-3d)	0.20(0.89)	0.34(0.89)	0.089	12
P7(2a-3e)	0.5(2.13)	0.95(2.13)	0.213	12
P8(2b-3a)	0.71(2.99)	0.61(2.99)	0.29	12
P9(2b-3b)	1.0(4.27)	1.0(4.27)	0.42	12
P10(2b-3c)	1.0(4.27)	1.24(4.27)	0.21	12
P11(2b-3d)	0.80(2.57)	0.48(2.57)	0.20	12
P12(2b-3e)	0.5(2.13)	0.95(2.13)	0.21	12
P13(2c-3a)	0.70(2.99)	0.61(2.99)	0.29	12
P14(2c-3b)	0.94(4.02)	0.94(4.02)	0.40	12
P15(2c-3c)	0.88(3.76)	1.09(3.76)	0.37	12
P16(2c-3d)	0.58(2.47)	0.95(2.47)	0.24	12
P17(2c-3e)	0.5(2.13)	0.94(2.13)	0.21	12

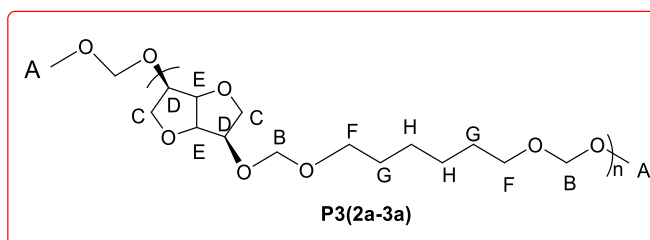
Table 3.3. Copolymerization conditions and brief polymerization protocol.

Copolyacetals	Copolymerization protocol
P3(2a-3a)	Temperature was raised from 60 °C-90 °C over a period of 1 hour, along with vacuum-argon purge cycles. Finally constant vacuum of 0.01 mbar was maintained at 90 °C for next 11 hours to give highly viscous copolymer.
P4(2a-3b)	Same as above, except; constant vacuum of 0.01 mbar was maintained at 90 °C for 5 hours to give highly viscous copolymer.
P5(2a-3c)	Temperature was raised from 60 °C-110 °C over a period of 1 hour, along with vacuum-argon purge cycles. Finally constant vacuum of 0.01 mbar was maintained at 110 °C for next 11 hours to obtain solid copolymer mass.
P6(2a-3d)	Same as P3(2a-3a) ; except that a solid copolymer was obtained.

P7(2a-3e)	Same as P6(2a-3d) .
P8(2b-3a)	Same as P3(2a-3a) .
P9(2b-3b)	Same as P3(2a-3a) .
P10(2b-3c)	Same as P3(2a-3a) ; except that a solid copolymer was obtained.
P11(2b-3d)	Same as P3(2a-3a) ; except that a solid copolymer was obtained.
P12(2b-3e)	Same as P3(2a-3a) ; except that a solid copolymer was obtained.
P13(2c-3a)	Same as P3(2a-3a) .
P14(2c-3b)	Same as P3(2a-3a) .
P15(2c-3c)	Same as P3(2a-3a) ; except that a solid copolymer was obtained.
P16(2c-3d)	Same as P3(2a-3a) ; except that a solid copolymer was obtained.
P17(2c-3e)	Same as P3(2a-3a) ; except that a solid copolymer was obtained.

3.4.3.1. Copolymerization of Isomannide-Diacetal (2a) with Linear Diacetals (3a-e) to P3(2a-3a)-P7(2a-3e):

P3(2a-3a):



$^1\text{H NMR}$ (200 MHz, CDCl_3 , 298 K) δ = 4.82 (br., s, H_B), 4.53 (m, H_E), 4.28 (m, H_D), 4.00 (br. s, H_C), 3.78 (br., s, H_C), 3.64 (t, $J_{\text{H-H}} = 7.7$ Hz, H_F), 1.61 (br., s, H_G), 1.36 (br., s, H_H).

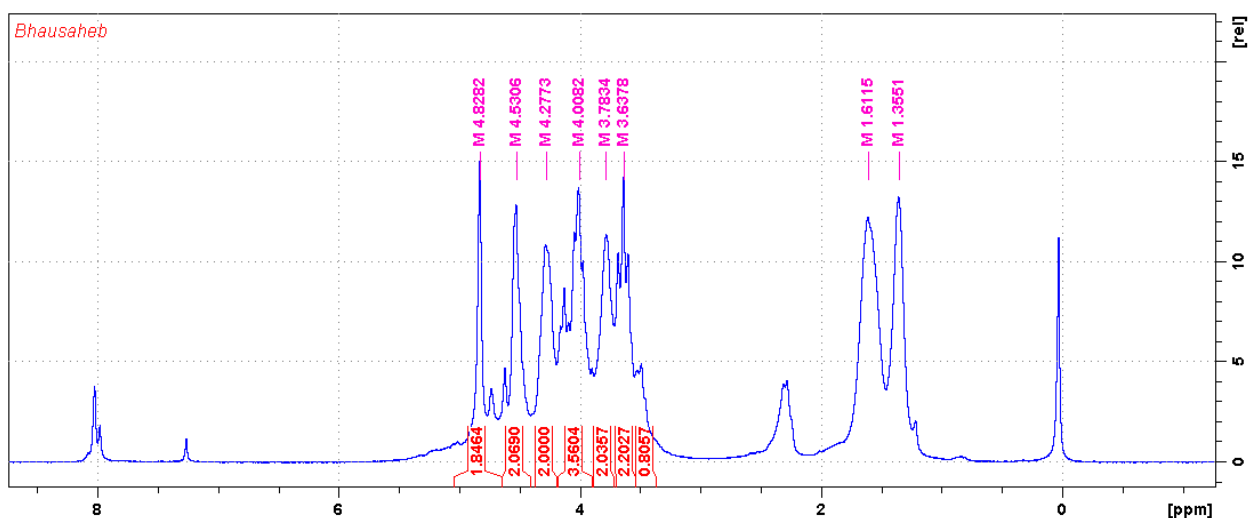


Figure 3.16. ^1H NMR spectrum of **P3(2a-3a)** in CDCl_3 (200 MHz at 298 K).

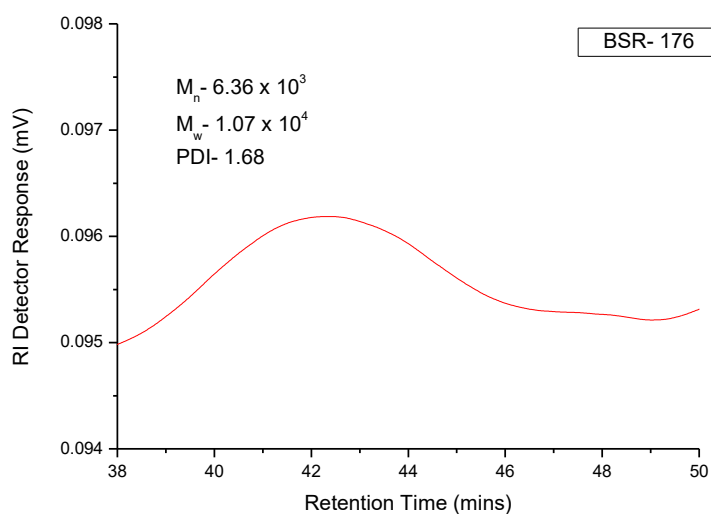
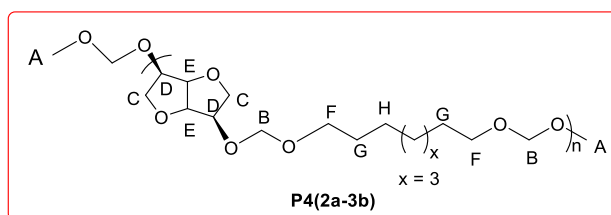


Figure 3.17. GPC chromatogram of **P3(2a-3a)** in chloroform at room temperature.

P4(2a-3b):



^1H NMR (500 MHz, CDCl_3 , 298 K) δ = 4.82-4.61 (m, H_B), 4.53 (br., s, H_E), 4.27(br., s, H_D), 4.00(br., s, H_C), 3.63 (br., s, H_C), 3.47 (br., s, H_F), 1.53 (br., s, H_G), 1.28 (br., s, H_H). ^{13}C

NMR (125 MHz, CDCl₃, 298 K) δ = 95.3-95.0 (br., s, C_B), 80.8 (s, C_E), 78.1 (s, C_D), 75.3 (s, C_C), 71.1 (s, C_C), 67.9 (s, C_F), 29.8-29.5 (m, C_G), 26.3 (br., s, C_H).

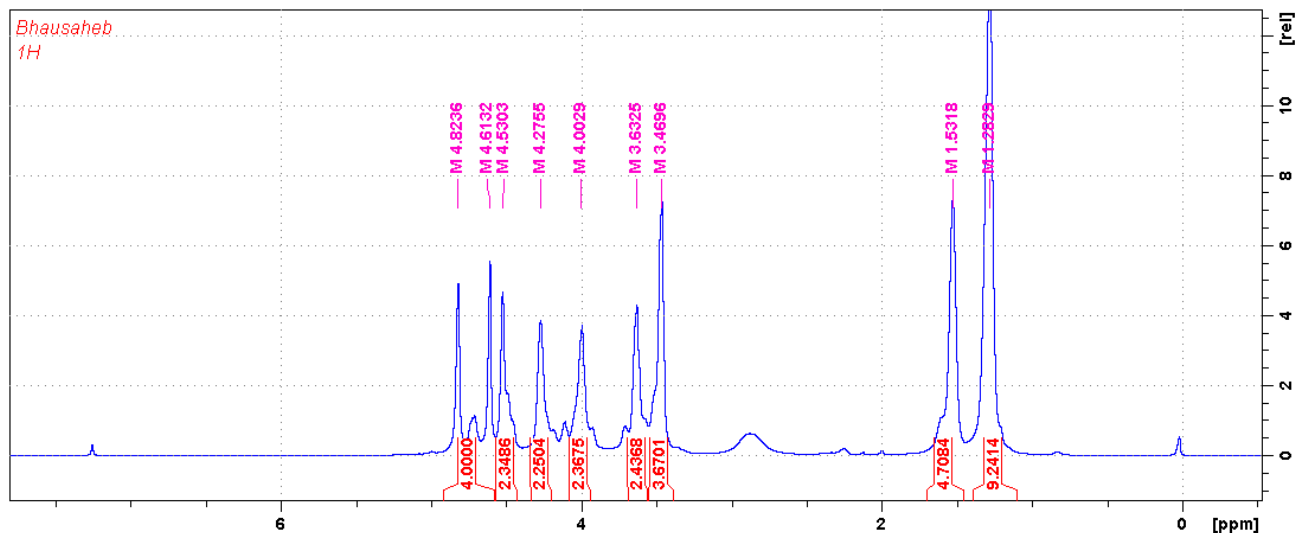


Figure 3.18. ¹H NMR spectrum of P4(2a-3b) in CDCl₃ (500MHz, at 298 K).

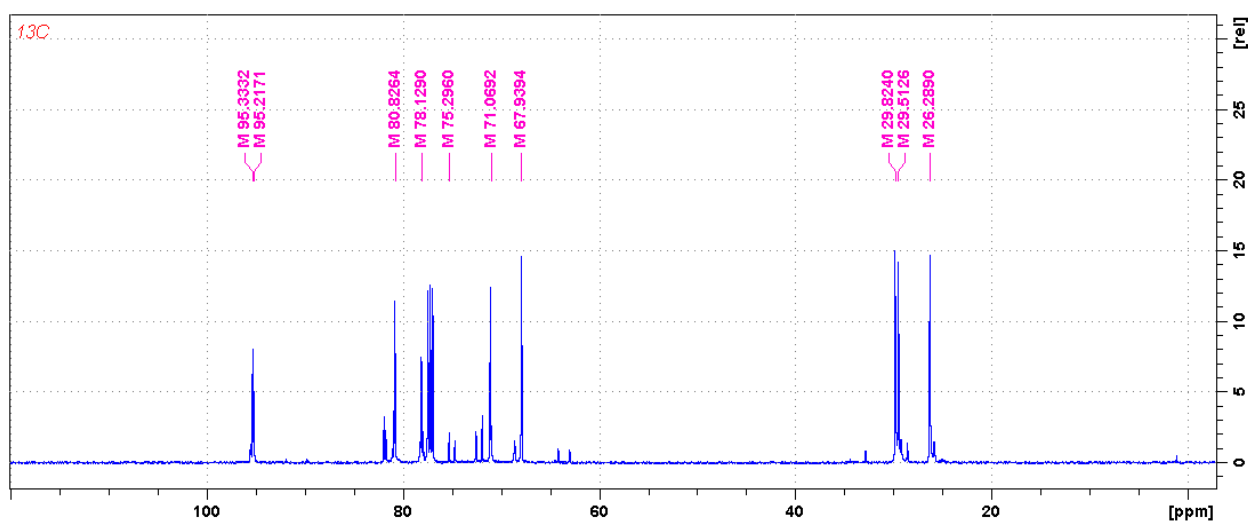


Figure 3.19. ¹³C NMR spectrum of P4(2a-3b) in CDCl₃ (125 MHz at 298 K).

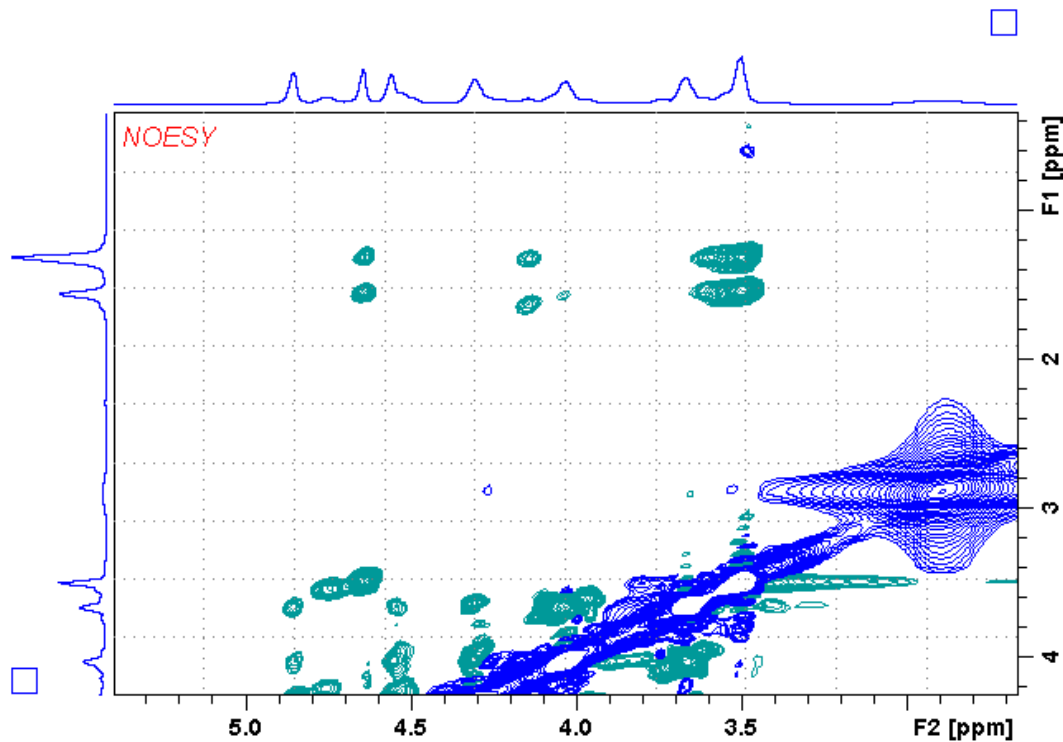


Figure 3.20. ^1H (NOESY) spectrum of **P4(2a-3b)** in CDCl_3 at (500 MHz at 298 K).

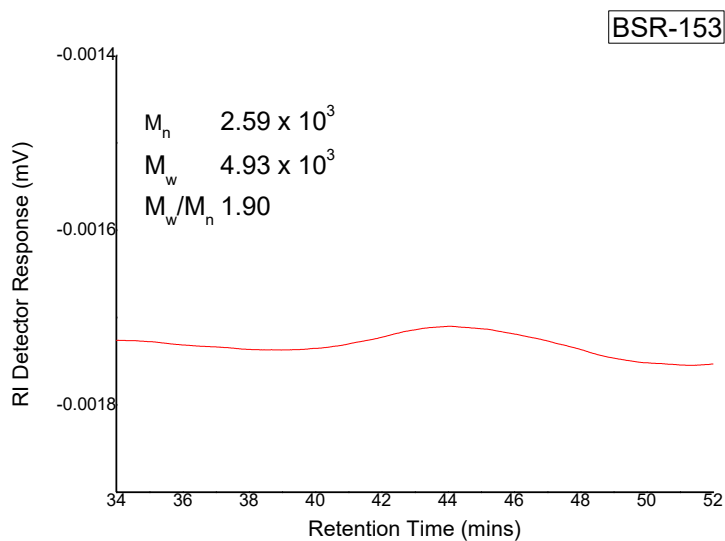
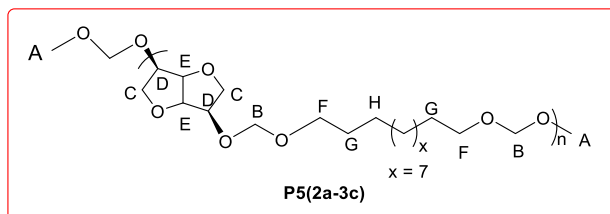


Figure 3.21. GPC chromatogram of **P4(2a-3b)** in chloroform at room temperature.

P5(2a-3c):

^1H NMR (500 MHz, CDCl_3 , 298 K) $\delta = 4.85\text{--}4.63$ (m, H_B), 4.54 (m, H_E), 4.29 (m, H_D), 4.01 (m, H_C), 3.65 (m, H_C), 3.48 (t, $J_{\text{H-H}} = 6.65$ Hz, H_F), 1.54 (br., s, H_G), 1.24 (br., s, H_H).

^{13}C NMR (125 MHz, CDCl_3 , 298 K) $\delta = 95.4$ (s, C_B), 81.8–80.9 (s, C_E), 78.2 (s, C_D), 75.4–74.8 (s, C_C), 71.1 (s, C_C), 67.9 (s, C_F), 29.8 (s, C_G), 26.4 (s, C_H).

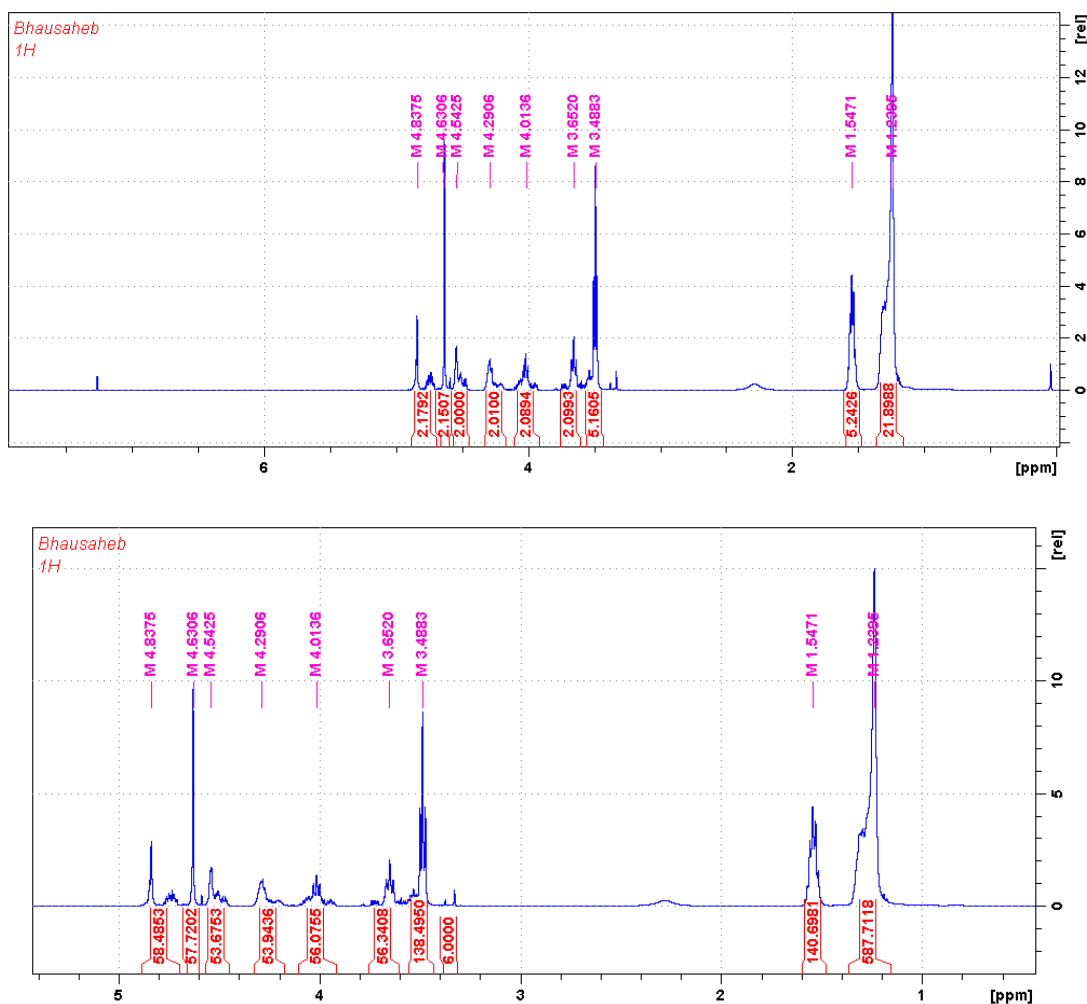


Figure 3.22. ^1H NMR spectrum of **P5(2a-3c)** in CDCl_3 (top) and determination of molecular weight by proton NMR (bottom) (500 MHz at 298 K).

Determination of molecular weight by proton NMR: The total number of protons in **Figure 3.22-bottom** is 1197 and number of protons in polymer repeat unit is 36.

Therefore, the number of repeat units in **P5(2a-3c)** = Total number of protons in **Figure 3.22** (bottom) divided by total number of protons in the repeat unit, i.e. $1197/36 = 33$.

Hence, molecular weight of the copolyacetal = number of repeat units multiplied by molar mass of the repeat unit, i.e. $33 \times 372 = 12276 \sim \mathbf{12300}$ g/mol.

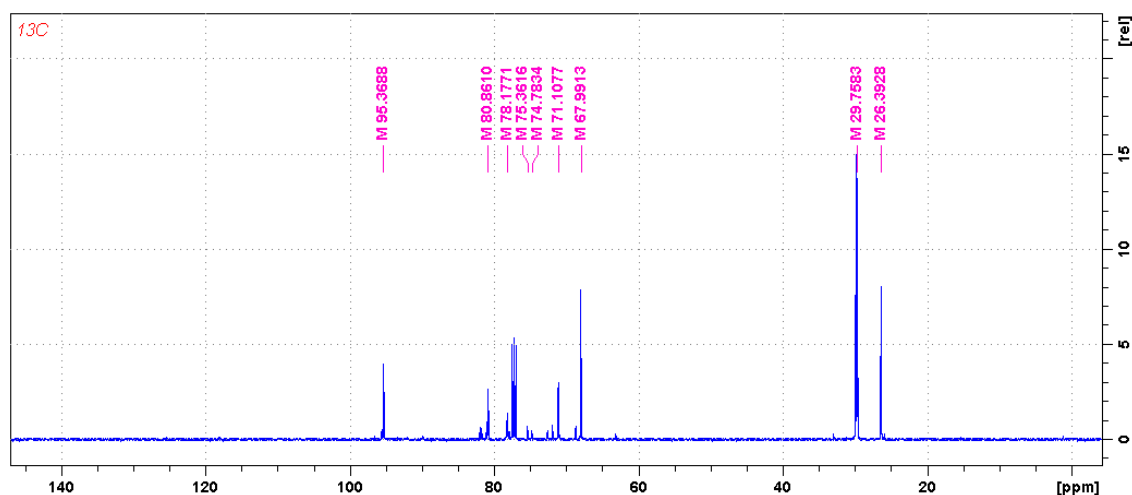


Figure 3.23. ^{13}C NMR spectrum of **P5(2a-3c)** in CDCl_3 (125 MHz at 298 K).

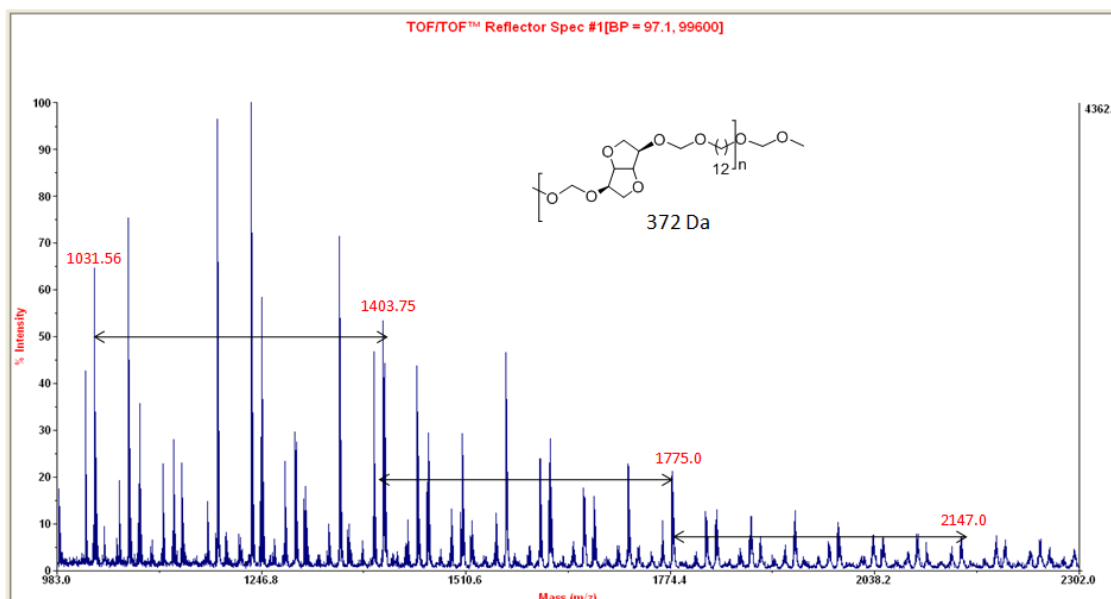


Figure 3.24. MALDI-ToF-MS spectrum of **P5(2a-3c)** recorded in dithranol.

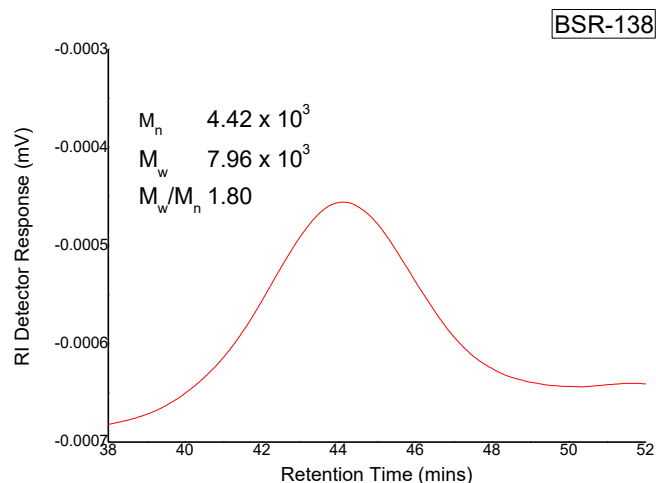
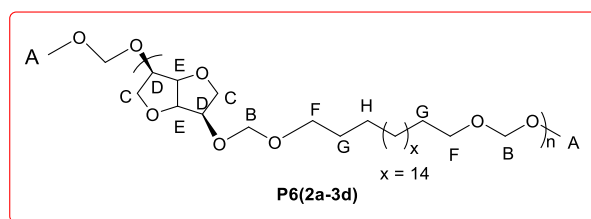


Figure 3.25. GPC chromatogram of **P5(2a-3c)** in chloroform at room temperature.

P6(2a-3d):



$^1\text{H NMR}$ (200 MHz, CDCl_3 , 298 K) $\delta = 4.88\text{--}4.65$ (m, H_B), 4.54 (br., s, H_E), 4.28 (br., s, H_D), 4.04 (br., s, H_C), 3.62 (m, H_C), 3.51 (m, H_F), 1.56 (br., s, H_G), 1.24 (br., s, H_H).

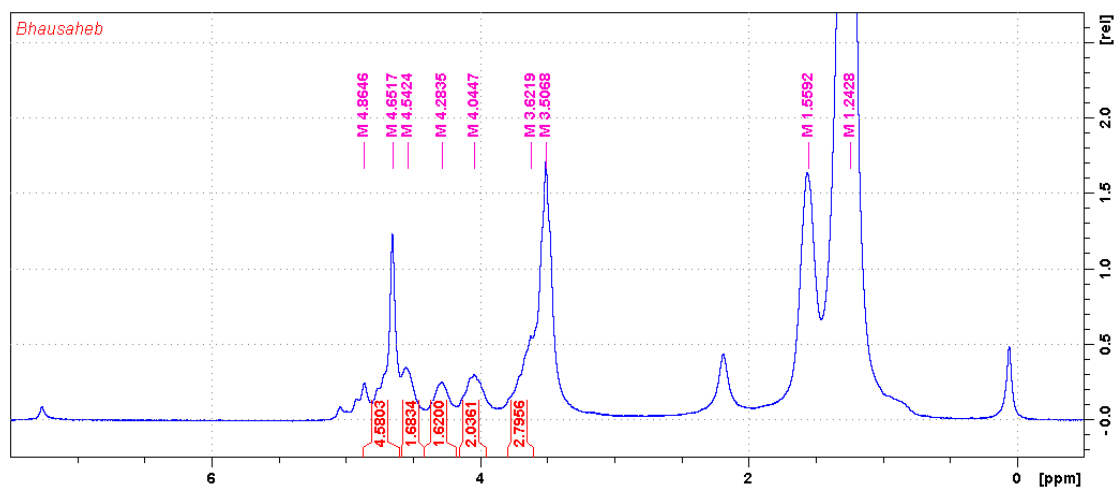


Figure 3.26. $^1\text{H NMR}$ spectrum of **P6(2a-3d)** in CDCl_3 (200 MHz at 298 K).

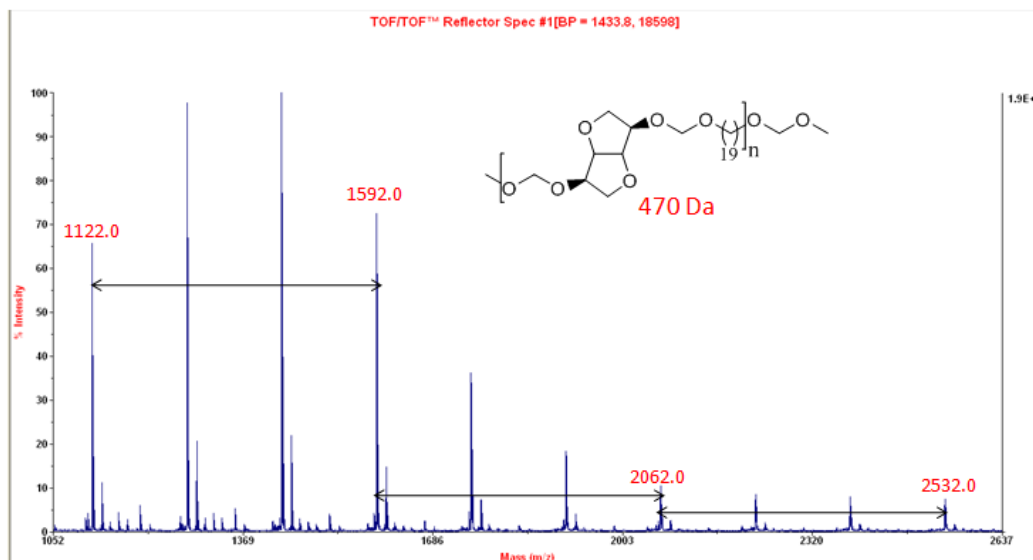


Figure 3.27. MALDI-ToF-MS spectrum of P6(2a-3d) recorded in dithranol.

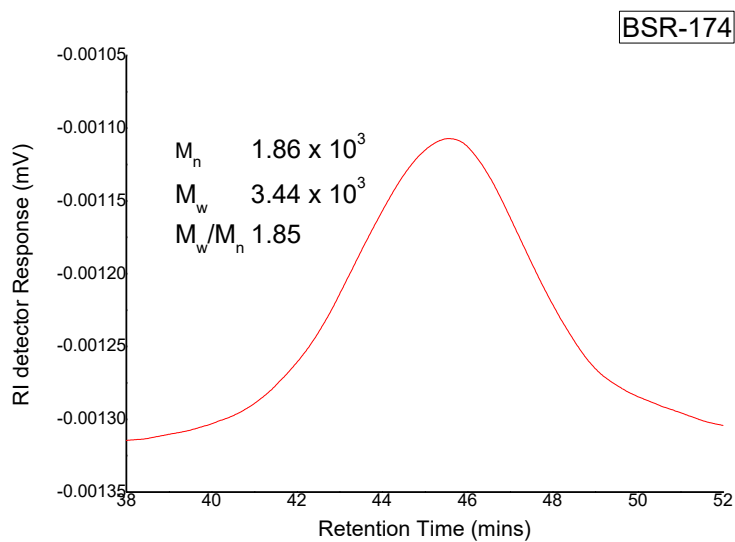
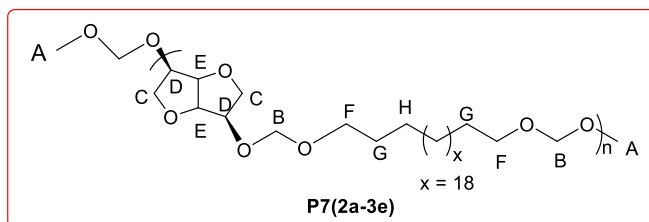


Figure 3.28. GPC chromatogram of P6(2a-3d) in chloroform at room temperature.

P7(2a-3e):

$^1\text{H NMR}$ (200 MHz, CDCl_3 , 298 K) δ = 4.87-4.65 (m, H_B), 4.57-4.49 (m, H_E), 4.30 (br., s, H_D), 4.03 (br., s, H_C), 3.67 (br., s, H_C), 3.51 (t, $J_{\text{H-H}} = 6.63$ Hz, H_F), 1.57 (br., s, H_G), 1.24 (m, H_H). $^{13}\text{C NMR}$ (50 MHz, CDCl_3 , 298 K) δ = 95.3 (s, C_B), 81.9-80.9 (m, C_E), 78.2 (s, C_D), 74.9 (s, C_C), 71.2 (s, C_C), 68.1 (s, C_F), 29.9 (s, C_G), 26.5 (s, C_H).

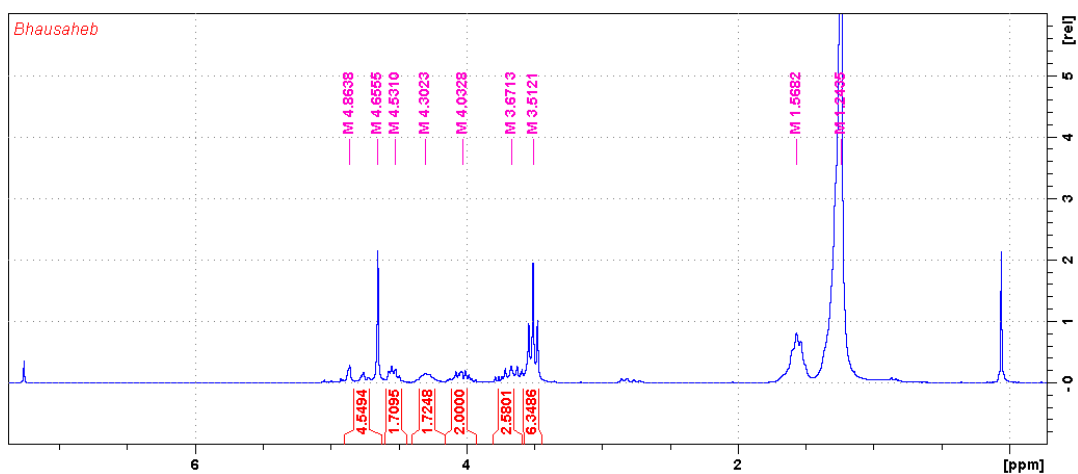


Figure 3.29. $^1\text{H NMR}$ spectrum of **P7(2a-3e)** in CDCl_3 (200 MHz at 298 K).

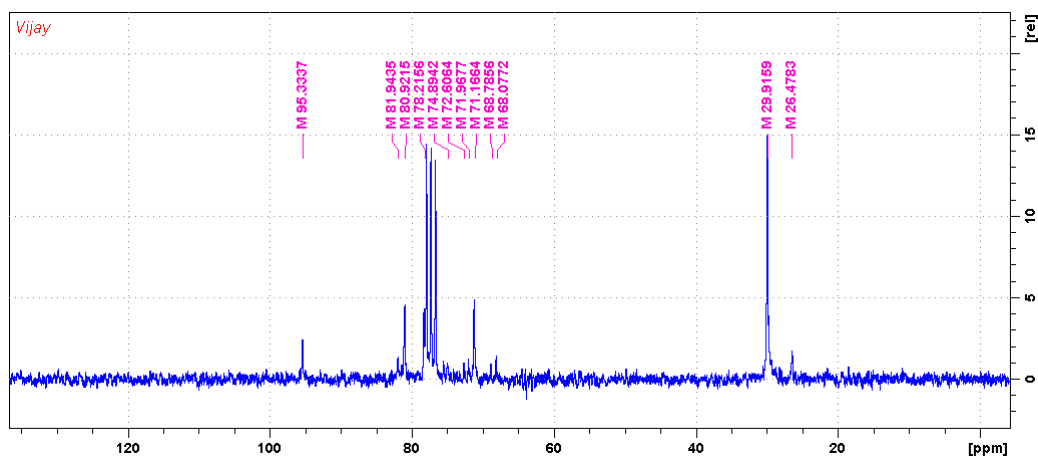


Figure 3.30. $^{13}\text{C NMR}$ spectrum of **P7(2a-3e)** in CDCl_3 (50 MHz at 298 K).

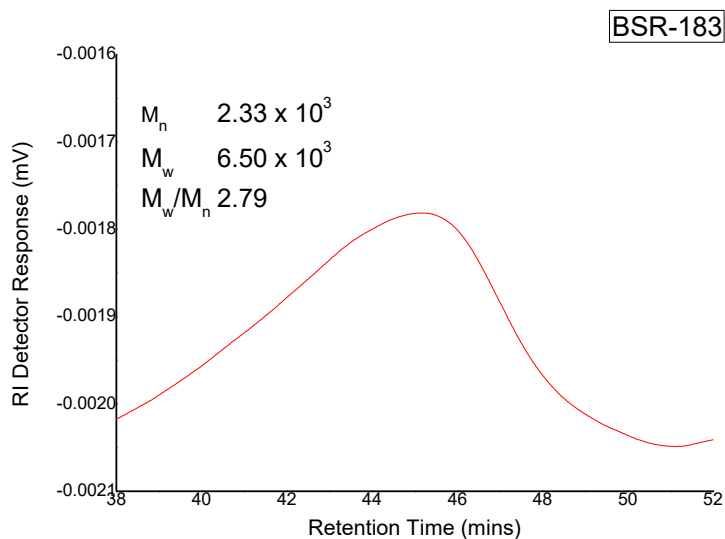
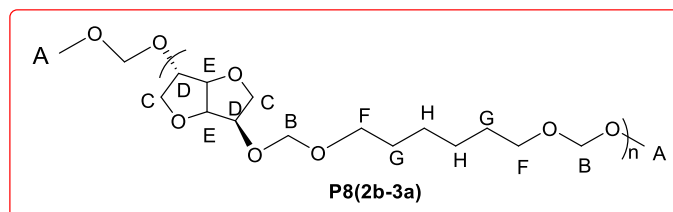


Figure 3.31. GPC chromatogram of **P7(2a-3e)** in chloroform at room temperature.

3.4.3.2. Copolymerization of Isosorbide-Diacetal (**2b**) with Linear Diacetals (**3a-e**) to **P8(2b-3a)**-**P12(2b-3e)**:

P8(2b-3a):



$^1\text{H NMR}$ (200 MHz, CDCl_3 , 298 K) δ = 4.85-4.74 (m, H_B), 4.53-4.33 (m, H_E), 4.33-4.25 (m, H_D), 4.24-4.08 (m, H_{E+D}), 4.07-3.81 (m, H_C), 3.70-3.41 (m, H_{C+F}), 1.58 (m, H_G), 1.37 (m, H_H).

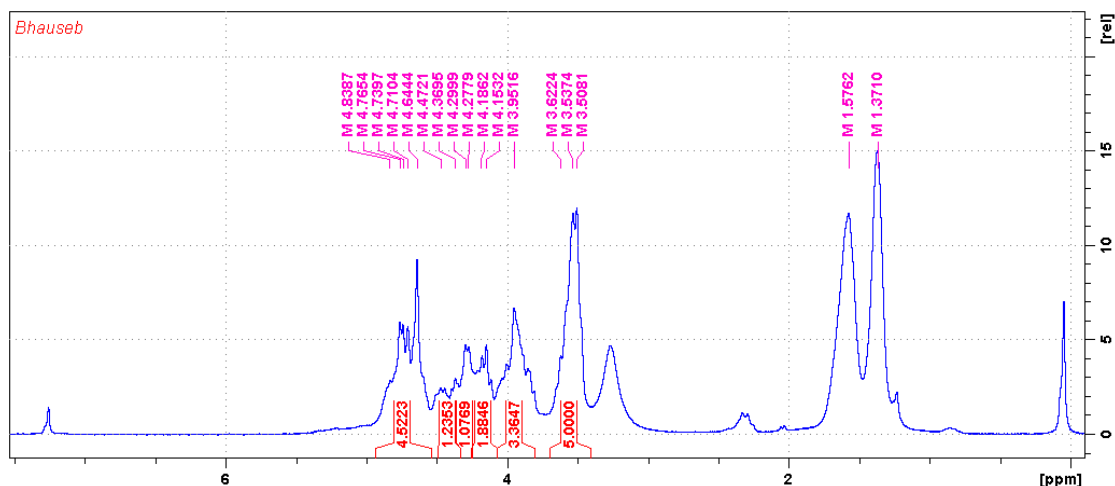


Figure 3.32. ^1H NMR spectrum of **P8(2b-3a)** in CDCl_3 (200 MHz at 298 K).

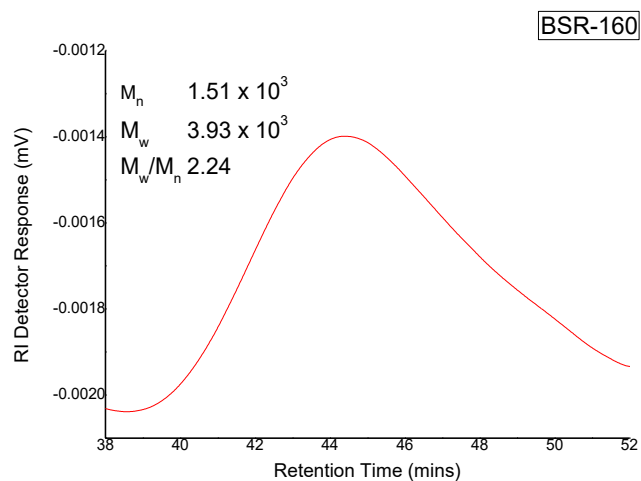
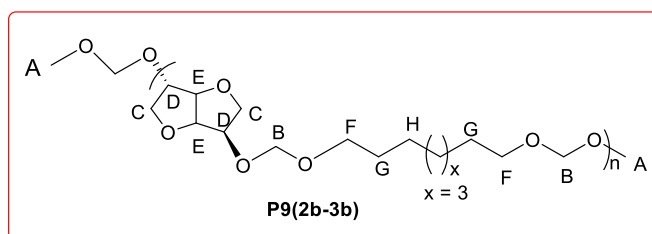


Figure 3.33. GPC chromatogram of **P8(2b-3a)** in chloroform at room temperature.

P9(2b-3b):



^1H NMR (200 MHz, CDCl_3 , 298 K) δ = 4.87-4.53 (m, H_B), 4.53-4.45 (m, H_E), 4.44-4.32 (m, H_D), 4.14 (br., s, H_{E+D}), 3.86 (br., s, H_C), 3.61-3.30 (m, H_{C+F}), 1.48 (m, H_G), 1.23 (m, H_H). ^{13}C NMR

(50 MHz, CDCl₃, 298 K) δ = 95.2-94.3 (m, C_B), 88.1 (s, C_E), 86.3 (s, C_D), 81.7-80.6 (m, C_E), 76.3-75.7 (m, C_D), 73.6-73.1 (m, C_C), 69.8 (s, C_C), 68.4-67.8 (m, C_F), 29.7-29.4 (m, C_G), 26.1-25.7 (m, C_H).

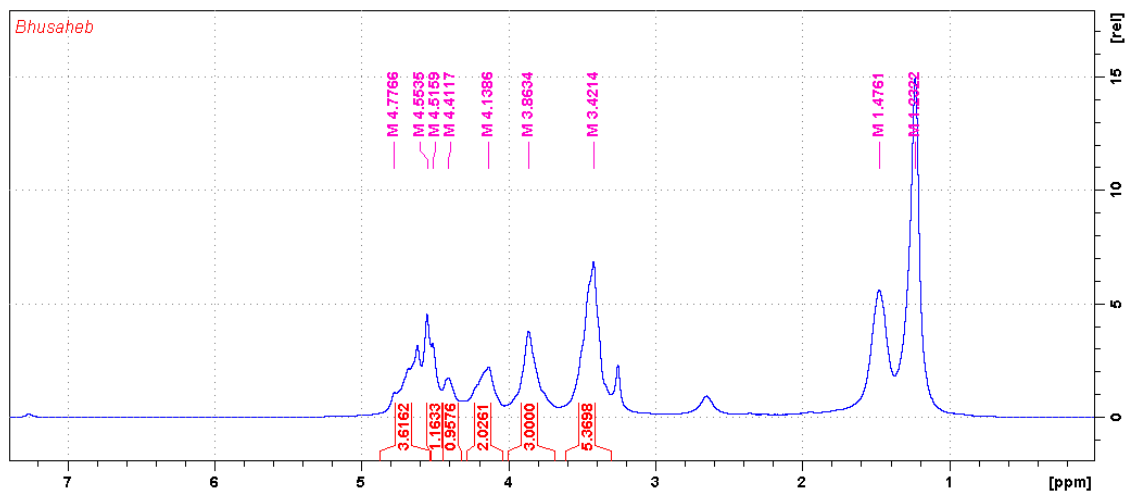


Figure 3.34. ¹H NMR spectrum of P9(2b-3b) in CDCl₃ (200 MHz at 298 K).

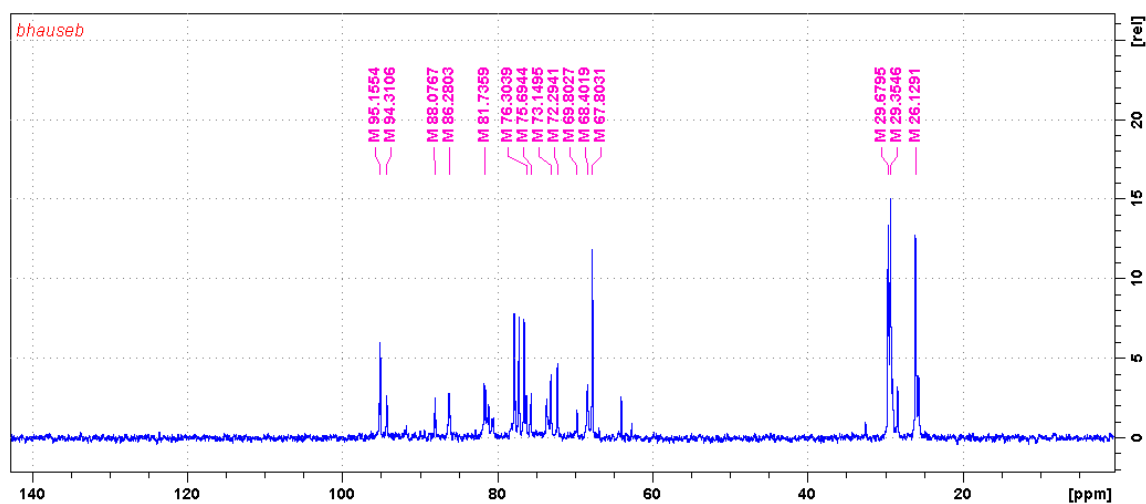


Figure 3.35. ¹³C NMR spectrum of P9(2b-3b) in CDCl₃ (50 MHz at 298 K).

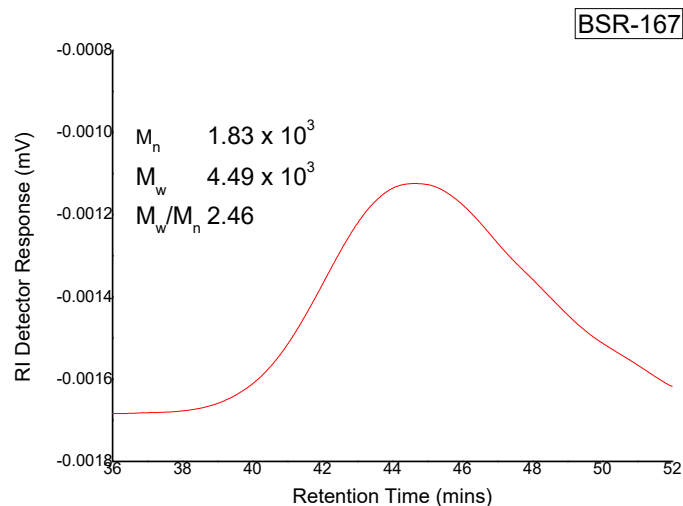
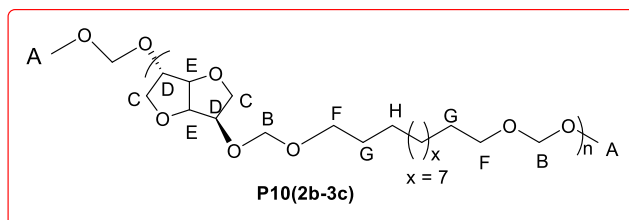


Figure 3.36. GPC chromatogram of **P9(2b-3b)** in chloroform at room temperature.

P10(2b-3c):



$^1\text{H NMR}$ (200 MHz, CDCl_3 , 298 K) $\delta = 4.88\text{-}4.60$ (m, H_B), $4.61\text{-}4.53$ (m, H_E), 4.48 (m, H_D), $4.34\text{-}4.11$ (m, H_{E+D}), $4.02\text{-}3.79$ (m, H_C), $3.64\text{-}3.38$ (m, H_{C+F}), 1.55 (br., s, H_G), 1.24 (m, H_H).

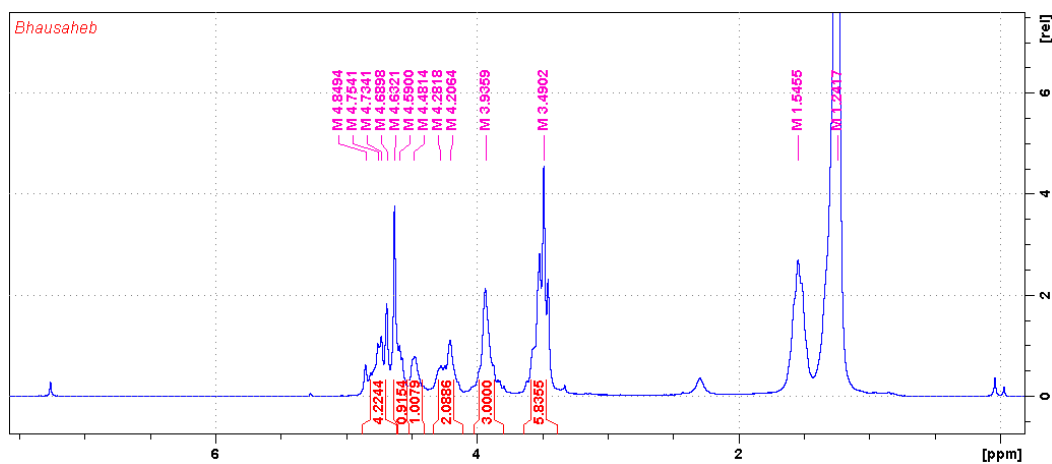


Figure 3.37. $^1\text{H NMR}$ spectrum of **P10(2b-3c)** in CDCl_3 (200 MHz at 298 K).

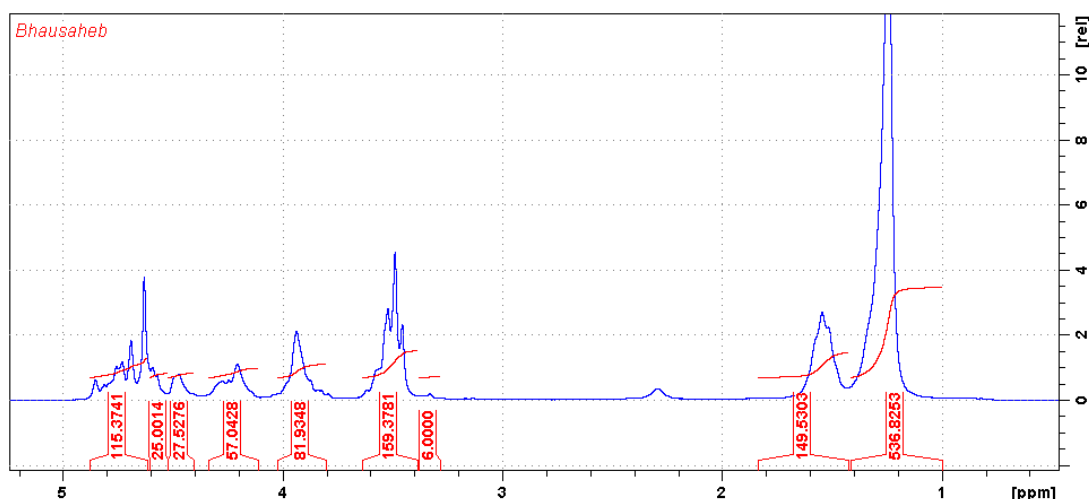


Figure 3.38. ^1H NMR spectrum of **P10(2b-3c)** in CDCl_3 (top), determination of molecular weight by NMR (bottom) (200 MHz at 298 K).

Determination of molecular weight by proton NMR: The total number of protons in **Figure 3.38-bottom** is 1152 and number of protons in polymer repeat unit is 36.

Therefore, the number of repeat units in **P10(2b-3c)** = Total number of protons in **Figure 3.38-bottom** divided by total number of protons in the repeat unit, i.e. $1152/36 = 32$.

Hence, molecular weight of the copolyacetal = number of repeat units multiplied by molar mass of the repeat unit, i.e. $32 \times 372 = 11904 \sim \mathbf{11900}$ g/mol.

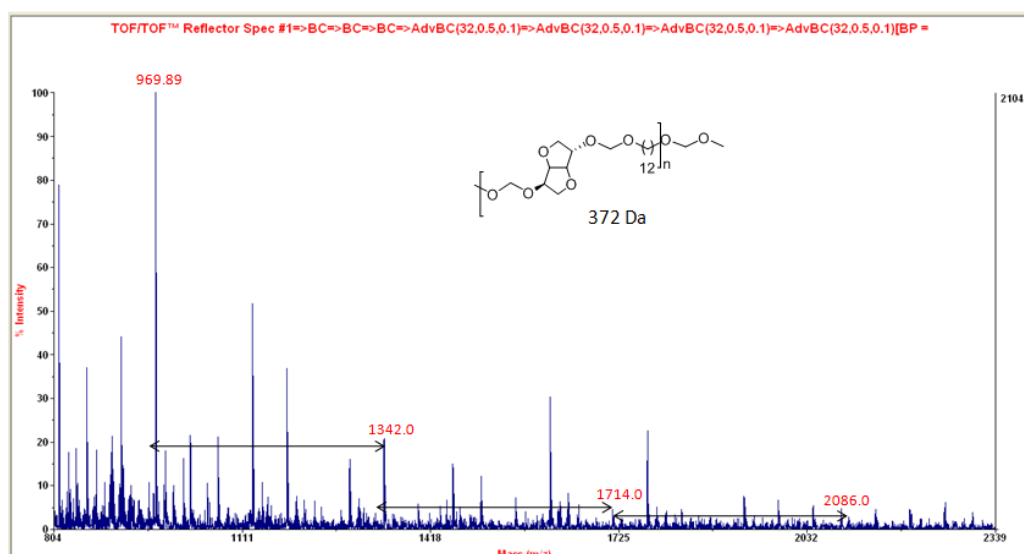


Figure 3.39. MALDI-ToF-MS spectrum of **P10(2b-3c)** recorded in dithranol.

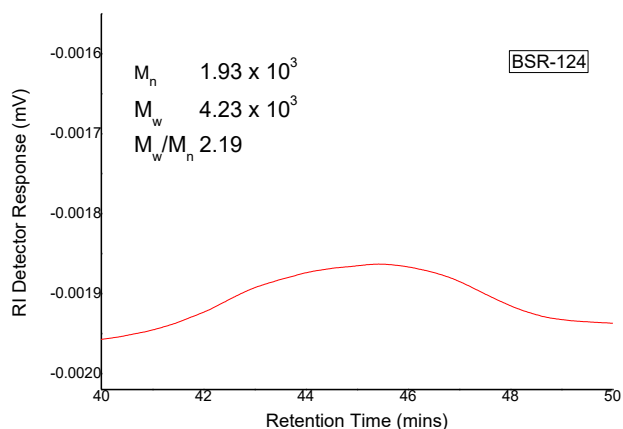
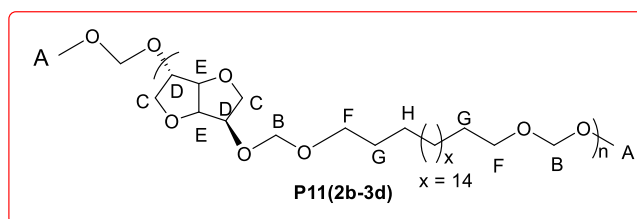


Figure 3.40. GPC chromatogram of **P10(2b-3c)** in chloroform at room temperature.

P11(2b-3d):



^1H NMR (500 MHz, CDCl_3 , 298 K) δ = 4.80-4.63 (m, H_B), 4.61 (br., s, H_E), 4.53-4.40 (m, H_D), 4.34-4.17 (m, $\text{H}_{\text{E}+\text{D}}$), 4.09-3.81 (m, H_C), 3.53-3.47 (m, $\text{H}_{\text{C}+\text{F}}$), 1.56 (br., s, H_G), 1.24 (br., s, H_H).
 ^{13}C NMR (125 MHz, CDCl_3 , 298 K) δ = 95.4-94.6 (m, C_B), 88.3 (s, C_E), 86.5 (s, C_D), 81.9-80.8 (m, C_E), 76.1-75.9 (m, C_D), 73.9-73.5 (m, C_C), 70.0 (s, C_C), 68.7-68.0 (m, C_F), 30.1-29.6 (m, C_G), 26.4 (m, C_H).

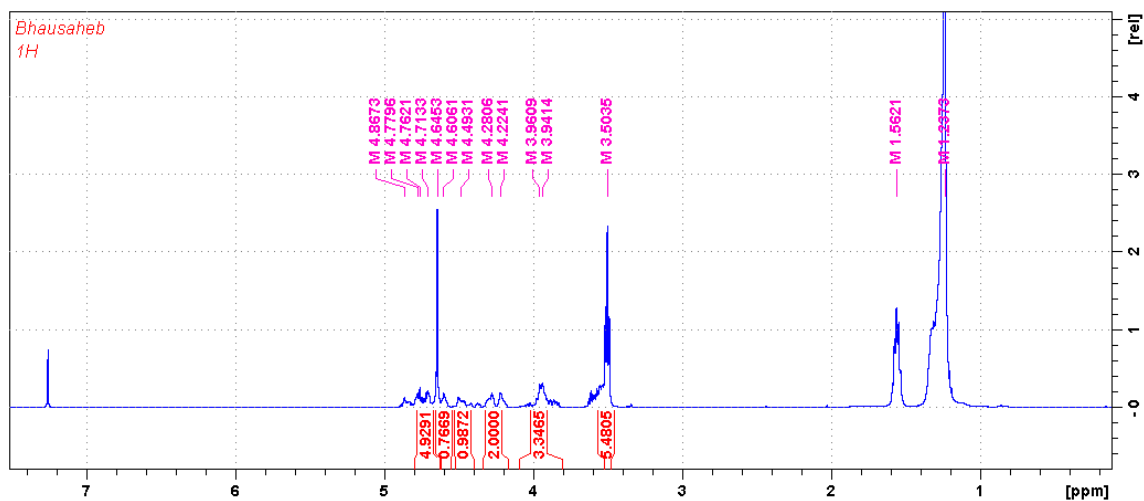


Figure 3.41. ¹H NMR spectrum of P11(2b-3d) in CDCl₃ (500 MHz at 298 K).

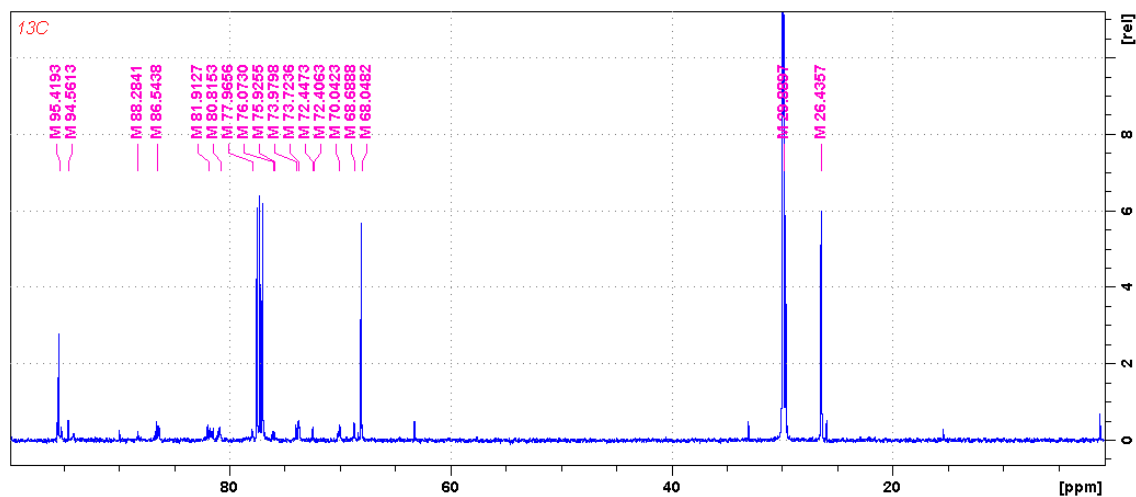


Figure 3.42. ¹³C NMR spectrum of P11(2b-3d) in CDCl₃ (125 MHz at 298 K).

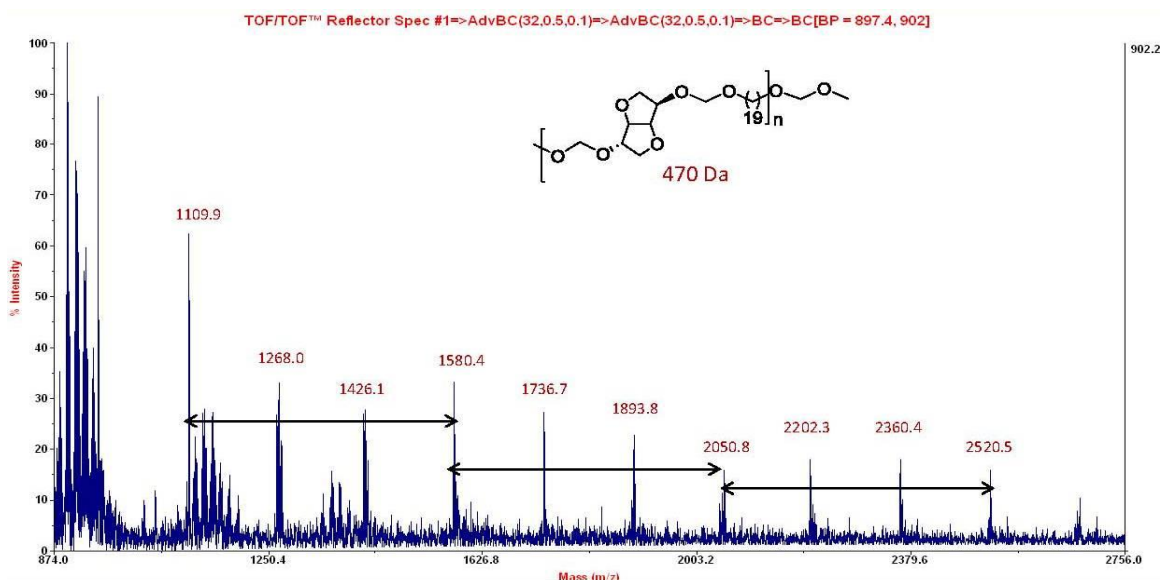


Figure 3.43. MALDI-ToF-MS spectrum of **P11(2b-3d)** recorded in dithranol.

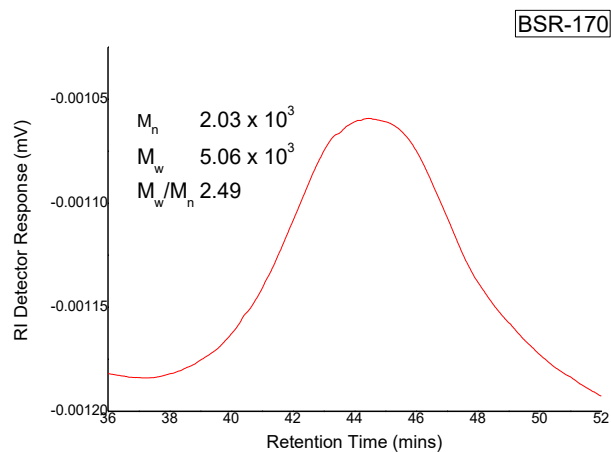
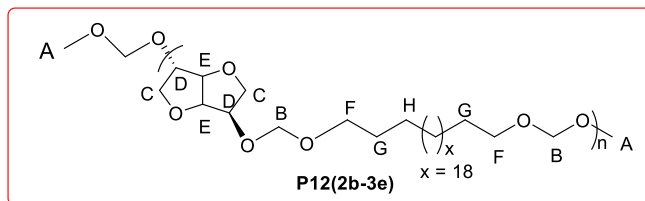


Figure 3.44. GPC chromatogram of **P11(2b-3d)** in chloroform at room temperature.

P12(2b-3e):



^1H NMR (400 MHz, CDCl_3 , 298 K) δ = 4.89-4.63 (m, $\text{H}_{\text{B}+\text{E}}$), 4.63-4.45 (m, H_{D}), 4.41-4.19 (m, $\text{H}_{\text{E}+\text{D}}$), 4.07-3.80 (m, H_{C}), 3.62 (m, H_{C}), 3.51 (m, H_{F}), 1.57 (br., s, H_{G}), 1.24 (br., s, H_{H}). ^{13}C NMR

(100 MHz, CDCl₃, 298 K) δ = 95.4-94.6 (m, C_B), 88.3 (br., s, C_E), 86.5 (br., s, C_D), 81.8 (m, C_E), 75.9 (s, C_D), 73.9 (s, C_C), 70.2-69.4 (br., m, C_C), 68.1 (s, C_F), 29.9 (br., s, C_G), 26.5 (s, C_H).

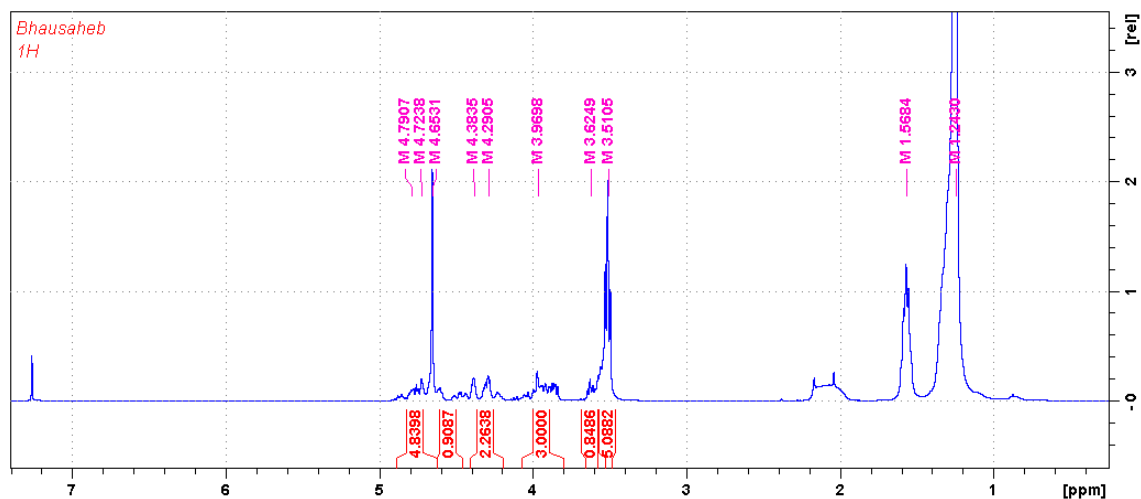


Figure 3.45. ¹H NMR spectrum of P12(2b-3e) in CDCl₃ (400 MHz at 298 K).

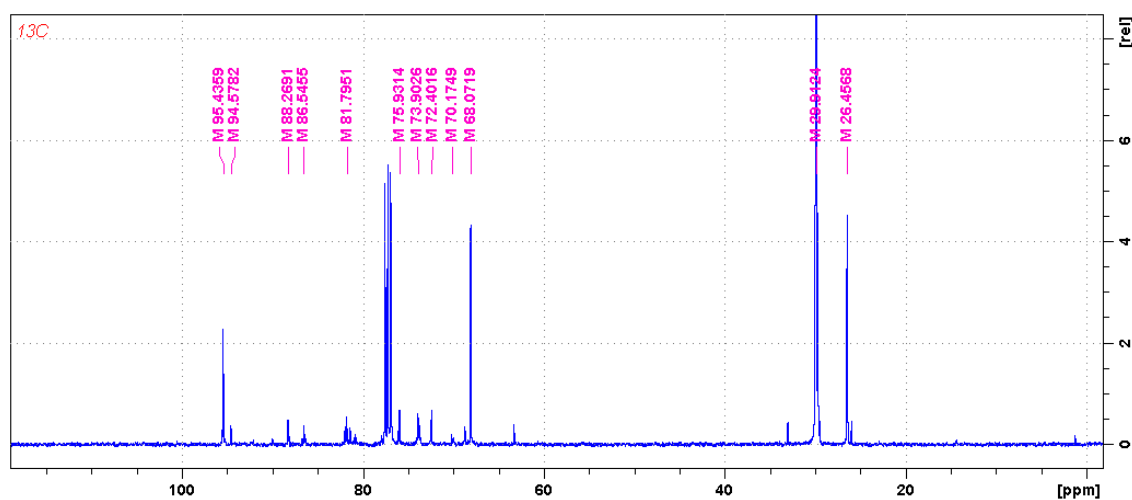


Figure 3.46. ¹³C NMR spectrum of P12(2b-3e) in CDCl₃ (100MHz at 298 K).

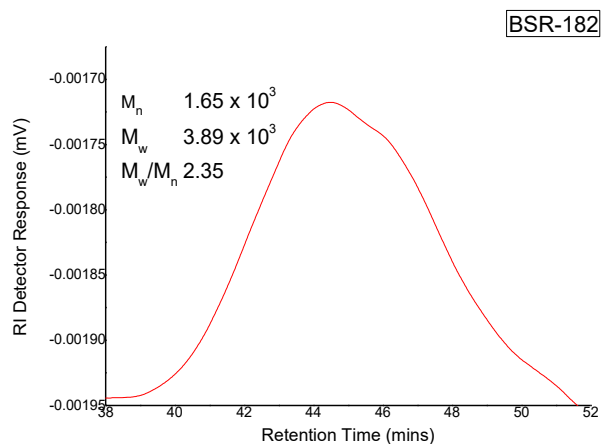


Figure 3.47. GPC chromatogram of **P12(2b-3e)** in chloroform at room temperature.

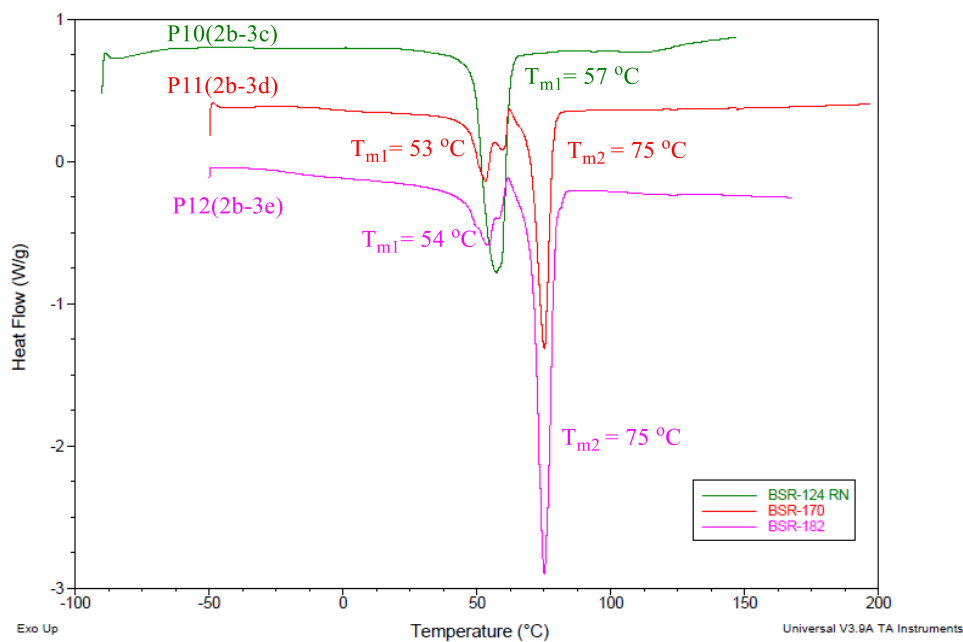


Figure 3.48. DSC heating curves for **P10(2b-3c)**-**P12(2b-3e)** under N₂ atmosphere. The data for **P10(2b-3c)** is from 1st heating cycle and for the remaining two copolyacetals is from second heating cycle.

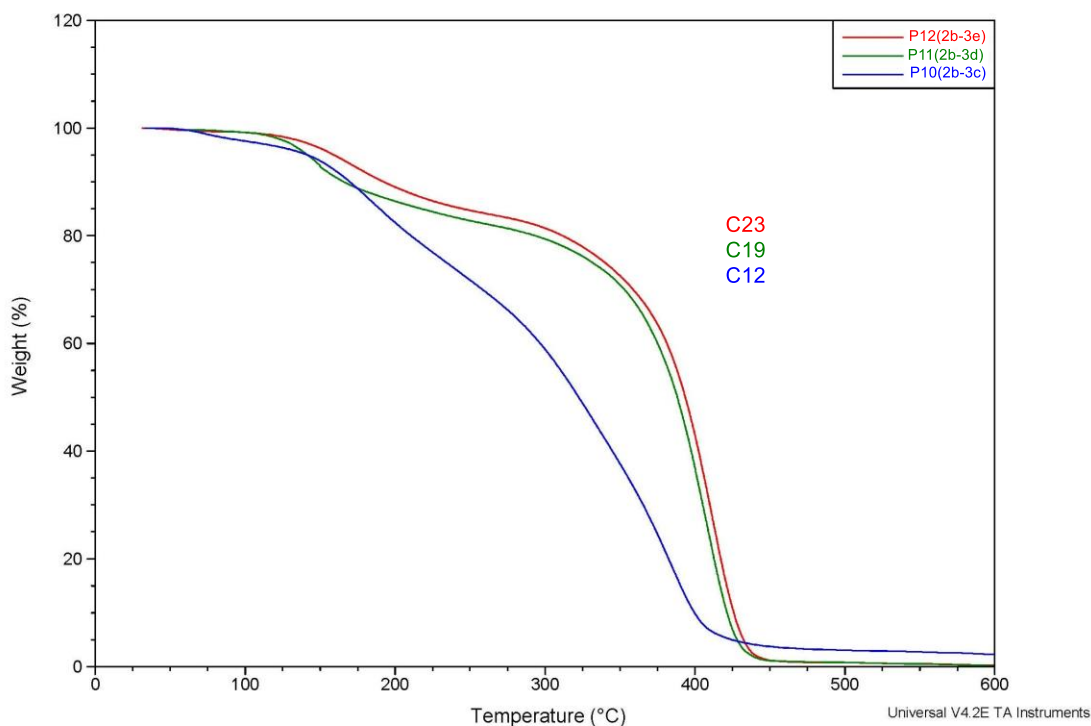
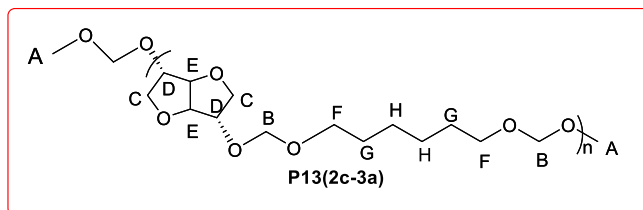


Figure 3.49. TGA traces of isosorbide-copolyacetals **P10(2b-3c)** to **P12(2b-3e)** recorded between 0-600 °C in N₂ atmosphere.

3.4.3.3. Copolymerization of Isosorbide-Diacetal (**2c**) with Linear Diacetals (**3a-e**) to **P13(2c-3a)**-**P17(2c-3e)**:

P13(2c-3a):



¹H NMR (200 MHz, CDCl₃, 298 K) δ = 4.85-4.61 (m, H_B), 4.61-4.44 (m, H_E), 4.31-4.16 (m, H_D), 3.97-3.67 (m, H_C), 3.60-3.40 (m, H_F), 1.57 (br., s, H_G), 1.36 (br., s, H_H).

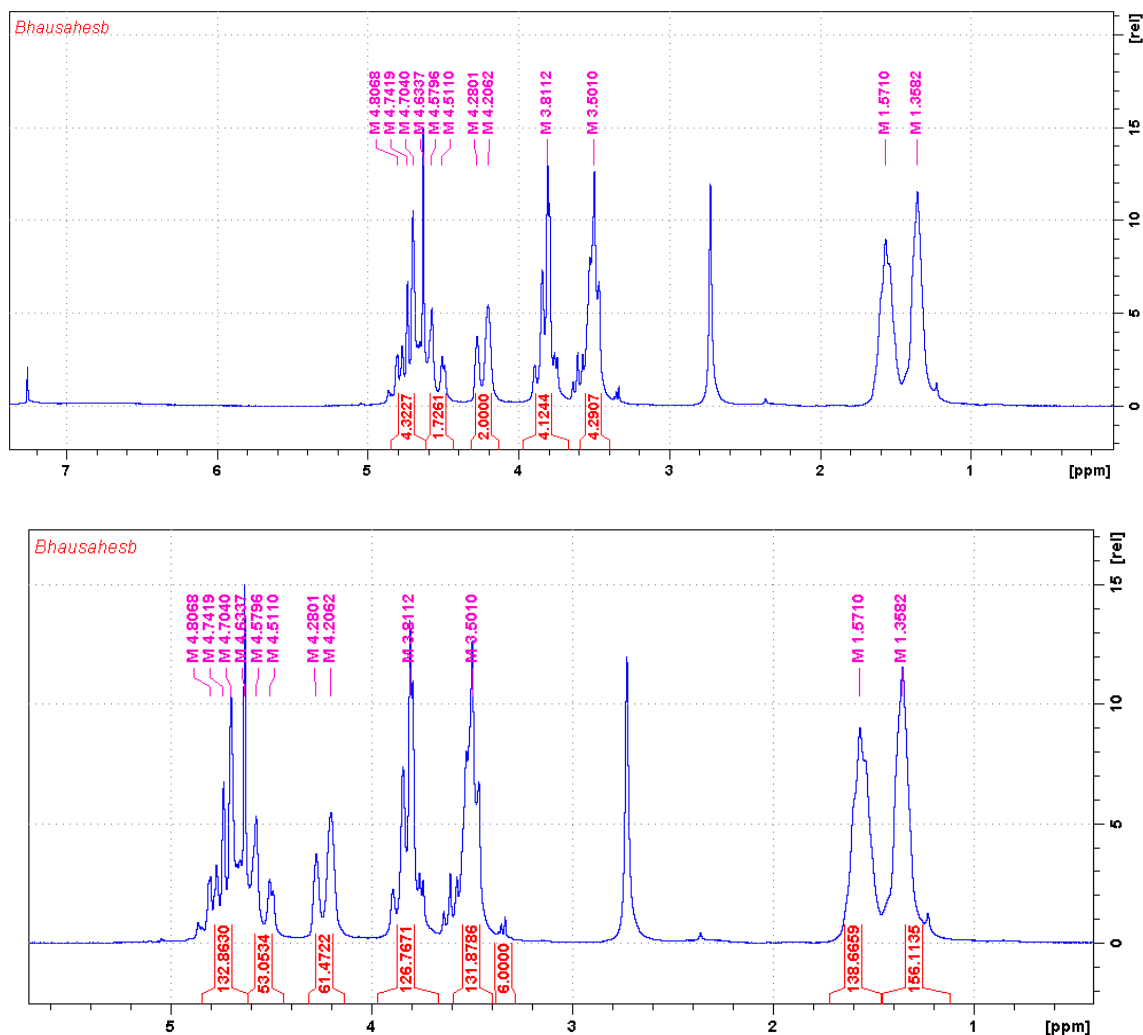


Figure 3.50. ¹H NMR spectrum of **P13(2c-3a)** in CDCl₃ (top) and determination of molecular weight by NMR (bottom) (200 MHz at 298 K).

Determination of molecular weight by proton NMR: The total number of protons in **Figure 3.50-bottom** is 800 and number of protons in polymer repeat unit is 24.

Therefore, the number of repeat units in **P13(2c-3a)** = Total number of protons in **Figure 3.50-bottom** divided by total number of protons in the repeat unit, i.e. $800/24 = 33$.

Hence, molecular weight of the copolyacetal = number of repeat units multiplied by molar mass of the repeat unit, i.e. $33 \times 288 = 9504 \sim \mathbf{9500}$ g/mol.

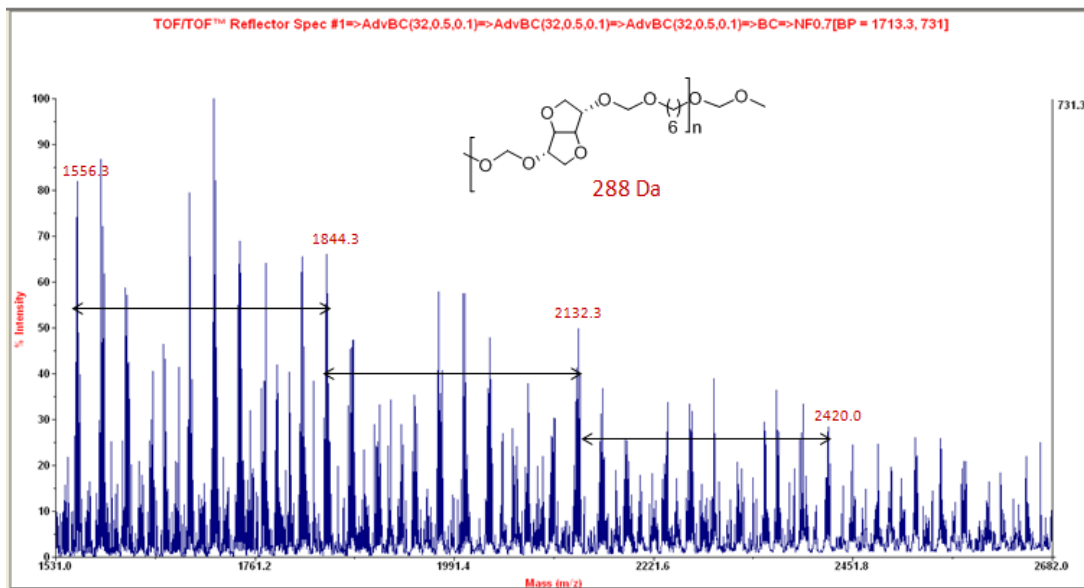


Figure 3.51. MALDI-ToF-MS spectrum of **P13(2c-3a)** recorded in the dithranol.

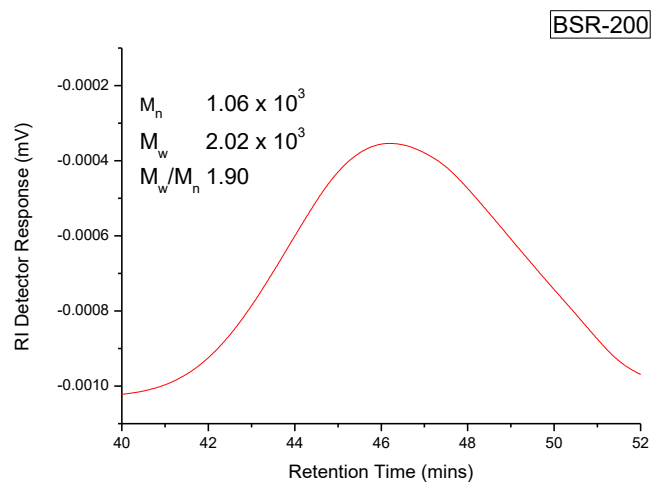
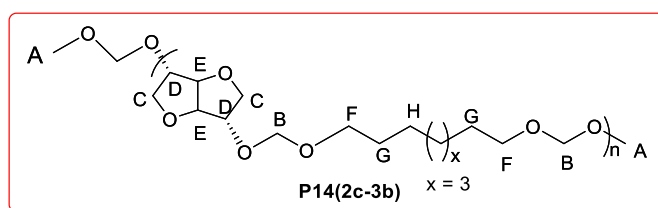


Figure 3.52. GPC chromatogram of **P13(2c-3a)** in chloroform at room temperature.

P14(2c-3b):



^1H NMR (200 MHz, CDCl_3 , 298 K) δ = 4.98-4.60 (m, H_B), 4.60-4.39 (m, H_E), 4.31-4.16 (m, H_D), 3.95-3.67 (m, H_C), 3.62-3.41 (m, H_F), 1.53 (br., s, H_G), 1.28 (br., s, H_H). ^{13}C NMR (50 MHz, CDCl_3 , 298 K) δ = 95.4-94.6 (m, C_B), 87.6-85.8 (m, C_E), 80.8 (br., s, C_D), 75.9 (s, C_D) 74.6-72.7 (m, C_C), 68.0 (s, C_F), 29.6 (m, C_G), 26.3 (m, C_H).

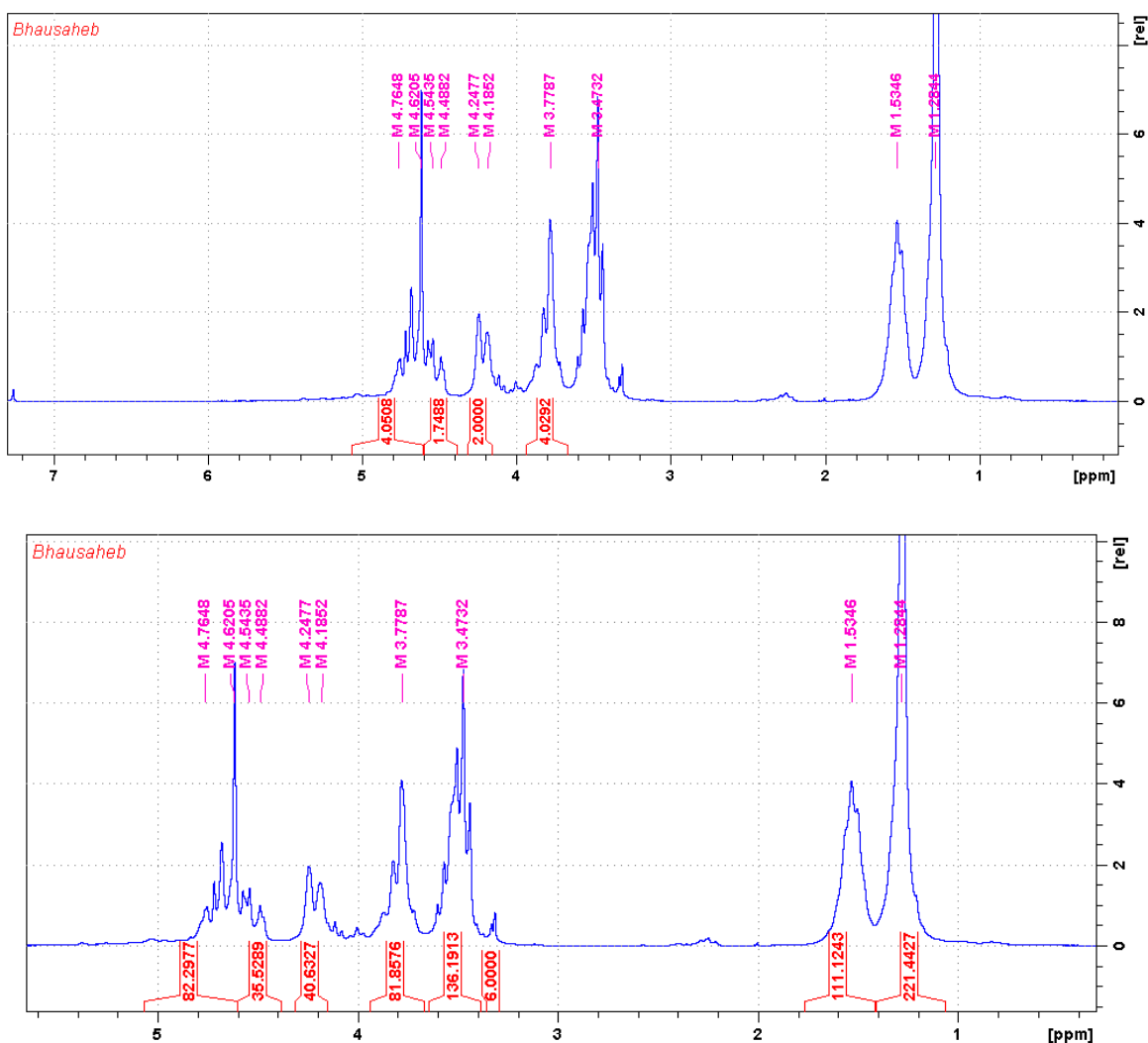


Figure 3.53. ^1H NMR spectrum of **P14(2c-3b)** in CDCl_3 (top) and determination of molecular weight by NMR (bottom) (200 MHz at 298 K).

Determination of molecular weight by proton NMR: The total number of protons in **Figure 3.53-bottom** is 709 and number of protons in polymer repeat unit is 28.

Therefore, the number of repeat units in **P14(2c-3b)** = Total number of protons in **Figure 3.53-bottom** divided by total number of protons in the repeat unit, i.e. $709/28 = 25$.

Hence, molecular weight of the copolyacetal = number of repeat units multiplied by molar mass

of the repeat unit, i.e. $25 \times 316 = 7900$ g/mol.

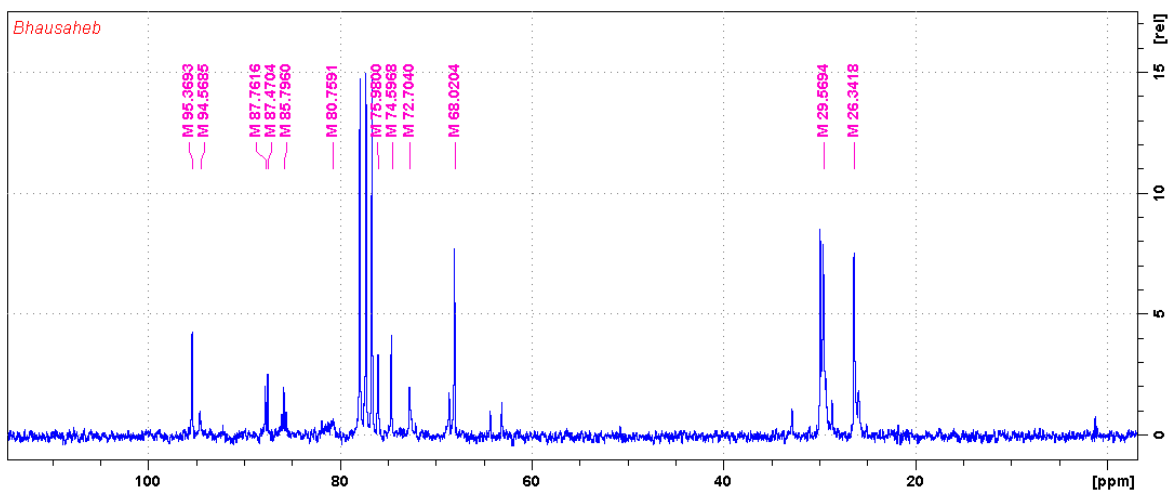


Figure 3.54. ^{13}C NMR spectrum of **P14(2c-3b)** in CDCl_3 (50 MHz at 298 K).

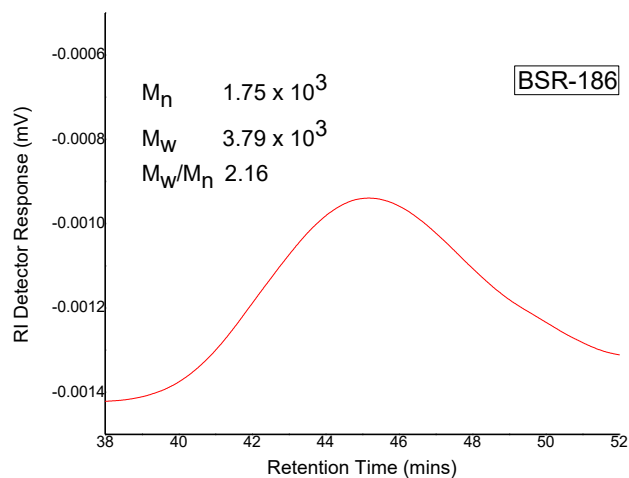
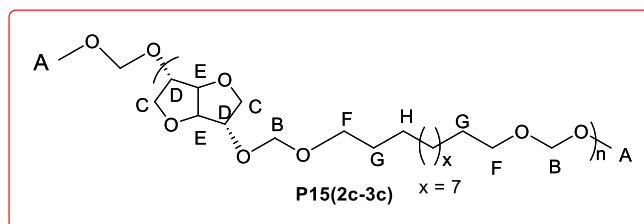


Figure 3.55. GPC chromatogram of **P14(2c-3b)** in chloroform at room temperature.

P15(2c-3c):



^1H NMR (200 MHz, CDCl_3 , 298 K) δ = 4.86-4.64 (m, H_B), 4.63-4.45 (m, H_E), 4.34-4.16 (m, H_D), 3.96-3.71 (m, H_C), 3.55 (t, $J_{\text{H-H}} = 6.7$ Hz, H_F), 1.56 (m, H_G), 1.25 (br., s, H_H). ^{13}C NMR (100 MHz, CDCl_3 , 298 K) δ = 95.4-94.5 (m, C_B), 87.8-85.8 (s, C_E), 81.8-80.5 (s, C_D), 76.0 (s, C_D), 74.6-72.7 (m, C_C), 68.0 (s, C_F), 29.79 (t, $J_{\text{C-C}} = 12.9$ Hz C_G), 26.4 (s, C_H).

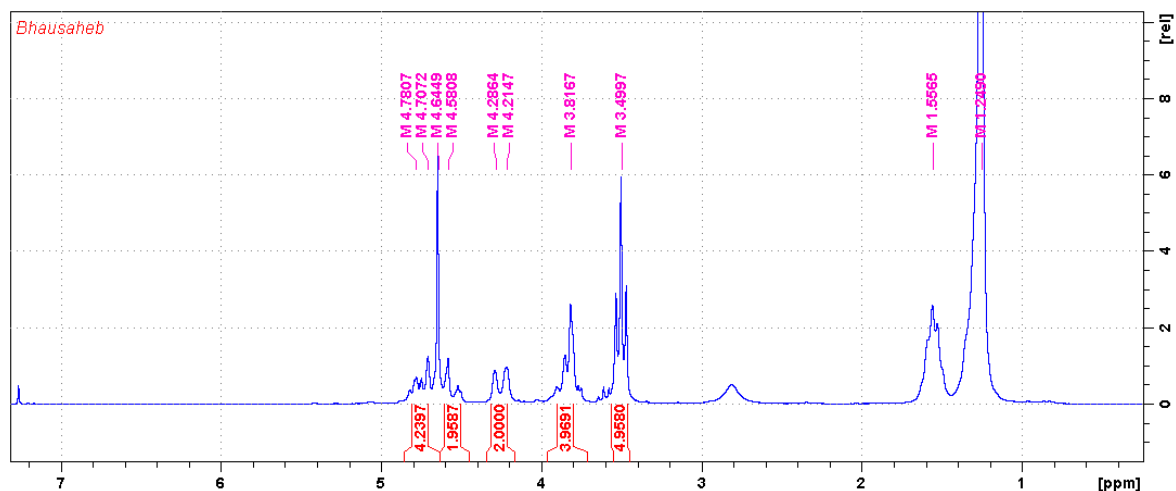


Figure 3.56. ^1H NMR spectrum of **P15(2c-3c)** in CDCl_3 (200 MHz at 298 K).

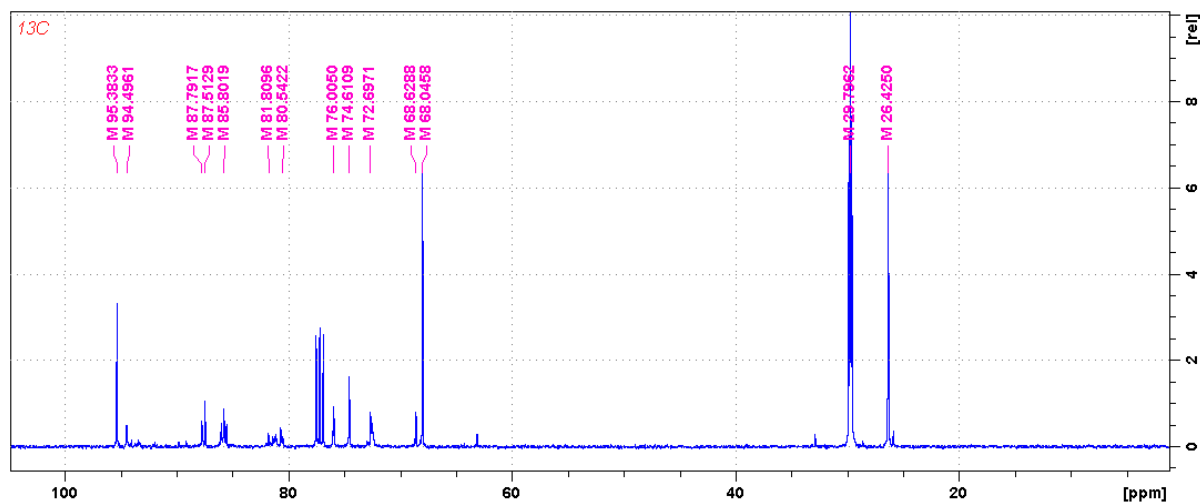


Figure 3.57. ^{13}C NMR spectrum of **P15(2c-3c)** in CDCl_3 (100 MHz at 298 K).

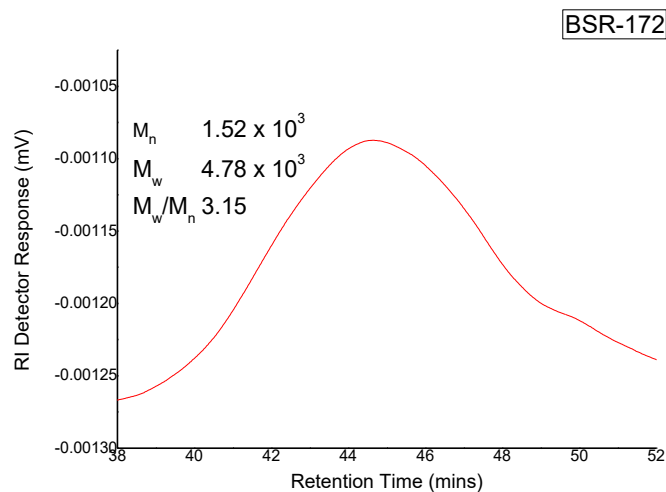
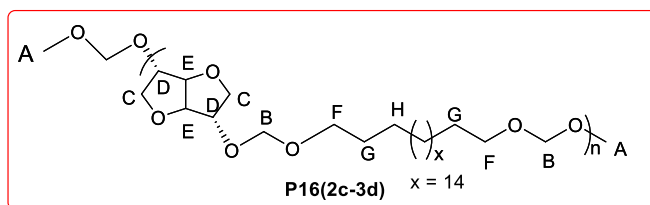


Figure 3.58. GPC chromatogram of **P15(2c-3c)** in chloroform at room temperature.

P16(2c-3d):



$^1\text{H NMR}$ (200 MHz, CDCl_3 , 298 K) $\delta = 4.91\text{-}4.62$ (m, H_B), $4.62\text{-}4.47$ (m, H_E), $4.36\text{-}4.17$ (m, H_D), $3.96\text{-}3.71$ (m, H_C), $3.67\text{-}3.41$ (m, H_F), 1.57 (br., s, H_G), 1.25 (m, H_H).

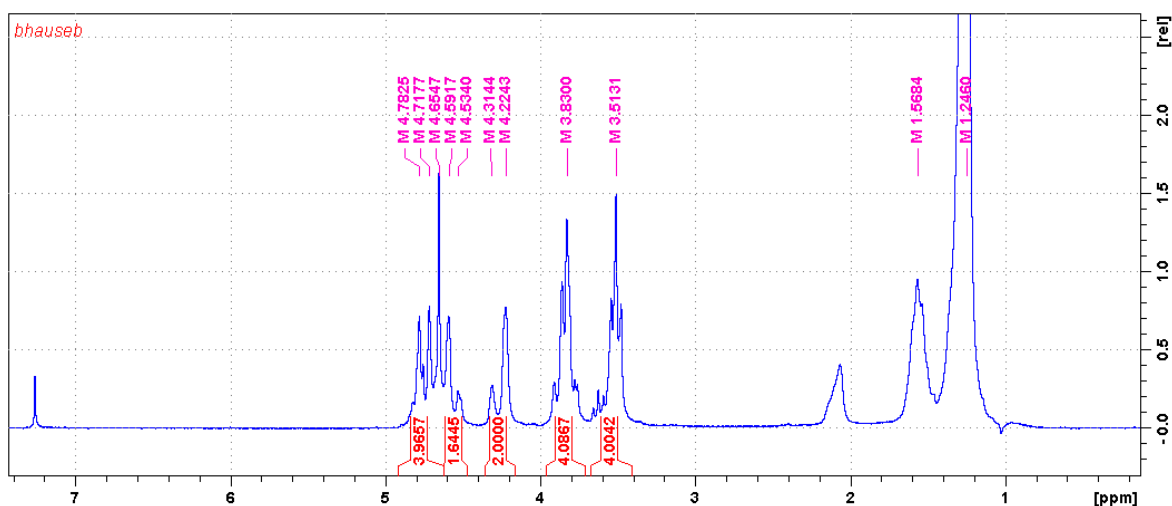


Figure 3.59. $^1\text{H NMR}$ spectrum of **P16(2c-3d)** in CDCl_3 (200 MHz at 298 K).

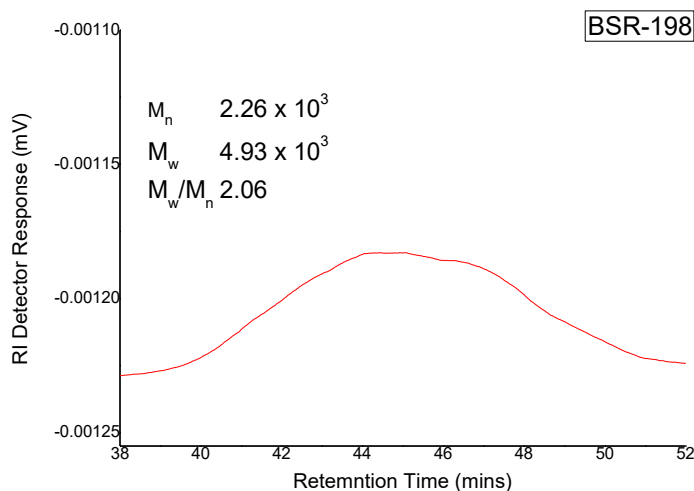
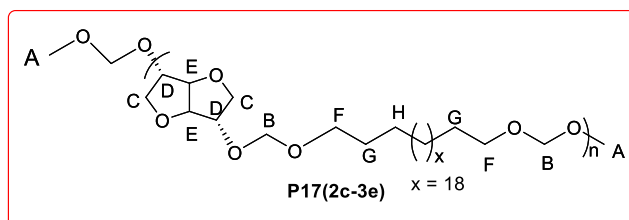


Figure 3.60. GPC chromatogram of **P16(2c-3d)** in chloroform at room temperature.

P17(2c-3e):



$^1\text{H NMR}$ (200 MHz, CDCl_3 , 298 K) $\delta = 4.99\text{--}4.63$ (m, H_B), $4.63\text{--}4.43$ (m, H_E), $4.39\text{--}4.27$ (m, H_D), $4.02\text{--}3.69$ (m, H_C), $3.68\text{--}3.40$ (m, H_F), 1.65 (m, H_G), 1.25 (m, H_H).

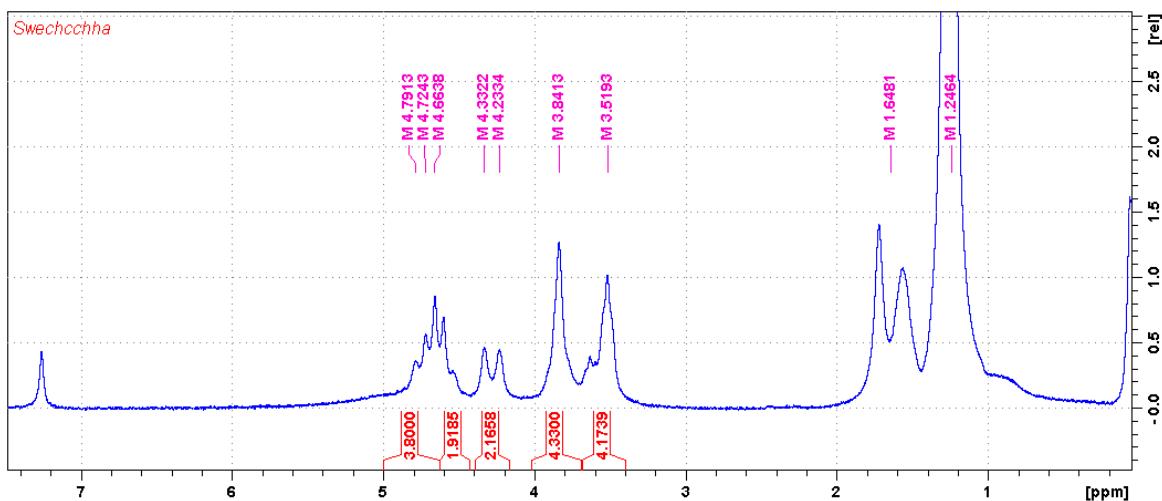


Figure 3.61. $^1\text{H NMR}$ spectrum of **P17(2c-3e)** in CDCl_3 (200 MHz at 298 K).

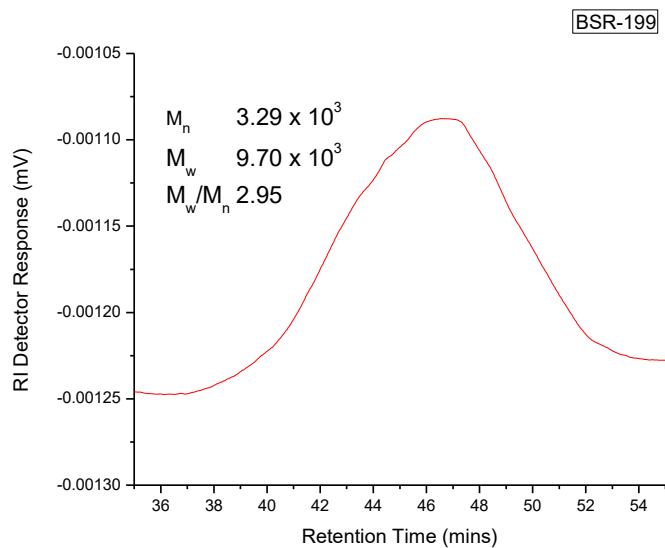


Figure 3.62. GPC chromatogram of **P17(2c-3e)** in chloroform at room temperature.

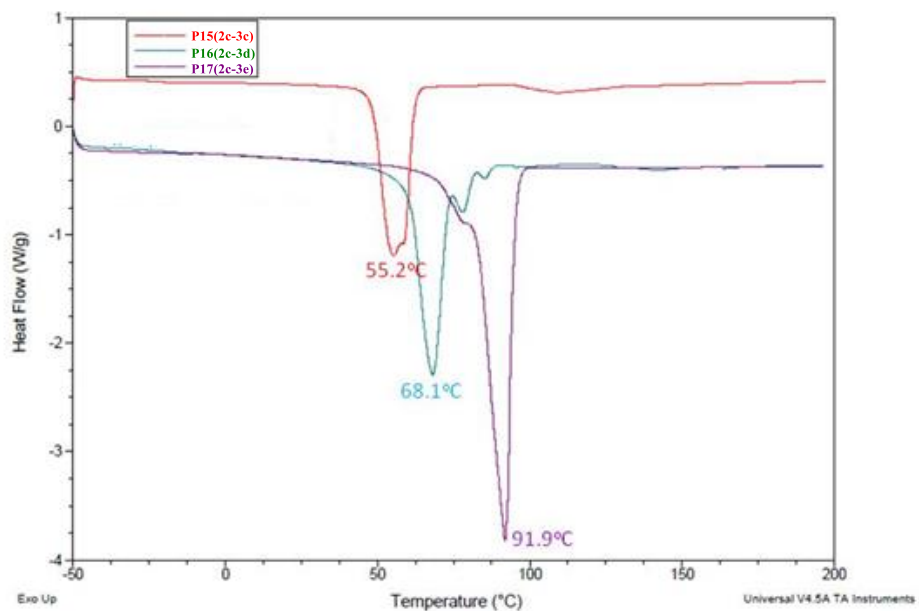


Figure 3.63. DSC heating and cooling curve of **P15(2c-3e)-P17(2c-3e)** under N_2 atmosphere data recorded from the first heating cycle).

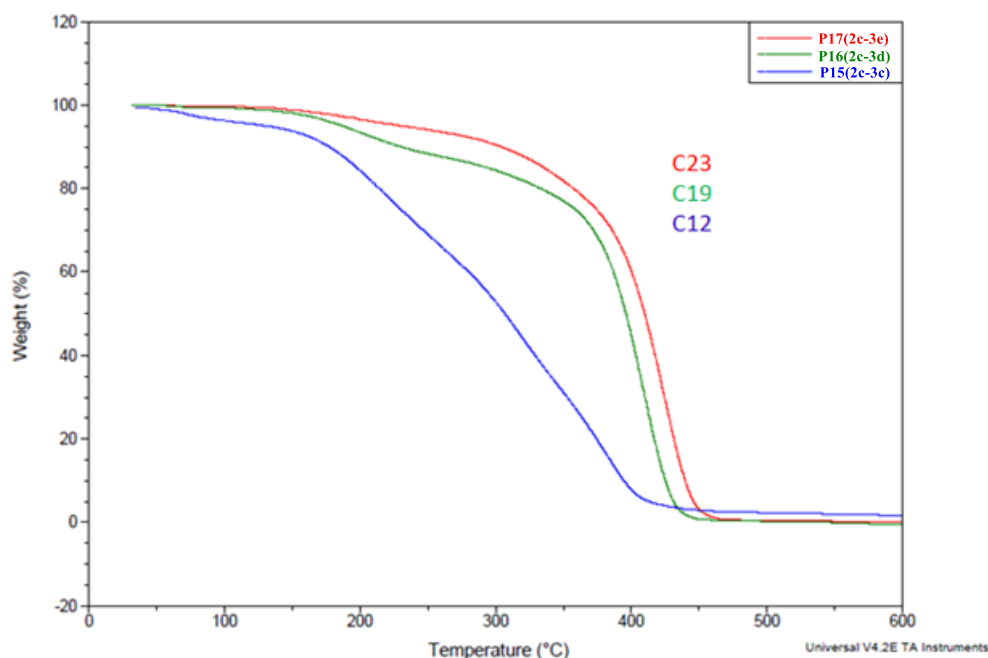


Figure 3.64. TGA traces of isoidide-copolyacetals **P15(2c-3c)** to **P17(2c-3e)** recorded between 0-900 °C in N₂ atmosphere.

3.4.4. Degradation of Copolyacetals:

3.4.4.1. Monitoring the Acid Induced Degradation by GPC:

17 mg of each of the copolymers **P5(2a-3c)**, **P7(2a-3e)**, **P10(2b-3c)**, **P12(2b-3e)**, **P15(2c-3c)** and **P17(2c-3e)** was weighed accurately in individual glass vial and 4 ml chloroform and 0.1 ml hydrochloric acid (1M in dioxane) was added to this to acidify the solution. The solution was allowed to stand for 20, 40 and 60 minutes after which the solvent was evaporated on rotary evaporator. The resultant material was fully dried on high vacuum to obtain the solid residue. The thus obtained residue was redissolved in 2 ml chloroform and the samples were injected. The GPC was recorded at room temperature with respect to the polystyrene standard and following plot (molecular weight Vs time) shows the most significant data (**Figure 3.65, 3.66**).

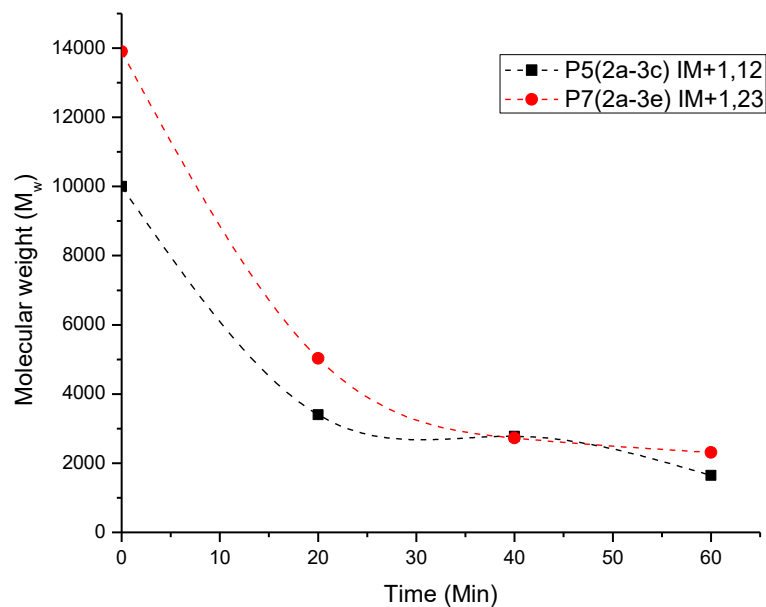


Figure 3.65: Monitoring degradation of **P5(2a-3c)** and **P7(2a-3e)** by GPC.

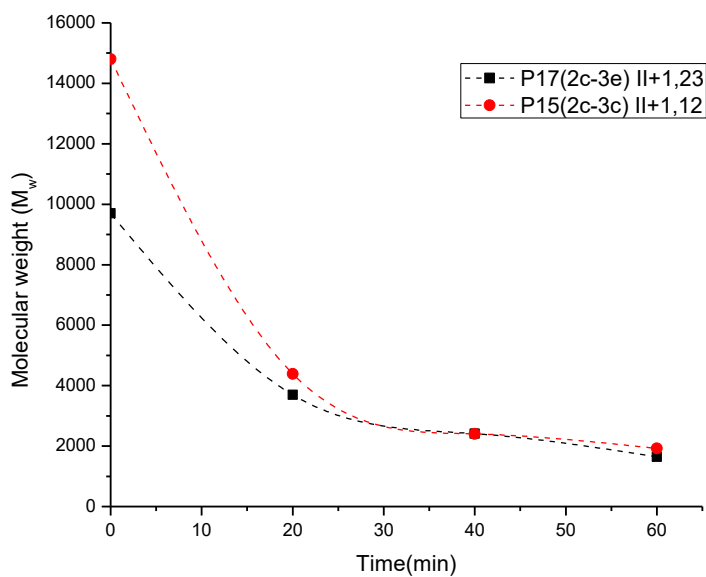


Figure 3.66. Time resolved degradation of copolyacetal **P15(2c-3c)** and **P17(2c-3e)** by GPC.

3.4.4.2. Hydrolytic Degradation of Copolyacetal:

Pellets of average weight 22-24 mg were prepared by melting the copolymer **P17(2c-3e)** in a DSC crucible-lid. The lid was cooled to room temperature, and the pellet was ejected by gentle shaking and dried for 2 h and stored under argon for further study. Similar weight of pellets are weighed and deep in the 5 ml HCl solution (3M and 9M) and kept at room temperature over a period of 5 days with slow stirring. After that, pellets are decanted and dried overnight (12h) in vacuum to get the constant weight. Next, the same pellet was suspended in a fresh acidic solution for next 10 and 15 days. Similar protocol was followed for pH 7 solution. The percent weight loss are shown in the **Figure 3.8** (see section 3.3.4.2) and representative degradation experiments in various media are summarized in **Table 3.4** (see below).

Table 3.4. Hydrolytic degradation of **P17(2c-3e)** pellets in pH 7, 3M and 9M hydrochloric acid solution over a period of 5, 10 and 15 days.

Entry	Initial wt. (mg)	Media	% wt. loss after 5 d	% wt. loss after 10 d	% wt. loss after 15 d
1	22.0	pH 7	NA	NA	7
2	23.6	3M.HCl	3	12	15
3	23.6	9M.HCl	12	23	30

3.4.4.3. Monitoring Acid Induced Degradation by NMR and Isolation of Degradation Products:

Hydrolytic degradation of **P5(2a-3c)** was also monitored by ^1H and ^{13}C NMR spectroscopy. 55 mg of copolymer **P5(2a-3c)** was added to an NMR tube and 0.6 ml of CDCl_3 and 0.1 ml of methanesulfonic acid (MSA) was added to the NMR tube. The proton NMR was recorded at 34 min., 77 min., 132 min. and 183 min. (**Figure 3.67-3.69**). The intensity of a $-\text{OCH}_2\text{O}-$ proton resonance at 4.6 & 4.8 ppm decreases suggesting that the copolymer is breaking or degrading to smaller fragments. Almost simultaneously, new peaks at 4.7, 4.9 and 5.1 ppm starts appearing, which can be assigned to various methylene protons originating from $-\text{ROCH}_2\text{OH}$ type fragments. Along the same line, the resonance at 3.5 ppm disappears and a new signal at 3.6 ppm appears. The 3.6 ppm resonance can be tentatively ascribed to a $-\text{RCH}_2\text{OH}$ fragment. The proton NMR findings were further supplemented by ^{13}C NMR, which revealed decreasing intensity of a resonance at 93-95 ppm (**Figure 3.70 & 3.71**).

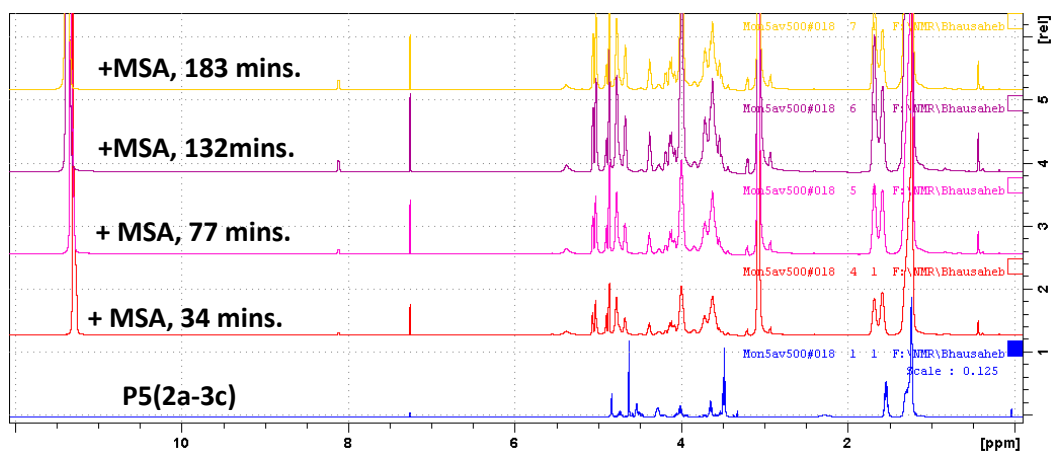


Figure 3.67. Time resolved, stacked ^1H NMR spectrum of **P5(2a-3c)** (bottom) and degradation products after addition of methanesulfonic acid (MSA) in CDCl_3 (500 MHz at 298 K).

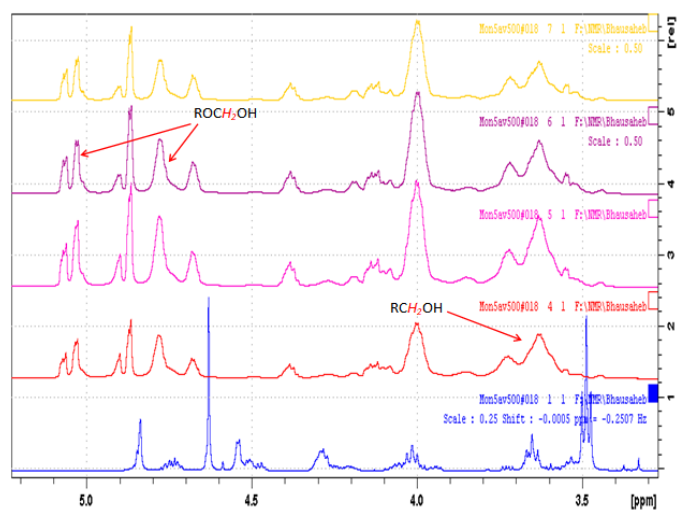


Figure 3.68. Expanded view of figure 3. 67 displaying characteristic decomposition products.

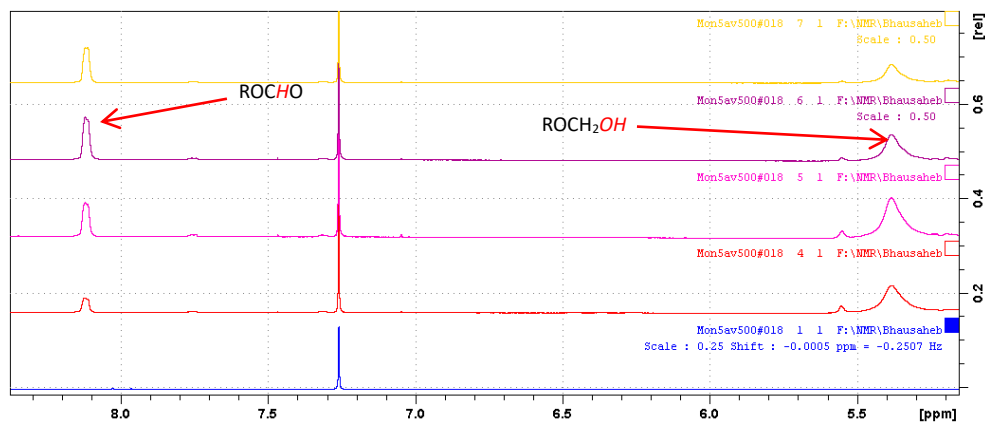


Figure 3.69. Expanded view of figure 3.67 displaying characteristic formate resonance and hemiacetal -OH protons.

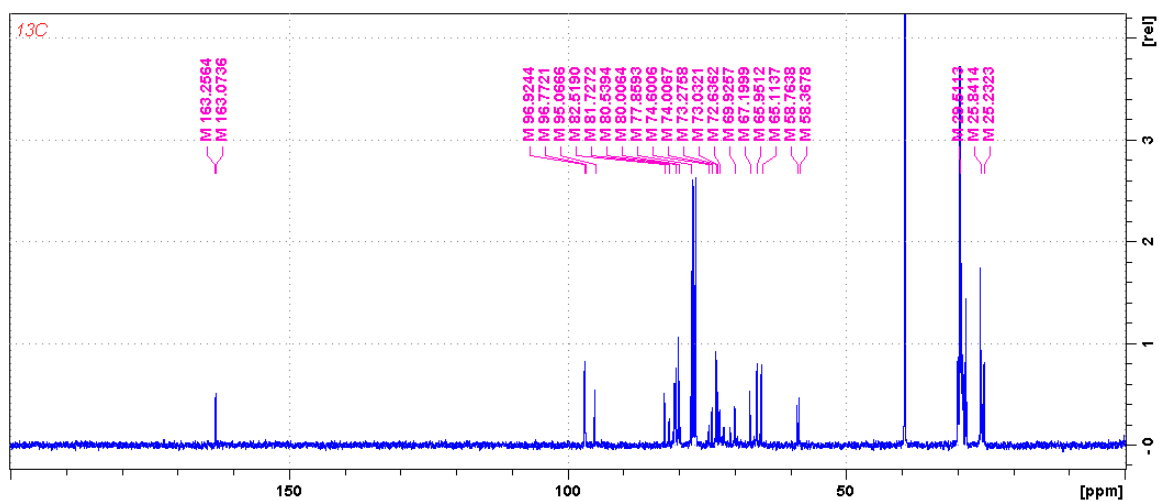


Figure 3.70. ¹³C NMR spectrum of degraded **P5(2a-3c)** in CDCl₃ (125 MHz at 298 K).

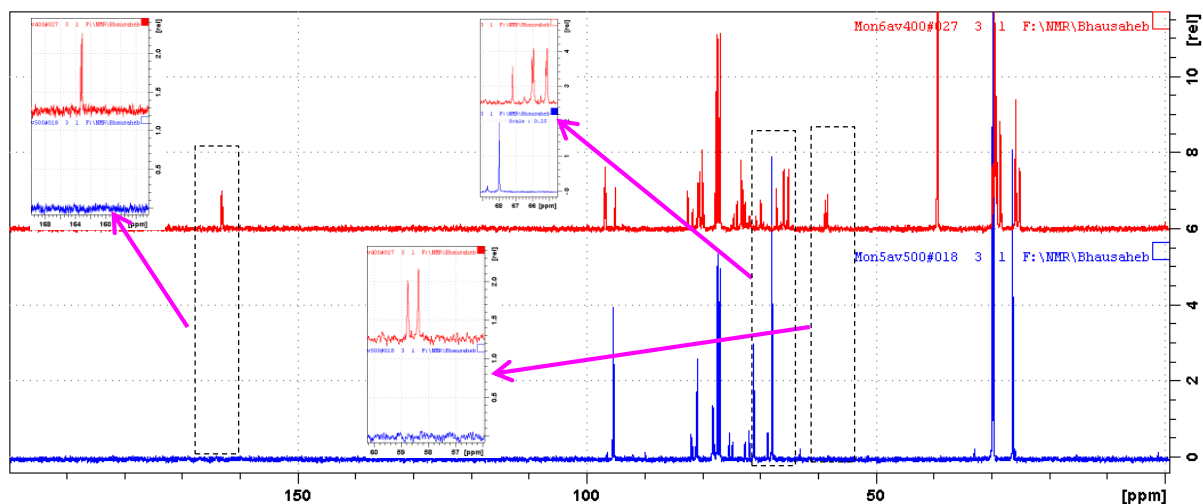


Figure 3.71. ¹³C NMR spectrum of **P5(2a-3c)** (bottom) and degradation products after addition of methanesulfonic acid (top) in CDCl₃. New resonances have been marked with dotted box and expanded view is presented (125 MHz at 298 K).

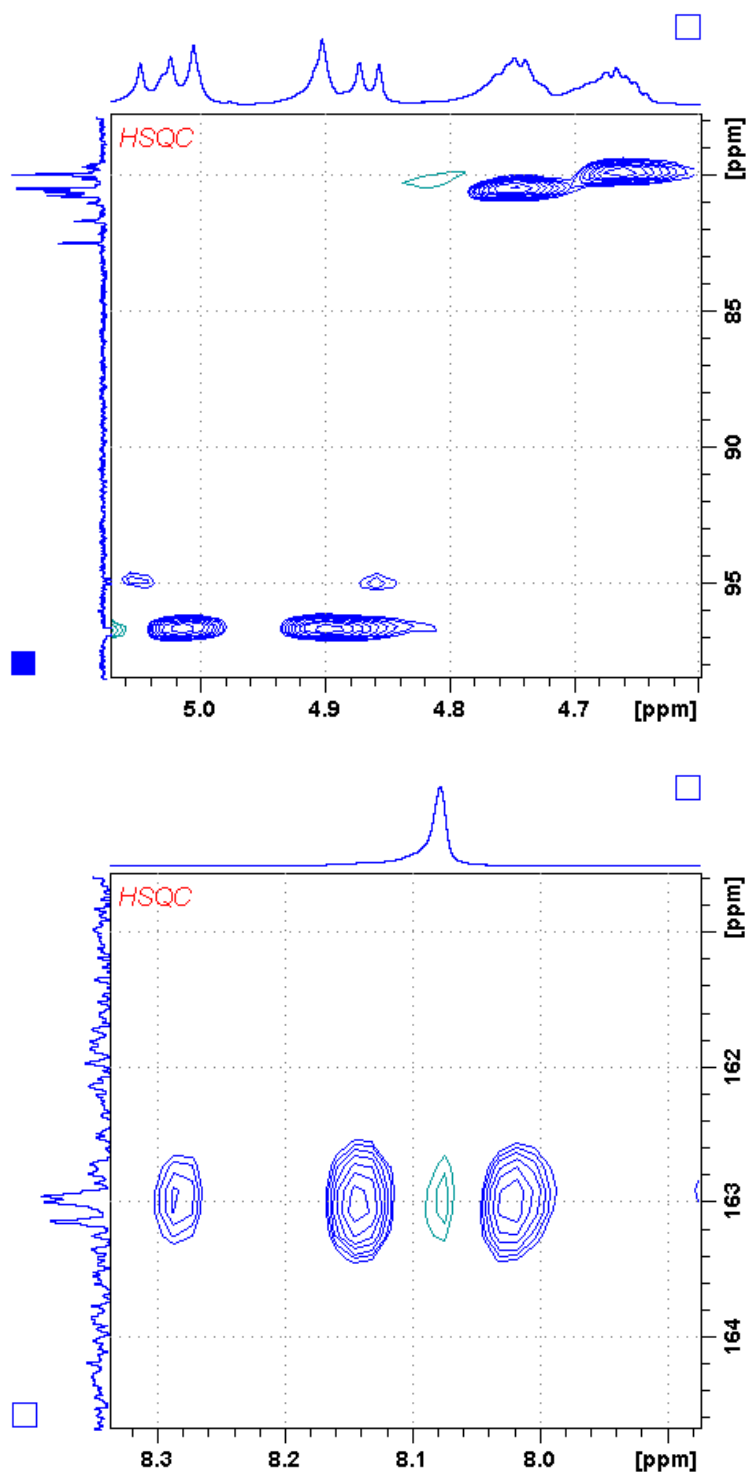


Figure 3.72. Direct C-H correlation (HSQC) spectrum of acid (MSA) induced degradation products of **P5(2a-3c)** in CDCl_3 (500 MHz, 298 K). Snapshots of the hemiacetal region (top) and formate region (bottom).

Isolation of Degradation Products:

In our attempts to identify the degradation products, 200 mg of copolyacetal **P5(2a-3c)** was dissolved in 20 ml chloroform and acidified by adding 1ml of hydrochloric acid (1M in dioxane) and the resultant mixture was kept for 24 hours. After 24 hours, volatiles were evaporated to obtain the residue, which displayed presence of acetal resonances. In order to further degrade the polyacetals, 0.5 ml of hydrochloric acid (1M in dioxane) was added and the copolymer was allowed to degrade for next 24 hours. Volatiles were evaporated and the residue was subjected to column chromatography. The first fraction (ethyl acetate: pet ether, 40:60) revealed presence of 1, 12-diol (**Figure 3.73, 3.74**) whereas, change of polarity (DCM: methanol, 80:20) was required to flush out the second fraction. The proton NMR of this fraction suggested presence of isomannide. The existence of isomannide was confirmed by comparing the ^1H NMR spectrum of commercially available isomannide and the one obtained after column chromatographic separation (**Figure 3.75, 3.76**).

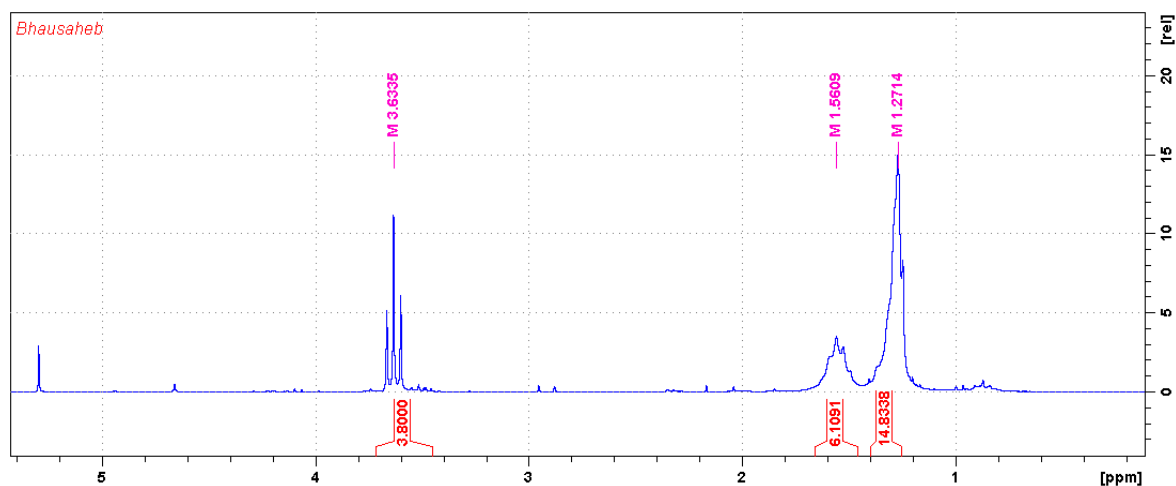


Figure 3.73. ^1H NMR spectrum of first fraction of degraded **P5(2a-3c)** which can be assigned to 1,12 dodecanediol (200 MHz, in CDCl_3 at 298 K).

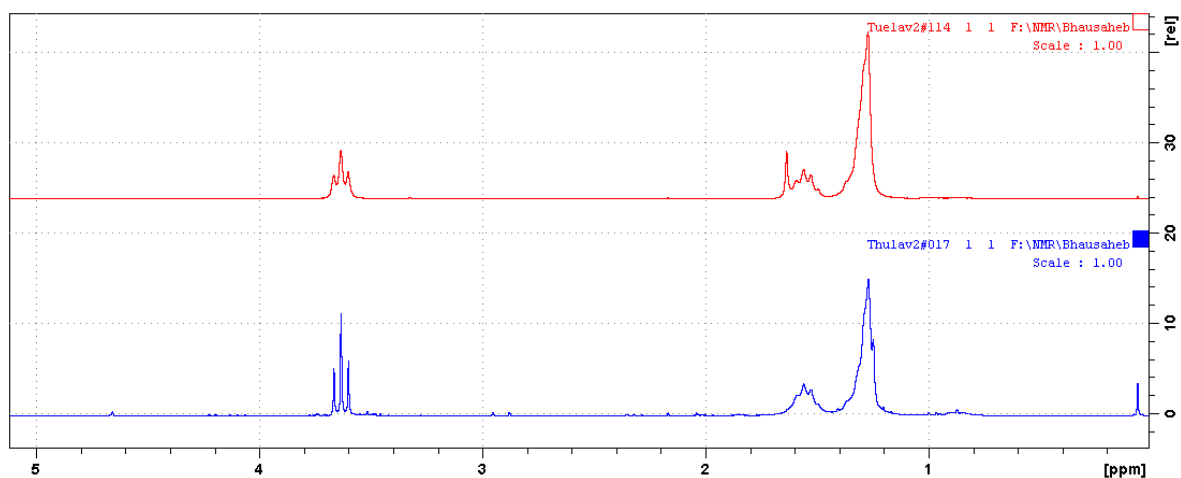


Figure 3.74. Comparative ¹H NMR spectrum of commercial 1, 12-dodecanediol (top) and first fraction of degraded **P5(2a-3c)** which can be assigned to 1, 12-dodecanediol (bottom) (200 MHz, in CDCl₃ at 298 K).

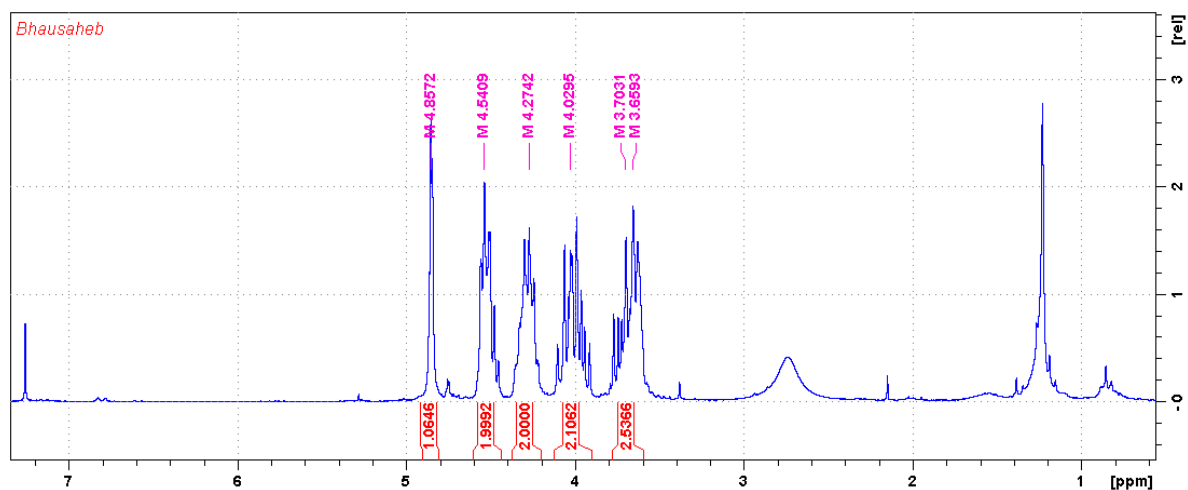


Figure 3.75. ¹H NMR spectrum of degraded **P5(2a-3c)** displaying signals corresponding to isomannide backbone (200 MHz, in CDCl₃ at 298 K).

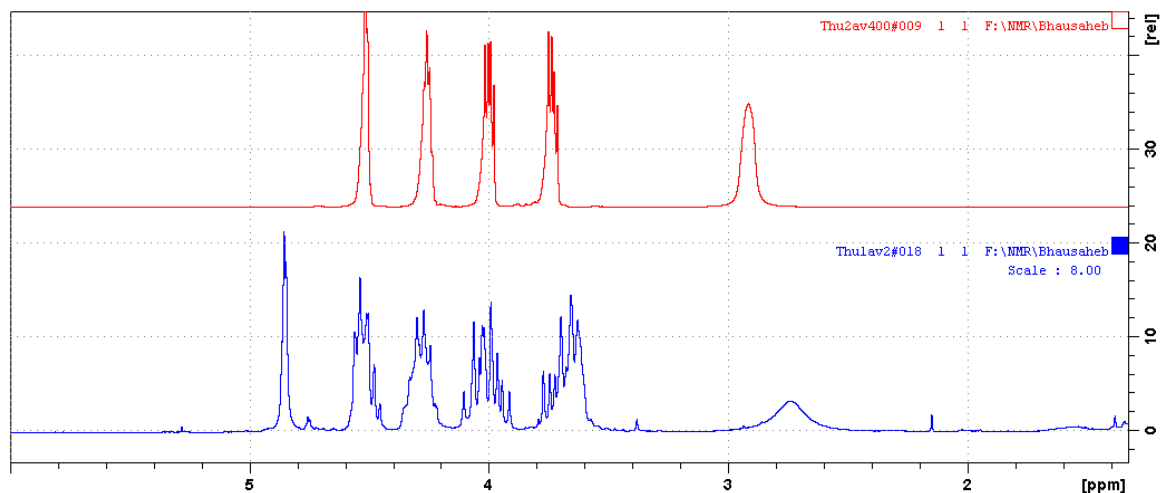


Figure 3.76. ¹H NMR spectrum of commercial isomannide (top) and isomannide obtained after degradation (bottom) (200 MHz, in CDCl₃ at 298 K).

3.5. Conclusions:

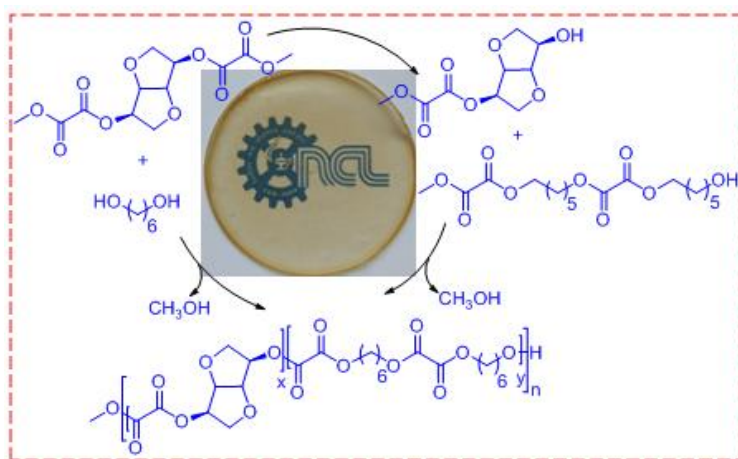
In summary, acid catalyzed Acetal Metathesis CoPolymerization (AMCP) of isohexide-diacetals with linear, plant oil derived long-chain diacetals has been reported. Typically, the polymerizations were carried out in a Schlenk tube equipped with mechanical stirrer and vacuum line (0.01 mbar) at 60-90 °C. Reduced intensity of the methoxy-protons and corresponding carbon indicated formation of desired copolyacetals. The proton NMR findings were corroborated by 2D NMR (NOESY, HSQC & HMBC), which established the correlation between the isohexide-segment and the linear aliphatic segment. Furthermore, ¹H NMR result indicates that the stereochemistry of the isohexide-diacetals **2a-c** is most likely retained during the copolymerization. The copolymer molecular weight was found to be in the range of 2000-11000 g/mol. The thermal behavior of the copolyacetals was investigated using DSC and TGA. Typically, the T_m of the copolyacetals was lower than the parent isohexide-polyacetals. This is partly due to the incorporation of flexible aliphatic segments in the parent isohexide-polyacetals. The copolyacetals **P10(2b-3c)**, **P15(2c-3c)**, **P16(2c-3d)**, **P17(2c-3e)** displayed a single melting transition indicating the presence of either perfectly alternating copolymer or one type of crystal form in the copolymers. It was observed that with an increasing carbon chain length of long chain diacetals (**2a-e**) the melting temperature of resultant copolyacetals increases. The copolyacetals were found to be thermally stable up to 325 °C. TGA analysis revealed that the copolyacetals

derived from long-chain diacetals are more stable compared to the copolyacetals derived from short-chain diacetals.

The biocompatibility of the copolyacetals was determined by subjecting the copolyacetal to various types of degradation. Acid induced degradation of copolyacetals was tracked by GPC (every 20 minutes), which revealed increasing degradation of copolyacetals over time. Thus, the time resolved molecular weight degradation investigations using GPC indicated slower degradation for long-chain copolyacetals as compared to their short-chain counterparts. Unlike the parent isohexide-polyacetals, hydrolytic degradation investigations revealed that the copolyacetals are relatively stable in acidic media over period of 15 days with only 30% weight loss in 9M HCl solution. Thus, the rate of degradation of the copolyacetals was found to be much slower than the parent isohexide-polyacetal homopolymers. The reduced rate of degradation can be attributed to incorporation of hydrophobic long chain segments in the copolyacetals. In-situ degradation investigation (based on 1-2D NMR) suggested formation of formates, hemiacetals and diols as degradation products. This was further corroborated by column chromatographic isolation of the parent diols. These findings imply that the properties of the copolyacetals can be tuned to suit a particular application. Thus, the present strategy provides an additional handle to control the rate of degradation by choosing the right combination of isohexide-diacetal and linear-diacetal monomers.

Chapter-4

Cross-Metathesis of Biorenewable Dioxalates and Diols to Film Forming Degradable Polyoxalates



This chapter has been adapted from following publication

Rajput, B. S.; Ram, F.; Menon, S. K.; Shanmuganathan, K.; Chikkali, S. H. *J. Polym. Sci., Part A: Polym. Chem.* **2018**, *56*, 1584-1592.

4.1. Abstract:

Starting from commonly available sugar derivatives, a single step protocol to access a small family of isohexide-dioxalates (**4a-c**) has been established. The synthetic competence of **4a-c** has been demonstrated by subjecting them to condensation polymerization. Quite surprisingly, the proton NMR of poly(isomannide-*co*-hexane)oxalate revealed a 1:2 ratio between isomannide-dioxalate (**4a**) and 1,6-hexanediol (**5a**) in the polymer backbone. This intriguing reactivity was found to be an outcome of a cross-metathesis reaction between **4a** and **5a**. The cross metathesis products **5a''** 6-hydroxyhexyl (6-(2-methoxy-2-oxoacetoxy)hexyl) oxalate and **4a'** (3R,6R)-6-hydroxyhexahydrofuro[3,2-b]-furan-3-yl methyl oxalate were isolated in a control experiment. Based on direct and indirect evidence, and control experiments, an alternative polymerization mechanism is proposed. Polymerization conditions were optimized to obtain polyoxalates **P18(4a-5a)-P26(4c-5c)** with molecular weights in the range of 14000-68000 g/mol. and narrow polydispersities. The identity of the polyoxalates was unambiguously established using 1-2D NMR spectroscopy, MALDI-ToF-MS and GPC measurements. The practical implication of these polymers is demonstrated by preparing transparent, mechanically robust films. The environmental footprint of the selected polyoxalates was investigated by subjecting them to solution and solid state degradation. The polyoxalates were found to be amenable to degradation.

4.2. Introduction:

Today the global production of polymers has reached the mark of 300 million metric tons a year and we cannot imagine life without polymers in this century.¹⁻² These polymers are sourced from non-renewable fossil fuel reserves.³ However, the supply of fossil fuels is finite and unsustainable, which calls upon sustainable strategies for nonstop and predictable supply of feedstocks. This has triggered a widespread research interest in sustainable chemicals and the search for renewable chemicals and materials has already begun.⁴ Renewable polymeric materials such as poly-lactic acid (PLA), polyhydroxyalkanoates (PHA)⁵ and sugarcane based polyethylene have been recently commercialized.⁶ However, the contribution of renewable polymeric materials to the total volume of polymers produced is negligible.⁷⁻⁸ Degradability is another material requirement for sustainable future and majority of the polymers produced today do not degrade over extended (100's of years) period of time.⁹⁻¹⁰ Thus, increasing consumption coupled with meager degradation has led to accumulation of alarming volumes of polymers and

has turned the planet into plastic soup.^{2, 11} Therefore, synthetic strategies that enable utilization of renewable feed-stocks and produce polymeric material which degrade within reasonably short time are highly desirable.¹²

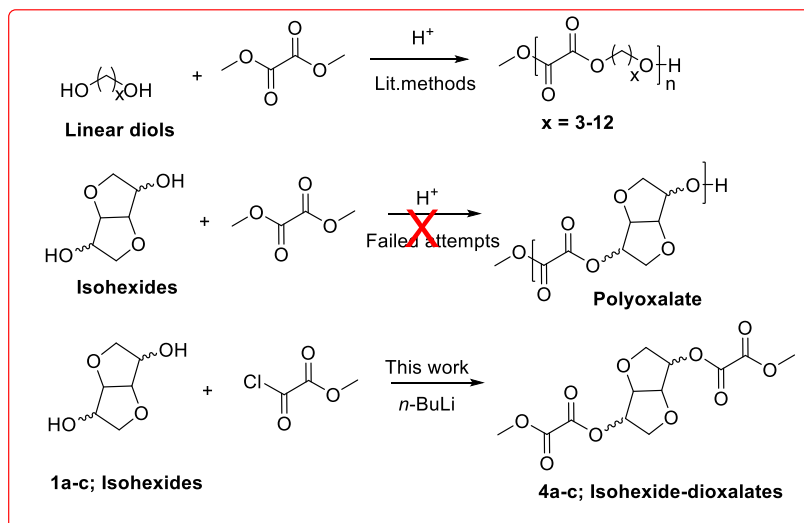
Among the accessible renewable feed-stocks, sugars and plant oils provide direct entry to chemical modification and functionalization.¹³⁻¹⁴ For instance, sugars can be easily converted to a host of new building blocks and enjoy naturally inbuilt chirality that can be creatively utilized to manufacture value added chiral reagents.¹⁵ These sugars can be readily converted to difunctional molecules called isohexides.¹⁶ Direct utilization of isohexides in polymerization is highly challenging. This is most likely due to the limited reactivity of secondary hydroxyl groups and hydrogen bonding between –OH groups and the ring C-H groups. These limitations have been partly addressed by Daan¹⁷ and Chikkali,¹⁸ among others.¹⁹ Thus, these fully bio-based monomers with enhanced reactivity were tested in different polymerization reactions and various polymers such as polyamides,²⁰ polyesters,²¹ co-polyesters,²² polyurethanes,²³ polyacetals^{4b, 24} and copolyacetals^{18a} have been successfully synthesized. Although considerable progress has been made, most of these polymers display limited molecular weight, decomposition remains unattempted and processing of these polymers to a useful item of daily use is largely missing.²⁵

In this chapter we report the synthesis of renewable feedstock chemicals with a degradable oxalate group incorporated into the building block. The synthetic utility of these feedstock chemicals is demonstrated by preparing corresponding film forming, high molecular weight, degradable, polyoxalates via an intriguing dioxalate-diol cross metathesis polymerization reaction.

4.3. Results and Discussion:

4.3.1. Synthesis of Isohexide-Dioxalates:

Synthesis of oxalates is routinely carried out by treating alcohols with acids or by treating diols with dimethyl oxalate in presence of Lewis acids (**Scheme 4.1**, top).²⁶⁻²⁷ Our initial attempts to prepare poly(isohexide)oxalates using literature reported method were largely unsuccessful and low molecular weight (~450 Da) tar like liquid could be obtained (see experimental section **Figure 4.15**). This is most likely due to the reduced reactivity of sterically encumbered secondary hydroxy groups installed on the rigid isohexides. In our pursuit to circumvent this



Scheme 4.1. Synthesis of polyoxalates, classical method (top), failed attempts (center) and this work (bottom).

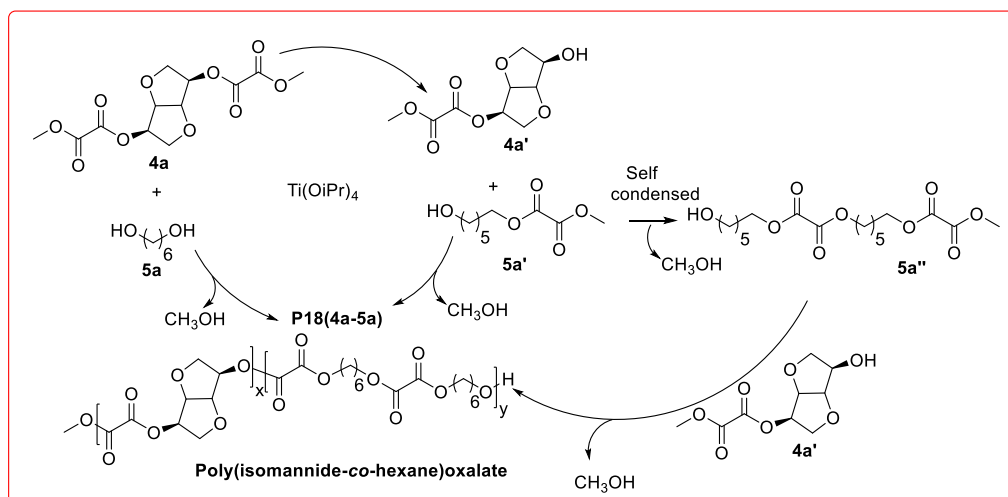
limitation, we developed a single step direct synthesis of dioxalates as depicted in **Scheme 4.1** (bottom). Treating isohexides with *n*-butyl lithium and methyl chlorooxalate led to the production of isohexide-dioxalates in excellent yields. Purification by column chromatography (pet ether: ethyl acetate 55:45) yielded **4a** as white solid (**4a** = 84%) (**Scheme 4.1**). A characteristic proton resonance at 3.89 ppm corresponding to the oxalate methoxy group indicated formation of isomannide-dioxalate **4a** (see experimental section and **Figure 4.3**). The proton NMR findings were corroborated by ^{13}C NMR which revealed a typical carbon signal at 157.6-156.8 ppm further confirming the formation of **4a** (**Figure 4.4**). In a direct carbon-proton (HSQC) correlation experiment, the proton resonance at 3.89 ppm revealed a cross peak to a carbon at 53.8 ppm, confirming the existence of a (-OCH₃) group (**Figure 4.5**). In addition, the proton signal at 5.20 ppm revealed a cross peak to a carbon at 75.7 ppm, verifying the existence of backbone CH-groups. A positive mode electrospray ionization mass spectroscopy disclosed molecular ion peak at $m/z = 341.04$ Da corresponding to [**4a**+Na]⁺ (**Figure 4.6**). Thus, the identity of **4a** was fully established using a combination of spectroscopic and analytical methods.

Along the same lines, isosorbide-dioxalate **4b** was isolated in 76% yield after column purification and the identity of **4b** was unambiguously ascertained using ^1H , ^{13}C NMR, mass spectroscopy. The third isomer, isoidide-dioxalate **4c** was prepared using same protocol and was isolated in moderate yields (53%) after column. **4c** was fully characterized using NMR, mass spectroscopy and elemental analysis (see experiential section for more details). The thus

prepared dioxalates **4a-4c** can serve as chiral building blocks for various applications, including monomers for polymerization.

4.3.2. Polymerization Mechanism and Poly(isohexide-co-alkane)oxalates:

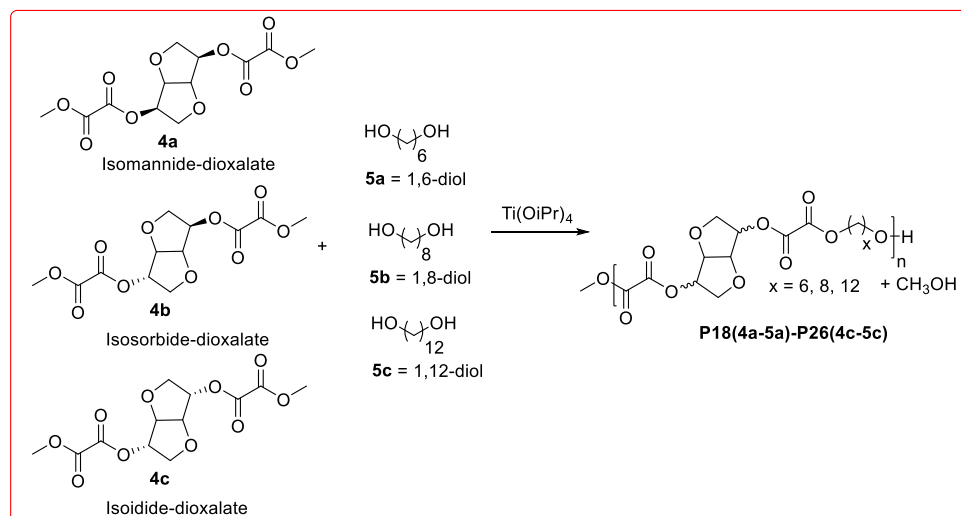
After having isolated **4a-4c**, their performance in oxalate metathesis polymerization (OMP) was examined.²⁷ It is anticipated that dioxalates will serve as **AA** type monomers and diols will behave as **BB** type monomers to yield **AABB** type polymers. The diol selection is based on their bio-renewability and degradability. An equimolar reaction between *O,O'*-((3*R,6R*)-hexahydrofuro[3,2-*b*]furan-3,6-diyl) dimethyl dioxalate **4a** and hexane-1,6-diol **5a** in presence of 1 mol% titanium isopropoxide was carried out in a Schlenk tube (see experimental section). The Schlenk tube was equipped with overhead high torque mechanical stirrer, heating and vacuum-purge arrangements. Polymerization was initiated by heating the mixture to 120 °C and the temperature was subsequently raised to 150 °C over a period of 2 hours with intermittent vacuum. Subsequently, the polymerization was continued at 150 °C for 46 hours under vacuum. After polymerization, the resultant highly viscous material was cooled to room temperature. The thus obtained solid was dissolved in chloroform and precipitated from methanol to yield poly-(isomannide-co-hexane)oxalate **P18(4a-5a)**. Reduced intensity of the terminal methoxy protons at 3.89 ppm (**Figure 4.29**) suggested formation of high molecular weight polymers. Surprisingly, the aliphatic protons were found to be double than the isomannide ring protons (2:1). This experiment was repeated several times, and it was found that **5a** protons are twice that of **4a** protons in each case. This puzzle could be addressed by assuming that the two monomers undergo oxalate cross metathesis with each other to yield monoxalates (**4a'** and **5a'**) as depicted in **Scheme 4.2**. Among the newly formed monomers, **5a'** is perhaps more reactive than **4a'** and might undergo faster self-condensation to **5a''**, than condensation with **4a'**. Perhaps this is the reason for higher content of **5a** in the resultant polymer than **4a**. This would also mean that some of the **4a'** is lost during precipitations. Indeed, analysis of the washing revealed existence of **4a'**.



Scheme 4.2. Proposed mechanism for the formation of poly(isomannide-co-hexane)oxalate.

In our pursuit to identify the reaction intermediates and unveil the mechanism, 1 equivalent of **4a** was treated with 1 equivalent of **5a** and the mixture was heated to 120 °C for 30 minutes. Subsequently, the reaction was quenched and the reaction mixture was subjected to column chromatography (see experimental section 4.4.3.2). Analyses of the resultant fractions revealed existence of **4a'** and **5a''** which were isolated and characterized. ^1H NMR spectroscopy established the existence of **5a''** which was corroborated by positive mode electron spray ionization mass spectrometry that displayed molecular ion peak at $m/z = 399.16$ [**5a''**+Na] $^+$ (**Figure 4.17**). These control experiments imply an oxalate cross metathesis to *in-situ* produce **5a''** during the initial stages of polymerization.

Due to the similarity between olefin cross-metathesis and the reactivity between a dioxalate and a diol to polyoxalate, this intriguing reaction can be named as Oxalate Cross-Metathesis Polymerization (OCMP).²⁷ The proposed *in-situ* formation of **4a'** and **5a'**, and polymerization to **P18(4a-5a)** is further supported by a control experiment between *ex-situ* prepared **4a'** and **5a'** (see experimental section 4.4.3.3.3). The two monoxalates **4a'** and **5a'** were independently prepared and subjected to polymerization to yield **P18(4a-5a)**. Thus, formation of the same polymer [**P18(4a-5a)**] from the two monoxalates unambiguously demonstrates the intermediacy of **4a'** and **5a'**. After having established the reactivity, polymerization conditions were optimized and **Table 4.1** summarizes the most significant results (see **Table 4.2** & **4.3** for details optimization). Isohexide-dioxalates were condensed with readily available, renewable diols in the presence of Lewis acids as catalysts (**Scheme 4.3**).



Scheme 4.3: Synthesis of poly(isohexide-*co*-alkane)oxalates.

Table 4.1. Polyoxalates derived from the renewable feedstocks and their properties.^a

Run	Monomers	Polymers	M_w^b	PDI ^b	T_m^c	Yield
1	4a:5a	P18(4a-5a)	40.6	2.00	NO	62
2 ^d	4a:5b	P19(4a-5b)	68.2	2.20	45	57
3 ^e	4a:5c	P20(4a-5c)	41.6	1.81	63	68
4	4b:5a	P21(4b-5a)	14.5	2.05	NO	72
5 ^f	4b:5b	P22(4b-5b)	31.9	1.94	44	62
6 ^g	4b:5c	P23(4b-5c)	23.4	2.16	50	74
7 ^h	4c:5a	P24(4c-5a)	23.3	1.83	NO	65
8 ^d	4c:5b	P25(4c-5b)	25.3	1.82	46	65
9 ^h	4c:5c	P26(4c-5c)	20.0	1.88	54	74

^aConditions: **4a-b**: 3.14 mmol, **5a-c**: 3.14 mmol, $\text{Ti}(\text{OiPr})_4$: 0.0314 mmol (1 mol%), Temp.: 120-150 °C, Time: 48 h, yields are listed in table 4.2, ^b M_w (into 10^3) and polydispersity index (PDI) were obtained from GPC in chloroform with respect to polystyrene standards, ^cObtained from DSC measurements, ^d2a/2c and 3b = 2.61 mmol, ^e2a and 3c = 2.47 mmol, ^f2b and 3b = 2.02 mmol, ^g2b and 3c = 2.68 mmol, ^h2c and 3a/3c = 2.83 mmol. NO = Could not be observed.

Initial catalyst optimization investigations pointed at $[\text{Ti}(\text{OiPr})_4]$ as the catalyst of choice which delivered high molecular weight poly(isohexide-*co*-alkane)oxalates (Table 4.2-4.3). Under the optimized conditions, reaction of **4a** with **5a** lead to high molecular weight (40600 g/mol) (Table 4.1, run 1) poly(isomannide-*co*-hexane)oxalate **P18(4a-5a)**. The existence of **P18(4a-5a)** was unambiguously established by 1-2D NMR, gel permeation chromatography

(GPC) and MALDI-ToF-MS (Figure 4.29-4.33) analysis. Along the same lines, treatment of **4a** with **5b** and **5c** produced corresponding polyoxalates **P19(4a-5b)** and **P20(4a-5c)** with high molecular weight (68200 and 41600 g/mol respectively, Table 4.1, run 2-3). The thermal properties of the polyoxalates were investigated by Differential Scanning Calorimetry (DSC) and Thermogravimetric Analysis (TGA). **P19(4a-5b)** with C8 aliphatic backbone revealed a T_m of 45 °C, whereas **P20(4a-5c)** with slightly longer chain (C12) aliphatic backbone displayed an enhanced melting temperature (T_m) of 63 °C. These melting temperatures are considerably lower than those reported for corresponding linear polyoxalates (Figure 4.40). We reasoned that this is most likely due to the presence of isomannide rings which disrupt the regular arrangement of polymeric chains and becomes relatively more amorphous. The thermal stability of polyoxalates was determined using TGA between 40 °C to 600 °C in nitrogen atmosphere (Figure 4.41). The polyoxalates **P18(4a-5a)-P20(4a-5c)** were found to be stable up to 300 °C after which the polymer starts decomposing. Almost 90% of the decomposition was observed between 300-400 °C. Likewise, isosorbide-dioxalate (**4b**) was treated with C6-C12 linear diols (**5a-c**) to yield corresponding polyoxalates **P21(4b-5a)-P23(4b-5c)** (Table 4.1 runs 4-6) and the identity of these polymers was unambiguously ascertained using a combination of spectroscopic and analytical methods. Once again, the ratio of aliphatic protons to the isosorbide backbone protons was found to be 2:1, a trend that was observed earlier for poly(isomannide-*co*-hexane)oxalate as well. This observation indicates that **P21(4b-5a)-P23(4b-5c)** follow the same mechanism as proposed in Scheme 4.2. Furthermore, the splitting pattern of the isosorbide backbone protons is same as in **4b**, indicating that the stereochemistry is retained during the polymerization (see experimental section 4.4.4.2).

Subsequently, the scope of OCMP was extended to the third isomer, isoidide. Under optimized conditions, isoidide dioxalate **4c** was polymerized with C6-C12 diols (**5a-c**) in presence of 1 mol% of Lewis acid [Ti(O*i*Pr)₄] catalyst to yield corresponding poly(isoidide-*co*-alkane)oxalates **P24(4c-5a)-P26(4c-5c)**. NMR investigation of poly(isoidide-*co*-alkane)oxalates reaffirmed the existence of 2:1 ratio of diol to isoidide protons, featuring the generality of the reactivity. The identity of **P24(4c-5a)-P26(4c-5c)** was fully established using 1-2D NMR, GPC and the thermal properties were evaluated by DSC and TGA (Figure 4.67 & 4.68). Interestingly, isomannide derived polyoxalates revealed highest molecular weight compared to their isosorbide and isoidide counterparts. The mostly likely reason for the differentiated behaviour could be the

mono-oxalate mechanism proposed in **Scheme 4.2**. Thus, a new synthetic protocol to prepare a small library of 9 renewable polyoxalates has been established.

4.3.3. Polyoxalate Film:

In our attempts to demonstrate the practical significance of these polymers, **P19(4a-5b)** was dissolved in chloroform and a transparent film could be obtained (**Figure 4.1**) by solution casting. It is well known that there is minimum molecular weight requirement to form entanglement networked structure of chains to obtain a film.²⁸ The formation of film (**Figure 4.1**) of **P19(4a-5b)** verifies that these polymers have high enough molecular weight with chain entanglements to form a network structure.²⁹ The intertwined network of long chains enables formation of a mechanically robust free standing film. Tensile testing of the film derived from **P19(4a-5b)** revealed a stress at break of 3.25 MPa and elongation at break of about 23% (**Figure 4.70-4.71**). The storage and loss modulus of **P19(4a-5b)** were 61.5 MPa and 11.5 MPa respectively. These modulus values correspond to a soft rubbery material. Thus, the polyoxalate **P19(4a-5b)** was found to be stable under solution casting conditions and yields a robust polymer film.



Figure 4.1. Solution casting of **P19(4a-5b)** to obtain a transparent film with CSIR-NCL logo in the background.

4.3.4. Degradation of Polyoxalates:

As the fate of next generation of polymeric materials will rely on their environmental footprint, degradation of aforementioned polyoxalates was examined.³⁰ The degradation of polyoxalates was evaluated i) by gel permeation chromatography (GPC), ii) in solution state by NMR, iii) in solid state, and degradation products were identified. In a solution state approach, defined quantity of **P20(4a-5c)** was dissolved in chloroform and 1M hydrochloric acid (in

dioxane) was added (see experimental section 4.4.6.1). The drop in molecular weight of the polymer was recorded after every 4 hours using GPC. **Figure 4.72** depicts drop in molecular weight versus time. As evident, the initial molecular weight of 41000 g/mol drops down to 5000 g/mol in 24 hours. Similar trend was observed for isosorbide and isoidide derived polyoxalates (**Figure 4.73, 4.74**). Thus, a poly(isosorbide-*co*-dodecane)oxalate **P23(4b-5c)** of molecular weight 23000 g/mol was found to degrade to 3900 g/mol after 24 hours. Whereas, isoidide derived poly(isoidide-*co*-dodecane)oxalate **P26(4c-5c)** displayed reduction in molecular weight from 20000 g/mol to 600 g/mol. These observations suggest the hitherto prepared polyoxalates are amenable to acid induced degradation. To investigate the solid state degradation, compact pellets of **P20(4a-5c)** with identical dimensions were prepared and their hydrolytic degradation was investigated.

Typically, the pellets were suspended in pH 7, 3M and 9M HCl solutions and the degradation was monitored over 15 days (**Figure 4.2**). There was 39% weight loss at pH 7, whereas 58% weight loss was observed in 3M HCl over 15 days. The highest weight loss of 84% in 15 days was observed in 9M HCl solution. These results indicate that the polyoxalates could be casted into films and are amenable to degradation. However, the identity of the degradation products remained unclear at this stage. To shed light on the degradation products, the degradation process was tracked by NMR spectroscopy. 30 mg of **P20(4a-5c)** in D₂O was taken in an NMR tube and 0.2 ml DCl in D₂O was added to above tube and an NMR was recorded over a period of 14 days (**Figure 4.75**). Initial proton NMR displayed only solvent peaks, however, isomannide backbone protons started appearing after 5 days. The intensity of these signals increased with increasing time and the new resonances clearly match with commercial isomannide sample. Even after 14 days, some part of the sample remained insoluble in NMR tube. The supernatant D₂O solution was decanted and the residue was fully dried. The residue was then dissolved in CDCl₃ and 1-2D NMR of the residue indicated presence of aliphatic hydroxy-oxalic acid derived segment (**Figure 4.77-4.80**). These NMR investigations point that the isomannide backbone cleaves off in acidic D₂O, whereas the aliphatic part of the polyoxalate dissolves in organic solvents. Thus, the combined NMR investigations suggest formation of isomannide and aliphatic hydroxy-oxalic acid as a degradation product.

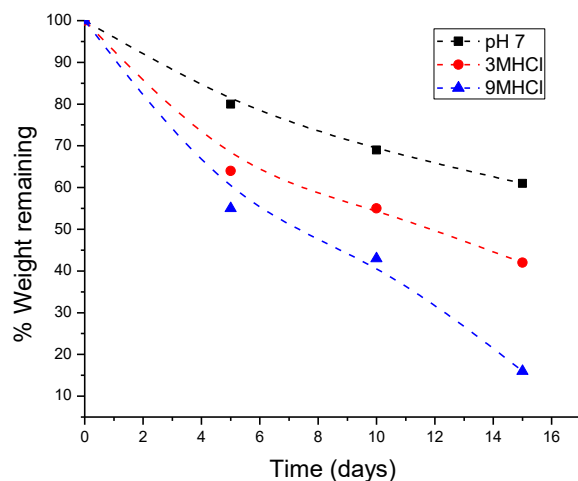


Figure 4.2. Monitoring hydrolytic degradation of **P20(4a-5c)** in, pH 7, 3M and 9M hydrochloric acid solutions.

4.4. Experimental Section:

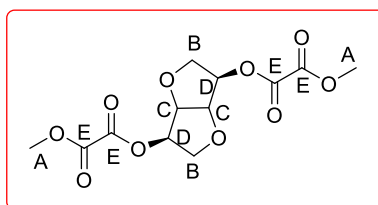
4.4.1. General Methods and Materials:

All manipulations involving moisture sensitive compounds were carried out under inert gas atmosphere using standard Schlenk or glove box techniques. Tetrahydrofuran (THF) was distilled from sodium/benzophenone under inert conditions. All other solvents were used as received without further purification. Isomannide, isosorbide, methyl chlorooxacetate, 1,8-octanediol, 1, 12-dodecanediol, sodium hydride, *n*-butyllithium solution (2.0 M in cyclohexane), sodium methoxide, deuterated chloroform, deuterium oxide, deuterium chloride solution 35 wt% in D₂O and titanium isopropoxide were purchased from Sigma Aldrich and used without further purification. 1, 6-hexanediol was purchased from Alfa Aesar. Diethyl azodicarboxylate, triphenyl phosphine, benzoic acid were purchased from Spectrochem Pvt Ltd and used without further purification. NMR spectra were recorded on a Bruker Avance 200, 400, 500 instruments. Chemical shifts are referenced to external reference TMS (¹H and ¹³C). Mass spectra were recorded on Thermo scientific Q-Exactive mass spectrometer, the column specification is Hypersil gold C18 column 100 x 3 mm diameter 3 um particle size mobile phase used is 90% methanol + 10 % water + 0.1 % formic acid. Elemental analysis was recorded on Flash EA 1112 series equipment. Differential scanning calorimeter (DSC) was carried out on DSC Q-100 from TA instruments with a heating and cooling rate of 10 K min⁻¹. Thermo-gravimetric analysis (TGA) was carried out on TA instrument STA 5000 model under nitrogen atmosphere.

GPC measurement was carried out on a Thermo Quest (TQ) GPC at 25 °C using chloroform (Merck, Lichrosolv) as the mobile phase. The analysis were carried out at a flow rate 1 mL/min using a set of five μ -styrigel HT columns (HT-2 to HT-6) and a refractive index (RI) detector. This column set enabled the determination of wide range of molecular weight from 10^2 to 10^6 . Columns were calibrated with polystyrene standard and the molecular weights reported are with respect to polystyrene standard. MALDI-ToF was performed on AB SCIEX TOF/TOF™ 5800 and matrix used is Dithranol. Tensile and viscoelastic properties of polymer films were measured using Dynamic Mechanical Analyzer (DMA), RSAIII (TA instrument). For tensile tests, rectangular film strips (5 nos) of 20 mm by 4 mm and 95 μ m thickness were stretched using strain rate 8.3×10^{-4} Hencky (1/s) and stress was recorded as function of percentage strain. Storage and loss modulus were measured using time sweep experiments at 30 °C and frequency of 1 Hz.

4.4.2. Syntheses of Isohexide-Dioxalates

4.4.2.1. Synthesis of *O, O'*-((3*R, 6R*)-Hexahydrofuran [3,2-*b*]furan-3,6-diyl) dimethyl dioxalates [Isomannide-Dioxalate] (4a):



To a stirred solution of isomannide (0.516 g, 3.53 mmol in 20 ml dry THF) was slowly added *n*-BuLi (4.1 ml, 8.12 mmol) at -78 °C and the mixture was stirred for 1 hour. After that, the resulting mixture is stirred at room temperature for an additional hour. To this mixture was added methyl chlorooacetate (0.74 ml, 8.12 mmol) at 0 °C and the reaction was stirred for next 48 hours at room temperature. Subsequently, the reaction mixture was washed with saturated sodium chloride solution (20 ml) and the aqueous phase was extracted with ethyl acetate (3×20 ml). The combined organic phase was dried over magnesium sulphate (MgSO_4), filtered and the filtrate was evaporated in vacuum to obtain a highly viscous material. Purification by column chromatography (pet ether-ethyl acetate 55:45) yielded highly viscous liquid. This residue was dissolved in ethyl acetate and was precipitated as a white solid after addition of excess pet ether. The white solid was isolated after evaporation of solvent, yielding 0.94 g of the desired isomannide-dioxalate **4a** (84%).

^1H NMR (400 MHz, CDCl_3 , 298 K) δ = 5.20-5.16 (m, 2H_D), 4.80-4.79 (m, 2H_C), 4.08-3.97 (m, 4H_B), 3.89 (s, 6H_A). ^{13}C NMR (100 MHz, CDCl_3 , 298 K) δ = 157.6-156.9 (m, C_E), 80.1 (s, C_C), 75.7 (s, C_D), 70.3 (s, C_B), 53.8 (s, C_A). **ESI-MS** (+ve mode) m/z = 341.04 $[\text{M}+\text{Na}]^+$. **Elemental analysis** (%): Calculated for $\text{C}_{12}\text{H}_{14}\text{O}_{10}$: C- 45.29, H- 4.43; Found: C- 45.97, H-4.23.

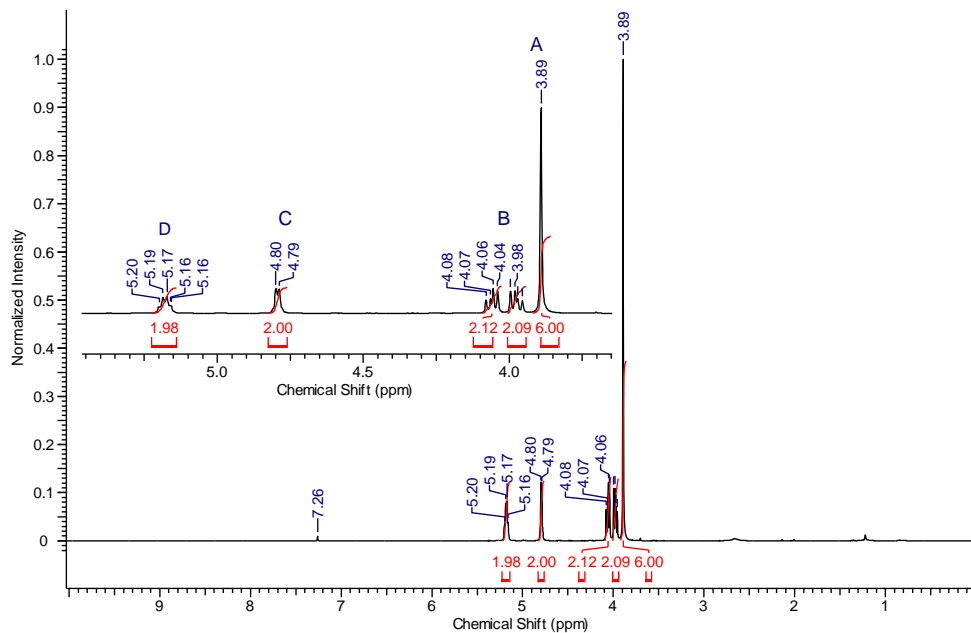


Figure 4.3. ^1H NMR spectrum of compound **4a** in CDCl_3 at (400 MHz at 298 K).

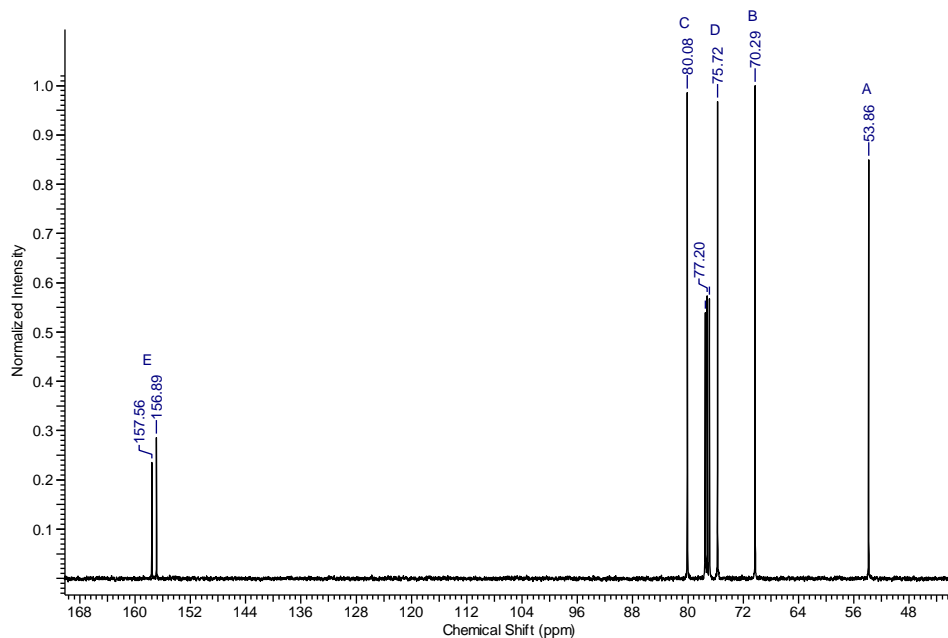


Figure 4.4. ^{13}C NMR spectrum of compound **4a** in CDCl_3 (100 MHz at 298 K).

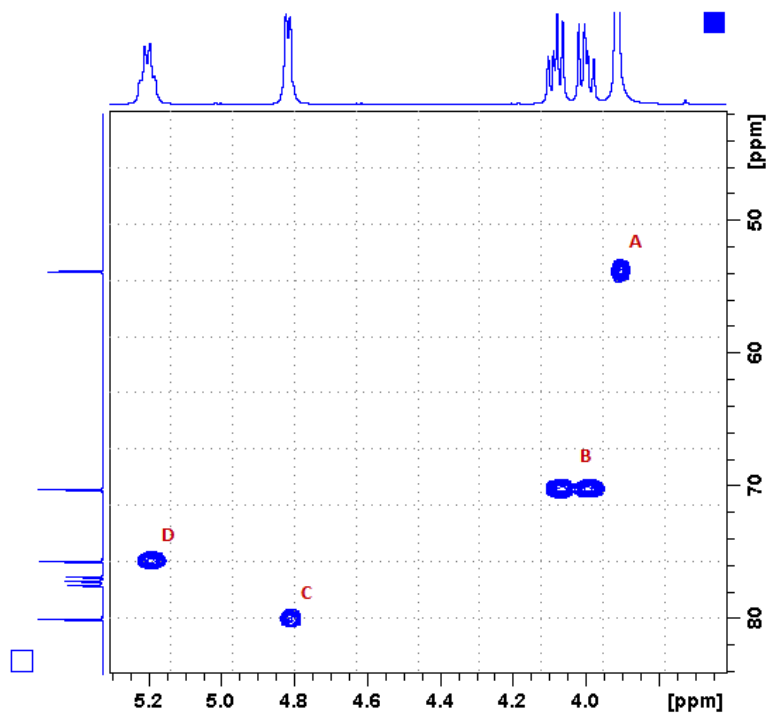


Figure 4.5. Short range C-H correlation (HSQC) spectrum of compound **4a** in CDCl_3 (at 298 K).

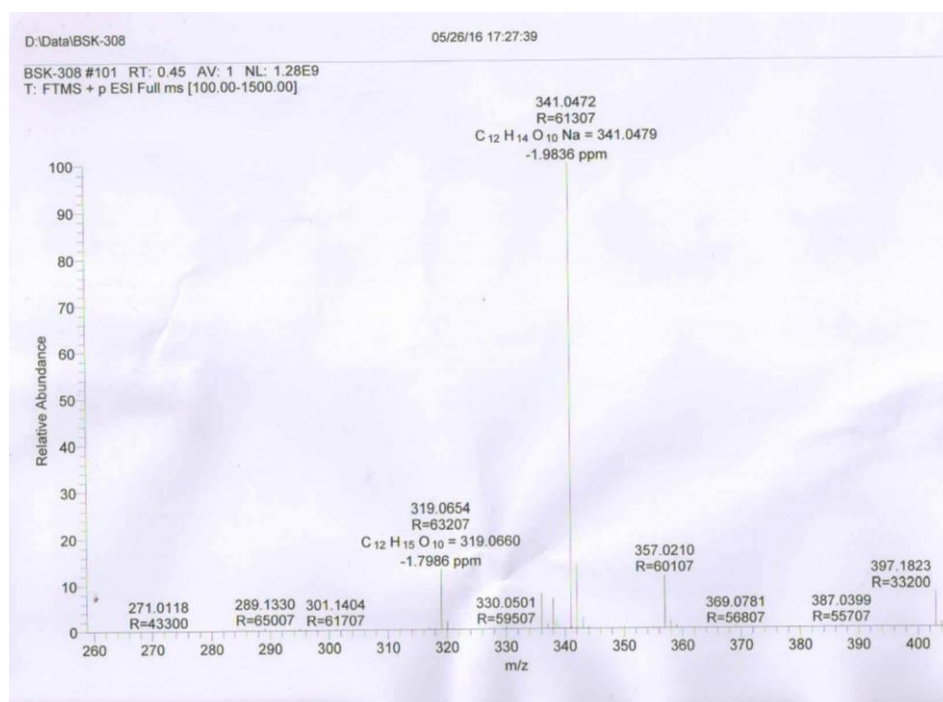
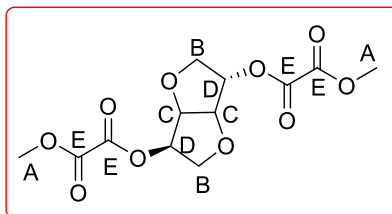


Figure 4.6. ESI-MS (+ve mode) spectrum of compound **4a** ($\text{C}_{12}\text{H}_{14}\text{O}_{10}$), $m/z = 341.04$ $[\text{M}+\text{Na}]^+$.

4.4.2.2. Synthesis of *O, O'*-(3*R, 6S*)-Hexahydrofuran [3,2-*b*]furan-3,6-diyl) dimethyl dioxalates [Isosorbide-Dioxalate] (4b**):**

To a stirred solution of isosorbide (0.516 g, 3.53 mmol in 20 ml dry THF) was slowly added *n*-BuLi (4.1 ml, 8.12 mmol) at -78 °C and the mixture was stirred for 1 hour. After that, the resulting mixture is stirred at room temperature for 1 more hour. To this mixture was added methyl chlorooxoacetate (0.74 ml, 8.12 mmol) at 0 °C and the reaction content was stirred for next 48 hours at room temperature. Subsequently, the reaction mixture was washed with saturated sodium chloride solution (20 ml) and the aqueous phase was extracted with ethyl acetate (3 × 20) ml). The combined organic phase was dried over MgSO₄, filtered and the filtrate was evaporated in vacuum to obtain a highly viscous material. Purification by column chromatography (pet ether-ethyl acetate 55:45) yielded highly viscous liquid. The residue was dissolved in ethyl acetate and was precipitated by adding excess pet ether. After evaporation of volatiles a white solid of the desired isosorbide-dioxalate **4b** (0.85 g, 76 %) was isolated.

¹H NMR (400 MHz, CDCl₃, 298 K) δ = 5.33-5.30 (m, 2H_D), 5.01-4.98 (m, 1H_C), 4.59-4.58 (m, 1H_C), 4.08-3.94 (m, 4H_B), 3.91-3.89 (s, 6H_A). **¹³C NMR** (100 MHz, CDCl₃, 298 K) δ = 157.7-156.8 (m, C_E), 85.8 (s, C_C), 80.9 (s, C_C), 80.3 (s, C_D), 76.2 (s, C_D), 73.1 (s, C_B), 70.8 (s, C_B), 53.9 (s, C_A). **ESI-MS** (+ve mode) *m/z* = 341.04 [M+Na]⁺. **Elemental analysis** (%): Calculated for C₁₂H₁₄O₁₀: C- 45.29, H- 4.43; Found: C- 45.90, H-4.33.

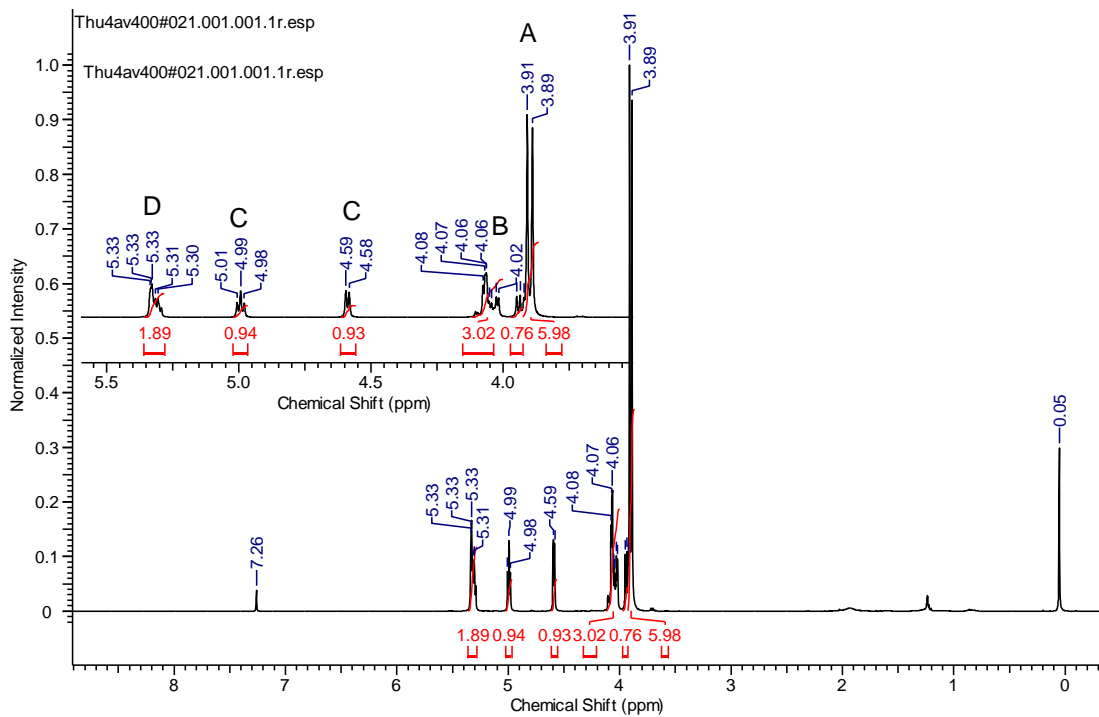


Figure 4.7. ¹H NMR spectrum of compound **4b** in CDCl₃ (400 MHz at 298 K).

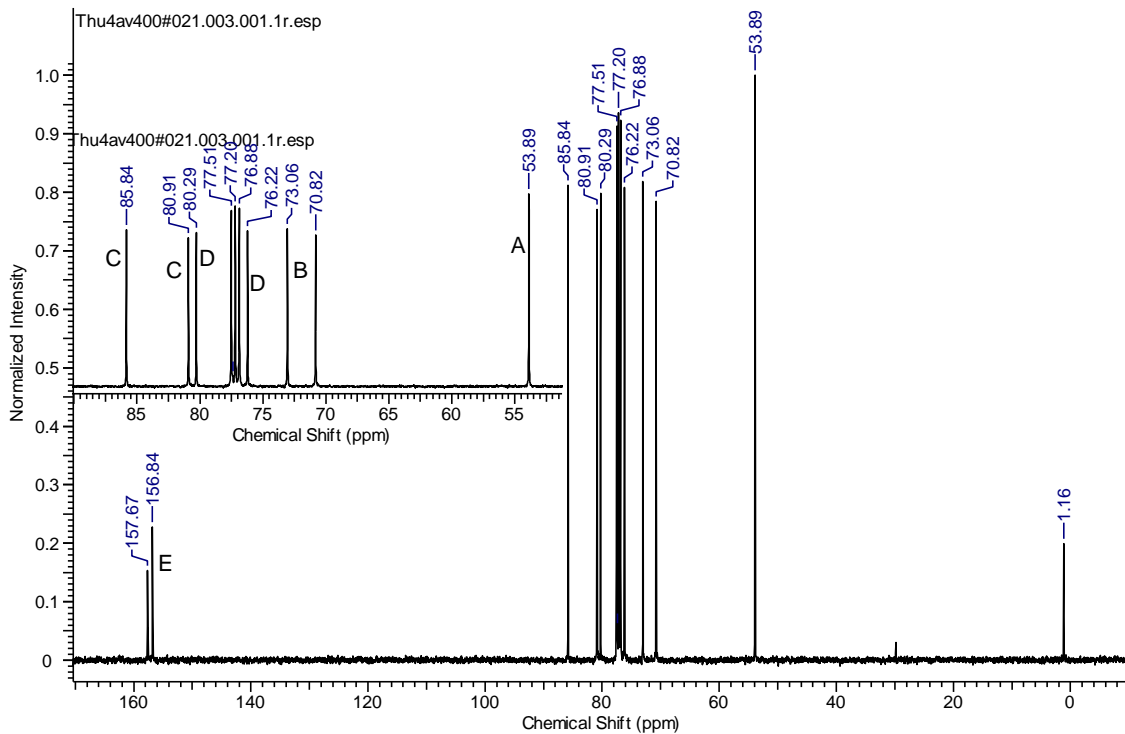


Figure 4.8. ¹³C NMR spectrum of compound **4b** in CDCl₃ (100 MHz at 298 K).

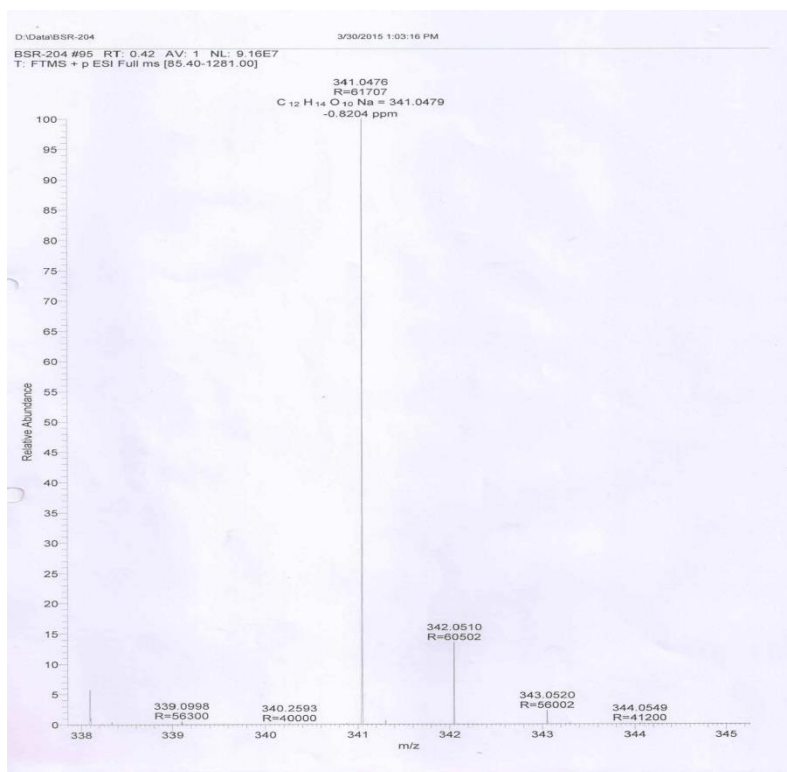
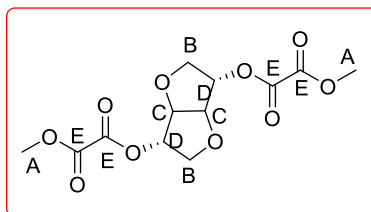


Figure 4.9. ESI-MS (+ve mode) spectrum of compound **4b** ($C_{12}H_{14}O_{10}$), $m/z = 341.04 [M+Na]^+$.

4.4.2.3. Synthesis of *O, O'*-((3*S*,6*S*)-Hexahydrofuran[3,2-*b*]furan-3,6-diyl) dimethyl dioxalates [Isoidide-Dioxalate] (**4c**):



To a stirred solution of isoidide^{4b} (0.516 g, 3.53 mmol) in 20 ml dry THF was slowly added *n*-BuLi (4.1 ml, 8.12 mmol) at $-78\text{ }^{\circ}\text{C}$ and the mixture was stirred for 1 hour. Next, the Schlenk tube was brought to room temperature and was stirred for an additional hour. Subsequently, the Schlenk tube was cooled to $0\text{ }^{\circ}\text{C}$ and methyl chlorooxoacetate (0.74 ml, 8.12 mmol) was added. The reaction mixture was warmed to room temperature and was stirred for next 48 hours. The resultant reaction mixture was washed with saturated sodium chloride solution (20 ml) and the aqueous phase was extracted with ethyl acetate (3×20 ml). The combined organic phase was dried over $MgSO_4$, filtered and the filtrate was evaporated in vacuum to obtain a highly viscous material. Purification by column chromatography (pet ether-

ethyl acetate 55:45) yielded highly viscous liquid. This residue was dissolved in ethyl acetate and was precipitated by adding excess pet ether to produce white solid. The white solid was isolated after evaporation of solvents yielding 0.60 g of the desired isoidide-dioxalate **4c** (53%).

$^1\text{H NMR}$ (400 MHz, CDCl_3 , 298 K) δ = 5.33 (s, 2H_D), 4.79 (s, 2H_C), 4.02 (s, 4H_B), 3.88 (s, 6H_A).

$^{13}\text{C NMR}$ (100 MHz, CDCl_3 , 298 K) δ = 157.2-156.3 (m, C_E), 84.8 (s, C_C), 79.5 (s, C_D), 71.9 (s, C_B), 53.6 (s, C_A). **ESI-MS** (+ve mode) m/z = 319.06 $[\text{M}+\text{H}]^+$. **Elemental analysis** (%):

Calculated for $\text{C}_{12}\text{H}_{14}\text{O}_{10}$: C- 45.29, H- 4.43; Found: C- 45.15, H-3.87.

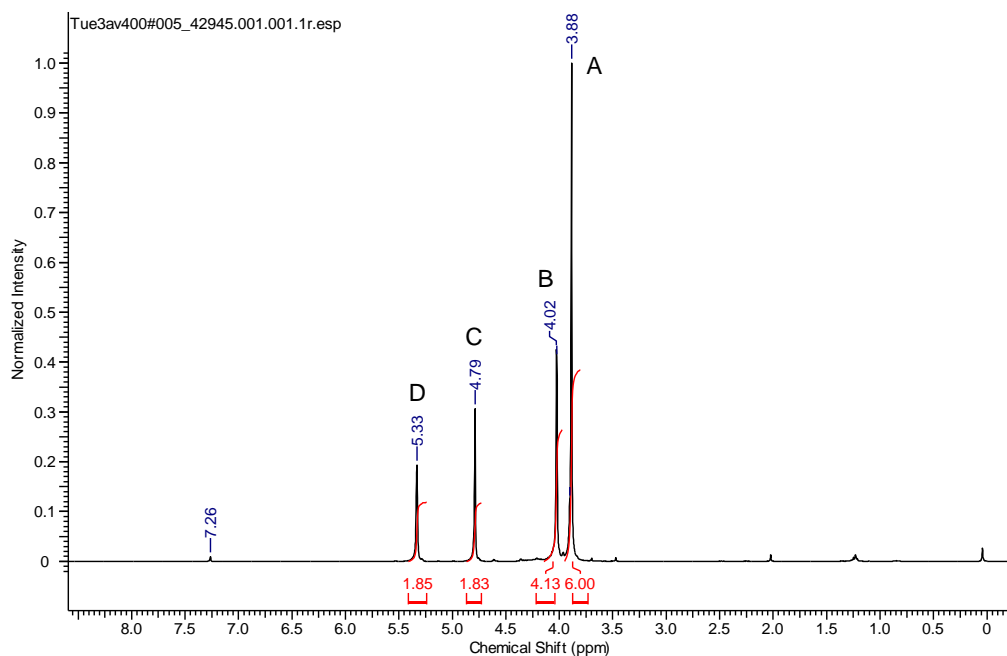


Figure 4.10. $^1\text{H NMR}$ spectrum of compound **4c** in CDCl_3 (400 MHz at 298 K).

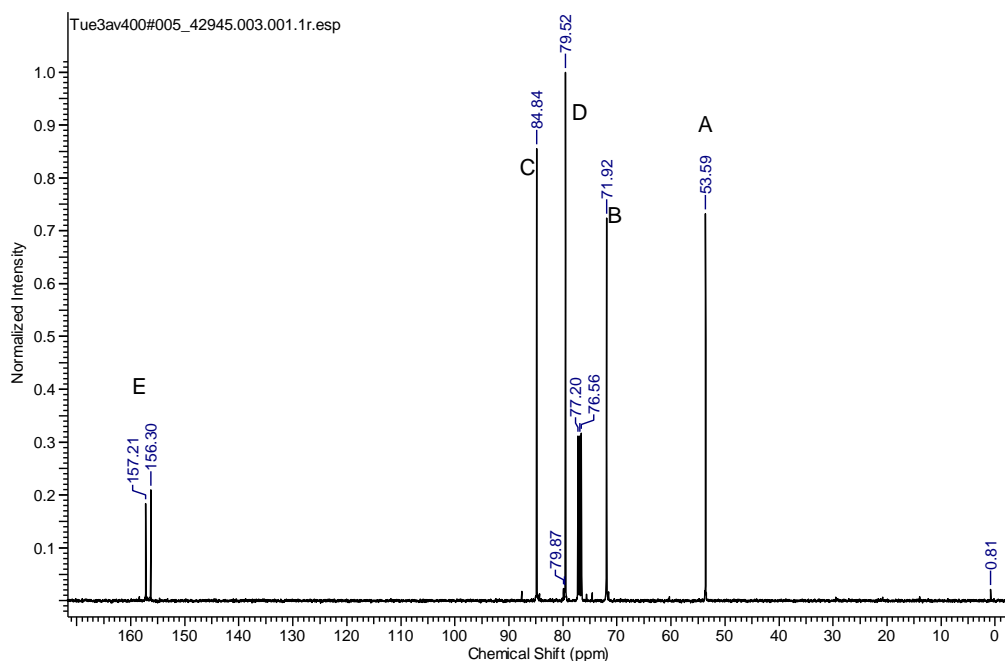


Figure 4.11. ^{13}C NMR spectrum of compound **4c** in CDCl_3 (100 MHz at 298 K).

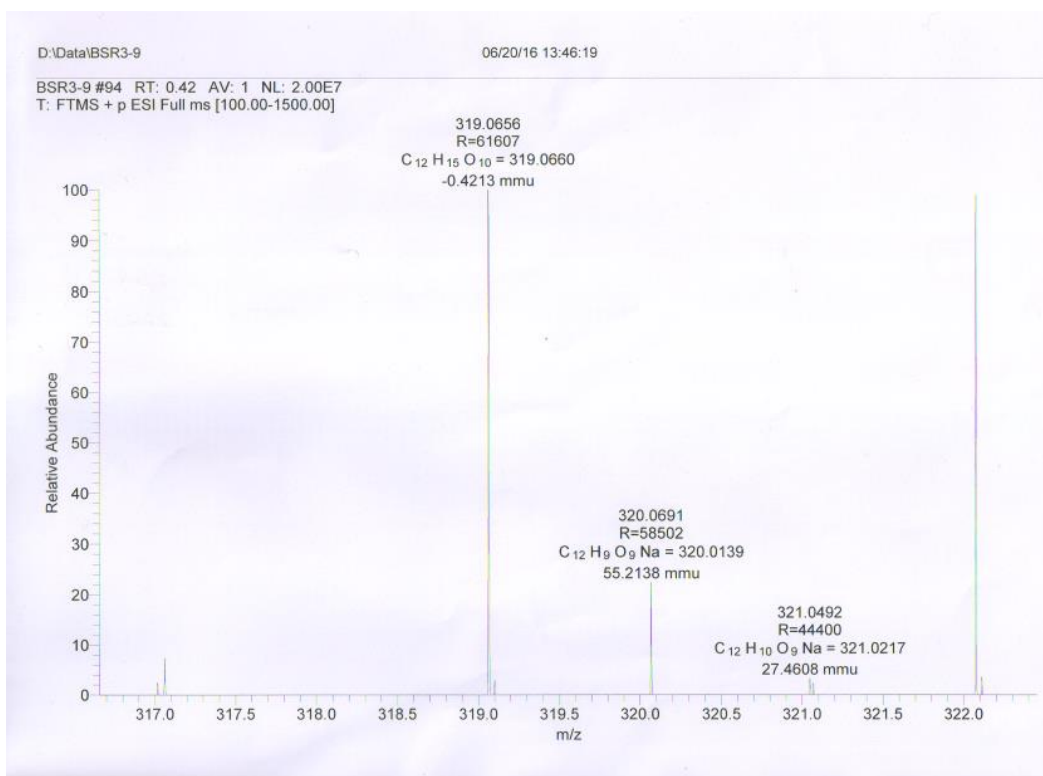
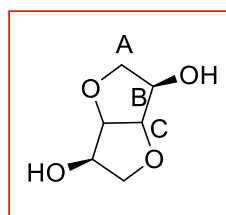


Figure 4.12. ESI-MS (+ve mode) spectrum of compound **4c** ($\text{C}_{12}\text{H}_{14}\text{O}_{10}$), $m/z = 319.06$ $[\text{M}+\text{H}]^+$.

4.4.3. Investigating the Reactivity and Control Experiments:

4.4.3.1. Direct Polymerization of Isomannide with Dimethyl Oxalate:

Polymerization of isomannide with dimethyl oxalate was carried out by following the literature procedure with slight modification.²⁷ In a 50 ml Schlenk tube one equivalent isomannide (1 gm, 6.84 mmol) and dimethyl oxalate (0.81 gm, 6.84 mmol) was taken. To this, 2 mol% (0.026 gm, 0.1368 mmol) of *p*-TSA catalyst was added under positive argon flow. The polymerization was started by heating the reaction mixture at 100 °C with constant stirring (using overhead mechanical stirrer) for 1 hour. After an hour, the temperature of the polymerization reaction was raised to 130 °C and polymerization was run for 2 hours under argon. For next one hour, slight vacuum was applied every 10-15 mins. to remove the byproduct (methanol). Finally, the content was stirred at 220 °C for next 3 hours under argon atmosphere. Polymerization was terminated by cooling the Schlenk to room temperature and finally the crude oily black color material was recovered. The ¹H and ¹³C NMR of crude oily material in D₂O shows the signals corresponding to the isomannide backbone along with the unreacted hydrolyzed dimethyl oxalate (see **Figure 4.13** and **4.14**). GPC results revealed only low molecular weight fractions ($M_w = 450$ Da) which actually touches lower detection limit of GPC (see **Figure 4.15**) and these numbers are therefore unreliable. These observations clearly indicate that the direct polymerization of isomannide with dimethyl oxalate fails to provide any polymer.



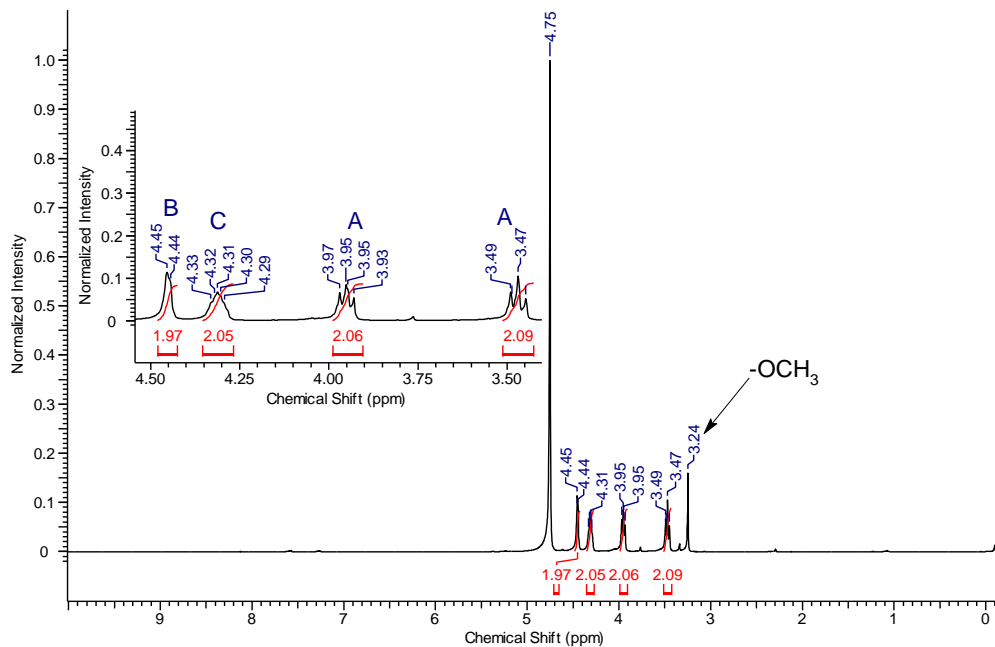


Figure 4.13. ¹H NMR spectrum of crude sample in D₂O (500 MHz at 298 K).

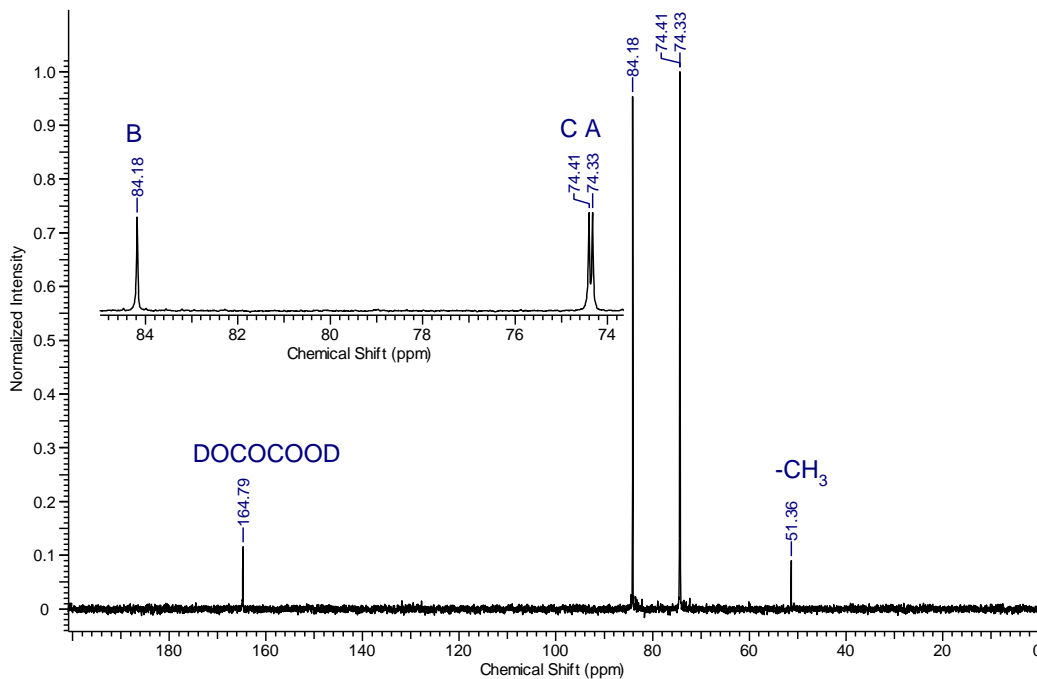


Figure 4.14. ¹³C NMR spectrum of crude sample in D₂O (100 MHz at 298 K).

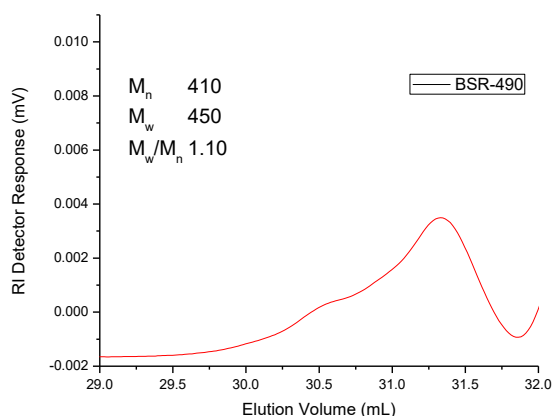


Figure 4.15. GPC chromatogram of crude sample in chloroform at room temperature.

4.4.3.2. Investigating the Reactivity of Isomannide-Dioxalate with **1**, 6-Hexane Diol:

In our attempts to identify the intermediates, reactivity of **4a** with **5a** in the initial stages of the polymerization reaction was investigated (see **Scheme 4.2**). In a 50 ml Schlenk tube isomannide-dioxalate **4a** (0.400 gm, 1.26 mmol), 1, 6-hexane diol **5a** (0.148 gm, 1.26 mmol) and 1 mol% of $[\text{Ti}(\text{OiPr})_4]$ (0.0036 gm, 0.0126 mmol) was added under positive argon flow. The reaction mixture was heated at 120 °C and stirred for 30 mins. The obtained crude reaction mixture was subjected to the column chromatographic (pet ether-ethyl acetate, 50:50) and various fractions were separated. A major fraction was found to be a dimer of 7-hydroxylheptyl methyl oxalate, **5a'**, that is, **5a''**. Unfortunately some of the isomannide-dioxalate fraction also elutes at the same polarity. The polarity of column was further increased (pet ether-ethyl acetate, 40:60) to eluate isomannide-monooxalate (**4a'**). A proton resonance at 3.87 ppm corresponds to the $-\text{OCH}_3$ group originating from dimer (**5a''**) and the multiplet at 3.54-3.64 ppm corresponds to the methylene protons next to the $-\text{OH}$ group (**Figure 4.16**).

The NMR findings were further supported by ESI-MS, that revealed molecular ion peak at $m/z = 399.16$ [**5a''**+Na]⁺ (**Figure 4.17**) corresponding to the dimer (**5a''**). The second fraction that could be isolated revealed a proton resonance at 3.91 ppm ($-\text{OCH}_3$ group) and all other signals match with expected chemical shifts (**Figure 4.18**) for isomannide-monooxalate (**4a'**). The proton NMR was corroborated by positive mode ESI-MS that showed a molecular ion peak at $m/z = 255.04$ [**4a'**+Na]⁺ (**Figure 4.19**). These observations clearly indicate that one of the oxalate from isomannide-dioxalate (**4a**) is transferred to the 1, 6-hexane diol (**5a**) leading to isomannide-monooxalate (**4a'**) and 1, 6-hexane monooxalate (**5a'**). The 1, 6-hexane monooxalate

5a' seems to be much more reactive and self-condenses to yield a dimer **5a''**, which has been isolated from the reaction in the initial stage.

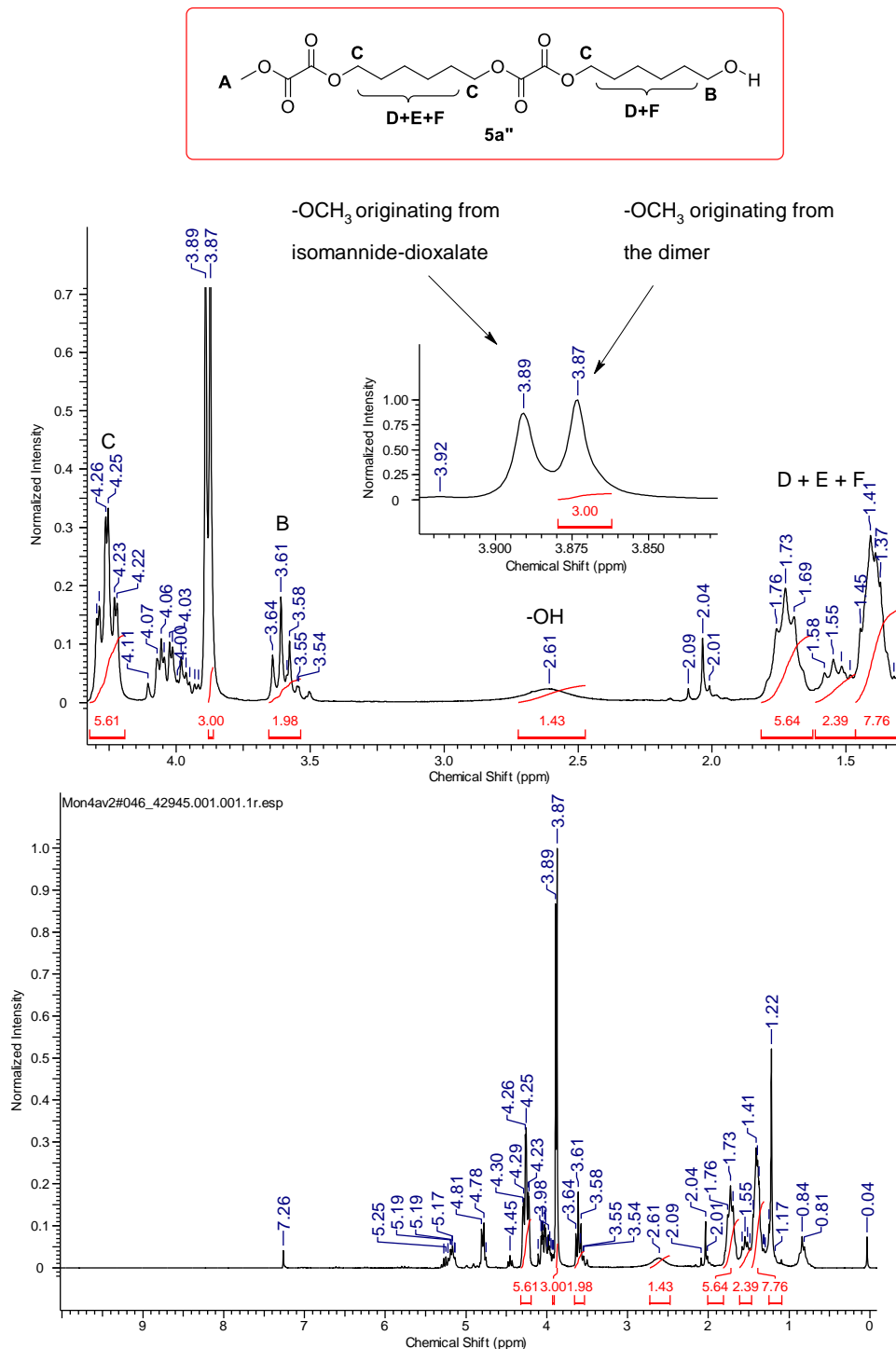


Figure 4.16. ¹H NMR spectrum of dimer (**5a''**) in CDCl₃ (200 MHz at 298 K).

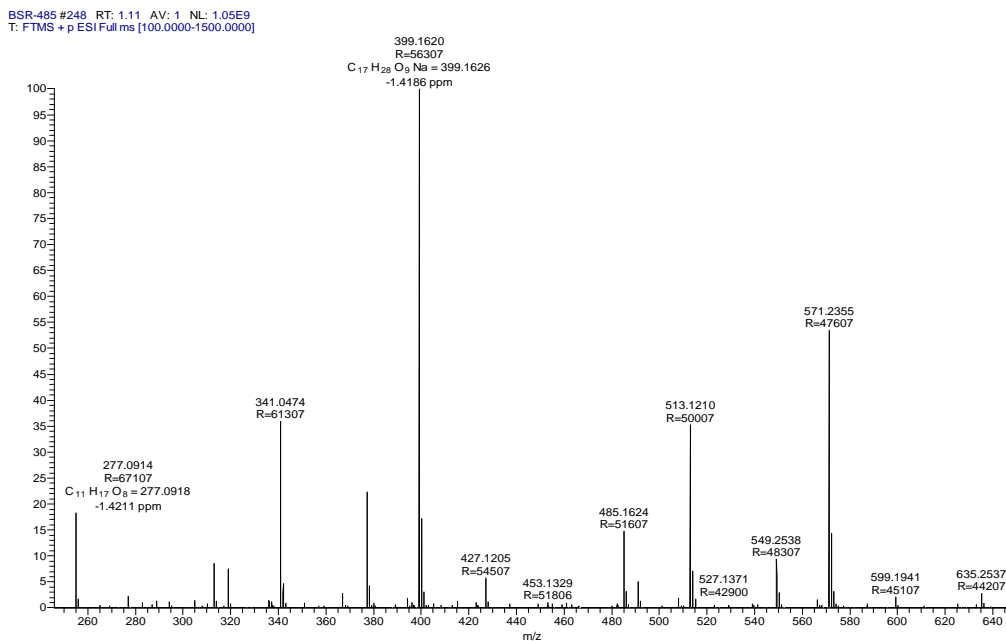


Figure 4.17. ESI-MS (+ve mode) spectrum of isolated dimer **5a''** (C₁₇H₂₈O₉), m/z = 399.16 [M+Na]⁺.

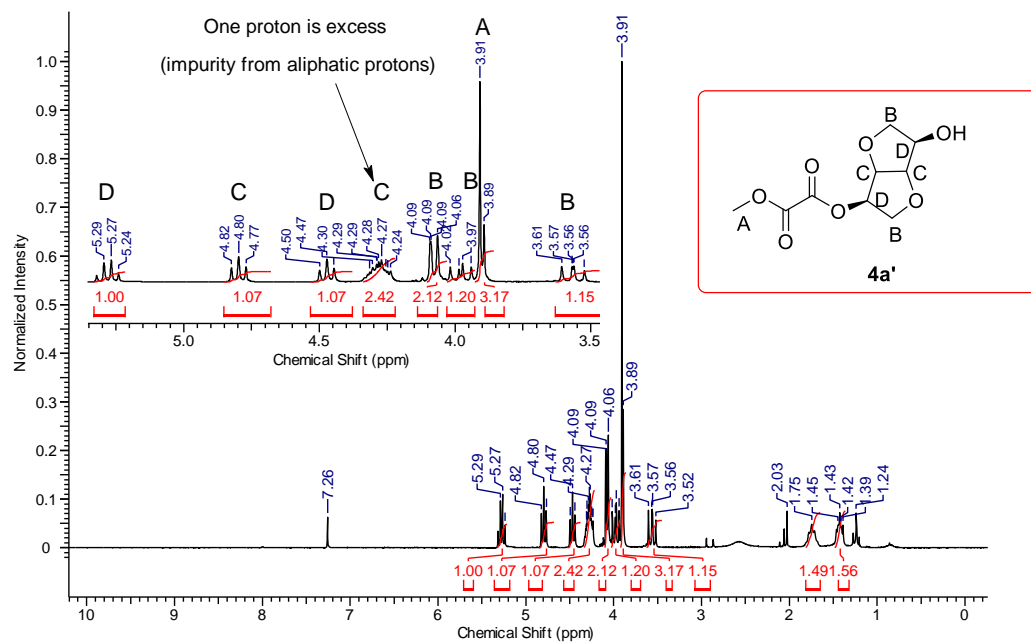


Figure 4.18. ¹H NMR spectrum of isolated isomannide-monooxalate (**4a'**) in CDCl₃ (200 MHz at 298 K).

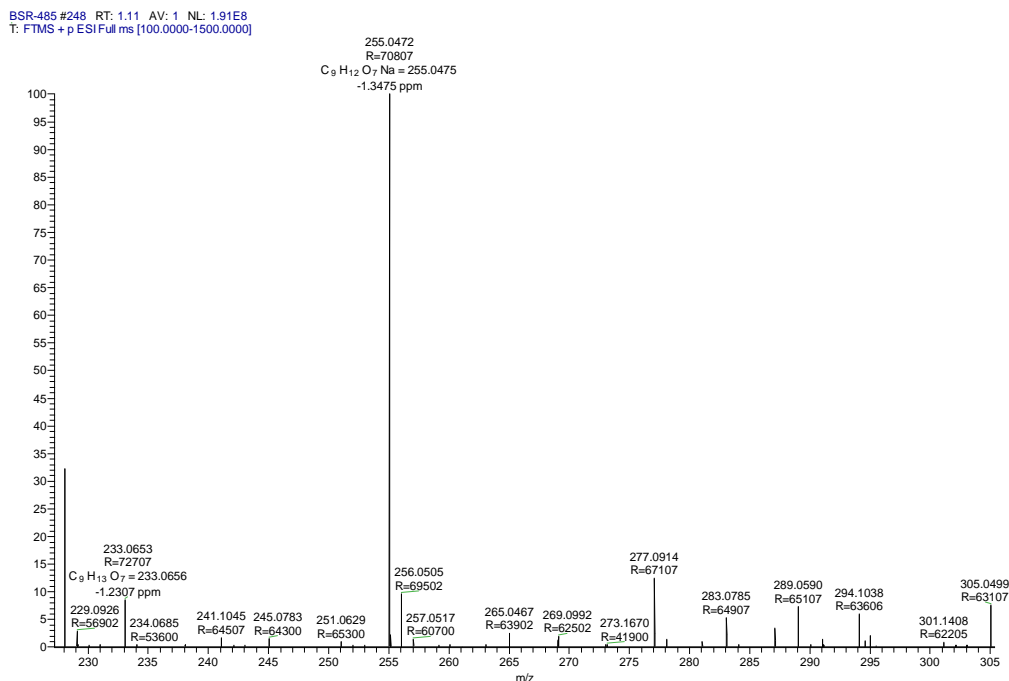


Figure 4.19. ESI-MS (+ve mode) spectrum of isolated isomannide-monooxalate **4a'** ($C_9H_{12}O_7$), $m/z = 255.04 [M+Na]^+$.

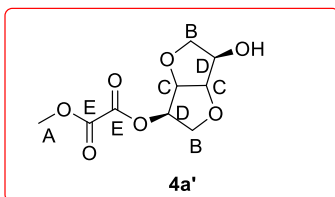
4.4.3.3. Polymerization of Isomannide-Monooxalate (**4a'**) with **1**, 6-Hexane Monooxalate (**5a'**):

Isomannide-monooxalate (**4a'**) and **1**, 6-hexane monooxalate (**5a'**) were synthesized separately as under. The detailed synthetic procedure and characterization is provided below.

4.4.3.3.1. Synthesis of Isomannide-Monooxalate (**4a'**):

In a 100 ml Schlenk flask, 0.39 g (16.43 mmol) of sodium hydride was accurately weighed and 30 ml of dry tetrahydrofuran was added. A THF solution of isomannide (2 g, 13.69 mmol, in 20 ml THF) was slowly added to above Schlenk tube over a period of 2 hours and the mixture was stirred for next 22 hours at room temperature. Subsequently, methyl chlorooxacetate (1.26 ml, 13.69 mmol) was added and the resultant reaction mixture was stirred for 24 hours at room temperature. Excess of sodium hydride present in reaction mixture was quenched with distilled water, the reaction mixture was washed with saturated sodium chloride (NaCl) solution (30 ml) and the aqueous phase was extracted with ethyl acetate (3×30 ml). The combined organic phase was dried over $MgSO_4$, filtered and the filtrate was evaporated in vacuum to obtain a highly viscous residue. Purification by column chromatography (pet ether-

ethyl acetate 50:50) yielded 0.93 g (4.0 mmol) of the desired (3R, 6R)-6-hydroxyhexahydrofuro[3,2-b]furan-3-yl methyl oxalate **4a'** (29%) as a white solid.



$^1\text{H NMR}$ (500 MHz, CDCl_3 , 298 K) δ = 5.28-5.25 (m, 1H_D), 4.79-4.77 (t, 1H_C), 4.46-4.44 (t, 1H_D), 4.28-4.24, (m, 1H_C), 4.09-4.03 (m, 2H_B), 3.97-3.94 (m, 1H_B), 3.89 (s, 3H_A), 3.56-3.53(t, 1H_B). $^{13}\text{C NMR}$ (125 MHz, CDCl_3 , 298 K) δ = 157.5-156.7 (s, C_E), 81.5 (s, C_D), 80.3 (s, C_C), 76.6 (s, C_D), 73.4 (s, C_B), 72.12 (s, C_C), 70.8 (s, C_B), 53.7 (s, C_A). **ESI-MS** (+ve mode) m/z = 255.04 $[\text{M}+\text{Na}]^+$.

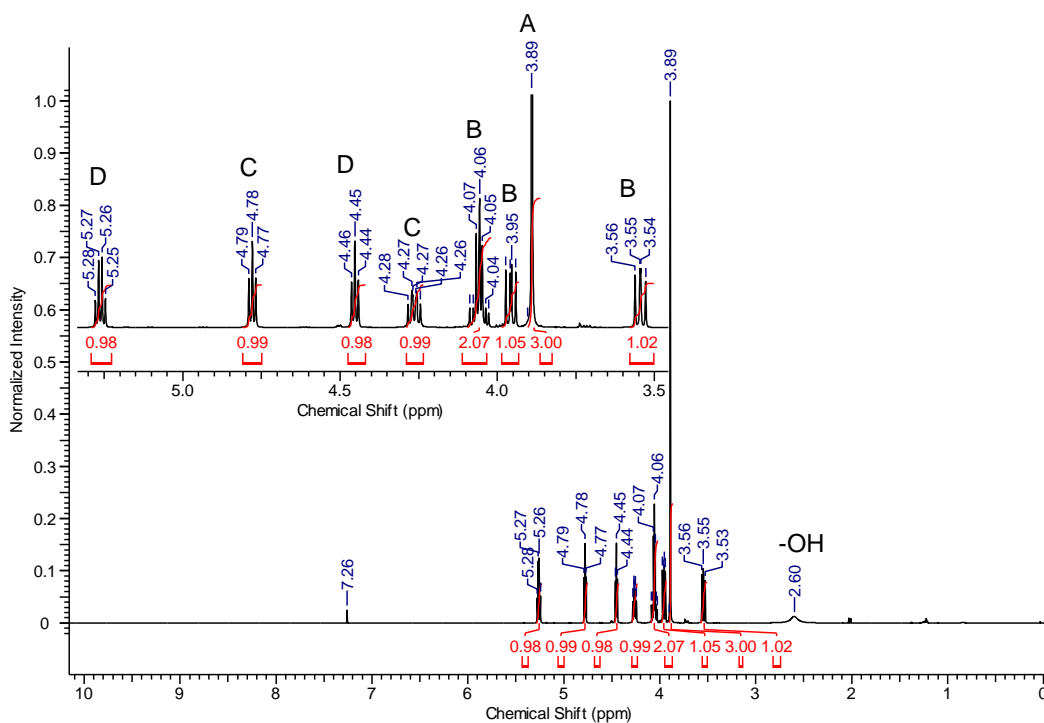


Figure 4.20. $^1\text{H NMR}$ spectrum of isomannide-monooxalate (**4a'**) in CDCl_3 (500 MHz at 298 K).

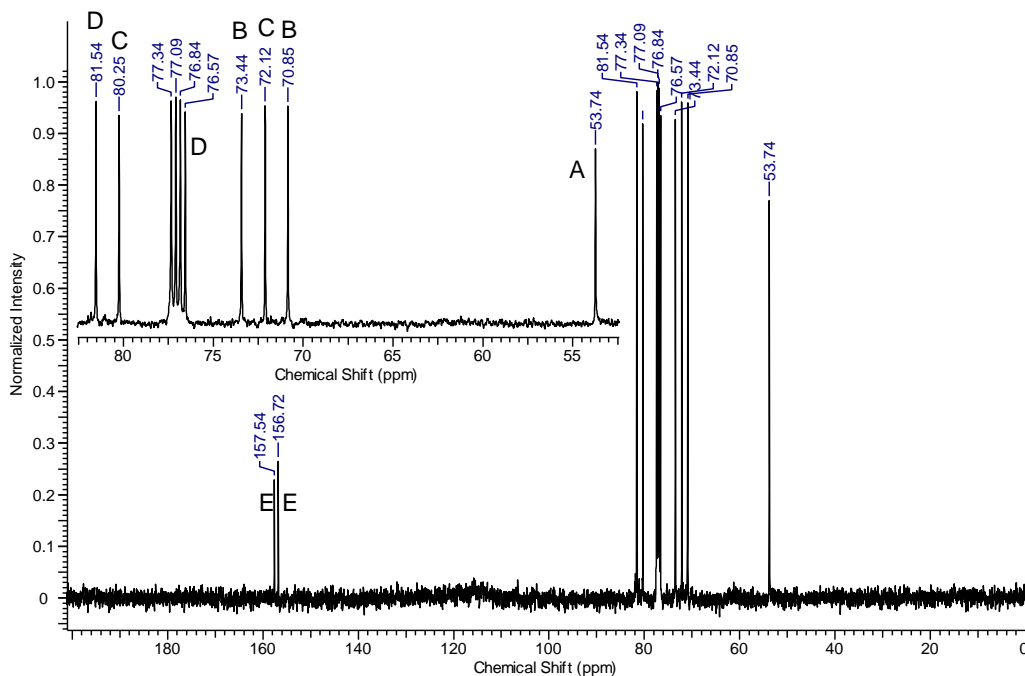


Figure 4.21. ^{13}C NMR spectrum of isomannide-monooxalate (**4a'**) in CDCl_3 (125 MHz at 298 K).

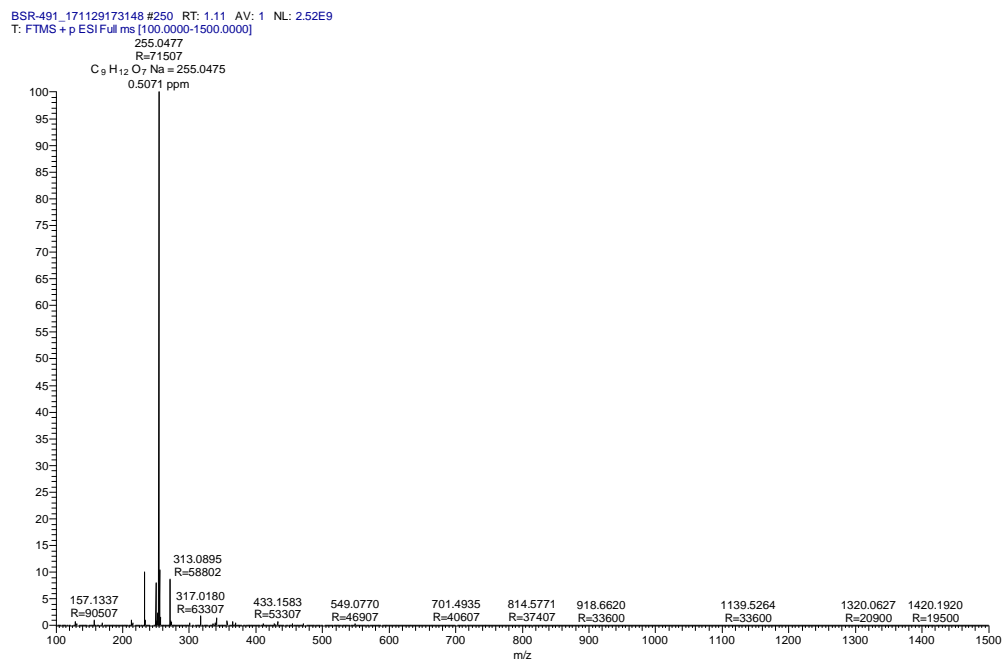
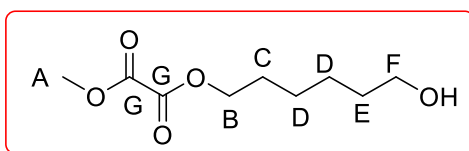


Figure 4.22. ESI-MS (+ve mode) spectrum of isomannide-monooxalate **4a'** ($\text{C}_9\text{H}_{12}\text{O}_7$), $m/z = 255.04$ $[\text{M}+\text{Na}]^+$.

4.4.3.3.2. Synthesis of 1, 6-Hexane Monoxalate (5a'):

In 100 ml Schlenk flask 0.49 g (20.30 mmol) of sodium hydride was weighed accurately and 40 ml of dry tetrahydrofuran was added. A THF solution of 1, 6-hexane diol (2 g, 16.92 mmol) in 20 ml THF was added to above Schlenk and reaction mixture was stirred over a period of 3 hours at room temperature. Methyl chlorooxoacetate (1.56 ml, 16.92 mmol) was slowly added to above Schlenk and the resultant reaction mixture was stirred for 16 hours at room temperature. Excess of sodium hydride was quenched with distilled water, the reaction mixture was washed with saturated sodium chloride (NaCl) solution (30 ml) and the aqueous phase was extracted with ethyl acetate (3 × 30 ml). The combined organic phase was dried over MgSO₄, filtered and the filtrate was evaporated in vacuum to obtain a highly viscous material. Purification by column chromatography (pet ether-ethyl acetate 65:35) yielded 1.36 g (6.66 mmol) of the desired 6-hydroxyhexyl methyl oxalate **5a'** (39%) as a viscous liquid.



¹H NMR (400 MHz, CDCl₃, 298 K) δ = 4.25-4.22 (t, 2H_B), 3.85 (s, 3H_A), 3.58-3.55 (t, 2H_F), 2.18 (broad, -OH), 1.71-1.68 (m, 2H_C), 1.53-1.50 (m, 2H_E), 1.37-1.36 (m, 4H_D). ¹³C NMR (100 MHz, CDCl₃, 298 K) δ = 158.2-157.6 (m, C_G), 67.1 (s, C_B), 62.5 (s, C_F), 32.4 (s, C_E), 28.2 (s, C_C), 25.5, 25.3 (s, C_D). **ESI-MS** (+ve mode) m/z = 227.08 [M+Na]⁺.

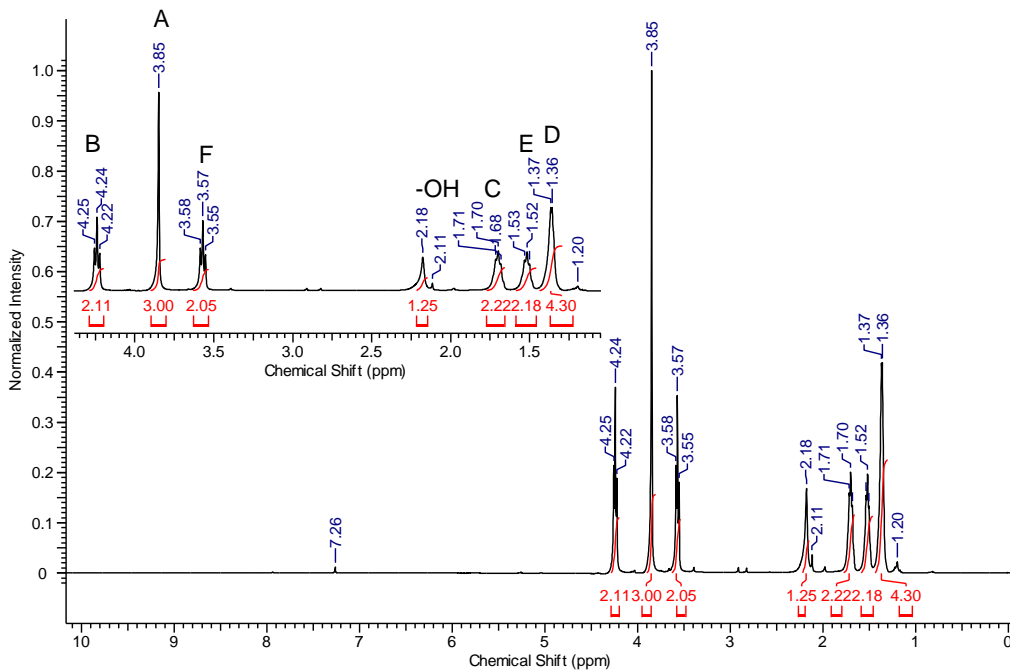


Figure 4.23. ^1H NMR spectrum of 1, 6-hexane monooxalate (**5a'**) in CDCl_3 (400 MHz at 298 K).

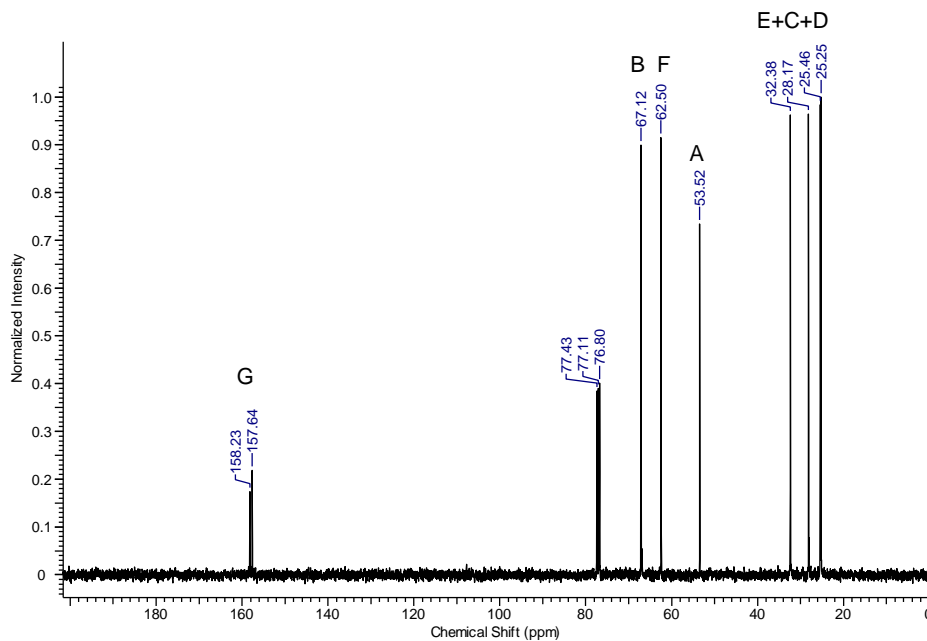


Figure 4.24. ^{13}C NMR spectrum of 1, 6-hexane monooxalate (**5a'**) in CDCl_3 (100 MHz at 298 K).

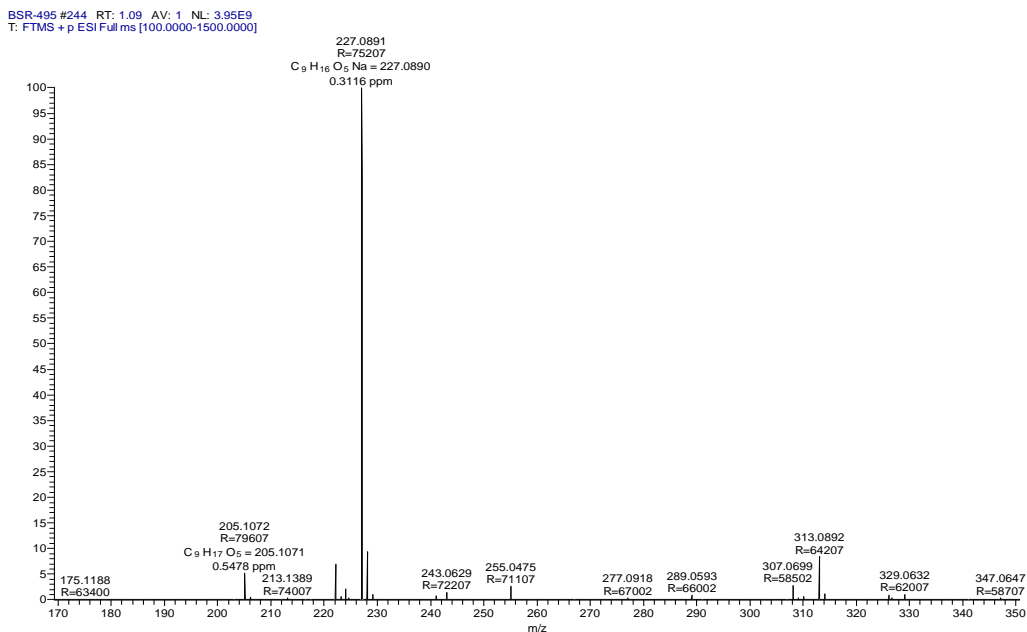
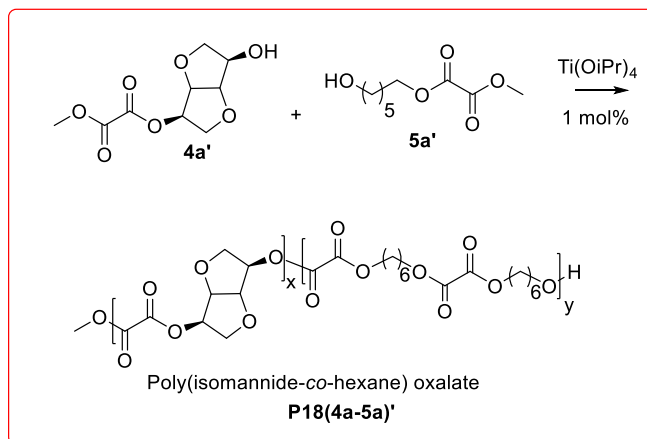


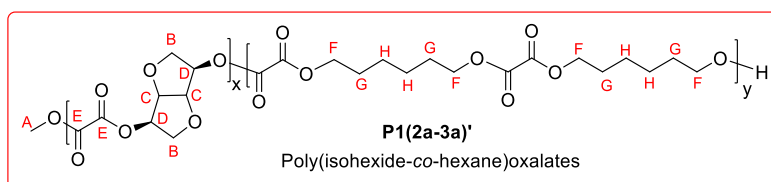
Figure 4.25. ESI-MS (+ve mode) spectrum of 1, 6-hexane monooxalate **5a'** (C₉H₁₆O₅), m/z = 227.08 [M+Na]⁺.

4.4.3.3. Polymerization of (4a') and (5a') to P18(4a-5a)':



The polyoxalates were prepared in a 50 ml Schlenk tube equipped with an overhead mechanical stirrer, heating arrangement and vacuum line. Isomannide-monoxalate (**4a'**) 0.937 g (4.04 mmol) and 1, 6-hexane monooxalate (**5a'**) 0.82 g (4.04 mmol) were transferred to the Schlenk tube and titanium isopropoxide (0.011 g, 0.0404 mmol, 1mol%) was added under positive argon flow. The polymerization was started at 120 °C and over a period of 2 hours the temperature was raised to 150 °C with intermittent vacuum in every 5 minutes to take out the byproduct (methanol). Subsequently, the polymerization is run at 150 °C for another 3 hours

with slight vacuum to avoid the monomer losses. Finally, the polymer melt was stirred for next 43 hours under reduced pressure (0.01 mbar). The thus obtained polymer was dissolved in chloroform (2 ml) and precipitated by pouring in methanol (~100 ml). The resultant polymer was isolated as a rubbery material after complete drying (0.83 g, 54%). ^1H NMR spectrum of this polymer revealed that the number of protons of aliphatic backbone is double than the isomannide protons ($5a':4a' = 2:1$) (Figure 4.26), which is in line with our observations for **P18(4a-5a)**. Proton NMR of the washing recovered after precipitation displayed presence of isomannide as major fractions (Figure 4.27). The GPC results revealed the molecular weight of 19200 g/mol (M_w 19200 g/mol, Figure 4.28).



^1H NMR (500 MHz, CDCl_3 , 298 K) $\delta = 5.18$ (br., 2H_D), 4.81 (br., s, 2H_C), 4.27 (br., s, 9H_F), 4.07 - 3.99 (br., s, 4H_B), 1.75 (br., s, 9H_G), 1.43 (br., s, 9H_H).

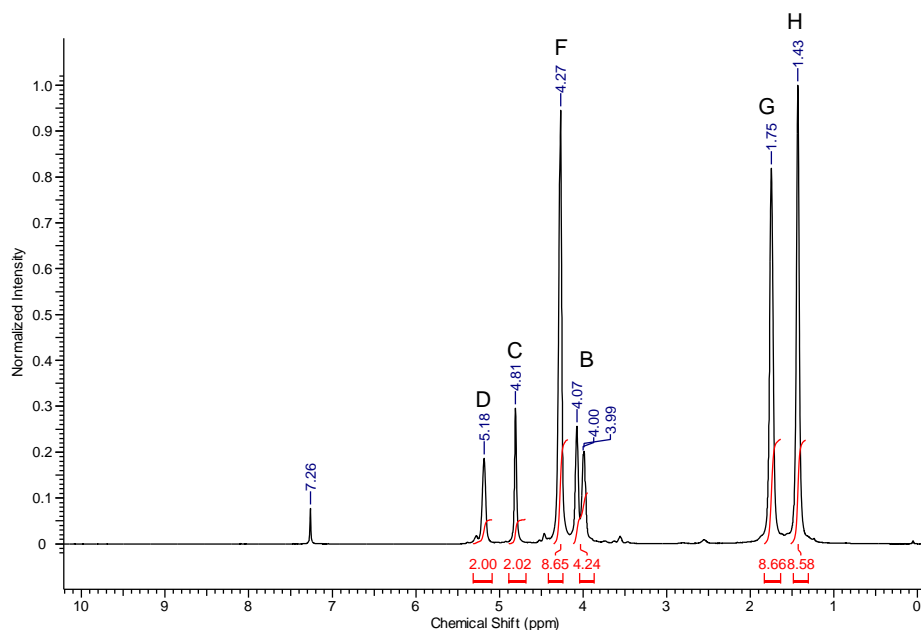


Figure 4.26. ^1H NMR spectrum of **P18(4a-5a)'** in CDCl_3 (500 MHz at 298 K).

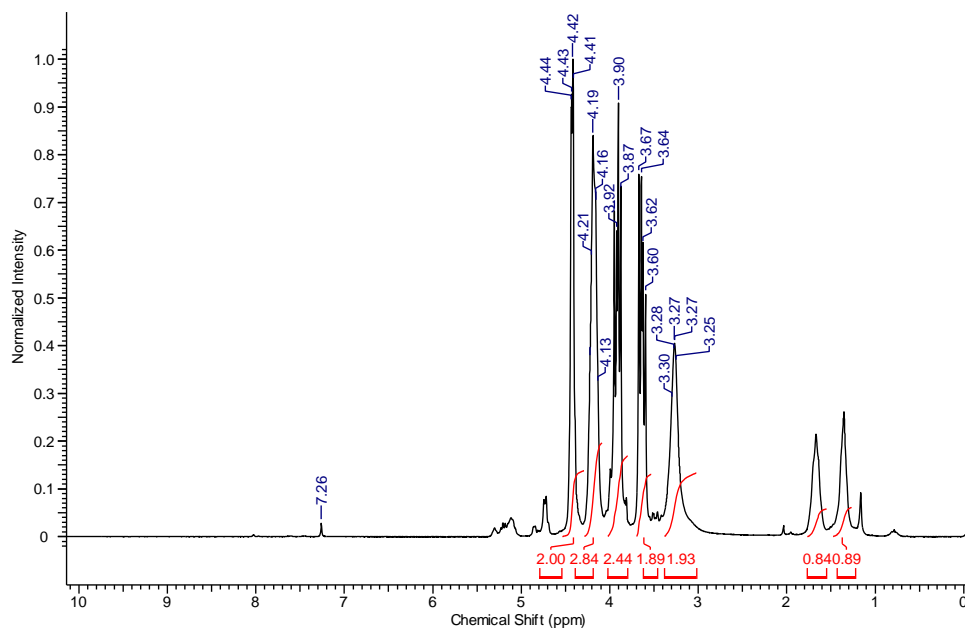


Figure 4.27. ^1H NMR spectrum of washing displaying isomannide as a major fraction in CDCl_3 (200 MHz at 298 K).

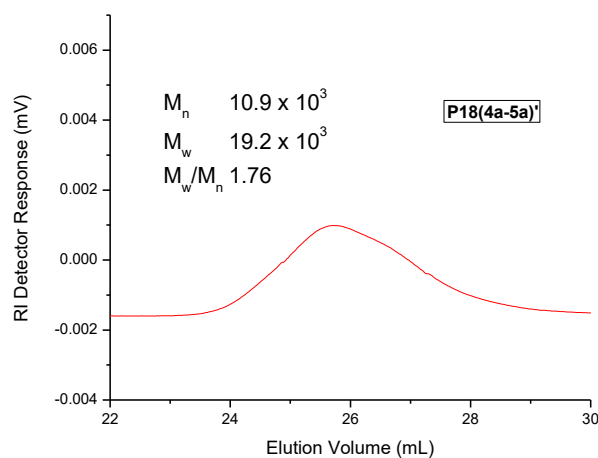


Figure 4.28. GPC chromatogram of **P18(4a-5a)'** in chloroform at room temperature.

4.4.4. General Procedure for Polymer Synthesis:

The polyoxalates were prepared in a 50 ml Schlenk tube equipped with an overhead mechanical stirrer, heating arrangement and vacuum-purge system. Isohexide-dioxalates (**4a-4c**) and linear-diols (**5a-5c**) were transferred to the Schlenk tube and catalyst (1 mol%) was added under positive argon flow. The monomers (neat monomers)

were melted by heating and polymerization was started at 120 °C. Next, over a period of 2 hours the temperature was raised to 150 °C with intermittent vacuum after every 3-5 minutes to knock-off the by-product (methanol). Finally, the polymer melt was stirred for next 46 hours under reduced pressure (0.01 mbar). The thus obtained polymer was dissolved in chloroform and precipitated by pouring in methanol (~100 ml). The resultant polymer was isolated as semi-solid material which was dried in vacuum. The quantitative details of various polyoxalates are summarized in **Table 4.2**. Synthesized polyoxalates were characterized using various analytical tools.

Table 4.2. Polymerization of isohexide-dioxalates (**4a-c**) and linear-diols (**5a-c**).

Run	Polyoxalates	4a-c g(mmol)	5a-c g(mmol)	Ti(OiPr) ₄ (mmol)	Theoretical yield (g)	Isolated yield (g)	Yield (%)
1	P18(4a-5a)	1.0(3.14)	0.37(3.14)	0.0314	1.17	0.73	62
2	P19(4a-5b)	0.83(2.61)	0.38(2.61)	0.0261	1.05	0.60	57
3	P20(4c-5c)	0.78(2.47)	0.50(2.47)	0.0247	1.13	0.77	68
4	P21(4b-5a)	1.0(3.14)	0.37(3.14)	0.0314	1.17	0.84	72
5	P22(4b-5b)	0.64(2.02)	0.29(2.02)	0.0202	0.81	0.50	62
6	P23(4b-5c)	0.85(2.68)	0.54(2.68)	0.0268	1.22	0.91	74
7	P24(4c-5a)	0.9(2.83)	0.33(2.83)	0.0283	1.05	0.69	65
8	P25(4c-5b)	0.83(2.61)	0.38(2.61)	0.0261	1.05	0.68	65
9	P26(4c-5c)	0.9(2.83)	0.57(2.83)	0.0283	1.29	0.95	74

Note: % yield = (mol of polymer isolated after precipitation) / (mol of monomer) × 100).

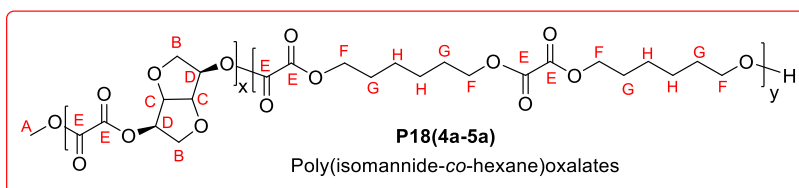
Table 4.3. Optimization of polymerization conditions for isosorbide-dioxalate (**4b**) polymerization with octane-1, 8-diol (**5b**) and dodecane-1, 12-diol (**5c**).

Run	Monomer	Polymers	Catalyst (mol%)	M _w (10) ³	PDI	T _m (°C)	Time (h)	Temp (°C)
1	4b-5b	P22(4b-5b)	<i>p</i> -TSA (10)	2.21	1.77	ND	8	150
2	4b-5c	P23(4b-5c)	<i>p</i> -TSA (10)	3.15	1.78	81	8	120
3	4b-5c	P23(4b-5c)	<i>p</i> -TSA (10)	4.35	2.11	ND	8	150
4	2b-5c	P23(4b-5c)	<i>p</i> -TSA (10)	4.73	2.25	74	8	200
5	4b-5b	P22(4b-5b)	Ti(OiPr) ₄ (5)	5.84	1.46	ND	4	150
6	4b-5b	P22(4b-5b)	Ti(OiPr) ₄ (5)	9.83	2.03	53	8	150
7	4b-5b	P22(4b-5b)	Ti(OiPr) ₄ (5)	22.5	2.51	49	12	150
8	4b-5b	P22(4b-5b)	Ti(OiPr) ₄ (5)	21.1	2.33	45	18	150
9	4b-5b	P22(4b-5b)	Ti(OiPr) ₄ (5)	16.4	2.16	ND	24	150
10	4b-5b	P22(4b-5b)	Ti(OiPr) ₄ (5)	22.6	1.83	ND	48	150
11	4b-5b	P22(4b-5b)	Ti(OiPr) ₄ (1)	20.8	2.10	ND	24	150
12	4b-5b	P22(4b-5b)	Ti(OiPr) ₄ (1)	31.9	1.94	44	48	150

ND: Not determined.

4.4.4.1. Polycondensation of Isomannide-Dioxalate (**4a**):

Poly(isomannide-co-hexane)oxalate: P18(4a-5a) Polymerization of isomannide-dioxalate (**4a**) with diol (**5a**) was performed as reported in the general procedure (section 4.4.4).



¹H NMR (500 MHz, CDCl₃, 298 K) δ = 5.18 (br., 2H_D), 4.80 (br., s, 2H_C), 4.26 (br., s, 8H_F), 4.07-3.98 (br., s, 4H_B), 1.74 (br., s, 8H_G), 1.42 (br., s, 8H_H). ¹³C NMR (125 MHz, CDCl₃, 298 K) δ = 157.9-156.4 (m, C_E), 79.9 (s, C_C), 75.6 (s, C_D), 70.2 (s, C_B), 67.1-66.8 (m, C_F), 28.1 (s, C_G), 25.3 (s, C_H).

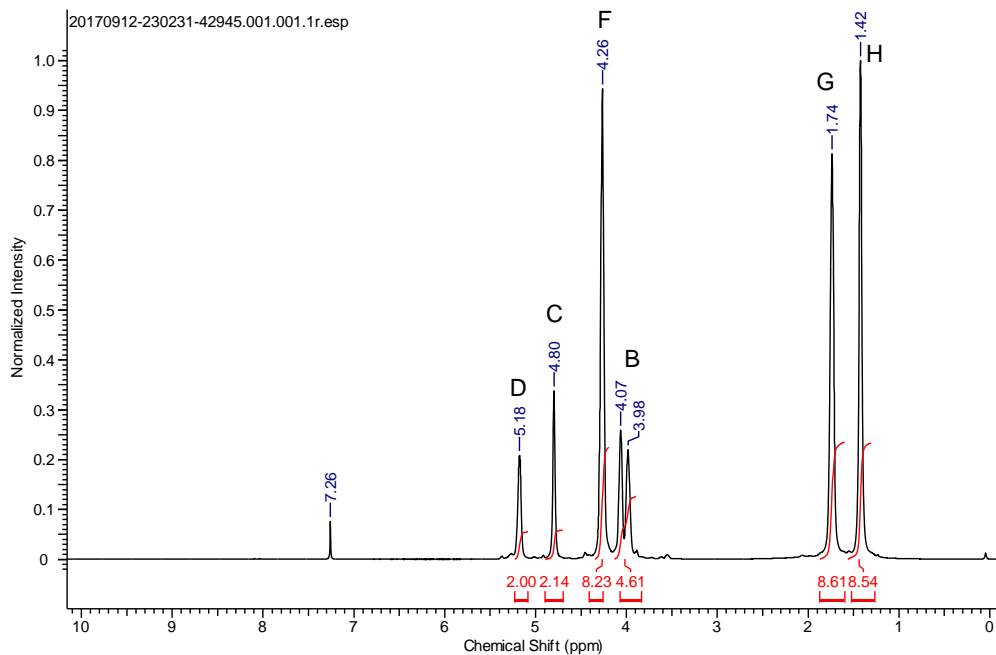


Figure 4.29. ^1H NMR spectrum of polyoxalate **P18(4a-5a)** in CDCl_3 (500 MHz at 298 K).

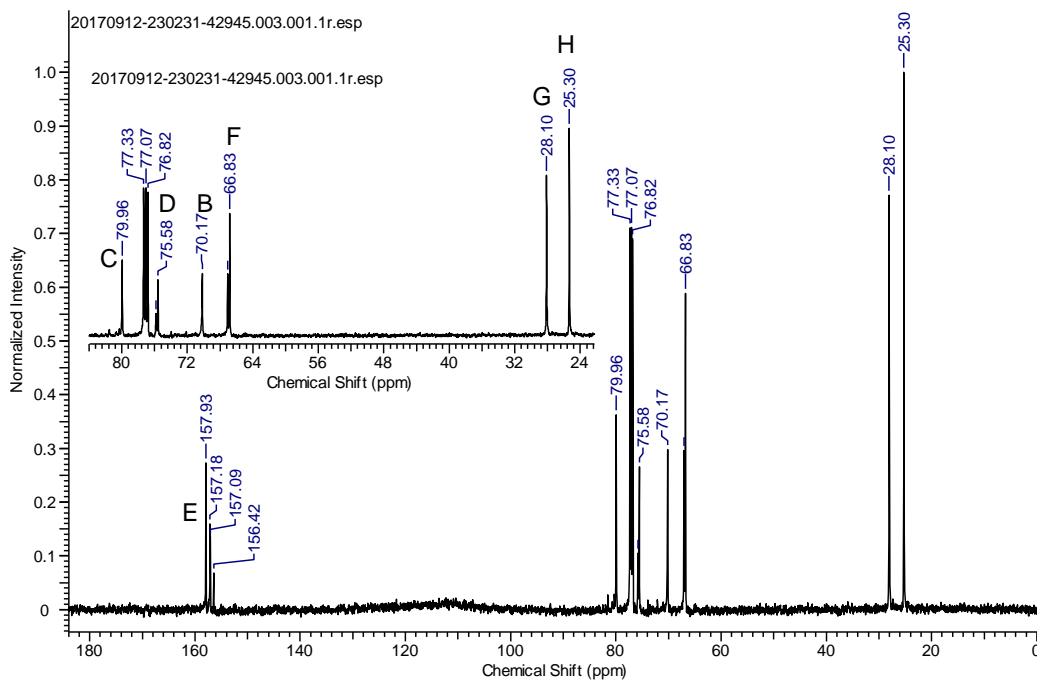


Figure 4.30. ^{13}C NMR spectrum of polyoxalate **P18(4a-5a)** in CDCl_3 (125 MHz at 298 K).

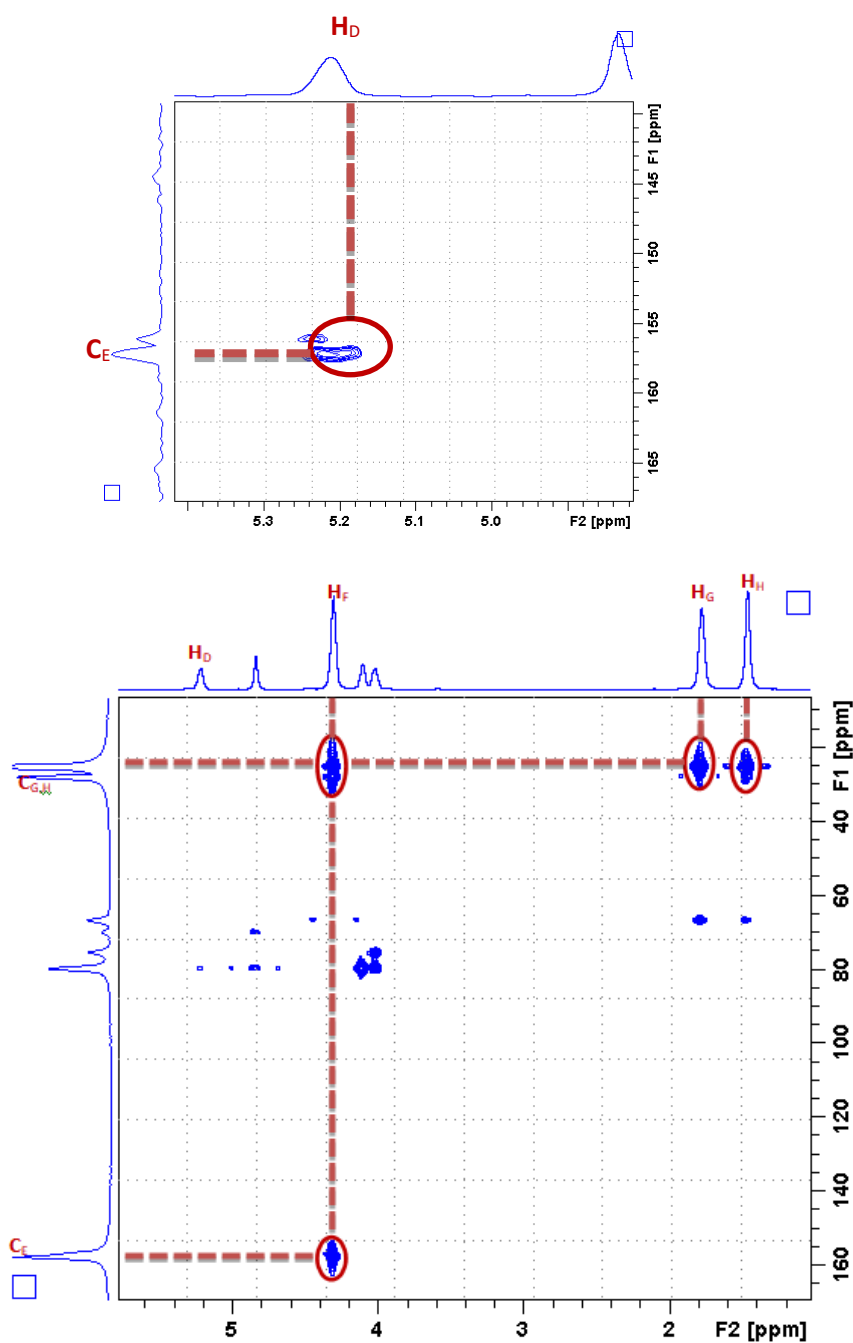


Figure 4.31. Long range C-H correlation (HMBC) spectrum of polyoxalate **P18(4a-5a)** in $CDCl_3$ (at 298 K).

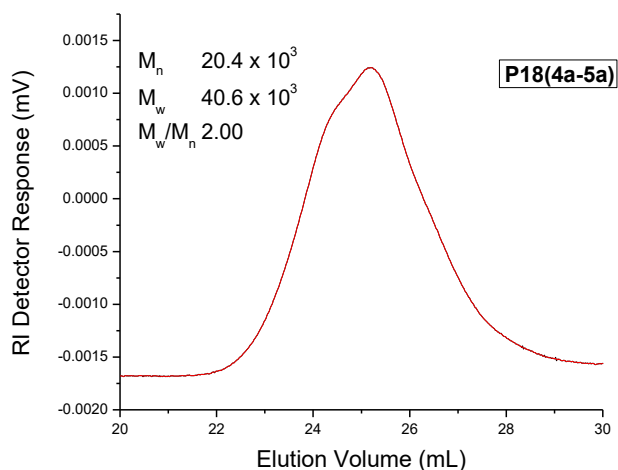


Figure 4.32. GPC chromatogram of P18(4a-5a) in chloroform at room temperature.

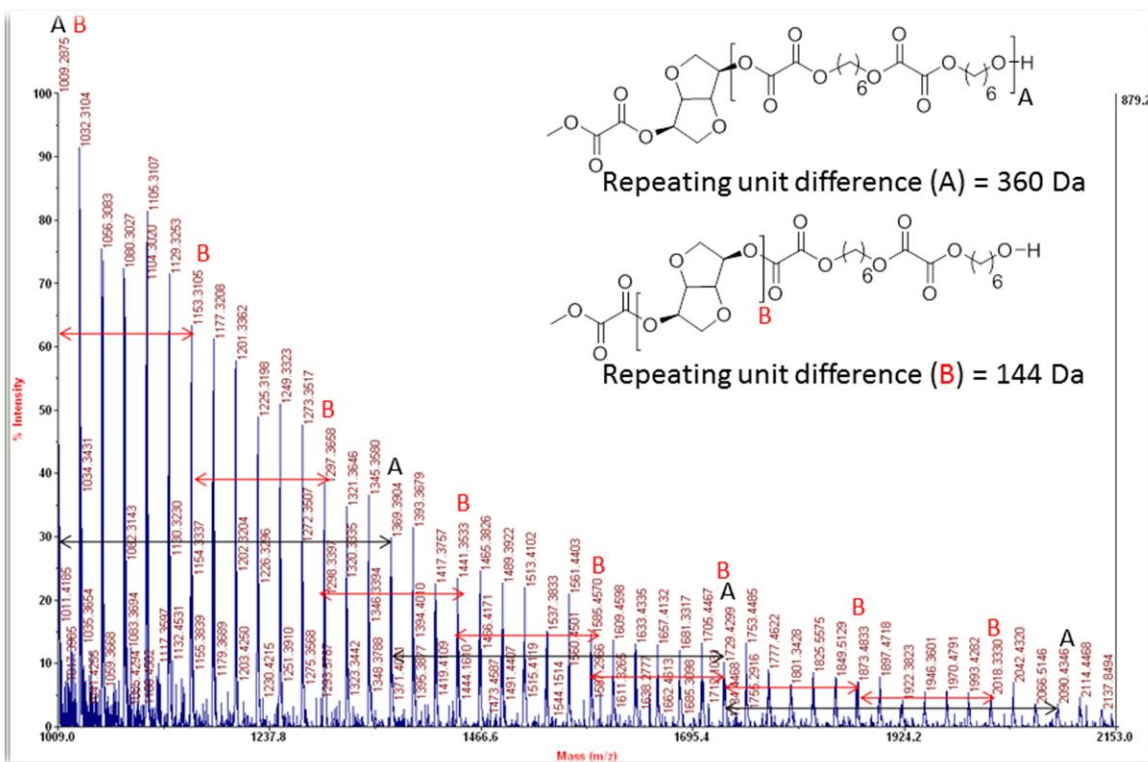
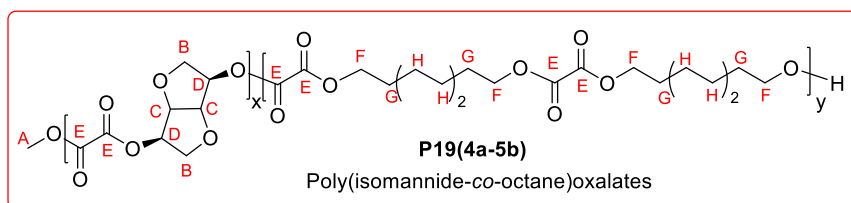


Figure 4.33. MALDI-ToF-MS spectrum of P18(4a-5a).

Poly(isomannide-co-octane)oxalate: P19(4a-5b) Polymerization of isomannide-dioxalate (**4a**) with diol (**5b**) was performed as reported in the general procedure (section 4.4.4).



$^1\text{H NMR}$ (400 MHz, CDCl_3 , 298 K) δ = 5.19 (br., 2H_D), 4.81 (br., s, 2H_C), 4.27 (br., s, 12H_F), 4.06 (br., s, 4H_B), 1.73 (br., s, 12H_G), 1.36 (br., s, 23H_H). $^{13}\text{C NMR}$ (100 MHz, CDCl_3 , 298 K) δ = 157.9-157.0 (m, C_E), 79.8 (s, C_C), 75.4 (s, C_D), 70.0 (s, C_B), 66.9 (m, C_F), 28.8 (s, C_G), 28.1-25.4 (s, C_H).

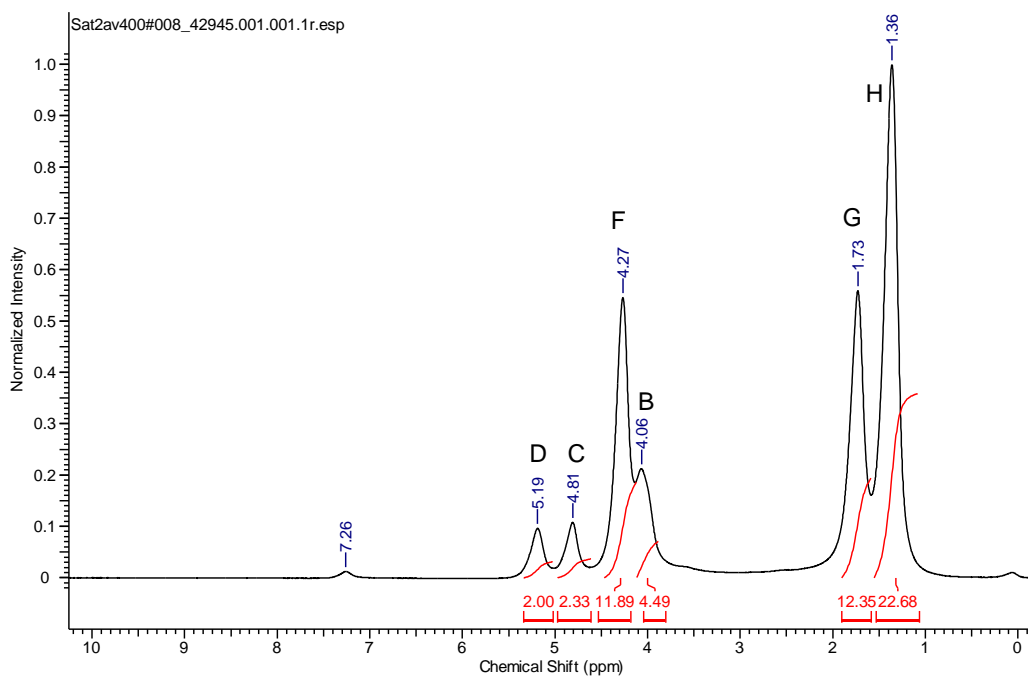


Figure 4.34. $^1\text{H NMR}$ spectrum of polyoxalate **P19(4a-5b)** in CDCl_3 (400 MHz at 298 K).

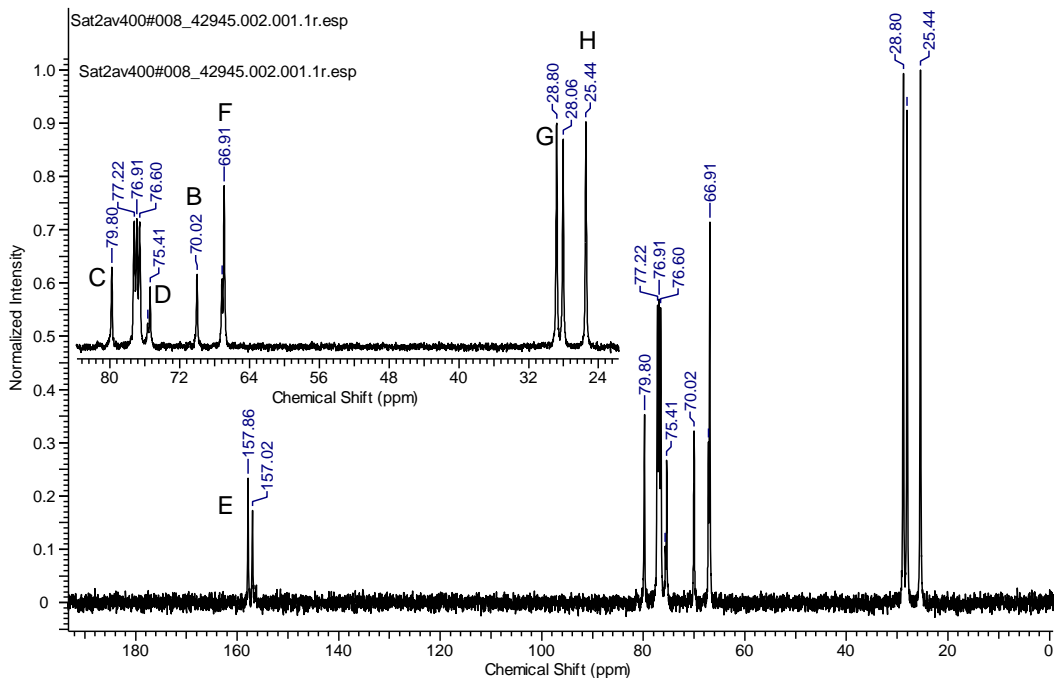


Figure 4.35. ^{13}C NMR spectrum of polyoxalate **P19(4a-5b)** in CDCl_3 (100 MHz at 298 K).

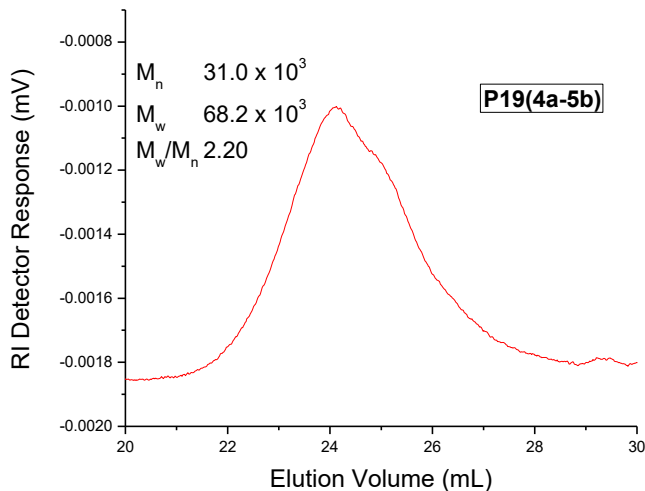
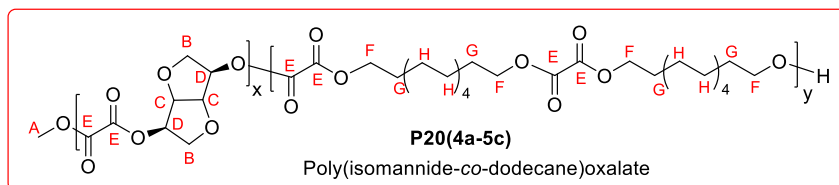


Figure 4.36. GPC chromatogram of **P19(4a-5b)** in chloroform at room temperature.

Poly(isomannide-co-dodecane)oxalate:P20(4a-5c) Polymerization of isomannide-dioxalate (4a) with diol (5c) was performed as reported in the general procedure (section 4.4.4).



$^1\text{H NMR}$ (400 MHz, CDCl_3 , 298 K) $\delta = 5.18$ (br., 2H_D), 4.81 (br., s, 2H_C), 4.26 (br., s, 8H_F), 4.07 - 4.00 (br., s, 4H_B), 1.72 (br., s, 9H_G), 1.26 (br., s, 34H_H). $^{13}\text{C NMR}$ (100 MHz, CDCl_3 , 298 K) $\delta = 157.9$ - 157.1 (m, C_E), 79.9 (s, C_C), 75.5 (s, C_D), 70.1 (s, C_B), 67.4 - 67.1 (m, C_F), 29.4 (s, C_G), 29.4 , 29.1 , 28.2 , 25.6 (s, C_H).

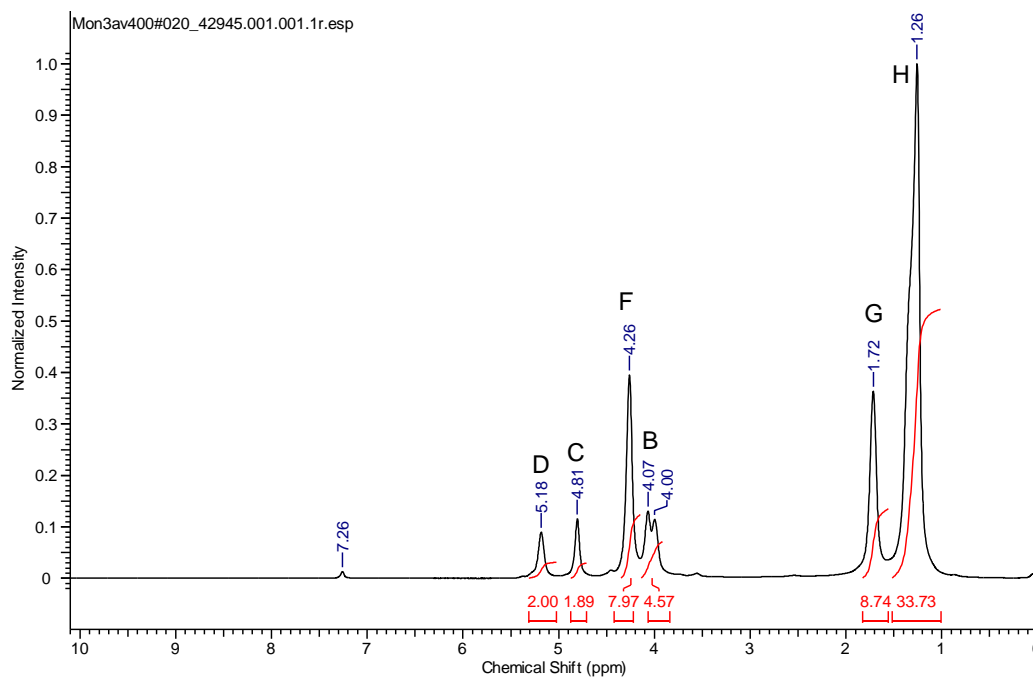


Figure 4.37. $^1\text{H NMR}$ spectrum of polyoxalate **P20(4a-5c)** in CDCl_3 (400 MHz at 298 K).

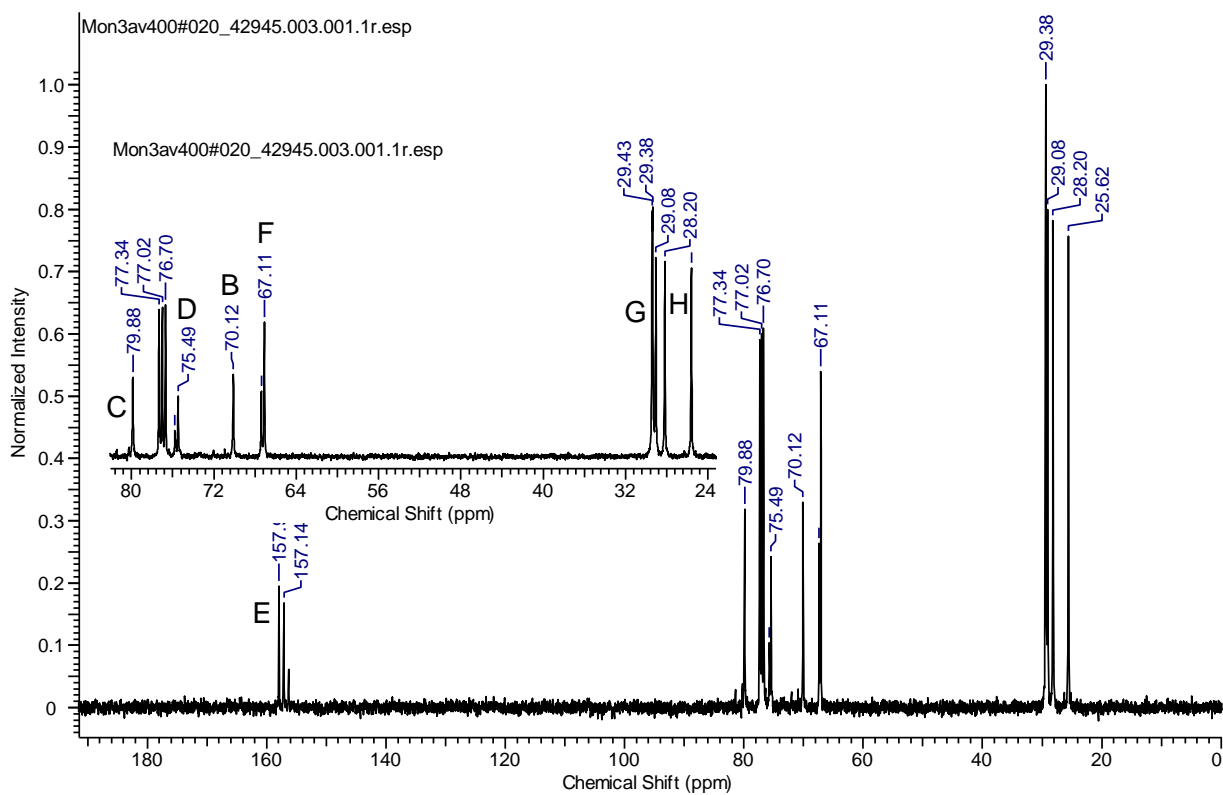


Figure 4.38. ^{13}C NMR spectrum of polyoxalate **P20(4a-5c)** in CDCl_3 (100 MHz at 298 K).

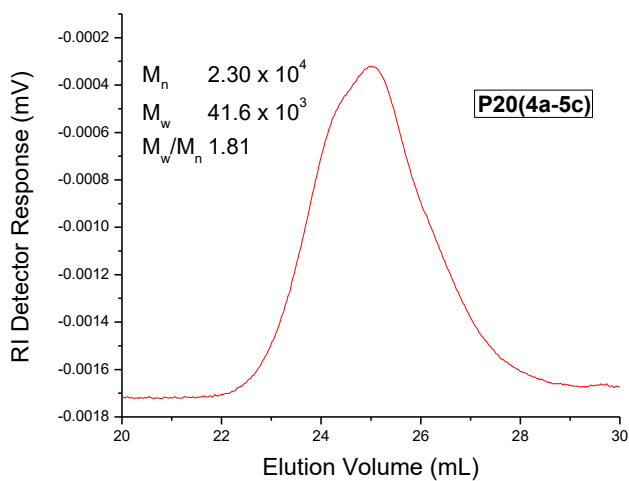


Figure 4.39. GPC chromatogram of **P20(4a-5c)** in chloroform at room temperature.

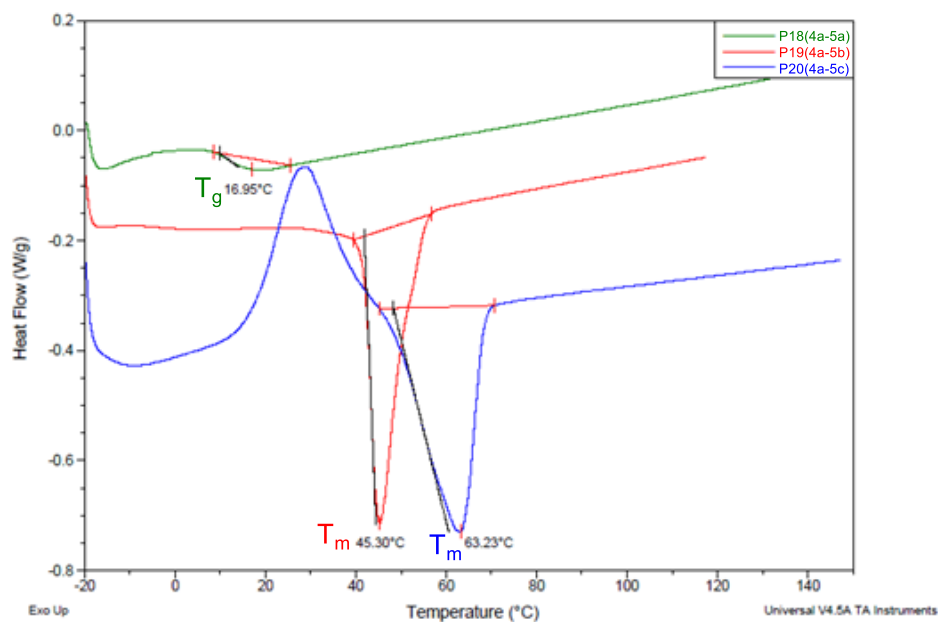


Figure 4.40. DSC heating curve of **P18(4a-5a)-P20(4a-5c)** (Run 1-3) under N_2 atmosphere, data recorded from the second heating cycle (except **P19(4a-5b)**: from 1st heating cycle).

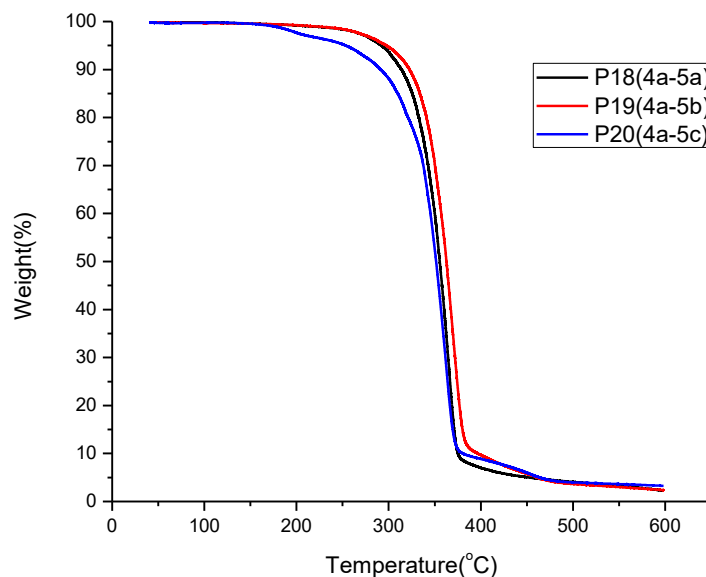
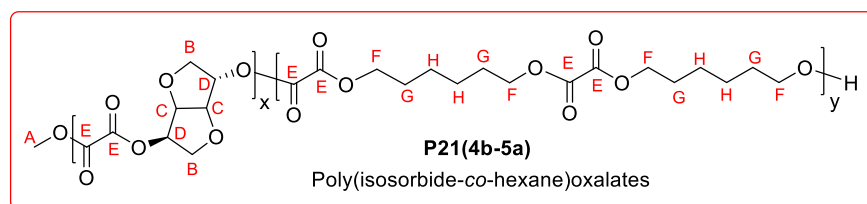


Figure 4.41. TGA trace of **P18(4a-5a)-P20(4a-5c)** (Run 1-3) recorded between 40-600 °C under the N_2 atmosphere.

4.4.4.2. Polycondensation of Isosorbide-Dioxalate (4b):

Poly(isosorbide-co-hexane)oxalate:P21(4b-5a): Polymerization of isosorbide-dioxalate (4b) with diol (5a) was performed as reported in the general procedure (section 4.4.4).



$^1\text{H NMR}$ (400 MHz, CDCl_3 , 298 K) δ = 5.31 (br., 2H_D), 4.98 (br., s, 1H_C), 4.58 (br., s, 1H_C), 4.26 (br., s, 6H_F), 4.05 (br., s, 3H_B), 3.92 (br., s, 1H_B), 1.74 (br., s, 6H_G), 1.42 (br., s, 6H_H). $^{13}\text{C NMR}$ (100 MHz, CDCl_3 , 298 K) δ = 157.9-156.9 (m, C_E), 85.7 (s, C_C), 80.8 (s, C_C), 80.1 (s, C_D), 76.0 (s, C_D), 72.9 (s, C_B), 70.7 (s, C_B), 67.1-66.8 (m, C_F), 28.1 (s, C_G), 25.3 (s, C_H).

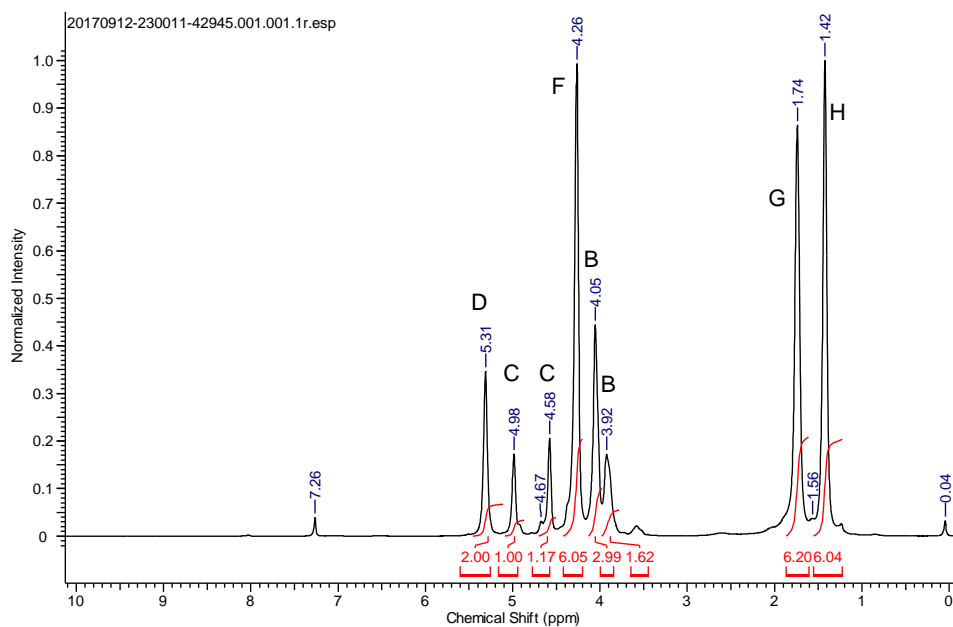


Figure 4.42. $^1\text{H NMR}$ spectrum of polyoxalate **P21(4b-5a)** in CDCl_3 (400 MHz at 298 K).

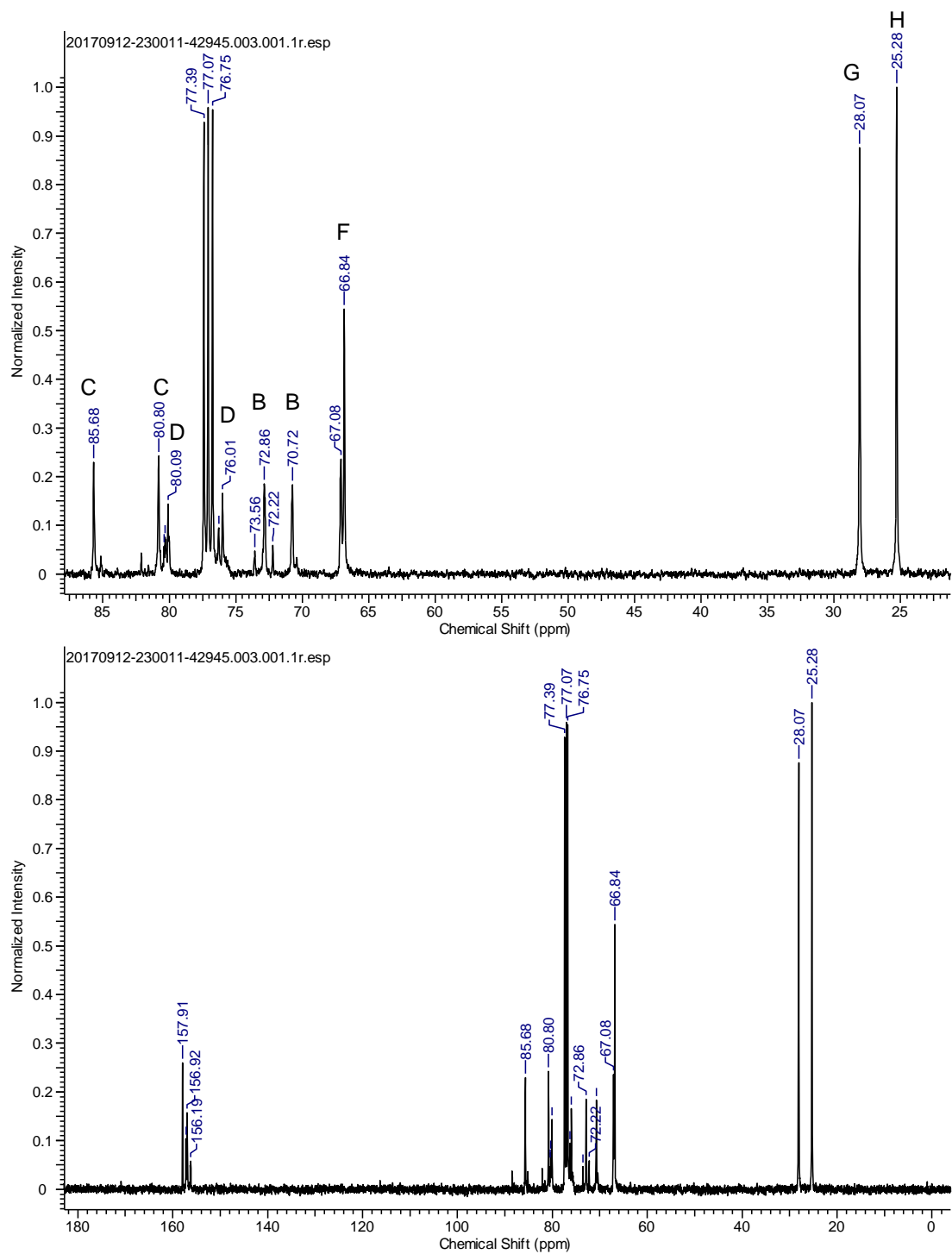


Figure 4.43. ^{13}C NMR spectrum of polyoxalate **P21(4b-5a)** in CDCl_3 (100 MHz at 298 K).

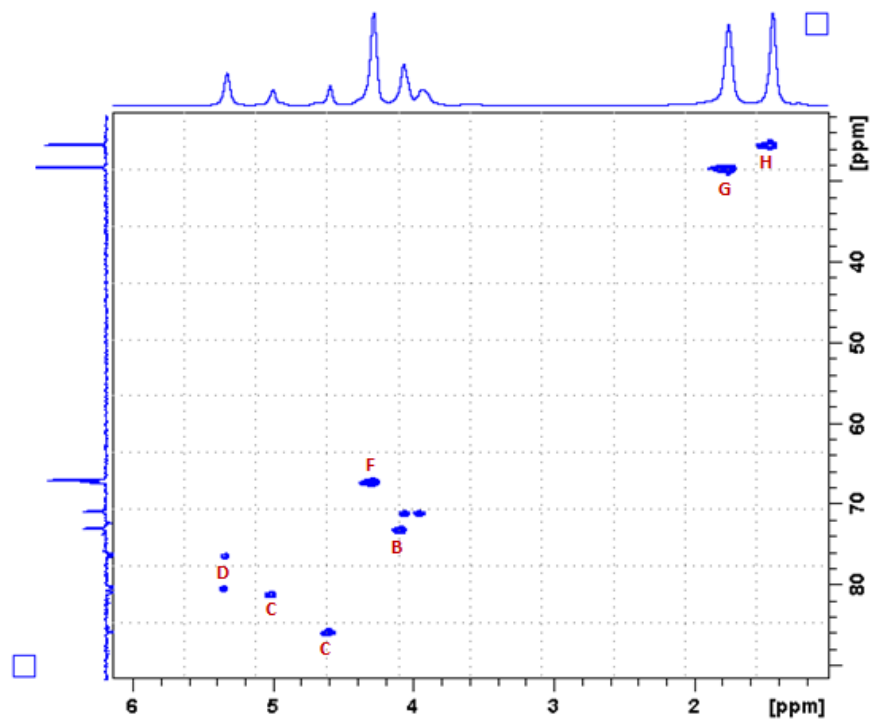


Figure 4.44. HSQC NMR spectrum of polyoxalate **P21(4b-5a)** in CDCl_3 (at 298 K).

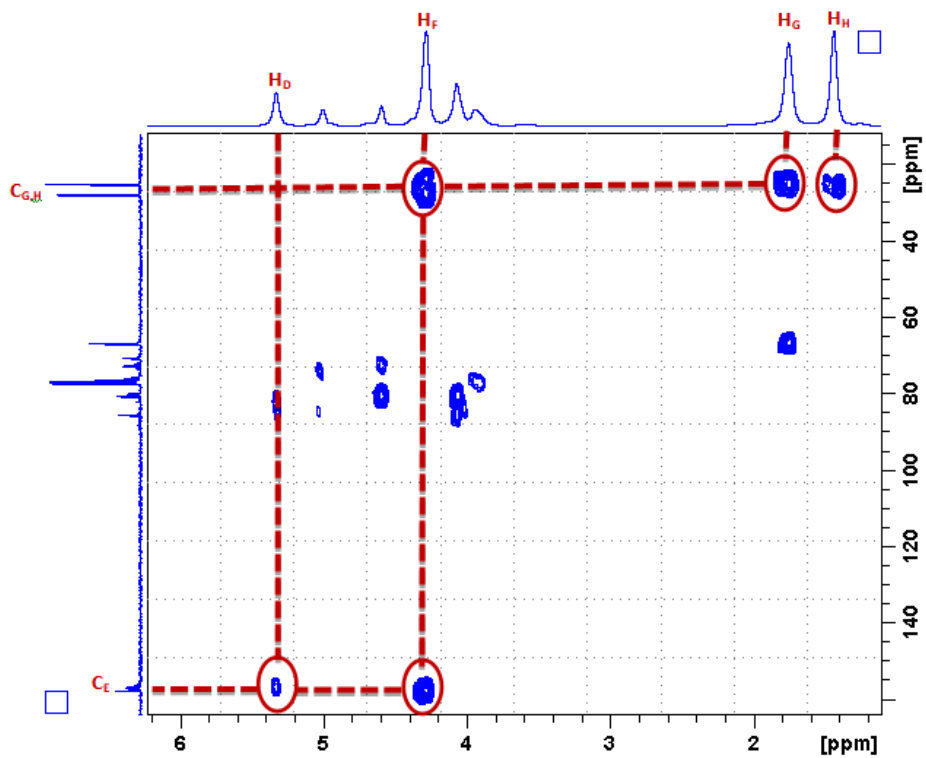


Figure 4.45. HMBC NMR spectrum of polyoxalate **P21(4b-5a)** in CDCl_3 (at 298 K).

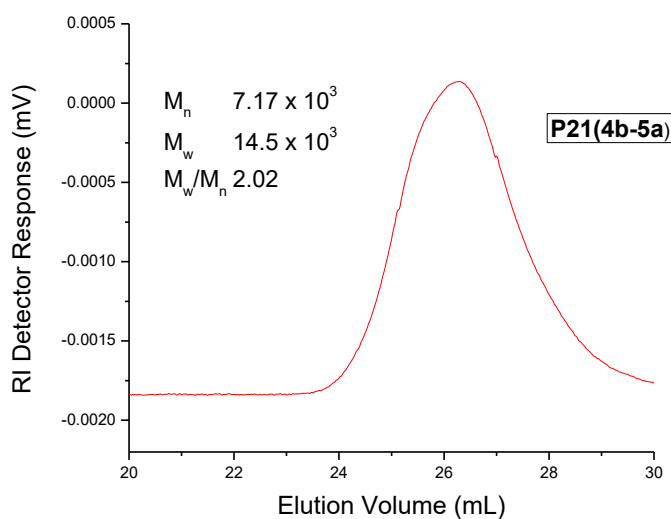
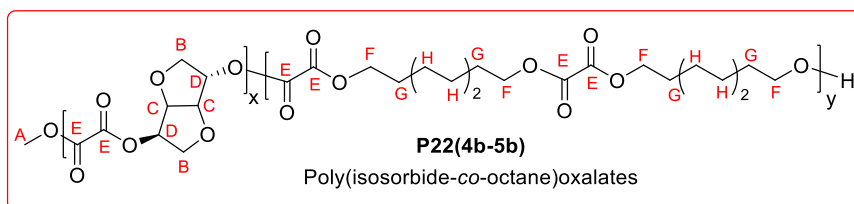


Figure 4.46. GPC chromatogram of **P21(4b-5a)** in chloroform at room temperature.

Poly(isosorbide-co-octane)oxalate:P22(4b-5b) Polymerization of isosorbide-dioxalate (**4b**) with diol (**5b**) was performed as reported in the general procedure (section 4.4.4).



¹H NMR (500 MHz, CDCl₃, 298 K) δ = 5.30 (br., 2H_D), 4.97 (br., s, 1H_C), 4.56 (br., s, 1H_C), 4.24 (br., s, 8H_F), 4.04 (br., s, 3H_B), 3.91-3.89 (br., s, 1H_B), 1.70 (br., s, 8H_G), 1.32 (br., s, 16H_H).

¹³C NMR (125 MHz, CDCl₃, 298 K) δ = 158.0-157.0 (m, C_E), 85.7 (s, C_C), 80.8 (s, C_C), 80.0 (s, C_D), 75.9 (s, C_D), 72.8 (s, C_B), 70.7 (s, C_B), 67.3-67.0 (m, C_F), 28.9 (s, C_G), 25.6 (s, C_H).

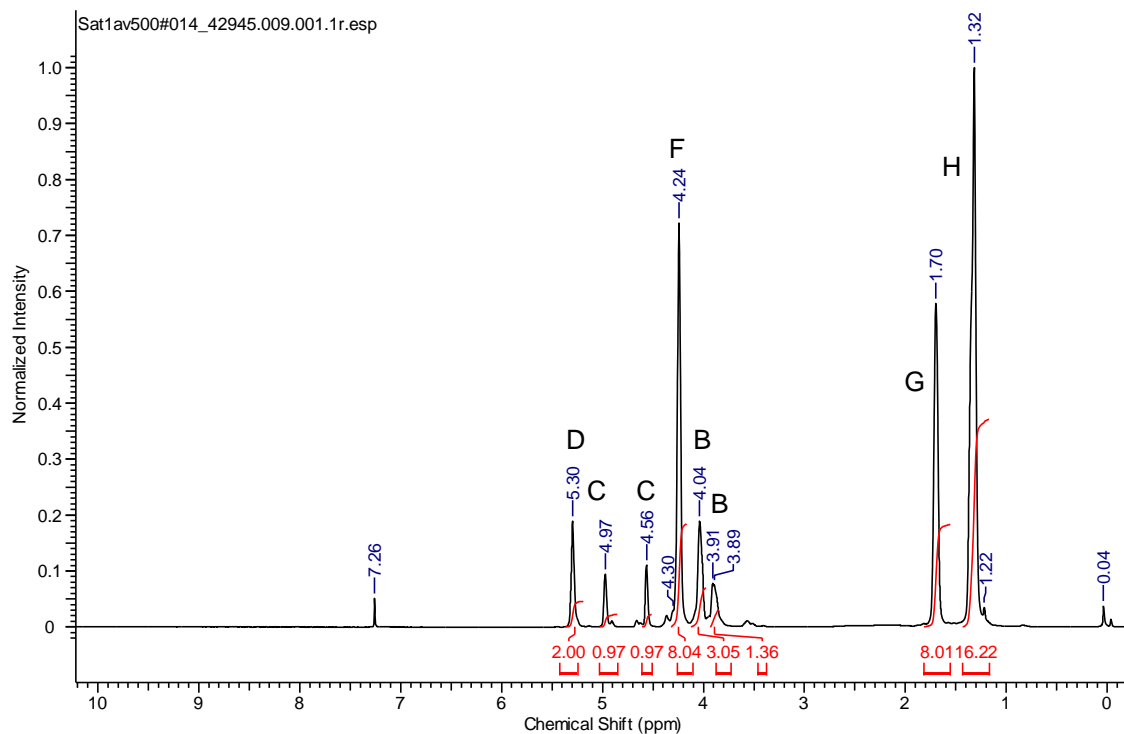


Figure 4.47. ^1H NMR spectrum of polyoxalate **P22(4b-5b)** in CDCl_3 (500 MHz at 298 K).

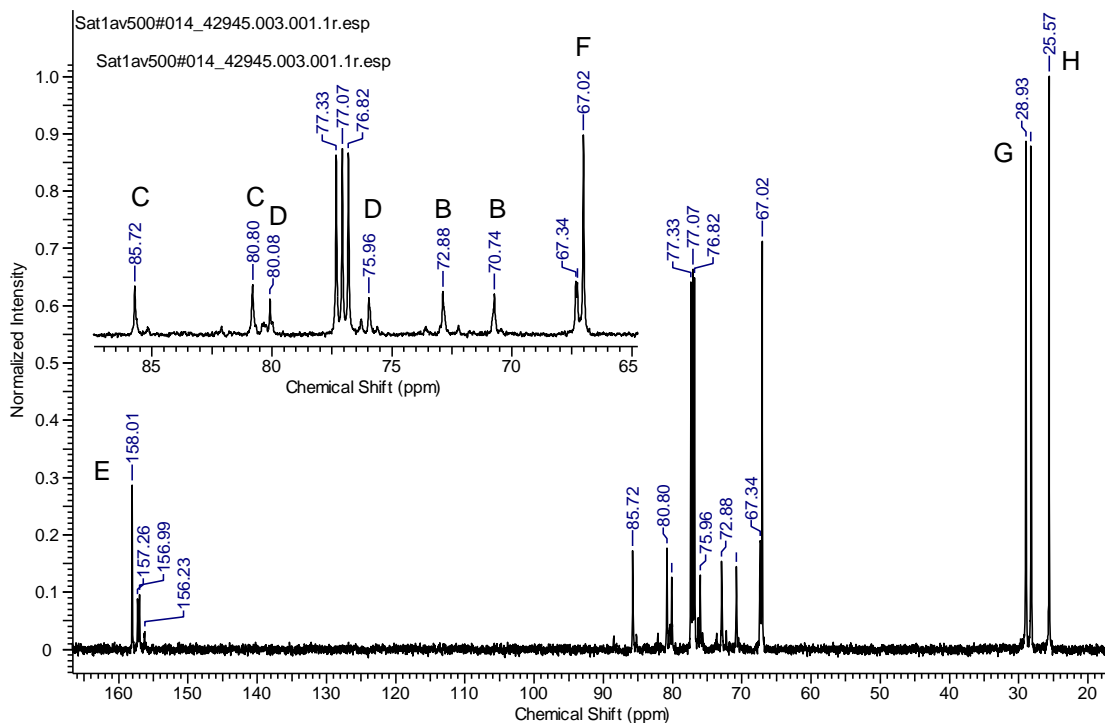


Figure 4.48. ^{13}C NMR spectrum of polyoxalate **P22(4b-5b)** in CDCl_3 (125 MHz at 298 K).

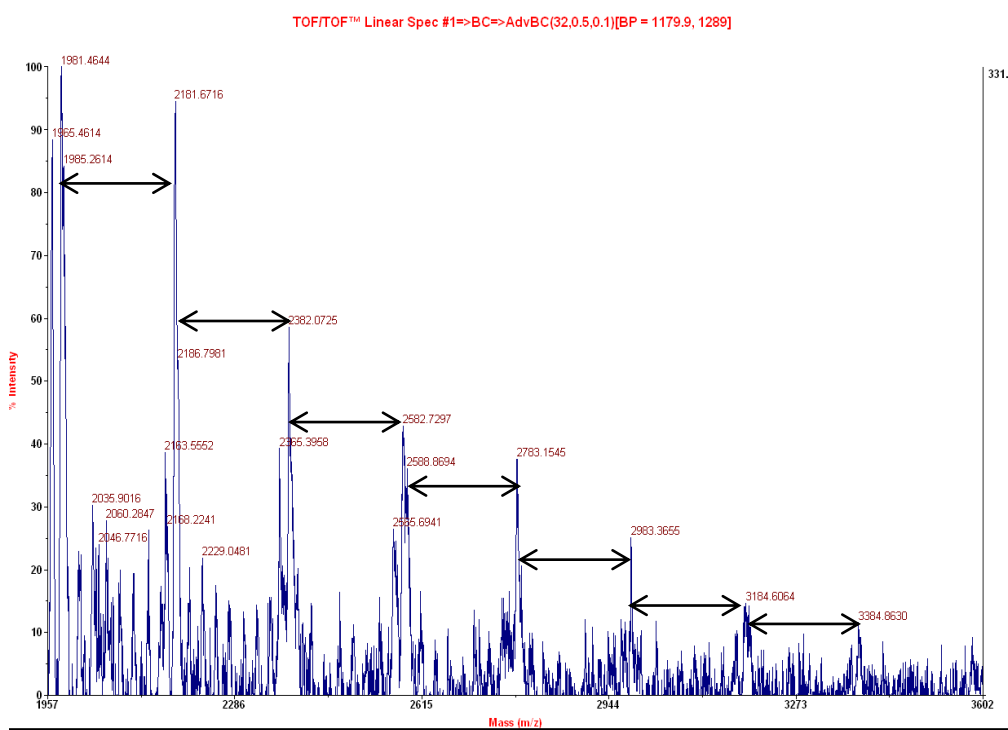


Figure 4.49. MALDI-ToF-MS spectrum of **P22(4b-5b)** recorded in dithranol (shows 200 Da repeat unit mass).

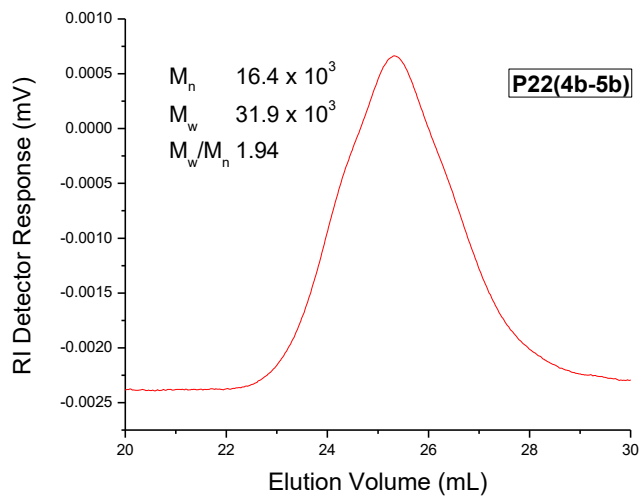
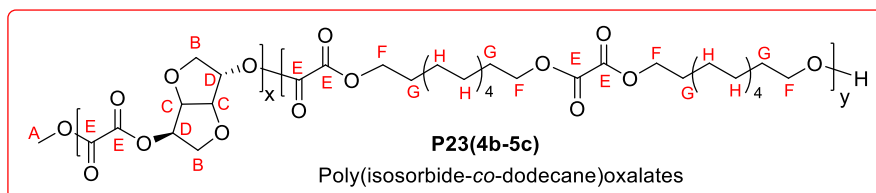


Figure 4.50. GPC chromatogram of **P22(4b-5b)** in chloroform at room temperature.

Poly(isosorbide-co-dodecane)oxalate:P23(4b-5c) Polymerization of isosorbide-dioxalate (**4b**) with diol (**5c**) was performed as reported in the general procedure (section 4.4.4).



$^1\text{H NMR}$ (400 MHz, CDCl_3 , 298 K) $\delta = 5.32$ (br., 2H_D), 4.99 (br., s, 1H_C), 4.59 (br., s, 1H_D), 4.27 (br., s, 6H_F), 4.06 (br., s, 4H_B), 1.72 (br., s, 7H_G), 1.28 (br., s, 25H_H). $^{13}\text{C NMR}$ (100 MHz, CDCl_3 , 298 K) $\delta = 158.0$ -157.0 (m, C_E), 85.7 (s, C_C), 80.7 (s, C_C), 80.0 (s, C_D), 76.2-75.9 (s, C_D), 72.8 (s, C_B), 70.7 (s, C_B), 67.5-67.1 (m, C_F), 29.4 (s, C_G), 29.1-25.6 (s, C_H).

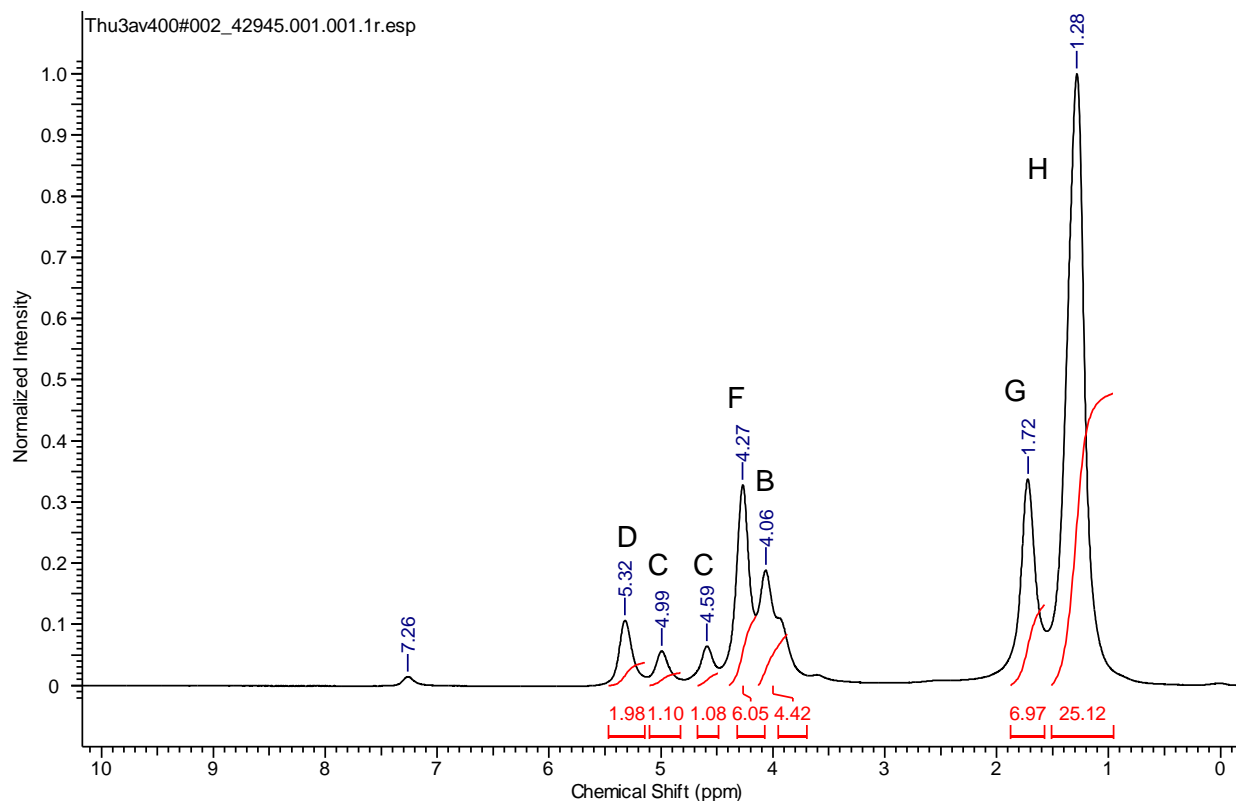


Figure 4.51. $^1\text{H NMR}$ spectrum of polyoxalate **P23(4b-5c)** in CDCl_3 (400 MHz at 298 K).

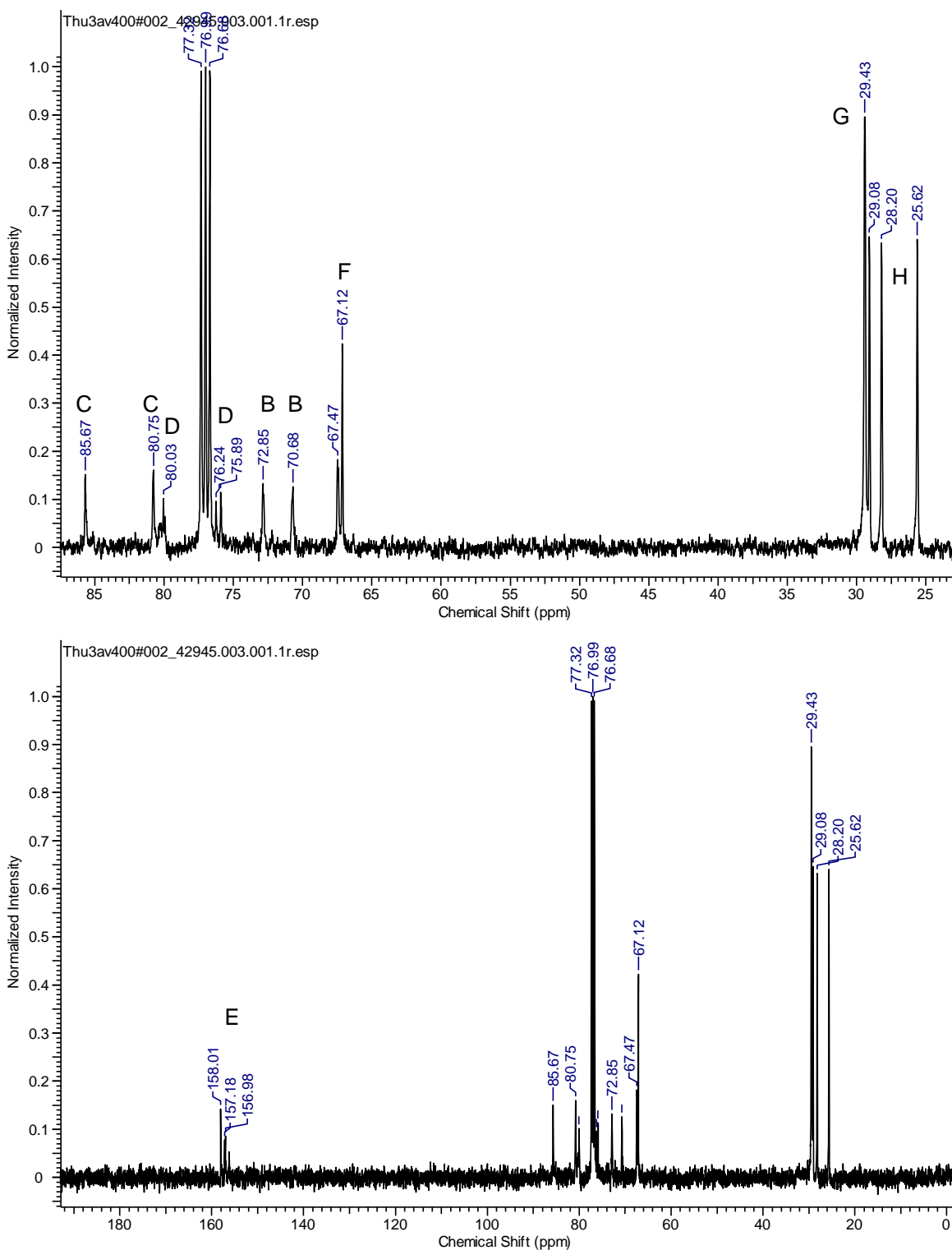


Figure 4.52. ^{13}C NMR spectrum of polyoxalate **P23(4b-5c)** in CDCl_3 (100 MHz at 298 K).

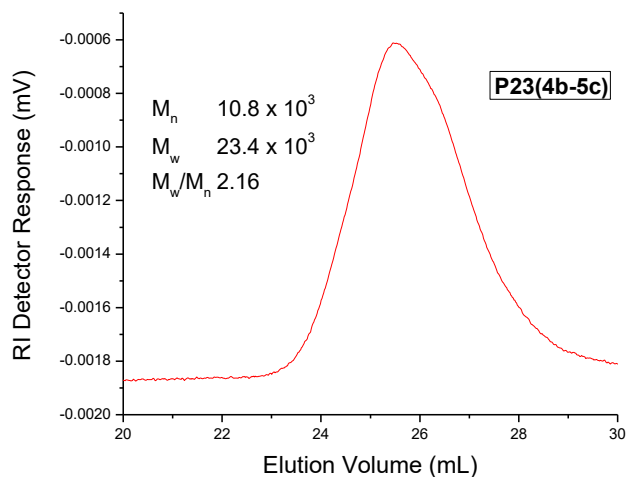


Figure 4.53. GPC chromatogram of **P23(4b-5c)** in chloroform at room temperature.

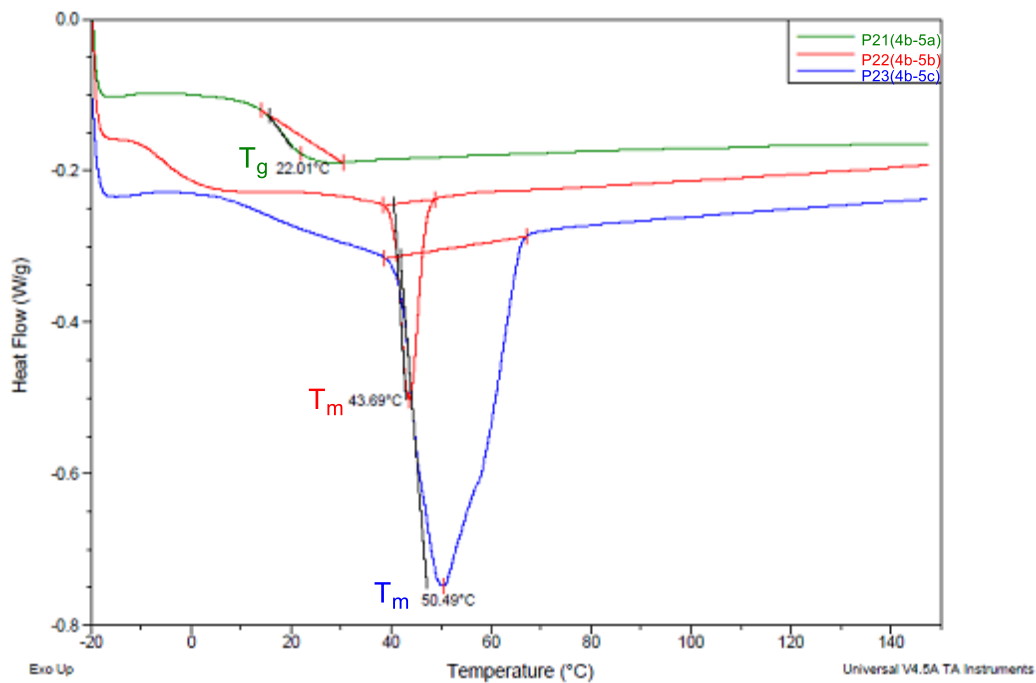


Figure 4.54. DSC heating curve for **P21(4b-5a)-P23(4b-5c)** (Run 4-6) under N_2 atmosphere (from the first heating cycle).

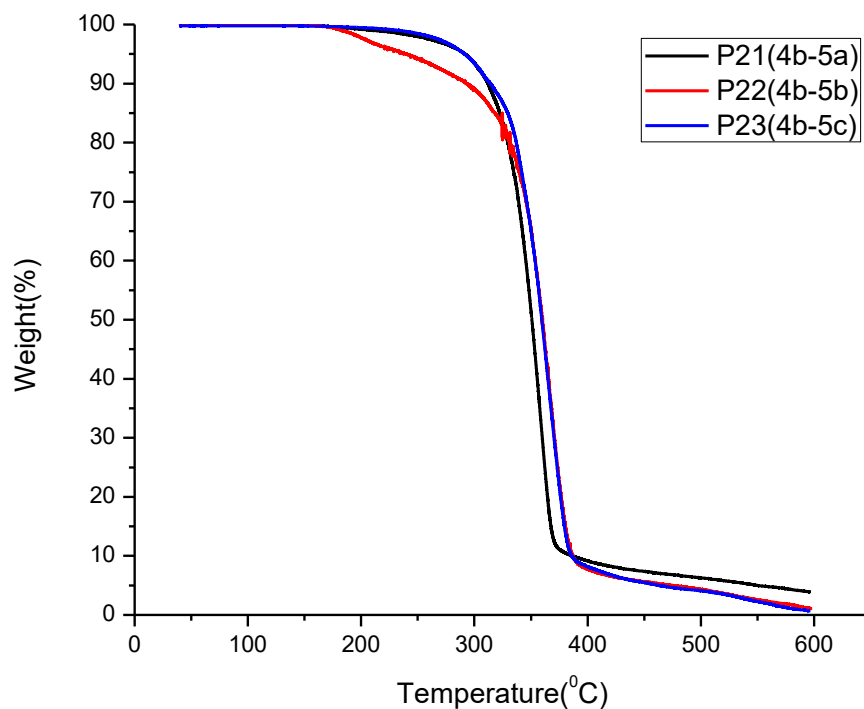
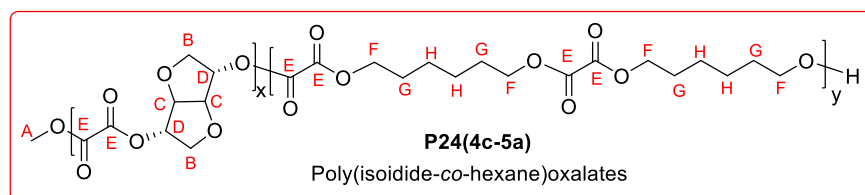


Figure 4.55. TGA traces for **P21(4b-5a)-P23(4b-5c)** (Run 4-6) recorded between 40-600 °C under the N₂ atmosphere.

4.4.4.3. Polycondensation of Isoidide-Dioxalate (**4c**):

Poly(isoidide-co-hexane)oxalate: P24(4c-5a) Polymerization of isoidide-dioxalate (**4c**) with diol (**5a**) was performed as reported in the general procedure (section 4.4.4).



¹H NMR (400 MHz, CDCl₃, 298 K) δ = 5.31 (br., 2H_D), 4.78 (br., s, 2H_C), 4.26 (br., s, 8H_F), 4.02 (br., s, 4H_B), 1.73 (br., s, 7H_G), 1.42 (br., s, 7H_H). ¹³C NMR (100 MHz, CDCl₃, 298 K) δ = 157.9-156.8 (m, C_E), 85.0 (s, C_C), 80.0-79.7 (m, C_D), 72.1 (s, C_B), 67.1-66.8 (m, C_F), 28.1 (s, C_G), 25.3 (s, C_H).

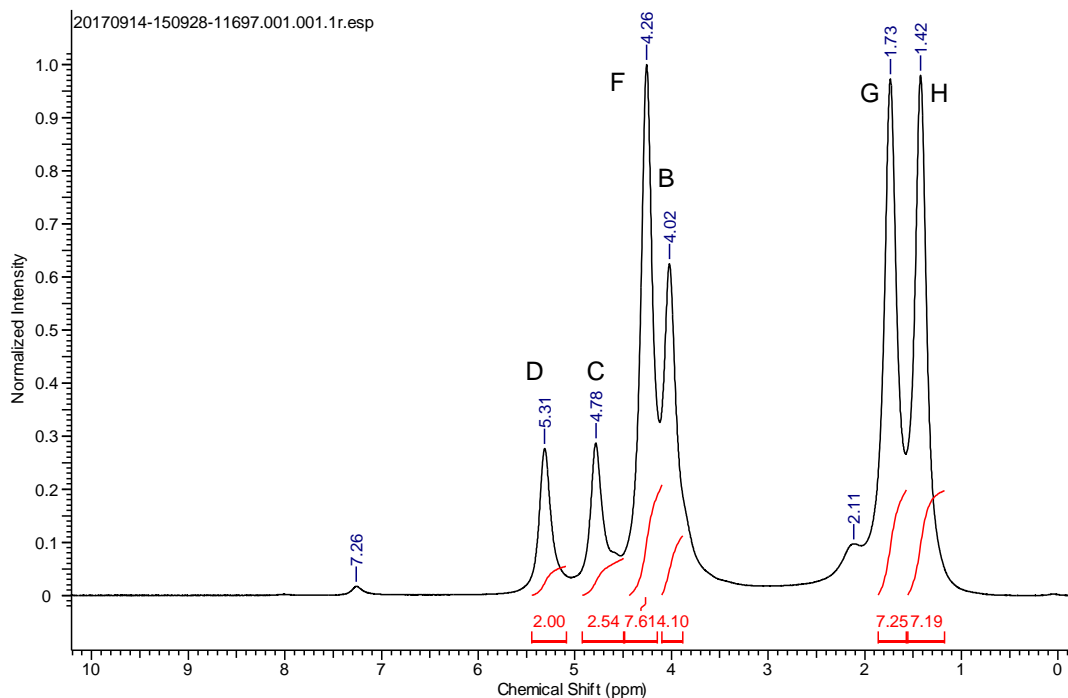


Figure 4.56. ^1H NMR spectrum of polyoxalate **P24(4c-5a)** in CDCl_3 (400 MHz at 298 K).

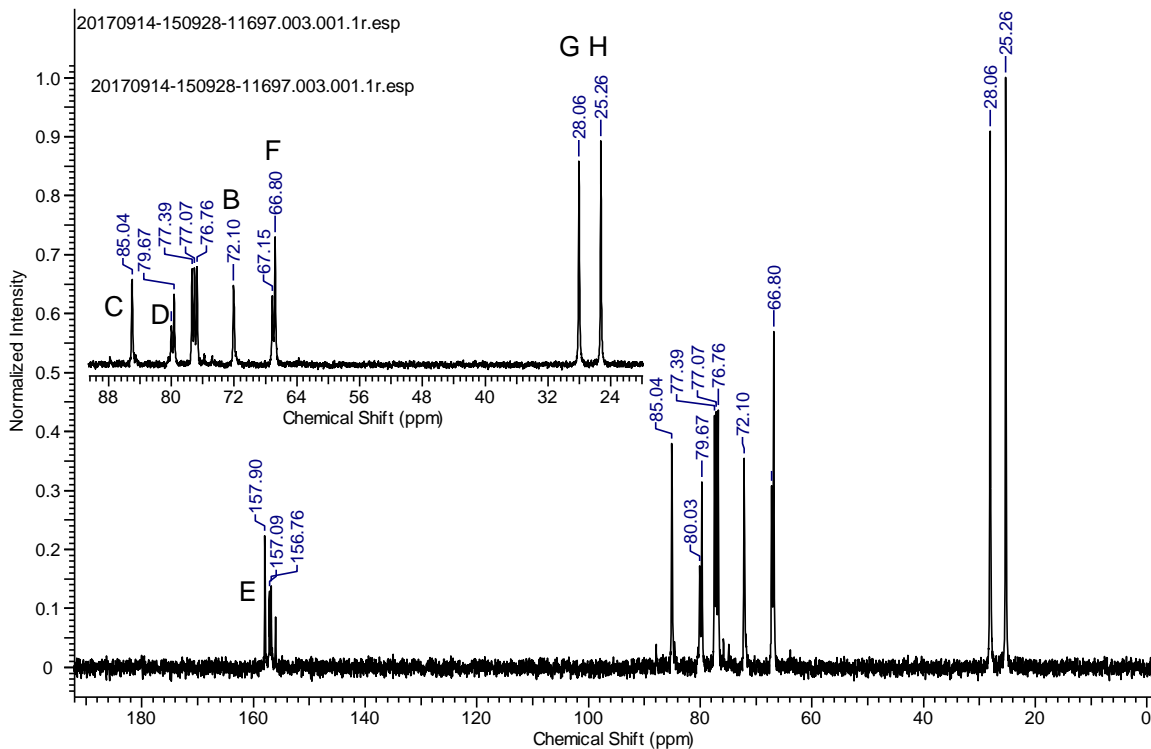


Figure 4.57. ^{13}C NMR spectrum of polyoxalate **P24(4c-5a)** in CDCl_3 (100 MHz at 298 K).

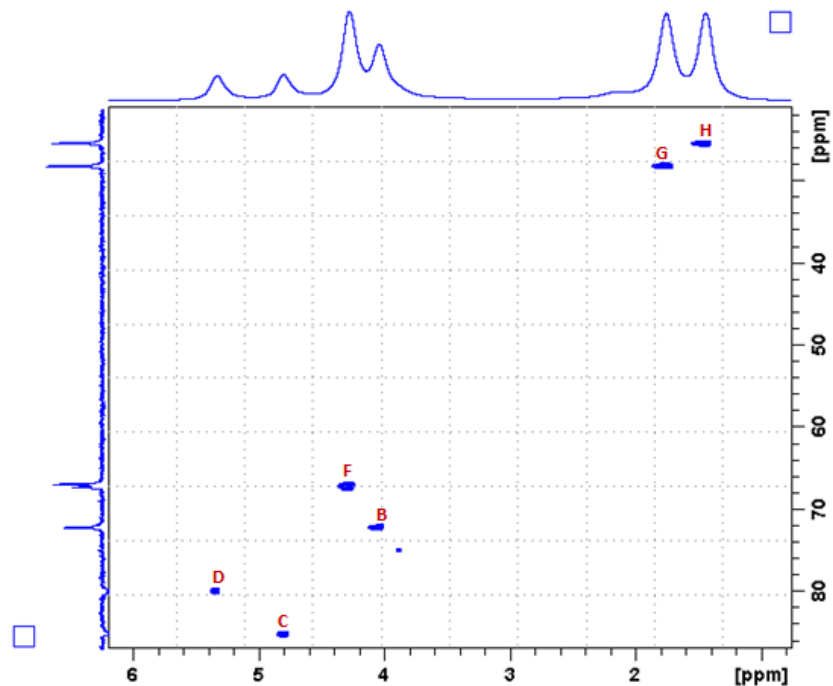


Figure 4.58. HSQC NMR spectrum of polyoxalate **P24(4c-5a)** in CDCl_3 (at 298 K).

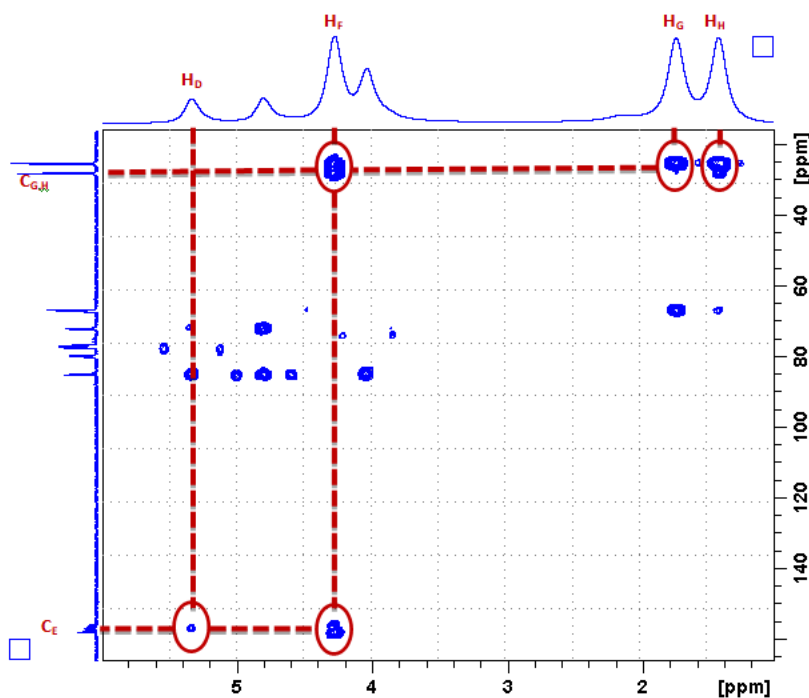


Figure 4.59. HMBC NMR spectrum of polyoxalate **P24(4c-5a)** in CDCl_3 (at 298 K).

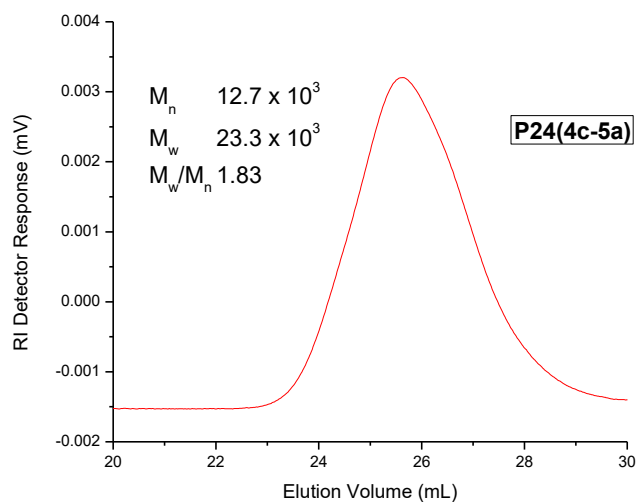
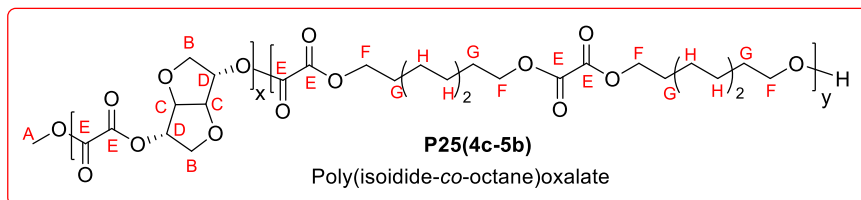


Figure 4.60. GPC chromatogram of **P24(4c-5a)** in chloroform at room temperature.

Poly(isoidide-co-octane)oxalate: P25(4c-5b) Polymerization of isoidide-dioxalate (**4c**) with diol (**5b**) was performed as reported in the general procedure (section 4.4.4).



$^1\text{H NMR}$ (500 MHz, CDCl_3 , 298 K) δ = 5.32 (br., 2H_D), 4.79 (br., s, 2H_C), 4.25 (br., s, 7H_F), 4.02 (br., s, 4H_B), 3.86 (br., 1H_A), 1.71 (br., s, 7H_G), 1.33 (br., s, 15H_H). $^{13}\text{C NMR}$ (125 MHz, CDCl_3 , 298 K) δ = 158.0-156.8(m, C_E), 85.1-85.0 (m, C_C), 79.7 (s, C_D), 72.1-72.0 (m, C_B), 67.4-67.0 (m, C_F), 28.9 (s, C_G), 28.2(s, C_H), 25.6 (s, C_H).

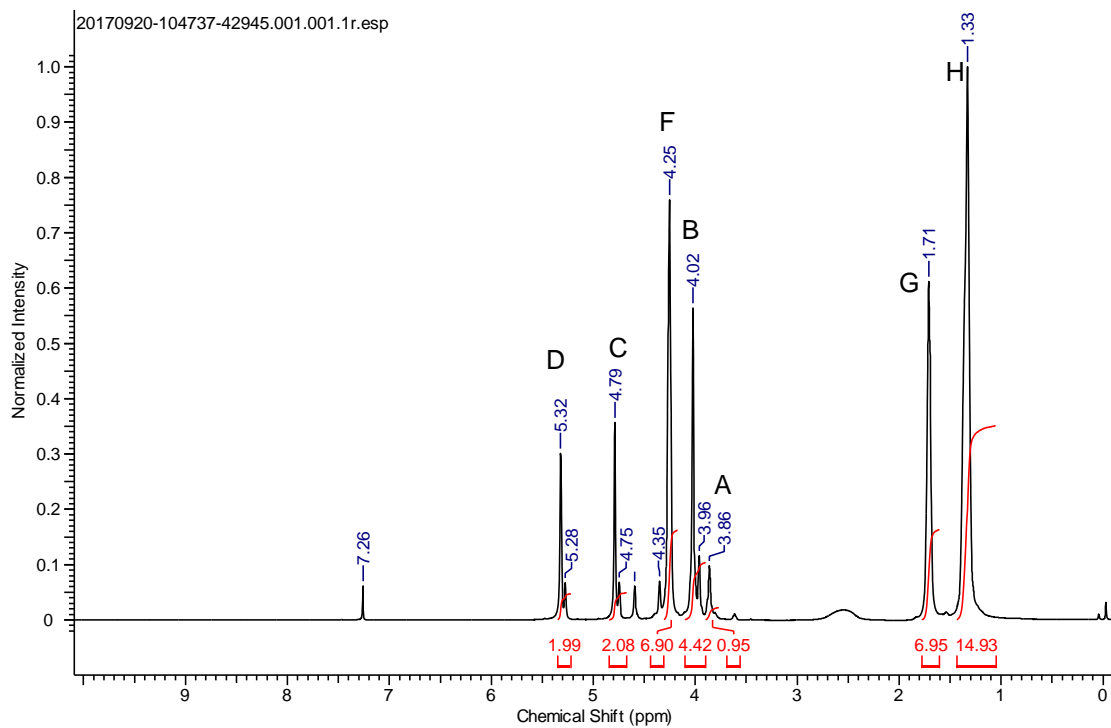


Figure 4.61. ^1H NMR spectrum of polyoxalate **P25(4c-5b)** in CDCl_3 (500 MHz at 298 K).

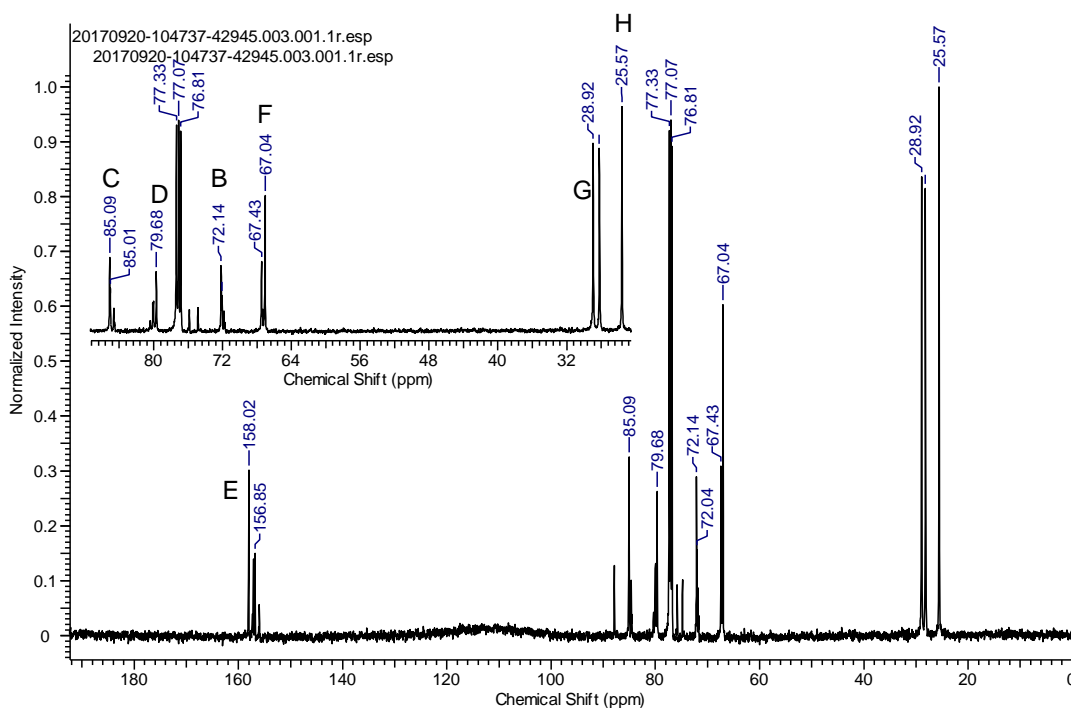


Figure 4.62. ^{13}C NMR spectrum of polyoxalate **P25(4c-5b)** in CDCl_3 (125 MHz at 298 K).

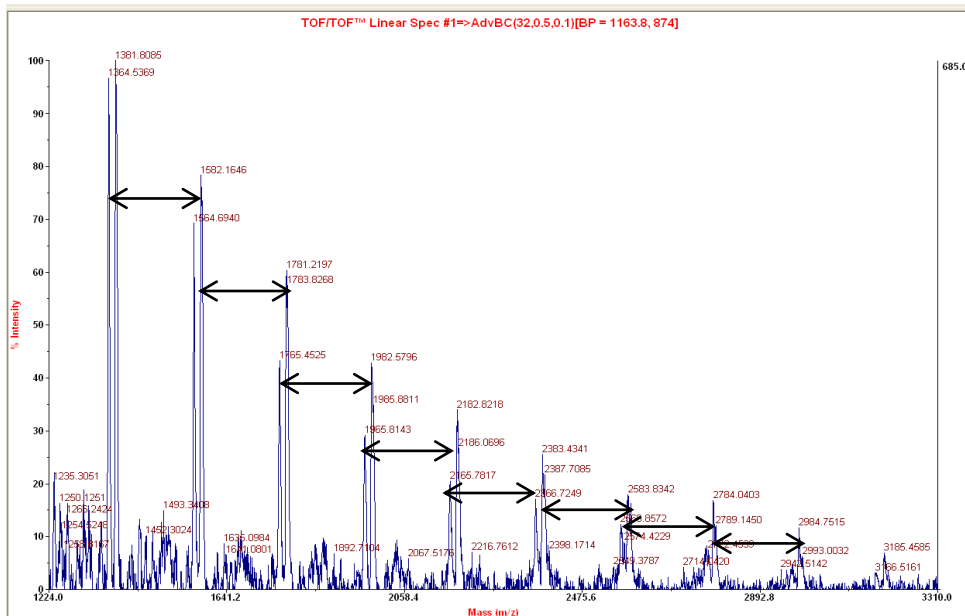


Figure 4.63. MALDI-ToF-MS spectrum of **P25(4c-5b)** recorded in dithranol (shows 200 Da repeat unit mass).

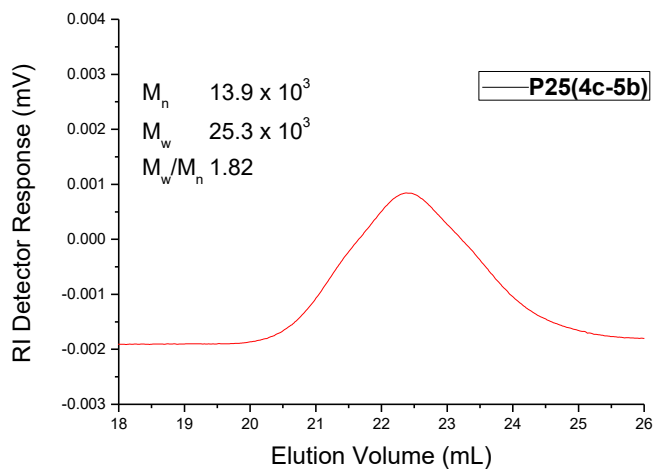
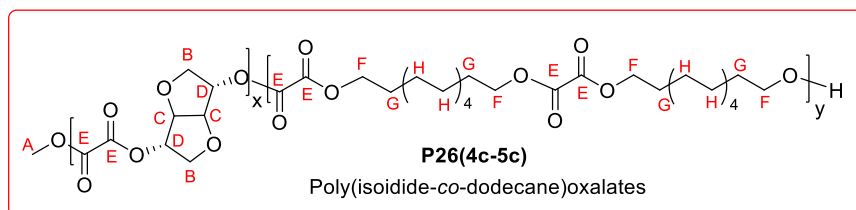


Figure 4.64. GPC chromatogram of **P25(4c-5b)** in chloroform at room temperature.

Poly(isoidide-co-dodecane)oxalate: P26(4c-5c) Polymerization of isoidide-dioxalate (**4c**) with diol (**5c**) was performed as reported in the general procedure (section 4.4.4).



$^1\text{H NMR}$ (500 MHz, CDCl_3 , 298 K) $\delta = 5.33$ (br., 2H_D), 4.80 (br., s, 2H_C), 4.27 (br., s, 7H_F), 4.04 (br., s, 4H_B), 1.72 (br., s, 8H_G), 1.28 (br., s, 27H_H). $^{13}\text{C NMR}$ (125 MHz, CDCl_3 , 298 K) $\delta = 158.1$ - 156.9 (m, C_E), 85.2 (s, C_C), 80.1 - 79.7 (m, C_D), 72.2 (s, C_B), 67.6 - 67.2 (m, C_F), 29.5 (s, C_G), 29.2 - 25.7 (m, C_H).

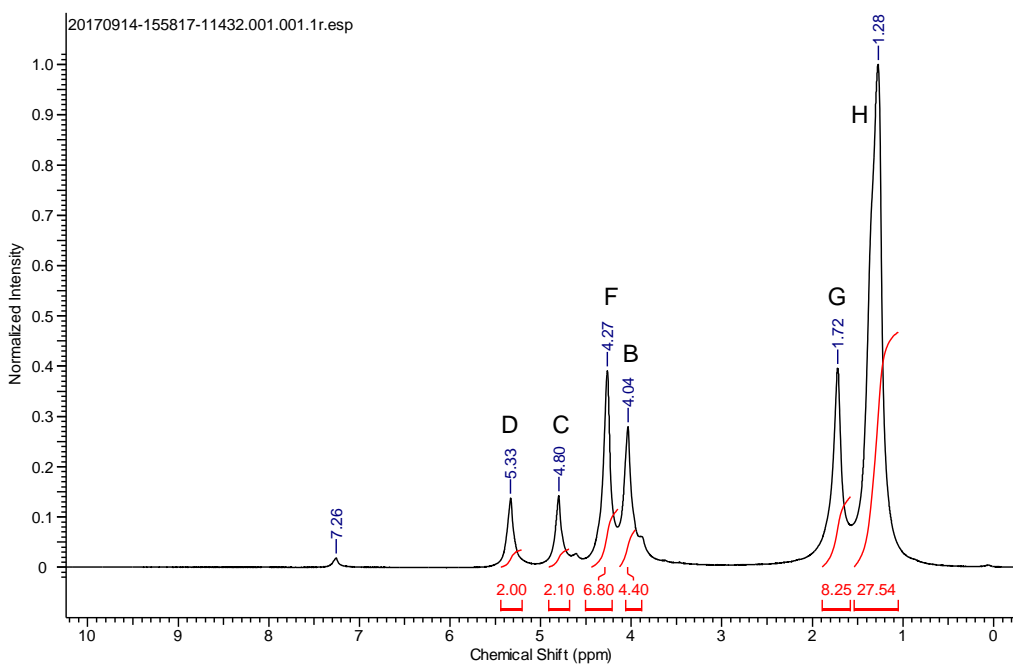


Figure 4.65. $^1\text{H NMR}$ spectrum of polyoxalate **P26(4c-5c)** in CDCl_3 (500 MHz at 298 K).

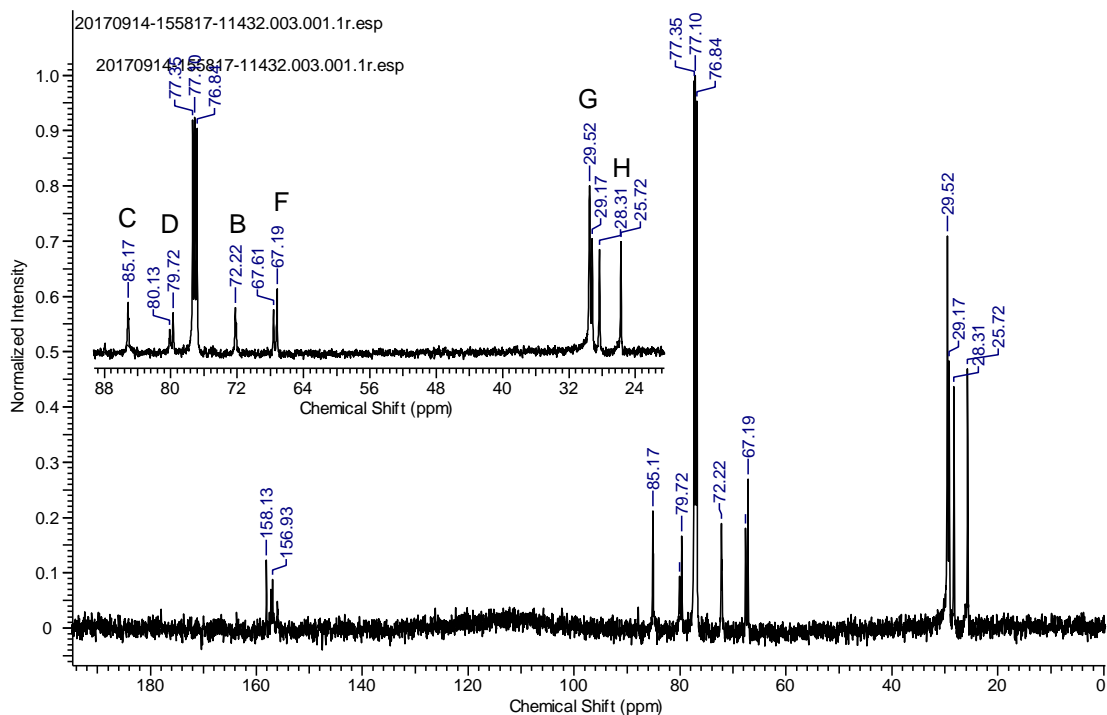


Figure 4.66. ^{13}C NMR spectrum of polyoxalate **P26(4c-5c)** in CDCl_3 (125 MHz at 298 K).

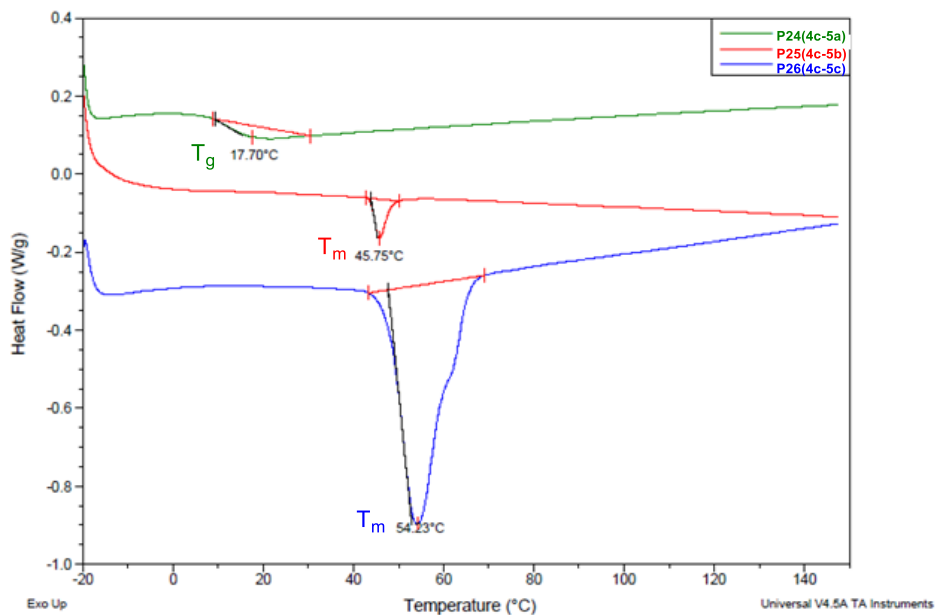


Figure 4.67. DSC heating curve for **P24(4c-5a)**-**P26(4c-5c)** (run 7-9) under N_2 atmosphere (first heating cycle; only for **P24(4c-5a)** from second heating cycle).

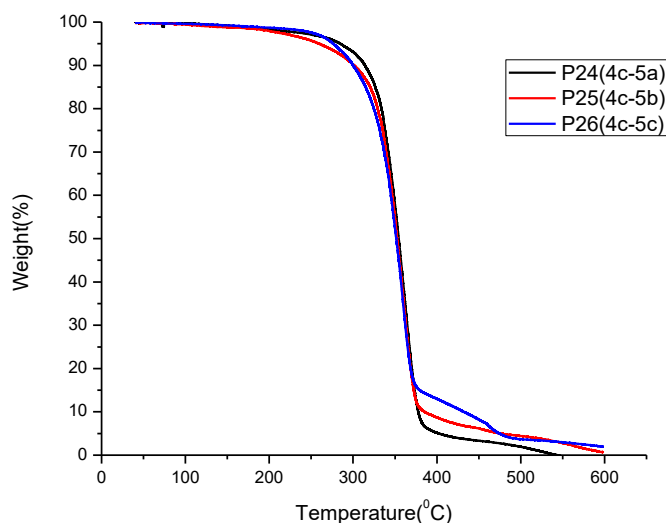


Figure 4.68. TGA trace for **P24(4c-5a)-P26(4c-5c)** recorded between 40-600 °C under the N₂ atmosphere.

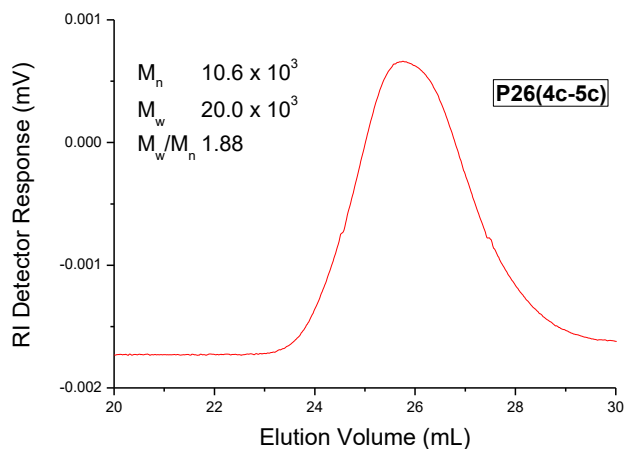


Figure 4.69. GPC chromatogram of **P26(4c-5c)** in chloroform at room temperature.

4.4.5. Polyoxalate Film and their Mechanical Properties:

A 10 wt% polymer solution was prepared in chloroform (3 ml). Homogeneous polymer solution was poured in a Teflon Petri dish and was air dried in a fume hood for 72 hours. The resultant film was sticky in nature and therefore it was further dried in a vacuum oven at 50 °C for another 48 hours to remove any residual solvent present. Film was peeled off gently from teflon Petri dish and was used as it is for characterization. Tensile testing of the film obtained

from polyoxalate **P19(4a-5b)** revealed a stress at break of 3.25 MPa and elongation at break of about 23% (Figure 4.70). The storage and loss modulus of **P19(4a-5b)** were 61.5 MPa and 11.5 MPa respectively (Figure 4.71). These modulus values correspond to a soft rubbery material.

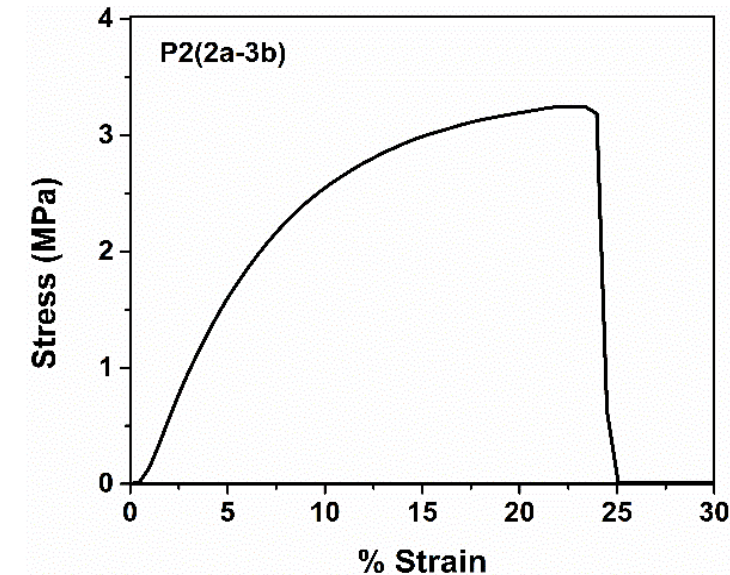


Figure 4.70. Stress-strain curve of **P19(4a-5b)**.

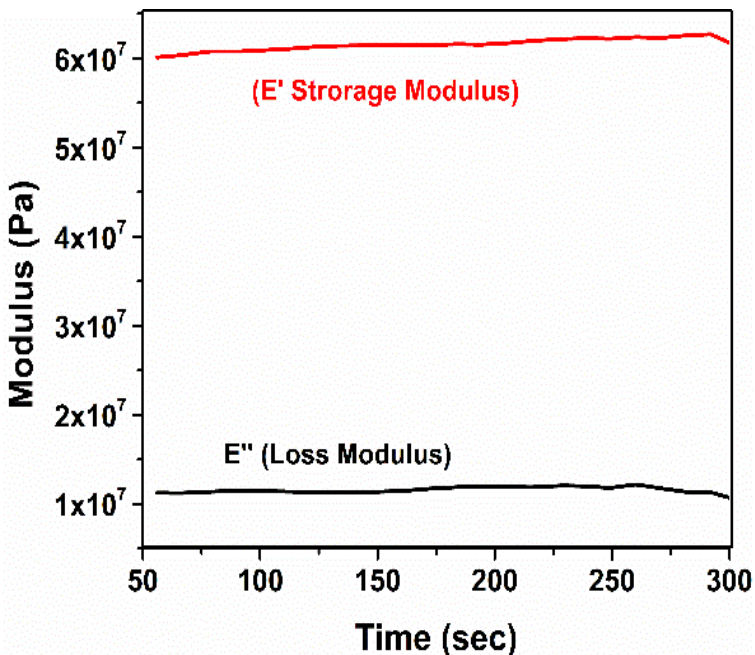


Figure 4.71. Storage and loss modulus of **P19(4a-5b)**.

4.4.6. Degradation of Polyoxalates:

4.4.6.1. Monitoring Acid Induced Degradation by GPC:

15 mg of polymer **P20(4a-5c)** was weighed accurately in individual vials and 4 ml of chloroform and 0.1 ml hydrochloric acid (1M in dioxane) was added to the vials to acidify the solution. The solution was kept for 4, 8, 12, 16, 20 and 24 hours for degradation, after which the solvent was evaporated on rotary evaporator. To ensure the complete removal of acid, the resultant material was fully dried under high vacuum. The thus obtained solid residue was again dissolved in 2 ml chloroform and the solution was filtered and injected in GPC. Similar protocol was followed for polymers **P23(4b-5c)** and **P26(4c-5c)**. The initial 41000 g mol⁻¹ molecular weight of polymer **P20(4a-5c)** is reduced to 5000 g mol⁻¹ (**Figure 4.72**) within 24 hours. Similar trend was observed for polyoxalates derived from isosorbide and isoidide. After 24 hours in acidic solution, the isosorbide derived polyoxalates **P23(4b-5c)** revealed decreased molecular weight of 3900 g mol⁻¹ from 23000 g mol⁻¹ (**Figure 4.73**) initial molecular weight. Whereas, isoidide derived polyoxalate **P26(4c-5c)** shows decrease in molecular weight from 20000 g mol⁻¹ to only 610 g mol⁻¹ (**Figure 4.74**). These results suggest that the polyoxalates are susceptible to degradation in acidic media. The following plots (molecular weight Vs time) shows the most significant data (**Figure 4.72-4.74**).

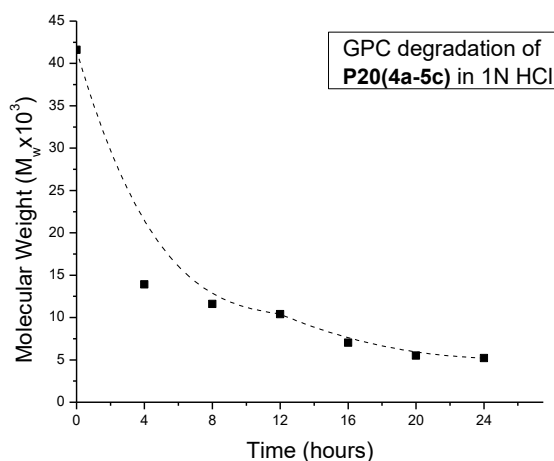


Figure 4.72. Acid induced degradation of polyoxalate **P20(4a-5c)**, molecular weight versus time by GPC.

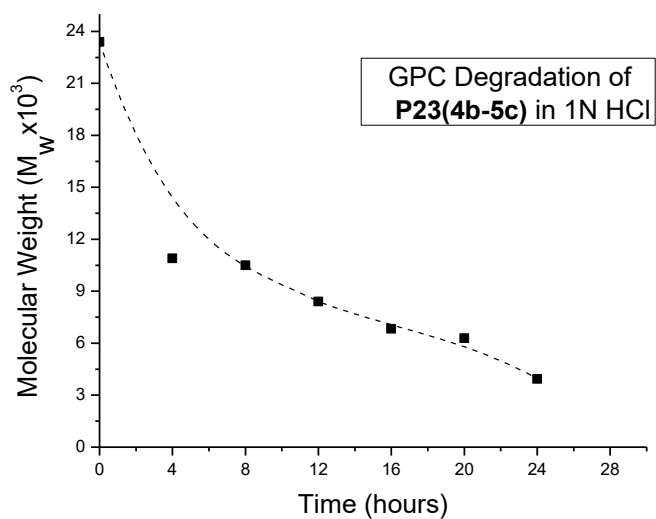


Figure 4.73. Acid induced degradation of polyoxalate **P23(4b-5c)**, molecular weight versus time by GPC.

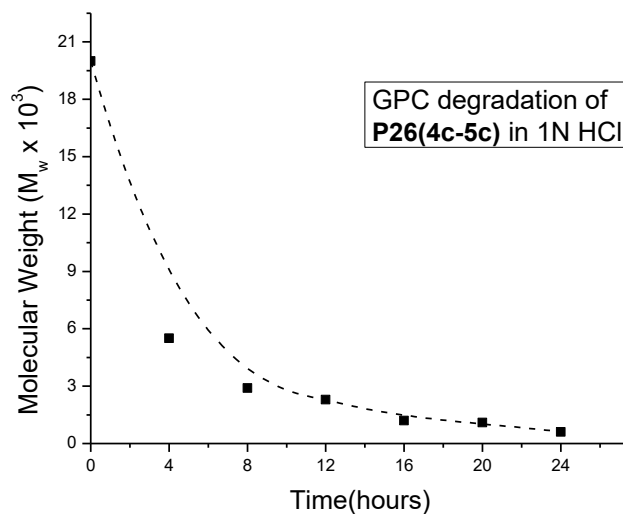


Figure 4.74. Acid induced degradation of polyoxalate **P26(4c-5c)** molecular weight versus time by GPC.

4.4.6.2. Solid-State Hydrolytic Degradation of Polyoxalate P20(4a-5c):

As a representative polyoxalate, **P20(4a-5c)** was selected and hydrolytic degradation was investigated. Compact pellets of identical dimensions were prepared from the polymer melt of **P20(4a-5c)** (20-23 mg) in a DSC crucible-lid. The lid was allowed to cool at room temperature, and the pellet was ejected with the help of forceps and dried for 4 hours and stored under argon. The thus obtained pellets were weighed and suspended in pH 7 solution or 5 ml HCl solution (3M and 9M) at room temperature over a period of 5 days. After that the supernatant was decanted and the pellets were dried for 7 hours in vacuum to get the constant weight. Next, the same pellet was suspended in a fresh solution for next 5 days (total 10 days) and same procedure as above was repeated. Subsequently, above cycle was repeated once again bring the total days of degradation to 15 days. Pellets derived from polyoxalate **P20(4a-5c)** in pH 7 solution revealed 39% weight loss after 15 days whereas, in 3M HCl solution 58% (in 15 days) degradation was observed. The maximum degradation of 84% was observed in 9M HCl solution after 15 days. Like the reported isohexides-polyacetals and copolyacetals^{4b, 18a} the present polyoxalates seem to be sensitive to acidic conditions. The percent weight loss is depicted in the **Figure 4.2** and the representative degradation experiments have been summarized in Table 4.3 (see below).

Table 4.3. Hydrolytic degradation of pellets derived from **P20(4a-5c)** in pH 7, 3M and 9M hydrochloric acid solution over a period of 5, 10 and 15 days.

Entry	Initial wt. (mg)	Media	%wt. loss after 5 d	%wt. loss after 10 d	%wt. loss after 15 d
1	21.0	pH 7	20	31	39
2	20.0	3M.HCl	36	45	58
3	23.1	9M.HCl	45	57	84

4.4.6.3. Tracking Acid Induced Degradation by NMR:

30 mg of polyoxalate **P20(4a-5c)** was taken in a NMR tube and to this was added 0.6 ml of D₂O. Proton NMR of this sample displayed only D₂O resonance at 4.7 ppm. Subsequently, 0.1 ml of 35 wt% of DCl in D₂O was added to above NMR tube and proton NMR was recorded. At this stage, only D₂O peak was visible. Hence, to accelerate the degradation, additional 0.1 ml of DCl in D₂O was added and an NMR was recorded. After 8 hours a proton NMR was recorded, which displayed very weak resonances in the range

of 3.0-5.0 ppm. Subsequently, the progress of the degradation was monitored after 5 days, 9 days and 14 days. These ^1H NMR results indicate that over a period of time intensity of new peaks that can be assigned to isomannide backbone increases (**Figure 4.75**). Furthermore, the ^1H NMR of commercial grade isomannide compares well with proton NMR of degraded polyoxalate (**Figure 4.75-top**). Likewise, the ^{13}C NMR of degraded sample compares well with the commercial isomannide ^{13}C NMR spectrum, confirming the existence of isomannide (**Figure 4.76**) as one of the degradation products. Even after 14 days, a solid precipitate was observed at the bottom of the NMR tube. The soluble part was decanted off and solid part was dried under vacuum and an NMR was recorded in CDCl_3 . The ^1H and ^{13}C NMR results indicated the existence of aliphatic mono-oxalate 2-((12-hydroxydodecyl)oxy)-2-oxoacetic acid as the only detectable product. The proton NMR of the D_2O insoluble but CDCl_3 soluble fraction of the polyoxalate revealed a proton resonance at 4.26-4.29 ppm that corresponds to the oxalates methylene protons (**Figure 4.77**). A ^{13}C NMR spectrum of this fraction revealed resonance at 158 ppm, which confirms the presence of oxalate carbon (**Figure 4.78**). Various 2D NMR experiments further corroborated the existence of 2-((12-hydroxydodecyl)oxy)-2-oxoacetic acid as one of the degradation products (**Figure 4.79-80**). In addition, the possibility of existence of 1, 12-dodecane diol cannot be fully ruled out.

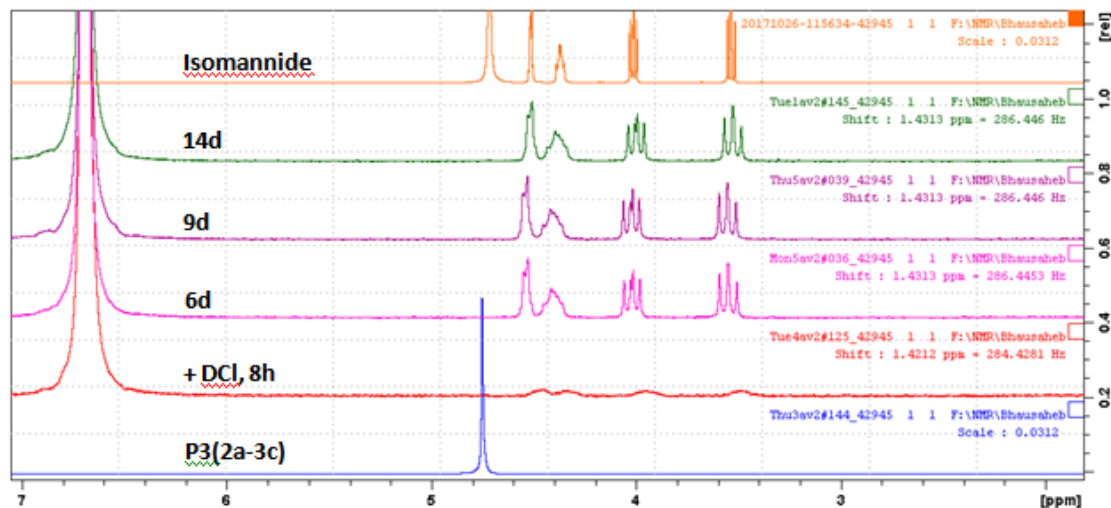


Figure 4.75. ^1H NMR of **P20(4a-5c)** in D_2O (bottom) and after addition of 0.2 ml of 35wt% DCl in D_2O over 14 days (200 MHz at 298 K).

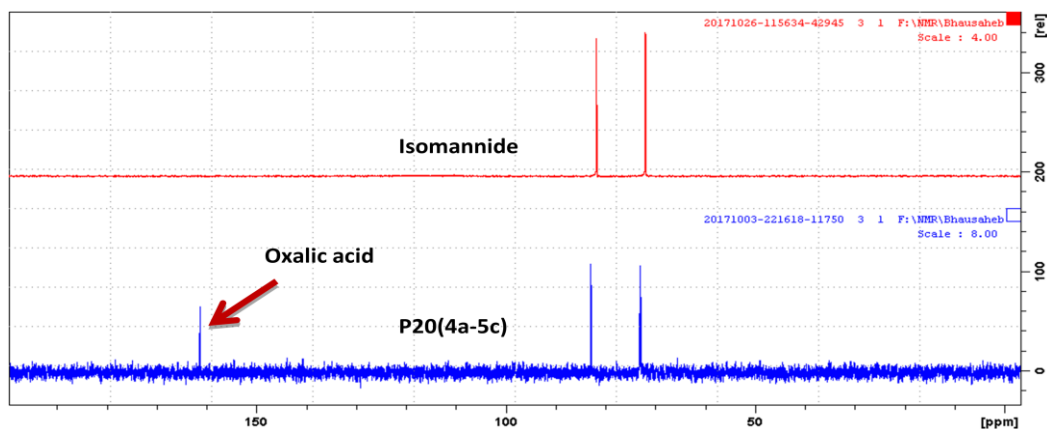


Figure 4.76. ^{13}C NMR of degraded **P20(4a-5c)** (bottom) and commercial isomannide (top) in D_2O (125 MHz at 298 K).

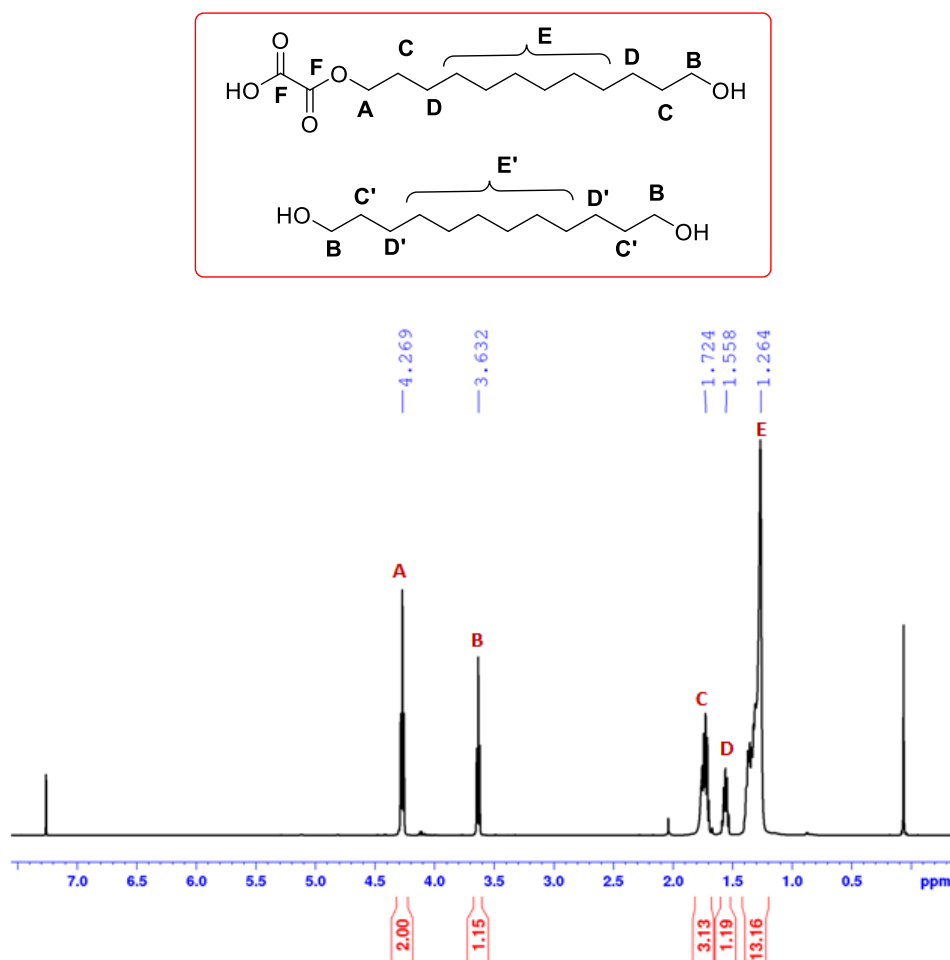


Figure 4.77. ^1H NMR spectrum of degraded aliphatic part of **P20(4a-5c)** in CDCl_3 (500 MHz at 298 K).

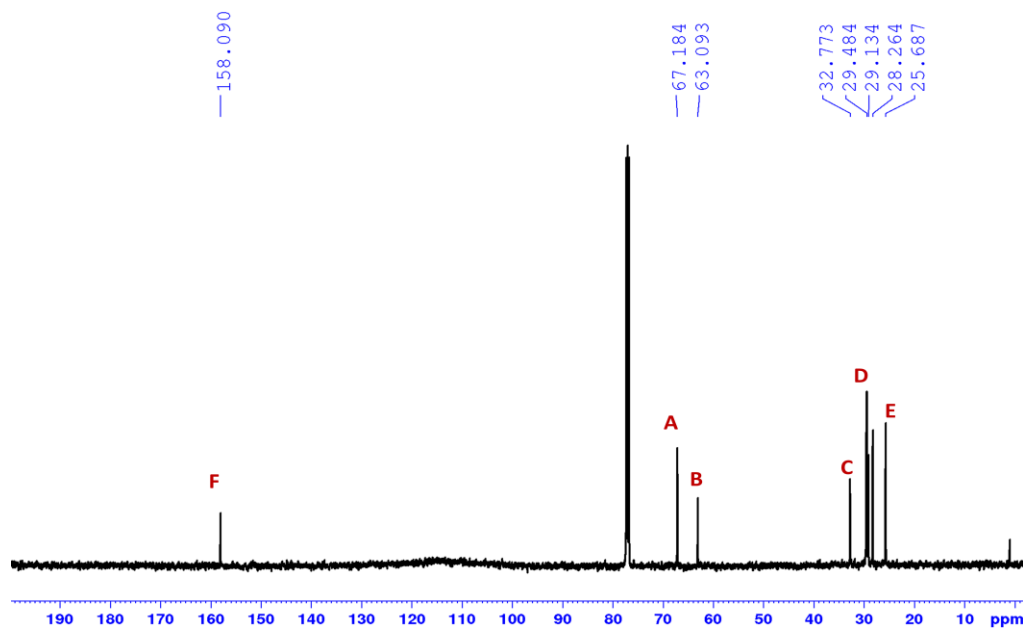


Figure 4.78. ^{13}C NMR spectrum of degraded aliphatic part of **P20(4a-5c)** in CDCl_3 (125 MHz at 298 K).

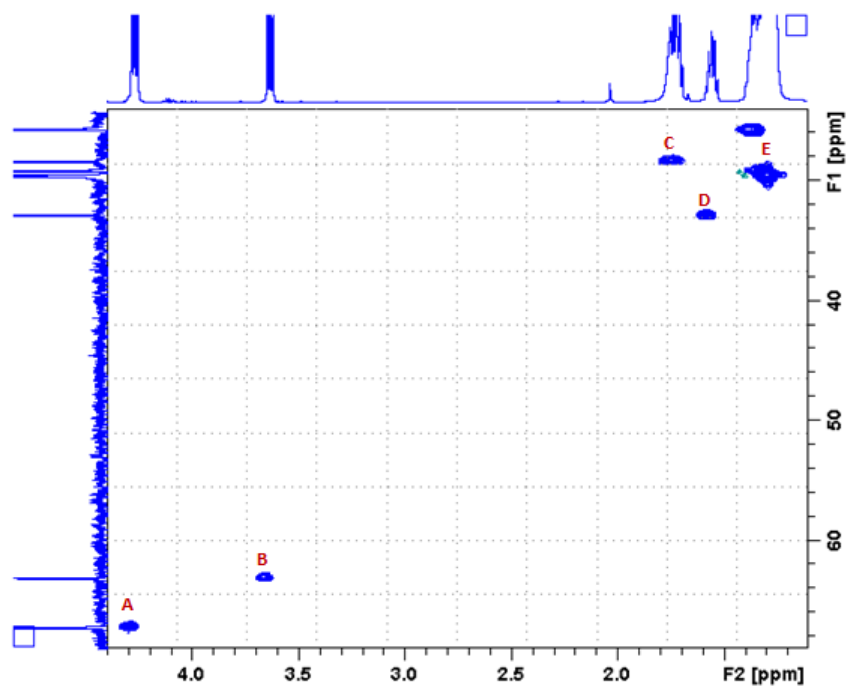


Figure 4.79. HSQC NMR spectrum of degraded **P20(4a-5c)** in CDCl_3 (at 298 K).

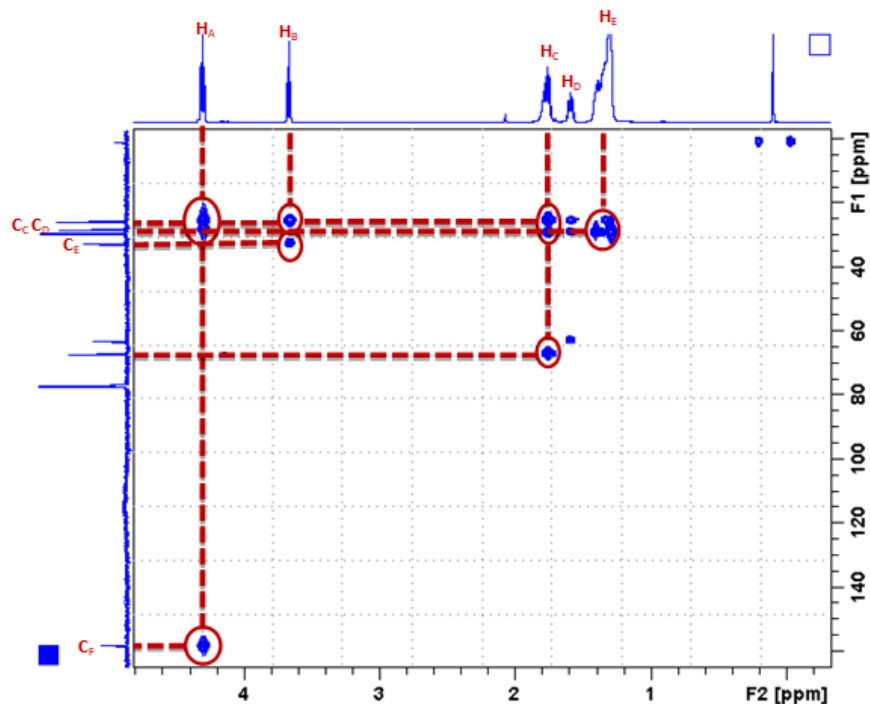


Figure 4.80. HMBC NMR spectrum of degraded **P20(4a-5c)** in CDCl₃ (at 298 K).

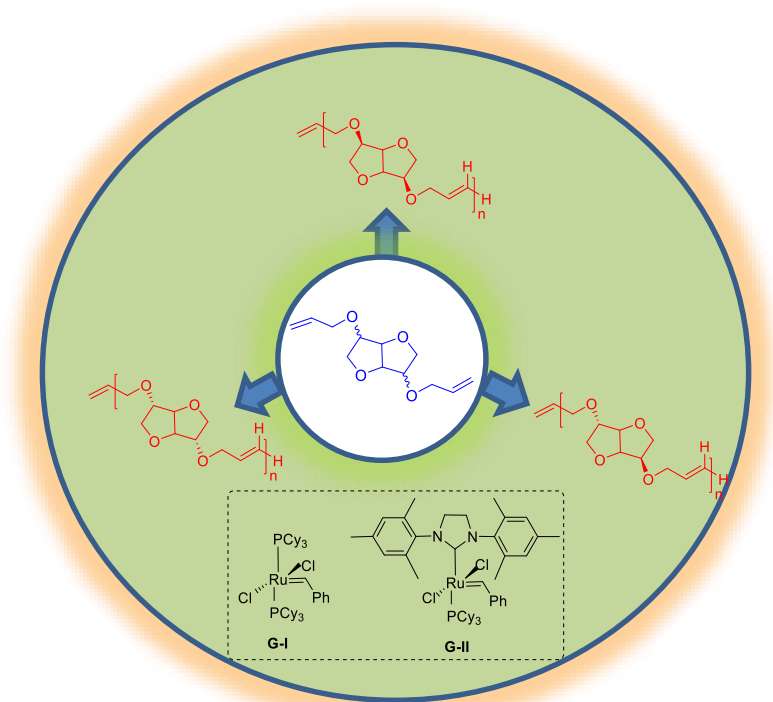
4.5. Conclusions:

In summary, single step synthesis of a small family of isohexide-dioxalates has been established. The identity of isomannide-dioxalate (**4a**), isosorbide-dioxalate (**4b**) and isoidide-dioxalate (**4c**) was unambiguously ascertained using a combination of 1-2D NMR, mass spectroscopy and analytical methods. The synthetic utility of these sugar derived dioxalates was examined in condensation polymerization. Condensing isohexide-dioxalates (**4a-c**) with aliphatic renewable diols (**5a-c**) in presence of Lewis acid catalyst leads to the production of poly(isohexide-*co*-alkane)oxalates. Quite surprisingly, the proton NMR of the polyoxalate **P18(4a-5a)** revealed a 2:1 ratio of 1,6-hexanediol (**5a**) and isomannide-dioxalate (**4a**) in the polymer backbone. This intriguing reactivity was found to be an outcome of cross metathesis between the two monomers **4a** and **5a**. Based on direct and indirect evidence, and control experiments, an alternative polymerization mechanism is proposed. In addition, identification and isolation of intermediate **5a''** 6-hydroxyhexyl (6-(2-methoxy-2-oxoacetoxy)hexyl) oxalate and **4a'** (3R, 6R)-6-hydroxyhexahydrofuro[3,2-*b*]-furan-3-yl methyl oxalate justified the 2:1 ratio of **5a**:**4a** observed in poly(isomannide-*co*-hexane)oxalate **P18(4a-5a)**.

Thereafter, polymerization conditions were optimized to obtain high molecular weight polyoxalates **P18(4a-5a)-P26(4c-5c)**. The existence of polyoxalates was unambiguously ascertained using a combination of spectroscopic and analytical methods. GPC analysis of these polymers revealed molecular weights in the range 14000–68000 g/mol. In an attempt to demonstrate direct application of aforementioned polymers, transparent films were casted and their mechanical properties indicated formation of soft films. Solid and solution state degradation investigations established that polyoxalates are amenable to degradation over extended period of time. Thus, utilization of renewable feed-stocks to prepare chiral building blocks and commercially attractive sustainable polyoxalates has been demonstrated for the first time.

Chapter-5

Synthesis of Isohexide-di(ether-ene)s and ADMET Polymerization



This chapter has been adapted from following publication

Rajput, B. S.; Lekshmy, K. G.; Menon, S. K.; Chikkali, S. H. *Green Materials* **2017**, 5, 63-73.

5.1. Abstract:

As the fossil fuel reserves deplete and the greenhouse gases increase, the scientific community is challenged to provide sustainable solutions. Sugar-based isohexides can be modified to prepare a library of isohexide-diene monomers for polymerization. Such isohexide diene monomers can be subjected to Acyclic Diene Metathesis Polymerization to obtain green materials. Here we report a single step synthetic protocol to access a small family of isohexide-di(ether-ene)s and the corresponding polymers. The isohexide di(ether-ene)s **6a-c** could be isolated in good to excellent yields under optimized conditions. The resultant isohexide-di(ether-ene)s **6a-c** are potential versatile building blocks for pharmaceuticals and material science. The synthetic utility of **6a-c** was demonstrated by subjecting them to ADMET polymerization using Grubbs 1st and 2nd generation catalysts. The resultant viscous material was evaluated using ¹H NMR and MALDI-ToF-MS, which suggests the formation of anticipated ADMET polymers. End group analysis of the polymers by NMR revealed molecular weight of 800-13800 g/mol. Slight improvement in the M_w was observed when benzoquinone was added or when the catalyst was added in two stages. Thus, the analysis of the poly(ether-ene)s suggests that low molecular weight polymers were formed under the optimized experimental conditions, and the molecular weight could not be improved beyond a point.

5.2. Introduction:

The demand for fossil fuels is increasing at a fast pace, while the fossil fuel reserves are dwindling with the same rate. Moreover, with increasing consumption of fossil fuels the amount of greenhouse gasses is also increasing, leading to climate change, and adverse effects on the environment.¹⁻² Driven by these challenges, last decade witnessed a resurgence in polymeric materials derived from renewable resources.³ Among the renewable feedstocks, sugars,⁴ and plant oils⁵ provide direct entry to chemical modification and functionalization.⁶⁻⁷ Utilisation of abundant renewable resources such as starch and cellulose to develop new chemicals and polymeric materials appears to be a sustainable solution.⁸⁻¹⁰ For instance, sugars can be easily converted to a host of new building blocks. The inbuilt chirality in sugars can be creatively utilized to manufacture value added chiral reagents. Sugars can be readily converted to bifunctional molecules called isohexides (isosorbide, isomannide, isoidide). The common C6-sugars such as glucose and mannose can be hydrogenated to produce sorbitol and mannitol respectively (**Figure 5.1**). The double dehydration of sorbitol and mannitol produces isohexides (Dianhydrohexitols).

These isohexides carry two free hydroxyl groups located at the C-2 and C-5 positions either pointing inwards (named as *endo*) or pointing outside (named as *exo*) the bicyclic ether ring. Based on the orientation of the two hydroxyl groups, three diastereoisomers are formed, which are known as 1,4:3,6-Dianhydro-D-glucitol (isosorbide, **1b**), 1,4:3,6-Dianhydro-D-mannitol (isomannide, **1a**) and 1,4:3,6-Dianhydro-L-iditol (isoidide, **1c**). The hydrogen bonding between the *endo*-hydroxyl group and the ether oxygen reduces the reactivity of these molecules.¹¹ Considering the steric effects and hydrogen bonding, isomannide with two *endo* hydroxyl groups is the least reactive compound compared with isoidide which has two *exo* hydroxyl groups and should be more attractive for biochemical applications.¹² Unfortunately, isoidide is rare in nature and remains largely inaccessible. The current method to obtain isoidide goes via inversion of chiral centers of isomannide.⁶ Isosorbide is the most widely and commercially available dianhydrohexitol. The orientation of the hydroxyl group at C-2 is *exo* and that at C-5 is *endo*, due to which isosorbide is more reactive isomer compared to isomannide. These isohexides can be either incorporated into the backbone of new polymers or converted to low molar mass additives for thermoplastics, thermosets or specialty applications. These can be also used as chiral auxiliaries, plasticizers, stabilizers or compatibilizers.¹²

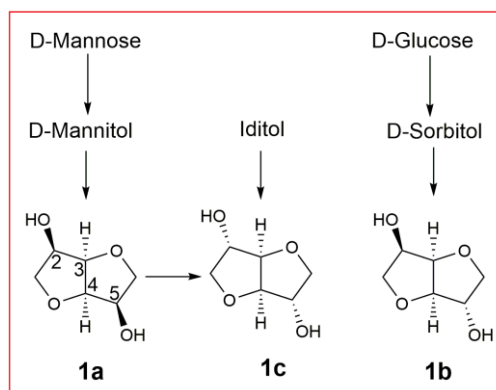


Figure 5.1. Stereoisomeric forms of isohexides.

Degradability is another material requirement for a clean and sustainable future. Isohexide and plant oil based polymers seem to meet these criteria which are very important for the next generation of sustainable materials.⁶⁻⁷ Commercially available isohexides (isosorbide and isomannide) have found multiple applications in polycondensates¹² but the direct utilization of isohexides usually requires harsh polymerization conditions and leads to dark, tar-like polymers with lower molecular weights.¹² This is mainly due to the hydrogen bonding in isohexides that limits their reactivity. In order to address these limitations, Daan and coworkers introduced 1-

carbon extension strategy and synthesized derivatives of isohexides (**1a**, **1b** and **1c**).¹³ Thus, these fully biobased monomers with enhanced reactivity after 1-carbon extension were tested in polymerization reactions and polymers such as polyamides,¹⁴ polyesters,¹⁵ co-polyesters with diols¹⁶ and polyurethanes¹⁷ were successfully synthesized. The resultant polymers were found to be less colored and displayed enhanced glass transition temperature (T_g) compared to their linear petroleum based analogues. Although fair amount of progress has been made to utilize isohexides, the scope of functionalization is limited to 1-carbon extension strategy. Therefore, utilization of isohexides calls for new synthetic strategies that can successfully convert the less reactive renewable resources into highly reactive functional molecules. One such strategy would be functionalizing the isohexides to isohexide-dienes. If accessible, the isohexide-dienes would open up new avenues in the area of chiral reagents or would serve as monomers for polymerization reactions.

One of the polymerization methods that uses diene as feed and requires catalytic amount of initiators is Acyclic Diene METathesis (ADMET) polymerization. Over the years acyclic diene metathesis polymerization has evolved into a very powerful technique for the preparation of a wide range of polymeric architectures, including linear polymers,¹⁸ polymers with a defined branching density¹⁹⁻²⁰ and block-copolymers from telechelics.²¹⁻²⁵ This metal catalyzed polymerization method tolerates various functional groups and produces high molecular weight polymers.^{19, 26} Acyclic diene metathesis polymerization follows a step growth mechanism and generates linear or cyclic polymers with double bonds in the main chain.²⁷ In ADMET, 2+2 cycloaddition reaction between two diene monomers produces four-membered metallacyclobutane intermediate, which is followed by ring opening to produce polyolefin and ethylene is liberated as by-product. Like in olefin metathesis, ADMET also goes through equilibrium mixtures and the driving force seems to be liberation of small molecules, which drives the equilibrium towards polymer (product) side.²⁸ Effective removal of ethylene by-product from the polymerization medium favors production of polymers with high molecular weight and high conversion.²⁹ The most commonly used catalysts for ADMET polymerization are based on ruthenium which tolerates a variety of functional groups.³⁰ As catalytic amount of initiator is required, ADMET represents a sustainable method of polymerization. Despite of considerable success of ADMET, isomerization of the diene/olefin has been identified as one of the side reactions in ADMET polymerization. It is known that second generation olefin metathesis catalysts show a temperature dependent double-bond isomerization.³¹ It appears that the formation of ruthenium-hydride species is responsible for these isomerization

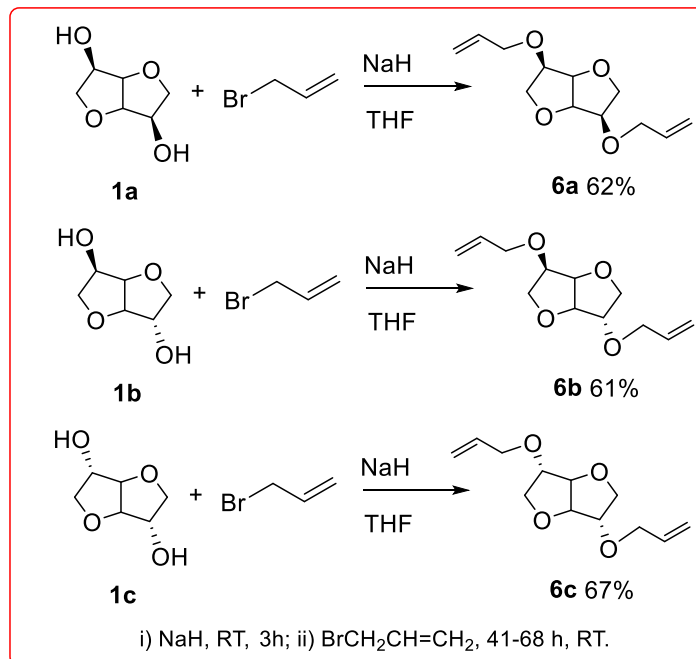
side reactions. The first generation Grubbs catalyst (**G-I**) generally showed very little isomerization, below 100 °C. Considerable isomerization was observed only at high temperatures (100°C and above).³² The extent of isomerization side reactions largely depends on the type of catalyst, the reaction temperatures, as well as other reaction conditions such as a continuous nitrogen purging as it is frequently applied during ADMET polymerizations. Therefore, it is highly desirable to prepare renewable monomers that can potentially undergo ADMET polymerization and produce green materials for sustainable future.

In this chapter, we report the synthesis of renewable isohexide-di(ether-ene) monomers **6a-c** and corresponding ADMET polymerization to renewable polymers.

5.3. Results and Discussion:

5.3.1. Monomer Synthesis:

Isohexide-di(ether-ene)s were synthesized in good yields in a single step, following our earlier synthetic protocol, with significant modifications.⁶ Isomannide and isosorbide were treated with 3 equivalent of sodium hydride which was followed by addition of excess allyl bromide in THF at room temperature. Stirring the reaction mixture for longer period afforded crude **6a** and **6b**. The reaction was quenched by addition of distilled water followed by washing with saturated sodium chloride solution. The aqueous phase was extracted with ethyl acetate and combined organic phase was dried on magnesium sulphate, filtered and the filtrate was evaporated to obtain pale yellow oily material. Purification by column chromatography (pet ether: ethyl acetate 90:10 for **6a** and 94:06 for **6b**) yielded corresponding di(ether-ene)s as colourless liquid in good yields (**6a** = 62% and **6b** = 61% respectively) (**Scheme 5.1**). Isoxide was prepared from isomannide by a modified literature method.⁶ Isoxide-di(ether-ene) **6c** was prepared by following a similar procedure as in the case of **6a** and **6b**. Work up of the resultant oily material and purification by column chromatography (pet ether: ethyl acetate, 70:30) gave the desired isoxide-di(ether-ene) as colourless liquid in 67% yield.



Scheme 5.1. Synthesis of isohexide-di(ether-ene)s.

The isolated monomers **6a-c** were characterized by various analytical and spectroscopic methods. The formation of isomannide-di(ether-ene) **6a** was confirmed by the ¹H NMR spectroscopy which revealed a characteristic resonance at 3.85-4.07 ppm (**Figure 5.2**). This signal can be ascribed to the methylene protons (OCH₂, 4H), although methylene protons overlap with backbone proton signals. A characteristic multiplet at 5.02-5.21 ppm can be assigned to the terminal allylic (=CH₂, 4H) protons and another multiplet at around 5.69-5.88 ppm can be designated to allylic C-H protons. The proton NMR findings were corroborated by ¹³C NMR spectra.

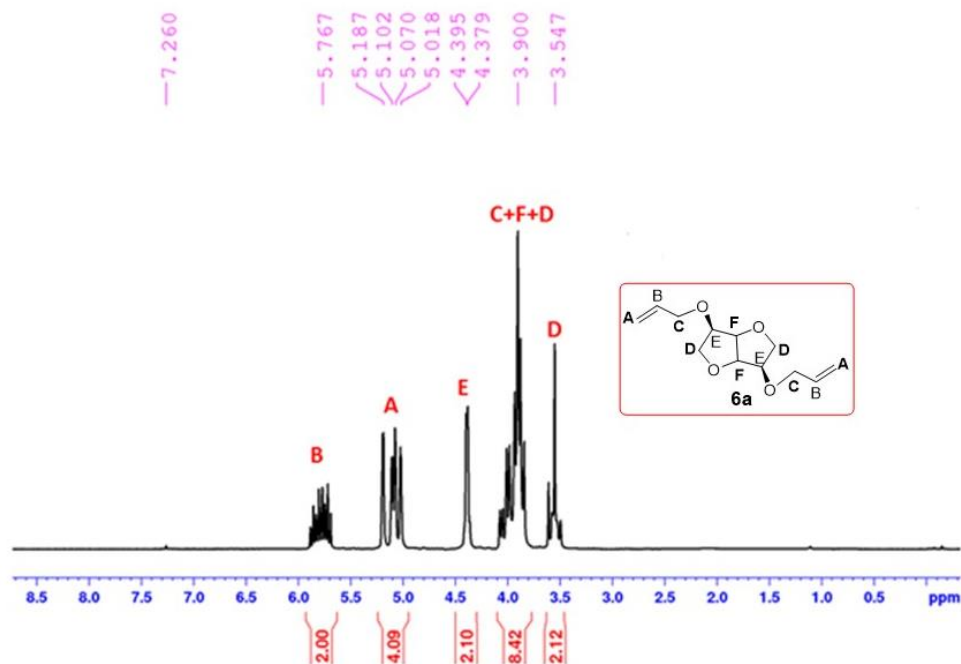
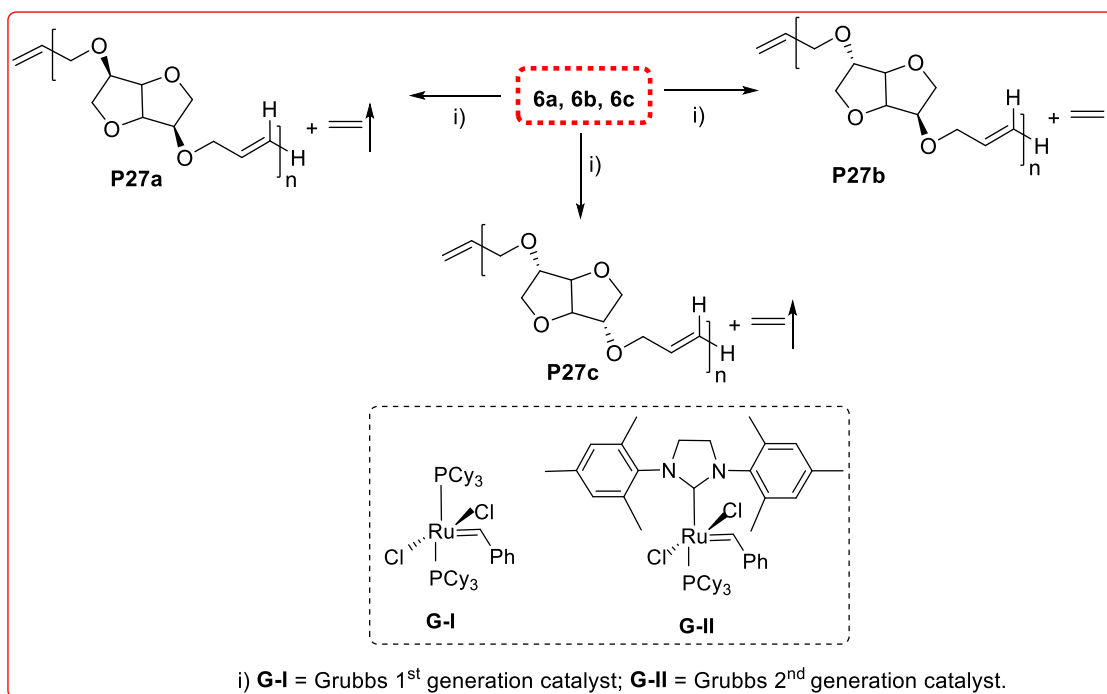


Figure 5.2. ^1H NMR spectrum of compound **6a** in CDCl_3 (200 MHz at 298 K).

A typical ^{13}C NMR of isosorbide-di(ether-ene) shows a characteristic resonance at 71.9 ppm that can be attributed to methylene carbon $-\text{OCH}_2$ (**Figure 5.4**). The identity of **6a** was further confirmed by mass spectroscopy (ESI-MS positive mode) which revealed a molecular ion peak at 227.12 $[\text{M}+\text{H}]^+$ and 249.10 $[\text{M}+\text{Na}]^+$ (**Figure 5.5**). The existence of **6b** was confirmed by a combination of spectroscopic and analytical methods. The crucial methylene ($-\text{OCH}_2$) protons appear as a multiplet between 3.89-4.25; unfortunately overlapping with the isosorbide backbone protons. However, clear evidence about the existence of $-\text{OCH}_2$ group was obtained from a proton-carbon (HSQC) 2D NMR experiment. In a direct proton-carbon correlation experiment, the proton resonance at 4.05 ppm revealed a cross peak to a carbon at 72.00 ppm, confirming the existence of a ($-\text{OCH}_2$) group (**Figure 5.8**). Furthermore, the proton signal at 5.16 ppm showed a cross peak to a carbon at 117.2 ppm, confirming the existence of $-\text{CH}_2$ group. The formation of isosorbide-di(ether-ene) has been also confirmed by mass spectrometry, which displayed $[\text{M}+\text{H}]^+$ peak at 227.12 and $[\text{M}+\text{Na}]^+$ peak at 249.10 (**Figure 5.9**). Along the same line, the identity of **6c** was established using a combination of ^1H , ^{13}C NMR spectroscopy and mass spectroscopy (**Figure 5.10-5.12**).

5.3.2. Acyclic Diene Metathesis (ADMET) Polymerization of Isohexide-di(ether-ene)s to Polyether-enes:



Scheme 5.2. ADMET polymerization of isohexide-di(ether-ene)s to polyethers.

The thus prepared monomers were subjected to Acyclic Diene Metathesis (ADMET) Polymerization using Grubbs generation I and generation II catalysts. The major driving force in these polymerization reactions is the loss of small molecules with low boiling point (ethylene). Usually, continuous removal of ethylene by-product is required to obtain high molecular weight polymers. Polymerization of **6a** was started at 60 °C with G-I catalyst and over a period of 1 hour the temperature of the polymerization vessel was raised to 100 °C. During this first one hour, slight vacuum was applied every 3-5 minutes to remove the by-product (ethylene). Next, the polymerization was continued at 100 °C for 1 hour with a slight vacuum. Finally, the polymerization is run for next 10 hours with constant vacuum (for detailed polymerization conditions see the experimental section). Further screening of polymerization parameters (temperature and time) indicated that molecular weight decrease above 100 °C and after 12 hours. After 10 hours the resultant colored viscous polymeric material was quenched with ethyl vinyl ether. The thus prepared material was dissolved in 2 ml chloroform and precipitation was attempted from ice-cold methanol. However, the precipitate could not be obtained, hence the

resultant brown coloured clear solution was concentrated on rotary evaporator to obtain viscous oily material.

Table 5.1. ADMET polymerization of **6a-6c**, molecular weights, molecular weight distributions and yields.^a

Run	Catalyst	M _n (theo) × 10 ^{3b}	M _n × 10 ^{3c}	M _w × 10 ^{3d} (PDI)	Theoretical yield in (gm)	Isolated yield in gm (%) ^e
P27a-1	G-I	19.8	1.3	0.9(1.36)	0.39	0.29(74)
P27a-2	G-II	19.8	2.5	0.7(1.38)	0.39	0.37(95)
P27b-1	G-I	19.8	2.1	1.2(2.01)	0.39	0.38(97)
P27b-2 ^f	G-I	19.8	0.8	2.4(2.00)	0.39	0.38(97)
P27b-3 ^g	G-I	19.8	1.4	1.8(1.75)	0.39	0.33(84)
P27b-4 ^h	G-I	19.8	1.4	2.9 (2.19)	0.39	0.37(95)
P27b-5	G-II	19.8	ND	0.6(1.21)	0.39	0.26(67)
P27c-1	G-I	19.8	13.8	1.5(1.58)	0.39	0.29(74)
P27c-2	G-II	19.8	ND	0.7(1.25)	0.39	0.31(80)

^aSee experimental section 5.4 for more details; G-I is the Grubbs first-generation catalyst and G-II is the Grubbs second-generation catalyst; ^bM_n (theoretical) = [M]₀/[C]₀ × molecular weight (monomer repeating unit) + molecular weight of end group (ethylene); ^cM_n determined by proton NMR: g/mol; ^dM_w and polydispersity index (PDI) were obtained from gel permeation chromatography in chloroform with respect to the polystyrene standard; ^eYield reported is of the crude material; ^f2 mol% of benzoquinone was added with respect to the monomer; ^gTwo-stage polymerization (initially 1 mol% catalyst addition, and after 4 h, further 1 mol% catalyst addition); ^h Combined 2 mol% of benzoquinone and 1 mol% of G-I catalyst were added (initially when polymerization is started and after 4 h); ND, not detected due to the absence of end groups.

Similar polymerization protocol was applied for G-II catalyst and the results are presented in **Table 5.1**, run **P27a-2**. The resultant polymer material was analyzed using various analytical tools. A proton NMR of **P27a-1** revealed reduced intensity of end group resonance at 5.09-5.26 ppm suggesting the formation of anticipated polymer (**Figure 5.13**). Similarly, polymerization of **6a** using Grubbs IInd generation catalyst produced polyether-ene (**P27a-2**) which displayed an end group resonance at around 5.14-5.31 ppm suggesting the formation of a polymer (**Figure 5.20**). The number average molecular weight was determined by end group analysis using proton NMR that displayed the molecular weight of 1300 and 2500 g/mol (for G-I and G-II catalysts respectively). When subjected to GPC analysis in chloroform; **P27a-1** and **P27a-2** revealed a relatively low molecular weight of 900 Da and 700 Da respectively (**Figure 5.19, 5.21**). This

difference in molecular weight between the NMR and GPC could be due to the polystyrene standards used in GPC, which might not be very suitable for this type of polymers. Formation of cyclic polymers could be the other reason for the observed difference in molecular weight. MALDI-ToF-MS spectrum of **P27a-1** displayed a repeat unit molar mass of 198 Da (**Figure 5.15**). MALDI-ToF-MS analysis is further supported by ESI-MS which shows the repeat unit molar mass difference of 198 Da (**Figure 5.17**). The splitting pattern of MALDI-ToF-MS (**Figure 5.16**) and ESI-MS (**Figure 5.18**) is matched with the respective simulated patterns. It is well established in olefin metathesis that vinyl-ether suppress the metathesis due to vicinal oxygen.³⁴ Although the olefinic double bond in monomer **6a** is one carbon away from the oxygen, it might be quite possible that the double bond isomerizes to internal position and *in-situ* generates vinyl ether, which then blocks the ADMET polymerization. Incidentally, ¹³C NMR of **P27a-1** further supports the *in-situ* formation of vinyl ether (~144 ppm for IM-O-CH=CH-CH₃; see **Figure 5.14**). Thus, ADMET polymerization of **6a** produced only high molecular weight oligomers, rather than high molecular weight polymers. Additionally, it could be the *endo-endo* orientation of the functional groups in **6a** which might boost the formation of cyclic polyethers under the current reaction conditions.

ADMET polymerization of isosorbide di(ether-ene) **6b** was attempted employing Grubbs 1st and 2nd generation catalysts and important runs are presented in **Table 5.1**. A Schlenk tube was loaded with **6b** and the tube was evacuated for 1 hour before heating. Then 1 mol% of Grubbs 1st generation catalyst was added and polymerization was initiated by heating the tube at 60 °C, for 2 hours, with vacuum-purge cycle after every 3 to 5 minutes. Next, the temperature of the tube was raised to 70 °C and the polymerization was continued for next 3 hours with an intermittent vacuum. Finally, the temperature was raised to 90 °C and the reaction continued for another 3 hours under constant vacuum. The polymerization was quenched by adding ethyl vinyl ether and the resultant polymer was found to be soluble in chloroform and methanol. A viscous material was obtained after evaporating the volatiles. Reduced intensity of the end group protons in a proton NMR indicated the formation of polymer **P27b-1** (**Figure 5.22**). End group analysis by NMR revealed a number average molecular weight of 2100 g/mol. GPC analysis of **P27b-1** revealed slightly better molecular weight of 1200 g/mol (**Figure 5.29**). ESI-MS analysis revealed monomeric repeating unit mass difference of 198 Da (**P27b-1**, **Figure 5.27**). The simulated splitting pattern for **P27b-1** closely matches with the observed splitting pattern (**Figure 5.28**). However, only low

molecular weight oligomers could be obtained, which could be due to the isomerisation of terminal double bonds to internal vinyl ethers.

It is known in the literature that addition of benzoquinone can suppress the isomerization of double bonds, which might enable formation of high molecular weight polymers.³⁵ Therefore, in a separate experiment, benzoquinone (2 mol%) was added to the reaction together with Grubbs 1st generation catalyst (see the detailed procedure in experimental section (5.4.6), method-B for **P27b-2**). As it is evident from the ¹³C NMR data, the vinyl ether carbons (~144 and 103 ppm) could not be observed (**Figure 5.25**). Along the same line, GPC results revealed marginal increase in the molecular weight (~2400 gm/mol, **Figure 5.30**). In our attempts to further increase the molecular weight of polymer, we performed two stage polymerization. After initial polymerization with 1 mol% Grubbs-I catalyst for 4 hours, a second batch of Grubbs-I (1 mol%) catalyst was added and the polymerization was run for another 4 hours (**Table 5.1**, run **P27b-3**). GPC analysis of this polymer displayed increased molecular weight of about 1800 gm/mol (**Figure 5.31**). Above two experimental observations indicates that the molecular weight is increased when we add the additional catalyst or benzoquinone. Since these two experiments were independently yielding higher molecular weight polymers, we set out to perform an experiment combining these two. In a separate experiment, polymerization of **6b** was initiated by adding 1 mol% of Grubbs-I catalysts and 2 mol% benzoquinone and a second batch of Grubbs-I catalyst along with benzoquinone (2 mol%) was added after four hours (see the detailed procedure in experimental section (5.4.6), method-D for **P27b-4**). The GPC analysis of the resultant polymer displayed a better molecular weight of 2900 g/mol (**Figure 5.32**). Thus, our efforts to improve the molecular weight of the polymer lead to the modest molecular weight of 2900 g/mol only.

The monomer **6c** was subjected to ADMET polymerization using 1 mol% of Grubbs 1st generation catalyst and the important runs are presented in **Table 5.1**. The monomer, along with catalyst was first heated to 60 °C, subsequently, the temperature was raised to 100 °C over a period of 1 hour with a slight vacuum. After the initial one hour, the temperature of the polymerization system was maintained at 100 °C and the polymerization was continued for next 7 hours under constant vacuum. Quenching followed by solvent evaporation produced viscous material. Proton NMR analysis of this materials revealed the formation of **P27c-1** with only traces of end groups (**Figure 5.35**), whereas end groups could not be detected for **P27c-2** (**Figure 5.39**). The end group analysis of **P27c-1** revealed an increased number average molecular weight of 13800 g/mol.

(**P27c-1**, **Figure 5.35**). Along the same line, GPC analysis of **P27c-1** displayed the molecular weight of 1500 g/mol (**Figure 5.38**), which is certainly comparable with **P27b-1**. An MALDI-ToF-MS spectrum of **P27c-1** is presented in **Figure 5.3**, which displayed a repeat unit mass of 198 Da, exactly corresponding to the molar mass of expected polymer repeat unit. MALDI-ToF-MS analysis is further supported by the ESI-MS analysis which revealed repeating unit mass difference of 198 Da (**Figure 5.36**). The observed and simulated splitting pattern of **P27c-1** closely matches (**Figure 5.37**). Overall, Grubbs 1st generation catalysts performed better than Grubbs 2nd generation catalysts and produced polymers with reasonable molecular weights.

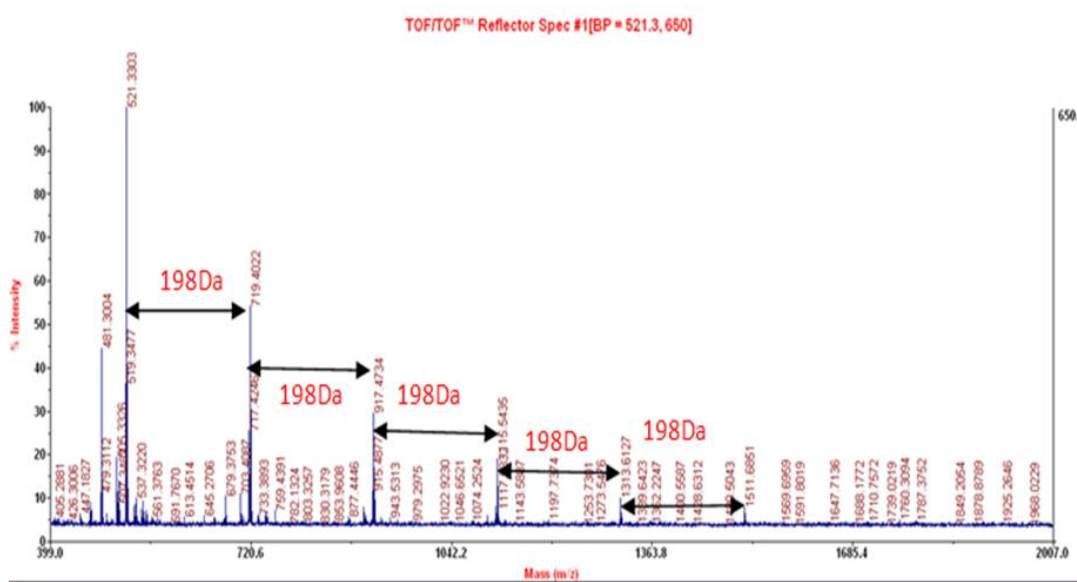


Figure 5.3. MALDI-ToF-MS spectrum of **P27c-1** (G-I) recorded in dithranol (shows 198 Da difference).

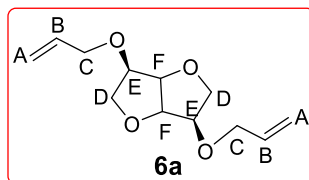
Thus, the analysis of the obtained materials **P27a-1** to **P27c-2** suggests that high molecular weight oligoethers or at the best, low molecular weight polymers are formed under the experimental conditions (see **Scheme 5.2**). It is most likely that the terminal olefin isomerized to internal olefin during the polymerization and generated vinyl-ethers *in-situ*. Such vinyl ethers are known to block the metathesis reaction, leading to low molecular weight polymers.

5.4. Experimental Section:

5.4.1. General Methods and Materials:

All manipulations involving moisture sensitive compounds were carried out under inert gas atmosphere using standard Schlenk or glove box techniques. Tetrahydrofuran was distilled from sodium/benzophenone under inert conditions.³³ All other solvents were used as received without further purification. Isomannide, isosorbide, Grubbs catalysts, sodium hydride and deuterated chloroform were purchased from Sigma Aldrich and used without further purification. Allyl bromide was purchased from Spectrochem Pvt. Ltd. and used without further purification. Benzoquinone was purchased from Alfa Aesar and used without further purification. NMR spectra were recorded on Bruker Avance 200, 400, 500 instruments. Chemical shifts are referenced to external reference TMS (¹H and ¹³C). Mass spectra were recorded on ThermoScientific Q-Exactive (the column specification is Hypersil gold C18 column 50 x 2.1 mm diameter 1.9 μm particle size mobile phase used is 90% methanol + 10 % water + 0.1 % formic acid) instrument. GPC measurement was carried out on a Thermo Quest (TQ) GPC at 25 °C using chloroform (Merck, Lichrosolv) as the mobile phase. The analysis was carried out at a flow rate 1 mL/min using a set of five μ-styragel HT columns (HT-2 to HT-6) and a refractive index (RI) detector. This column set enabled the determination of wide range of molecular weight from 10² to 10⁶. Columns were calibrated with polystyrene standard and the molecular weights reported are with respect to a polystyrene standard. MALDI-ToF-MS was performed on AB SCIEX TOF/TOFTM 5800 and matrix used is dithranol.

5.4.2. Synthesis of Isomannide-di(ether-ene) 6a:



0.98 g (41.04 mmol) of sodium hydride was suspended in 30 ml dry tetrahydrofuran. A THF solution of isomannide (2 g, 13.68 mmol in 20 mL THF) was slowly added to the sodium hydride suspension over a period of 3 hours. To this mixture was added allyl bromide (3.55 mL, 41.04 mmol) over a period of 2 hours and the resultant reaction mixture was stirred for next 13 hours. Excess allyl bromide (24.85 ml, 287.28 mmol) was added to the above reaction mixture and the content was stirred for next 50 hours. The reaction was quenched with distilled water and the

organic phase was washed with saturated sodium chloride solution. The aqueous phase was extracted with the ethyl acetate (3×20 mL). Combined organic phase was dried over MgSO_4 , filtered and the filtrate was evaporated in vacuum to obtain pale yellow oily material. Purification by column chromatography (pet ether: ethyl acetate, 90:10) yielded 1.89 g (62%) of colorless oily isomannide di(ether-ene) **6a**.

$^1\text{H NMR}$ (200 MHz, CDCl_3 , 298 K) δ = 5.88-5.69 (m, 2H_B), 5.21-5.02 (m, 4H_A), 4.41-4.38 (m, 2H_E), 4.07-3.85 (m, $8\text{H}_{\text{C}+\text{F}+\text{D}}$), 3.61-3.49 (m, 2H_D). $^{13}\text{C NMR}$ (50 MHz, CDCl_3 , 298 K) δ = 134.9 (s, C_B), 117.9 (s, C_A), 80.8 (s, C_E), 80.0 (s, C_F), 71.9 (s, C_C), 71.4 (s, C_D). **ESI-MS** (+ve mode) m/z = 227.12 $[\text{M}+\text{H}]^+$ and 249.11 $[\text{M}+\text{Na}]^+$.

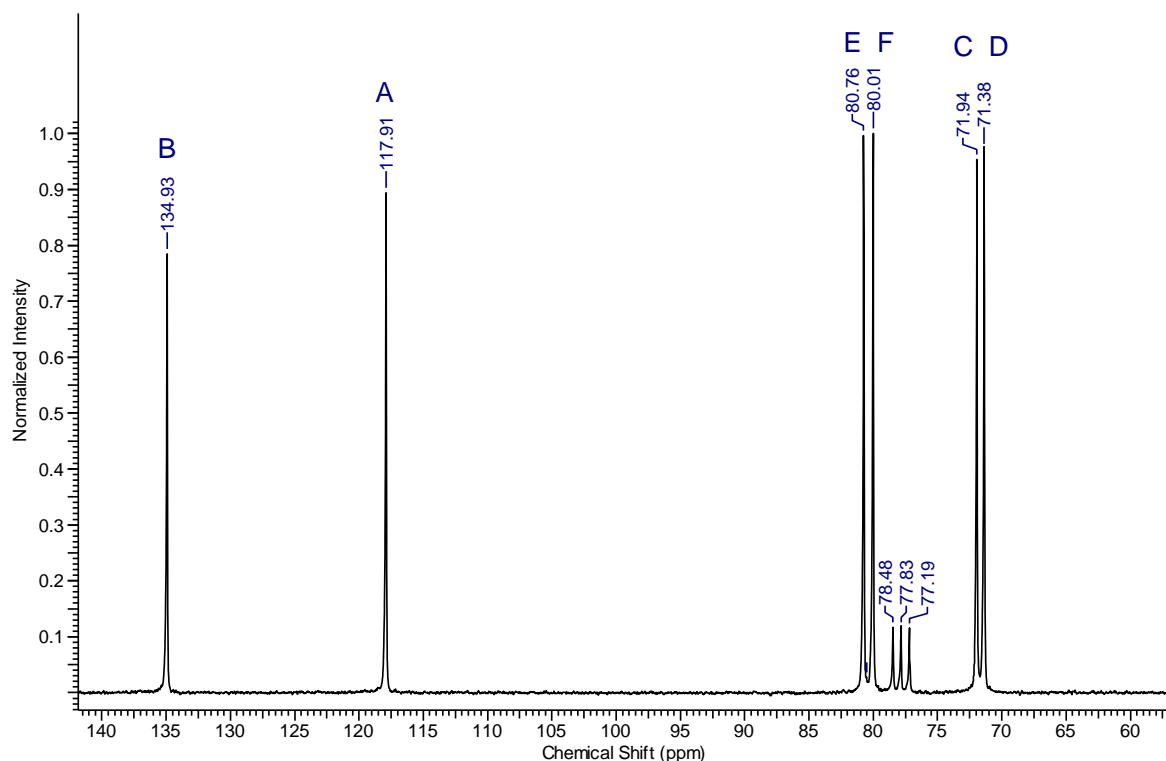


Figure 5.4. $^{13}\text{C NMR}$ spectrum of compound **6a** in CDCl_3 (50 MHz at 298 K).

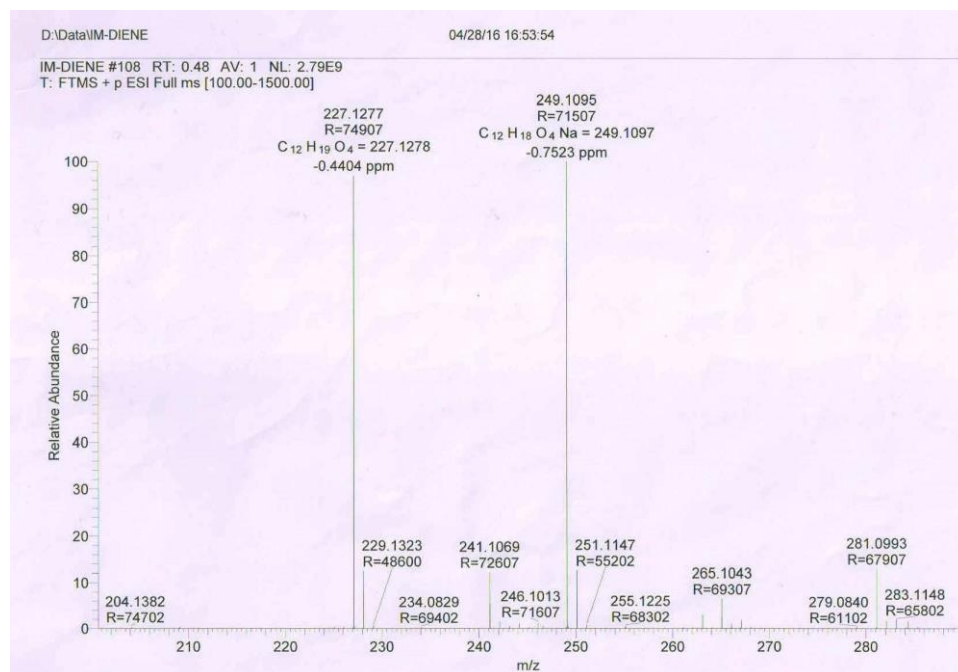
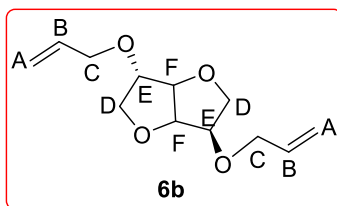


Figure 5.5. ESI-MS (+ve mode) spectrum of compound **6a** ($C_{12}H_{18}O_4$), $m/z = 227.12$

$[M+H]^+$, 249.10 $[M+Na]^+$.

5.4.3. Synthesis of Isosorbide-di(ether-ene) **6b**:



2.46 g (102.63 mmol) of sodium hydride was suspended in 30 ml dry tetrahydrofuran. A THF solution of isosorbide (5 g, 34.21 mmol in 40 mL THF) was slowly added to the sodium hydride suspension over a period of 3 hours. To this mixture was added allyl bromide (6.51 mL, 75.26 mmol) over a period of 2 hours and the resultant reaction mixture was stirred for next 16 hours. To achieve full conversion, excess allyl bromide (6.51 ml, 75.26 mmol) was added and the reaction mixture was stirred for next 45 hours. The reaction was quenched with distilled water and the organic phase was washed with saturated sodium chloride solution. The aqueous phase was extracted with ethyl acetate (3×30 mL). Combined organic phase was dried over $MgSO_4$, filtered and filtrate was evaporated in vacuum to obtain pale yellow oily material. Purification by column chromatography (pet ether: ethyl acetate, 94:06) yielded 4.71 g (61%) of colorless oily isosorbide di(ether-ene) **6b**.

$^1\text{H NMR}$ (200 MHz, CDCl_3 , 298 K) $\delta = 6.01\text{-}5.85$ (m, 2H_B), $5.35\text{-}5.16$ (m, 4H_A), $4.65\text{-}4.52$ (m, 2H_E), $4.25\text{-}3.89$ (m, $8\text{H}_\text{F+C+D}$), $3.63\text{-}3.55$ (m, 2H_D). $^{13}\text{C NMR}$ (100 MHz, CDCl_3 , 298 K) $\delta = 134.3\text{-}134.0$ (s, C_B), $117.2\text{-}116.9$ (s, C_A), 85.9 (s, C_E), 83.5 (s, C_F), 79.9 (s, C_E), 79.2 (s, C_F), $73.1\text{-}71.2$ (s, C_C), $70.3\text{-}69.5$ (s, C_D). **ESI-MS** (+ve mode) $m/z = 227.12$ $[\text{M}+\text{H}]^+$ and 249.11 $[\text{M}+\text{Na}]^+$.

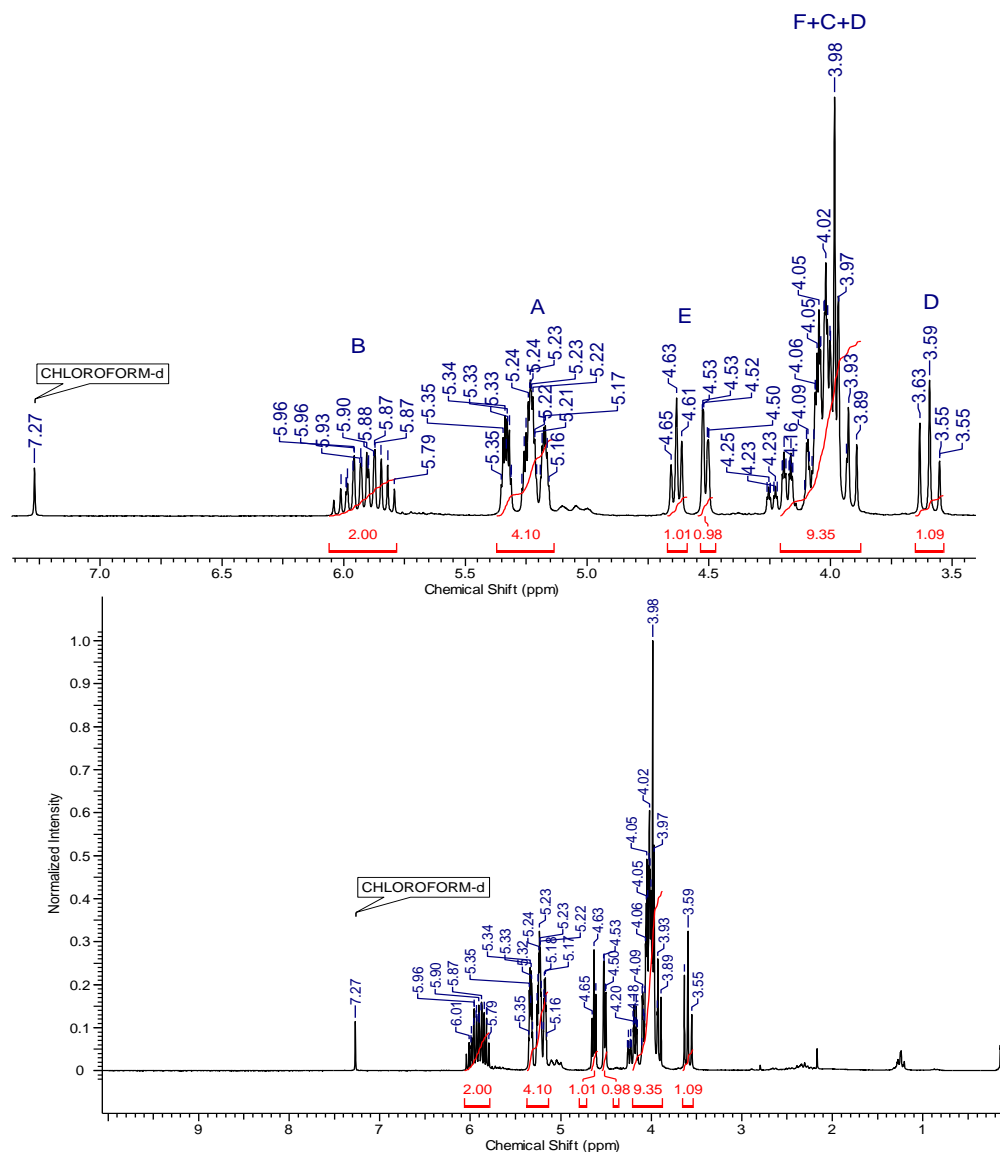


Figure 5.6. $^1\text{H NMR}$ spectrum of compound **6b** in CDCl_3 (bottom) and expanded view (top) (200 MHz at 298 K).

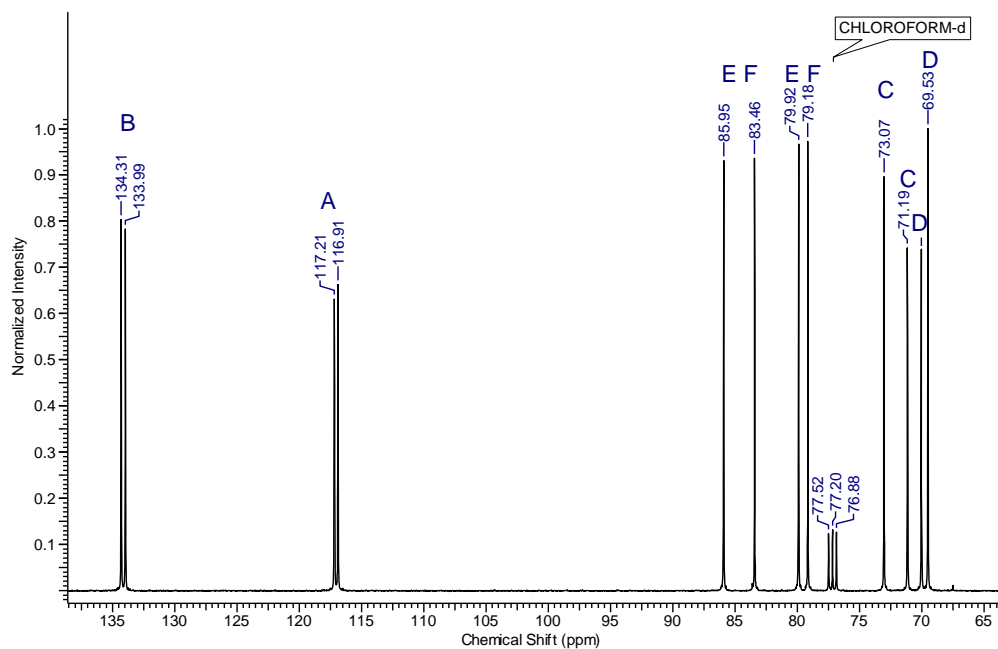


Figure 5.7. ^{13}C NMR spectrum of compound **6b** in CDCl_3 (100 MHz at 298 K).

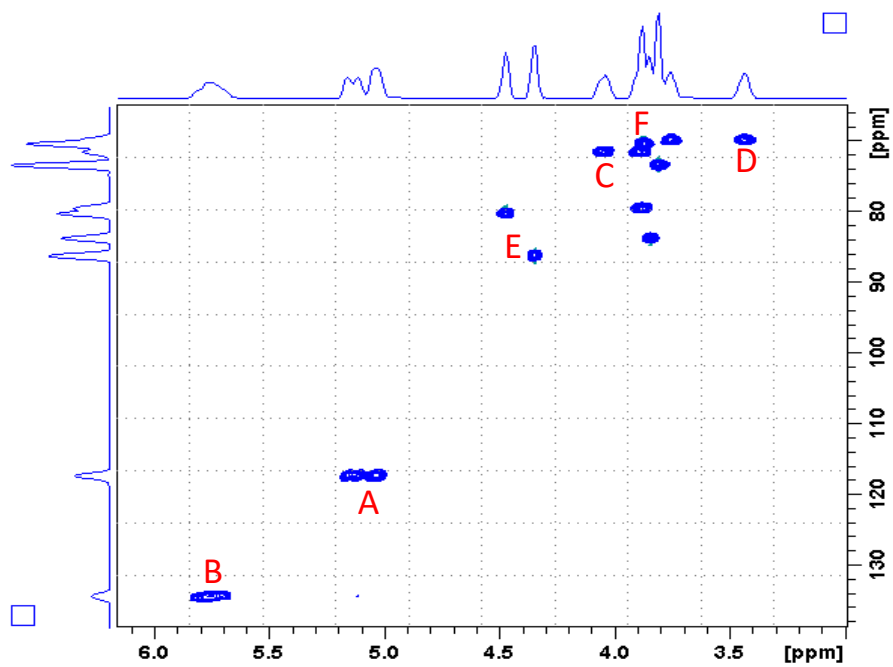


Figure 5.8. A direct C-H correlation (HSQC) spectrum of **6b** in CDCl_3 at room temperature (400 MHz at 298 K).

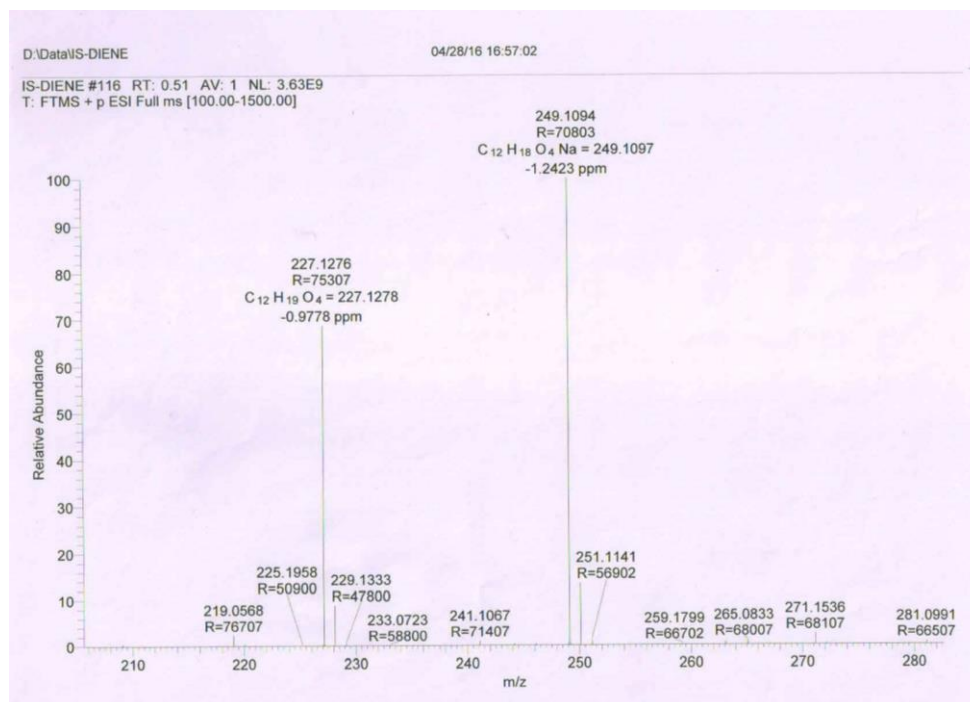
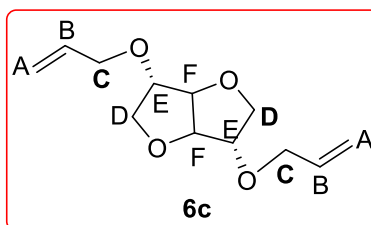


Figure 5.9. ESI-MS (+ve) mode spectrum of compound **6b** ($C_{12}H_{18}O_4$), $m/z = 227.12$

$[M+H]^+$, 249.10 $[M+Na]^+$.

5.4.4. Synthesis of Isoidide-di(ether-ene) **6c**:



0.66 g (27.73 mmol) of sodium hydride was suspended in 30 ml dry tetrahydrofuran. A THF solution of isoidide (1.35 g, 9.24 mmol in 20 mL THF) was slowly added to the sodium hydride suspension over a period of 3 hours. To this mixture was added allyl bromide (3.0 mL, 34.68 mmol) over a period of 2 hours and the resultant reaction mixture was stirred for next 20 hours. To achieve full conversion, excess allyl bromide (6 mL, 69.36 mmol) was added and the reaction mixture was stirred for next 16 hours. The reaction was quenched with distilled water and the organic phase was washed with saturated sodium chloride solution. The aqueous phase was extracted with ethyl acetate (3×20 mL). Combined organic phase was dried over $MgSO_4$, filtered and the filtrate was evaporated in vacuum to obtain pale yellow oily material. Purification by

column chromatography (pet ether: ethyl acetate, 70:30) yielded 1.39 (67%) of colorless oily isoidide di(ether-ene) **6c**.

$^1\text{H NMR}$ (200 MHz, CDCl_3 , 298 K) $\delta = 5.96\text{--}5.76$ (m, 2H_B), $5.31\text{--}5.13$ (m, 4H_A), 4.58 (s, 2H_E), $4.04\text{--}3.96$ (m, $6\text{H}_{\text{F+C}}$), $3.87\text{--}3.75$ (m, 4H_D). $^{13}\text{C NMR}$ (50 MHz, CDCl_3 , 298 K) $\delta = 134.2$ (s, C_B), 117.4 (s, C_A), 85.4 (s, C_E), 82.9 (s, C_F), 72.2 (s, C_C), 70.5 (s, C_D). **ESI-MS** (+ve mode) $m/z = 249.11$ $[\text{M}+\text{Na}]^+$.

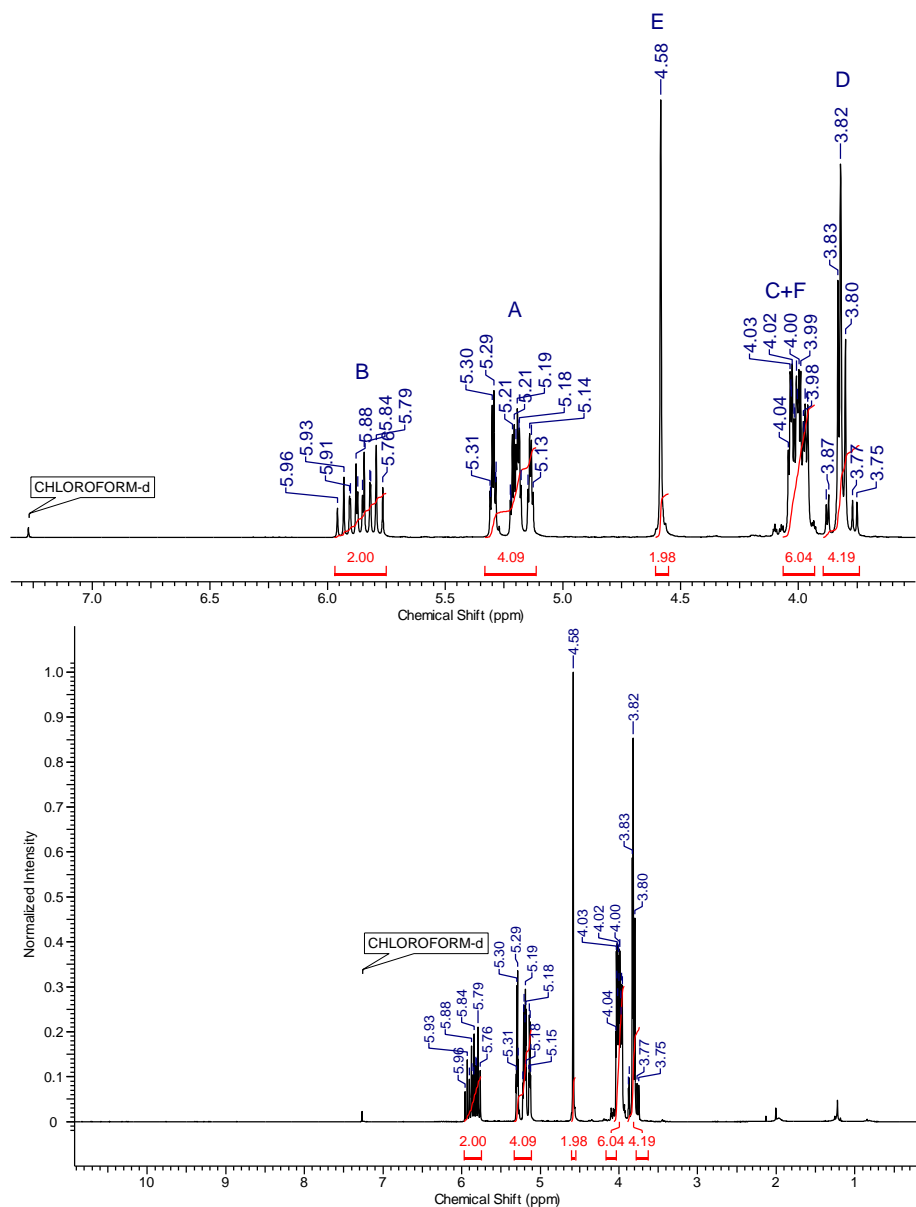


Figure 5.10. $^1\text{H NMR}$ spectrum of compound **6c** in CDCl_3 (bottom) and expanded view (top) (200 MHz at 298 K).

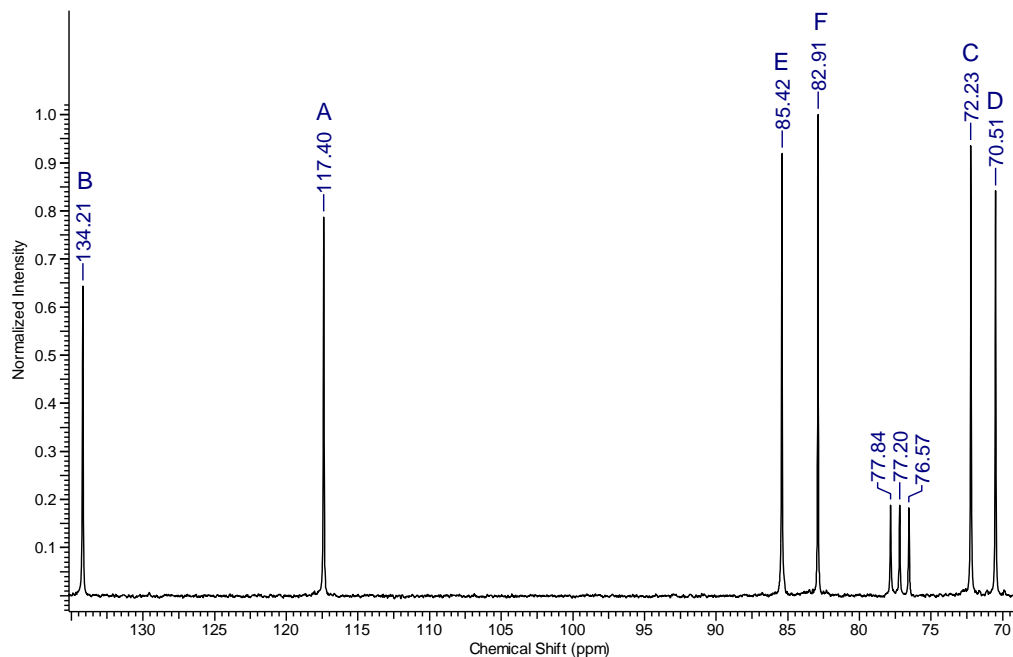


Figure 5.11. ^{13}C NMR spectrum of compound **6c** in CDCl_3 (50 MHz at 298 K).

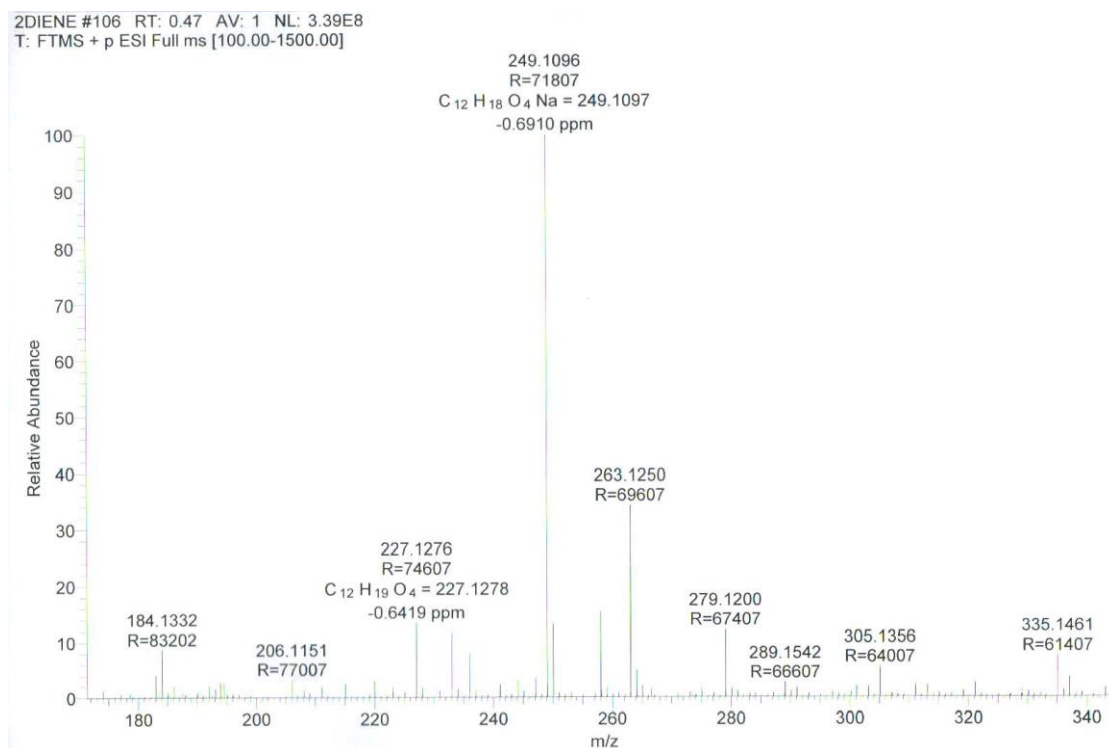


Figure 5.12. ESI-MS (+ve mode) spectrum of compound **6c** ($\text{C}_{12}\text{H}_{18}\text{O}_4$), $m/z = 249.10$ $[\text{M}+\text{Na}]^+$.

5.4.5. ADMET Polymerization of Isomannide-di(ether-ene) to P27a-1-P27a-2:

In a 10 ml Schlenk tube, 0.447 g (1.97 mmol) of isomannide-di(ether-ene) was accurately weighed and the Schlenk was evacuated for one hour at room temperature to remove traces of moisture etc. To this was added 1 mol% (0.016 g, 1.97×10^{-5} mol) of Grubbs 1st generation catalyst under positive argon flow. Polymerization was started at 60 °C and over a period of 1 hour the temperature was increased to 100 °C with the slight vacuum after every 3-5 min. to remove the by-product (ethylene). The polymerization was continued for 1 hour at 100 °C with a slight vacuum. Finally, the polymerization was continued for next 10 hours at 100 °C under constant vacuum to obtain viscous material. The polymerization was quenched with ethyl vinyl ether and the residue was dissolved in chloroform and precipitation was attempted from ice-cold methanol. However, no precipitation was observed and a clear solution was obtained. The solvent was evaporated using rotary evaporator to get viscous material (0.29 gm, 74.3 %). A similar protocol was followed for the Grubbs-II generation catalyst except the polymerization time (which was 8 hours).

P27a-1

¹H NMR (200 MHz, CDCl₃, 298 K) δ = 6.26-5.69 (m, vinyl 12H_B), 5.26-5.09 (m, 4H_A), 4.91-4.75 (m, 4H_E), 4.54-4.39 (m, 18H_{E+C}), 4.27-3.79 (m, 45H_{C+F+D}), 3.68-3.32 (m, 16H_D). **¹³C NMR** (125 MHz, CDCl₃, 298 K) δ = 144.7-143.7 (s, vinyl gr. IM-O-CH=CH-CH₃), 134.0 (s, C_B), 117.0 (s, C_A), 102.1-100.4 (s, vinyl gr. IM-O-CH=CH-CH₃), 80.6-79.7 (s, C_E), 79.2-76.7 (s, C_F), 71.1-71.0 (s, C_C), 70.6-69.8 (s, C_D), 11.9 (s, vinyl gr. IM-O-CH=CH-CH₃).

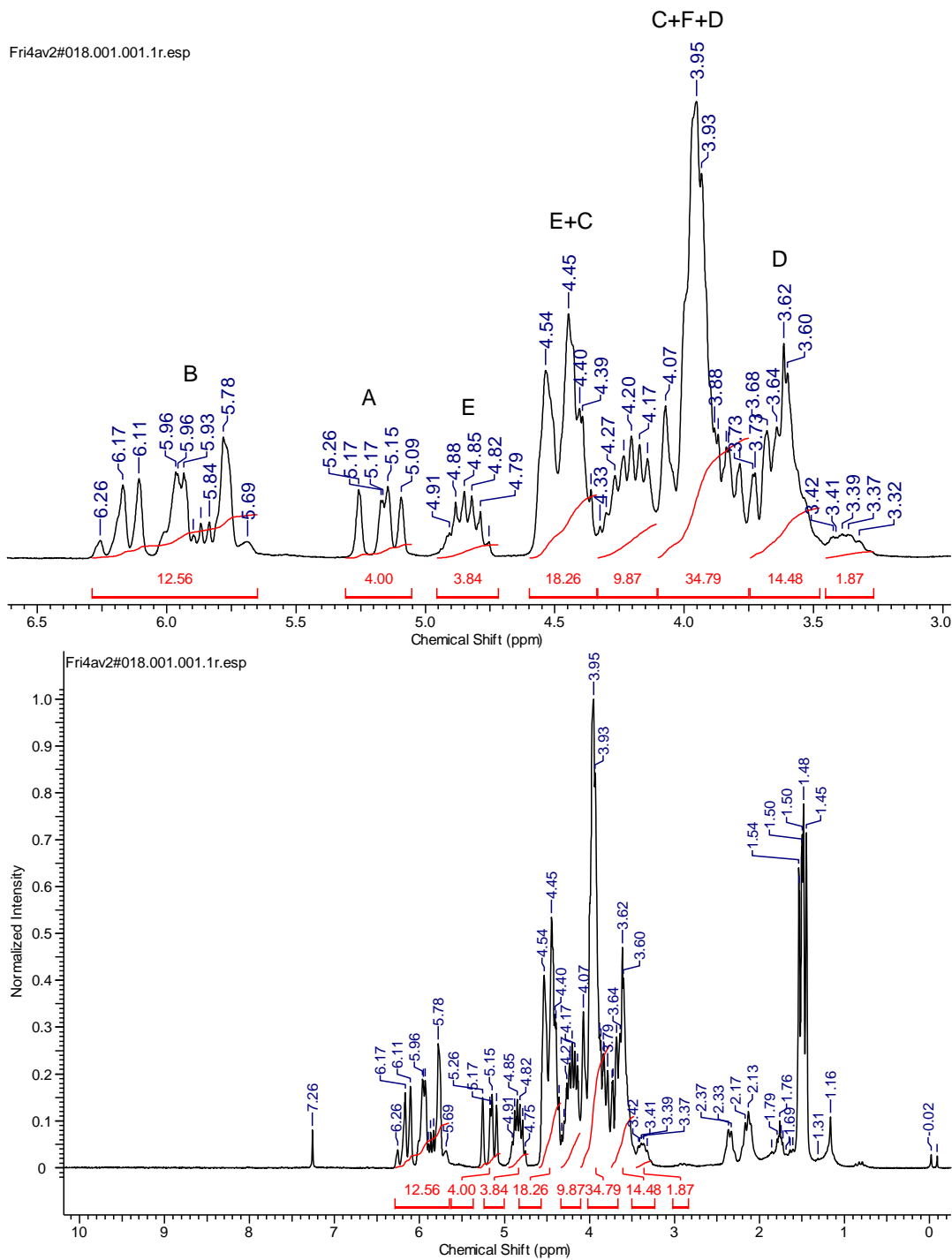


Figure 5.13. ¹H NMR spectrum of compound **P27a-1** (with **G-I**) in CDCl₃ (bottom) and zoomed-in spectrum (top) (200 MHz at 298 K).

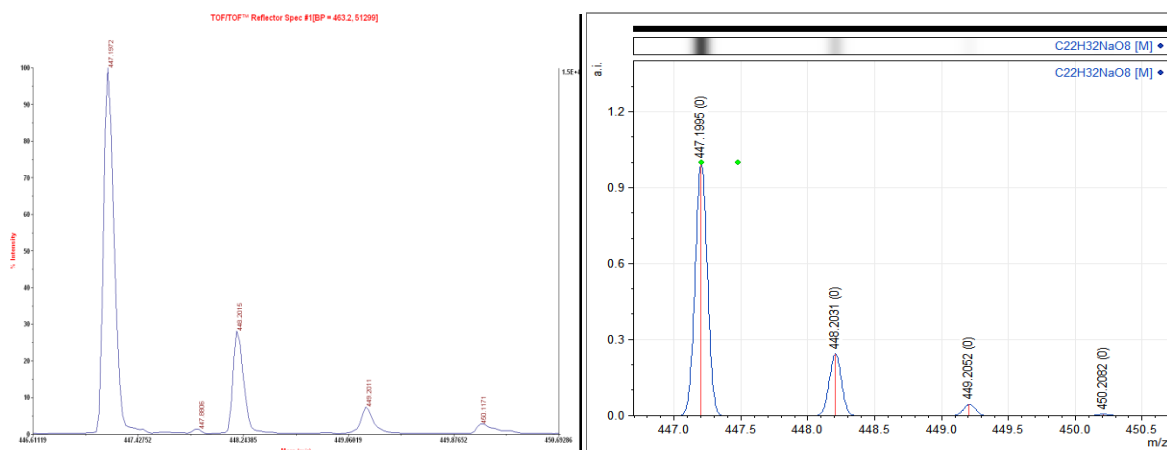


Figure 5.16. Expanded view of figure 5.15 **P27a-1 (G-I)** (left) and their simulated spectra (right) for comparison.

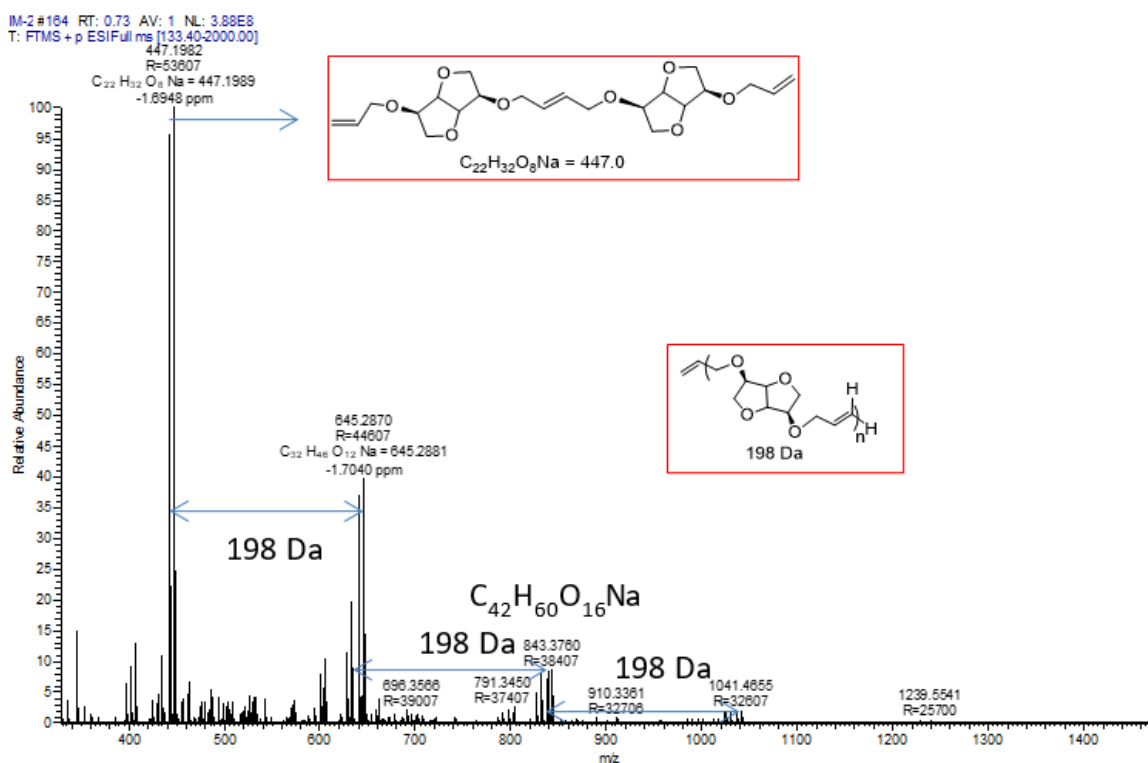


Figure 5.17. ESI-MS (+ve mode) spectrum of **P27a-1(G-I)** $[M+Na]^+$ shows the 198 Da difference.

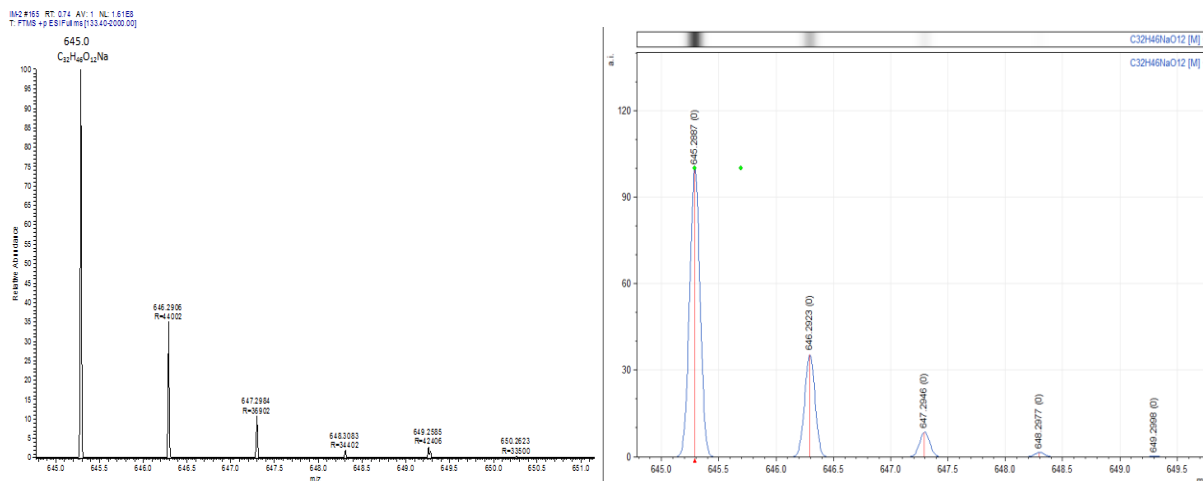


Figure 5.18. Expanded view of figure 5.17 **P27a-1(G-I)** (left) and their simulated spectra (right) for comparison.

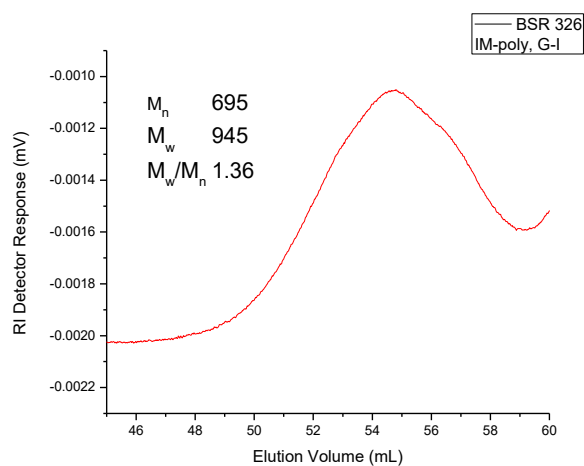


Figure 5.19. GPC chromatogram of **P2a-1(G-I)** in chloroform at room temperature.

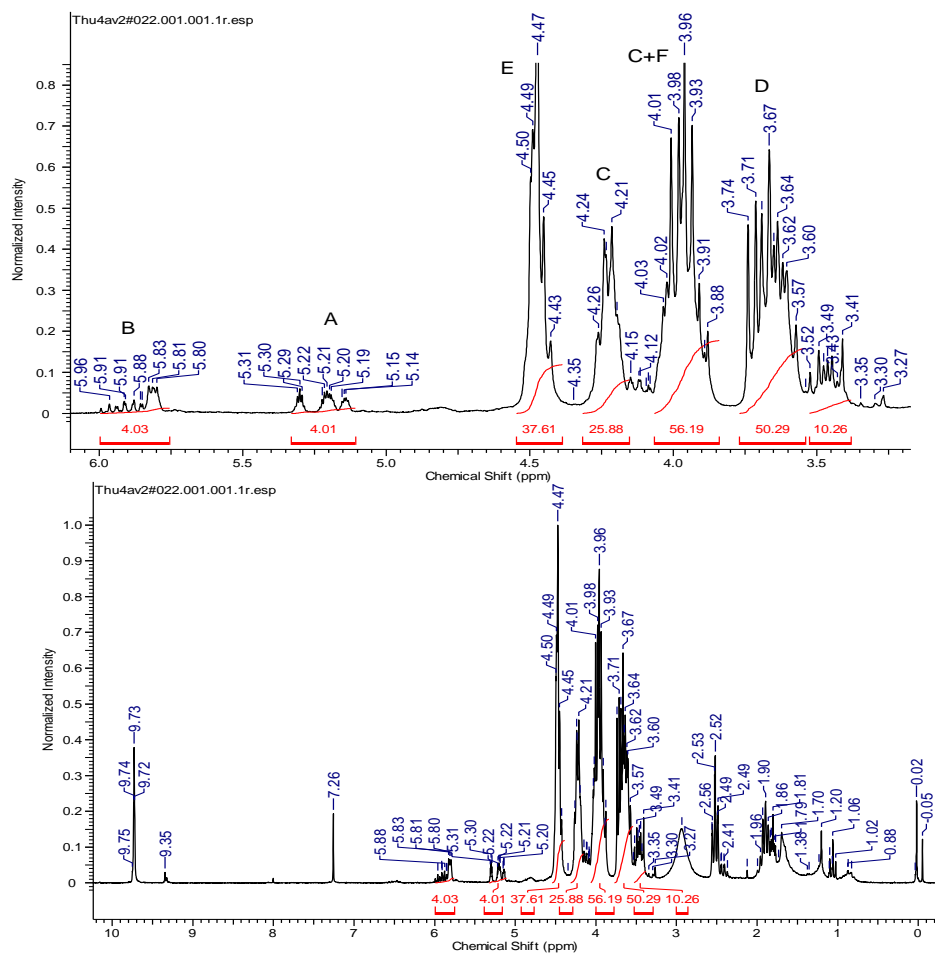


Figure 5.20. ¹H NMR spectrum of compound **P27a-2** (with **G-II**) in CDCl₃ (bottom) and expanded view (top) (200 MHz at 298 K).

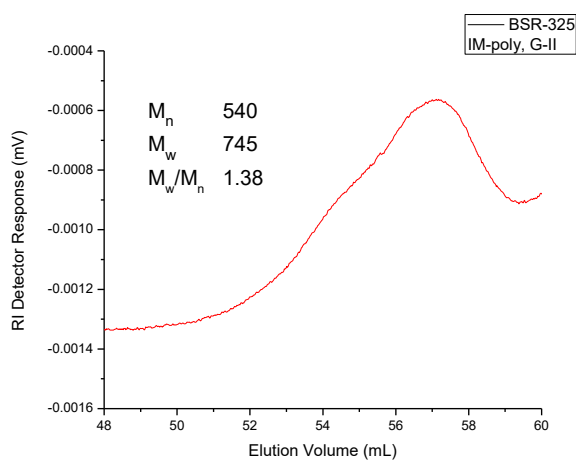


Figure 5.21. GPC chromatogram of **P27a-2** (**G-II**) in chloroform at room temperature.

5.4.6. ADMET Polymerization of Isosorbide-di(ether-ene) to P27b-1-P27b-2:

Method A:

In a 10 ml Schlenk tube 0.447 g (1.97 mmol) of isosorbide-di(ether-ene) was accurately weighed and the Schlenk was evacuated for one hour at room temperature to remove traces of moisture. To this was added 1 mol% (0.016 g, 1.97×10^{-5} mol) Grubbs 1st generation catalyst under positive argon flow. Polymerization was started at 60 °C and kept over a period of 2 hours with slight vacuum in every 3-5 min. to remove the by-product (ethylene). Polymerization was continued for another 3 hours at 70 °C with a slight vacuum. Finally, the polymerization was continued for next 3 hours at 90 °C under constant vacuum to get the viscous material. The residue was quenched with ethyl vinyl ether and dissolved in chloroform and precipitation from ice-cold methanol was attempted. However, a clear solution was observed after the addition of methanol. The solvent was evaporated on rotary evaporator to get the viscous material (0.38 gm, 97.0 %). A similar protocol was followed for Grubbs 2nd generation catalyst, except that the temperature was maintained at 100 °C.

Method B:

In a 10 ml Schlenk tube 0.447 g (1.97 mmol) of isosorbide-di(ether-ene) was accurately weighed and the Schlenk was evacuated for one hour at room temperature to remove traces of moisture. To this was added 2 mol% (0.004 g, 3.94×10^{-5} mol) of benzoquinone and 1 mol% (0.016 g, 1.97×10^{-5} mol) Grubbs 1st generation catalyst under positive argon flow. Polymerization was started at 60 °C and kept over a period of 2 hours with slight vacuum in every 3-5 min. to remove the by-product (ethylene). Polymerization was continued for another 3 hours at 70 °C with a slight vacuum. Finally, the polymerization was continued for next 3 hours at 90 °C under constant vacuum to get the viscous material. The residue was quenched with ethyl vinyl ether and dissolved in chloroform and precipitation from ice-cold methanol was attempted. However, a clear solution was observed after the addition of methanol. The solvent was evaporated on rotary evaporator to get viscous material (0.38 gm, 97.0 %).

Method C:

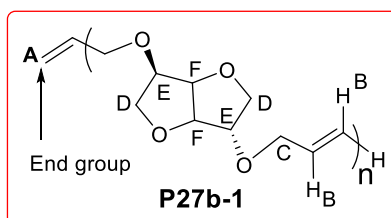
In a 10 ml Schlenk tube, 0.447 g (1.97 mmol) of isosorbide-di(ether-ene) was accurately weighed, and the Schlenk was evacuated for one hour at room temperature to remove traces of moisture. To this was added 1 mol% (0.016 g, 1.97×10^{-5} mol) Grubbs 1st generation catalyst under positive argon flow. Polymerization was started at 60 °C and kept over a period of 2 hours

with slight vacuum every 3-5 min. to remove the by-product (ethylene). Polymerization was continued for another 2 hours at 70 °C with a slight vacuum. To this was added second batch of 1 mol% (0.016 g, 1.97×10^{-5} mol) Grubbs 1st generation catalyst under positive argon flow. Then the polymerization was run for 1 hour with slight vacuum and finally, the polymerization was continued for next 3 hours at 90 °C under constant vacuum to get the viscous material. The residue was quenched with ethyl vinyl ether and dissolved in chloroform and precipitation from ice-cold methanol was attempted. However, a clear solution was observed after the addition of methanol. The solvent was evaporated on rotary evaporator to get the viscous material (0.33 gm, 84.0 %).

Method D:

In a 10 ml Schlenk tube 0.447 g (1.97 mmol) of isosorbide-di(ether-ene) was accurately weighed and the Schlenk was evacuated for one hour at room temperature to remove traces of moisture. To this was added 2 mol% (0.004 g, 3.94×10^{-5} mol) of benzoquinone and 1 mol% (0.016 g, 1.97×10^{-5} mol) Grubbs 1st generation catalyst under positive argon flow. Polymerization was started at 60 °C and kept over a period of 2 hours with slight vacuum in every 3-5 min. to remove the by-product (ethylene). Polymerization was continued for another 2 hours at 70 °C with a slight vacuum. To this was added a second batch of 2 mol% (0.004 g, 3.94×10^{-5} mol) benzoquinone and 1 mol% (0.016 g, 1.97×10^{-5} mol) Grubbs 1st generation catalyst under positive argon flow. The polymerization was continued for 1 hour with slight vacuum and finally, the polymerization was continued for next 3 hours at 90 °C under constant vacuum to get the viscous material. The residue was quenched with ethyl vinyl ether and dissolved in chloroform and precipitation from ice-cold methanol was attempted. However, a turbid solution was observed after the addition of methanol. The solvent was evaporated on rotary evaporator to get the viscous material (0.37 gm, 95.0 %).

P27b-1



¹H NMR (200 MHz, CDCl₃, 298 K) δ = 6.23-5.69 (m, 22H_B), 5.32-5.14 (m, 4H_A), 4.96-4.60 (m, 19H_E), 4.53-4.10 (m, 37H_C), 4.05-3.42 (m, 78H_{F+C+D}). ¹³C NMR (125 MHz, CDCl₃, 298 K) δ = 145.0-142.9 (s, vinyl gr. IS-O-CH=CH-CH₃), 104.0-101.1 (s, vinyl gr. IS-O-CH=CH-CH₃), 86.2-

84.7 (s, C_{E,F}), 82.6-78.7(s, C_{E,F}), 73.4-73.2 (s, C_C), 70.6-69.8 (s, C_D), 12.4-12.3 (s, vinyl gr. IS-O-CH=CH-CH₃).

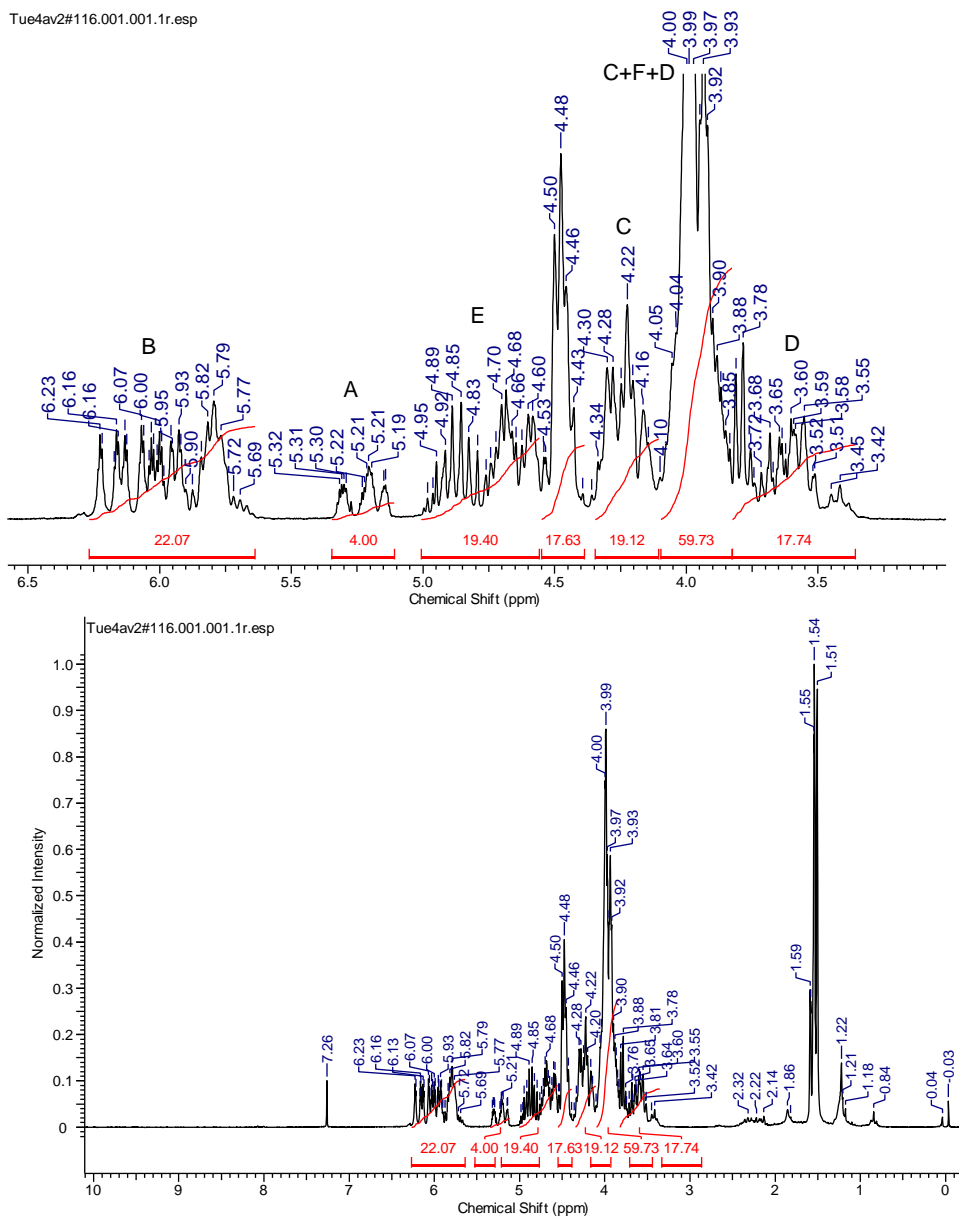


Figure 5.22. ¹H NMR spectrum of compound **P27b-1** (with **G-I**) in CDCl₃ (bottom) and expanded view (top) (125 MHz at 298 K).

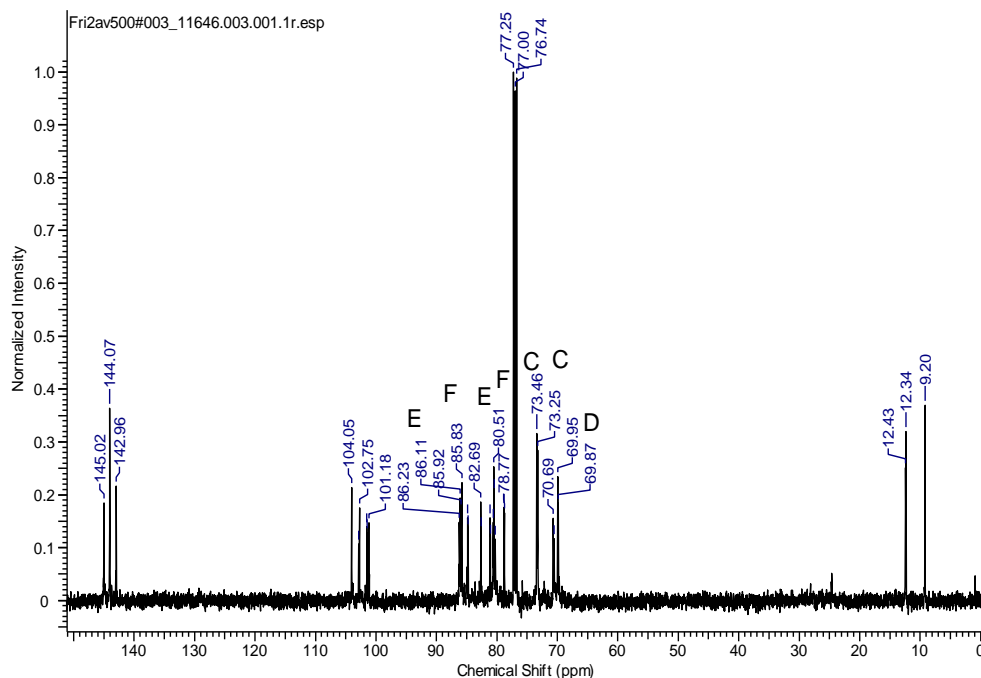


Figure 5.23. ^{13}C NMR spectrum of compound P27b-1 (with G-I) in CDCl_3 (125 MHz at 298 K).

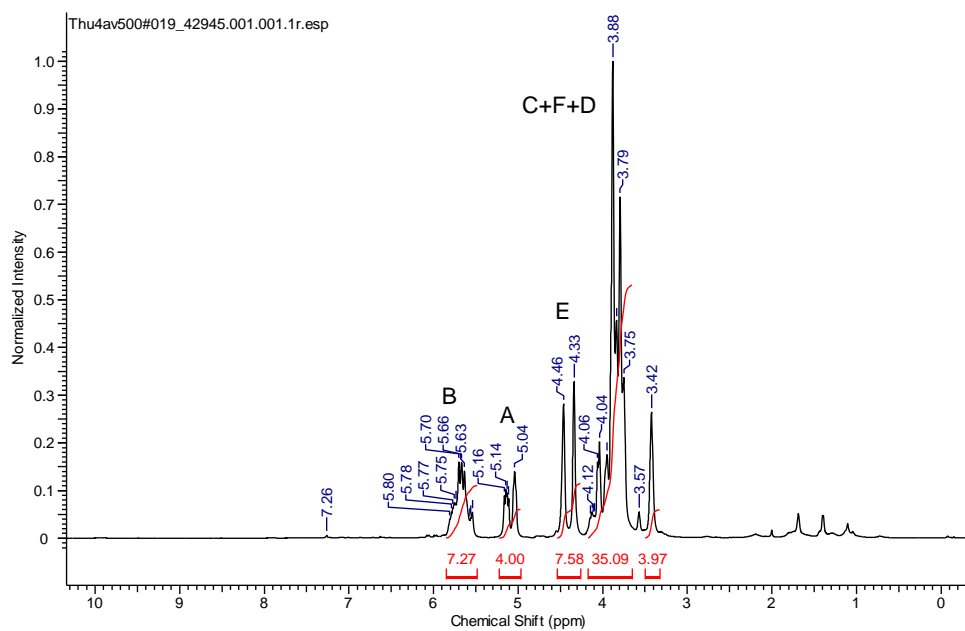


Figure 5.24: ^1H NMR spectrum of compound P27b-1 (G-I) with (2 mol% of benzoquinone) in CDCl_3 (500 MHz at 298 K).

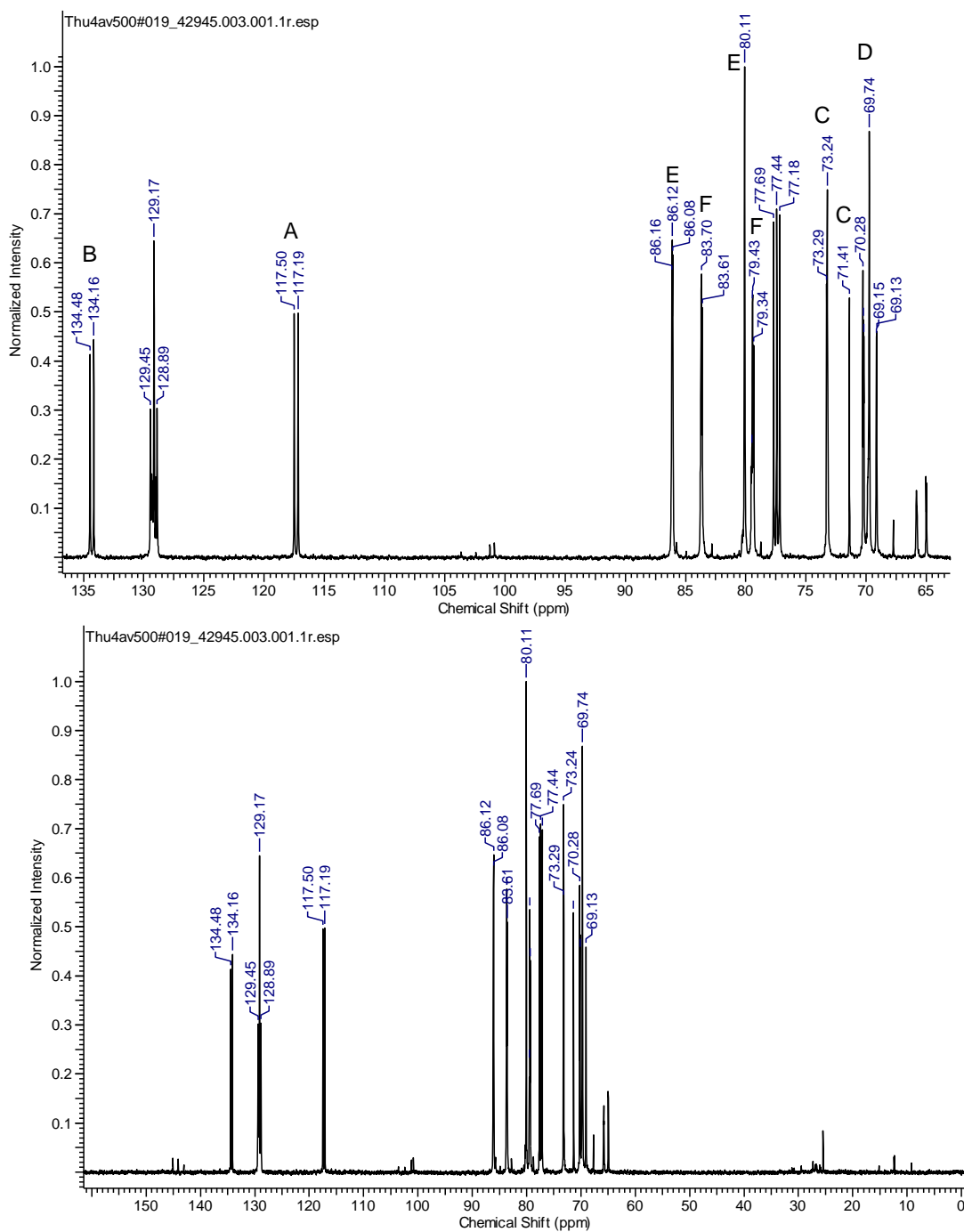


Figure 5.25. ^{13}C NMR spectrum of compound P27b-1 (G-1) with (2 mol% of benzoquinone) in CDCl_3 (bottom) and expanded view (top) (125 MHz at 298 K).

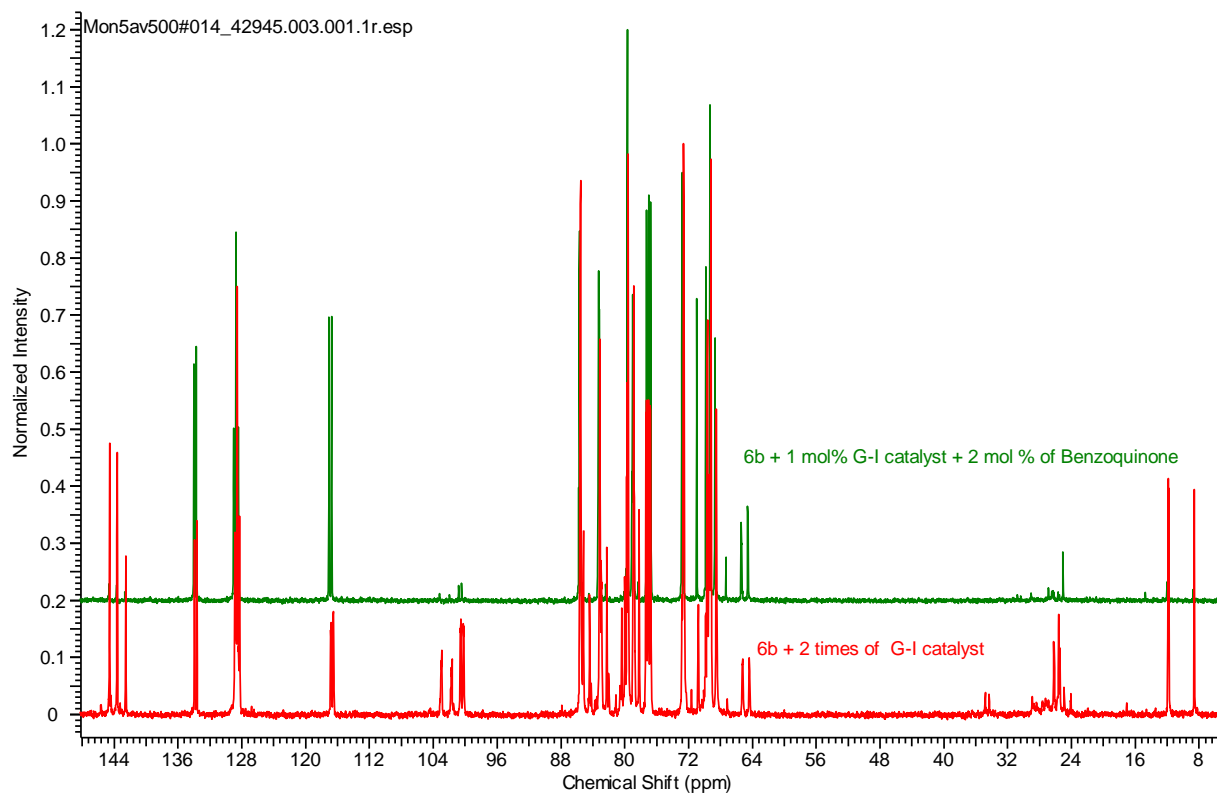


Figure 5.26. ^{13}C NMR spectrum of compound **P27b-1** showing overlay of two experiments with double amount of G-I catalyst added (bottom-red) and 2 mol % of benzoquinone added (top-green).

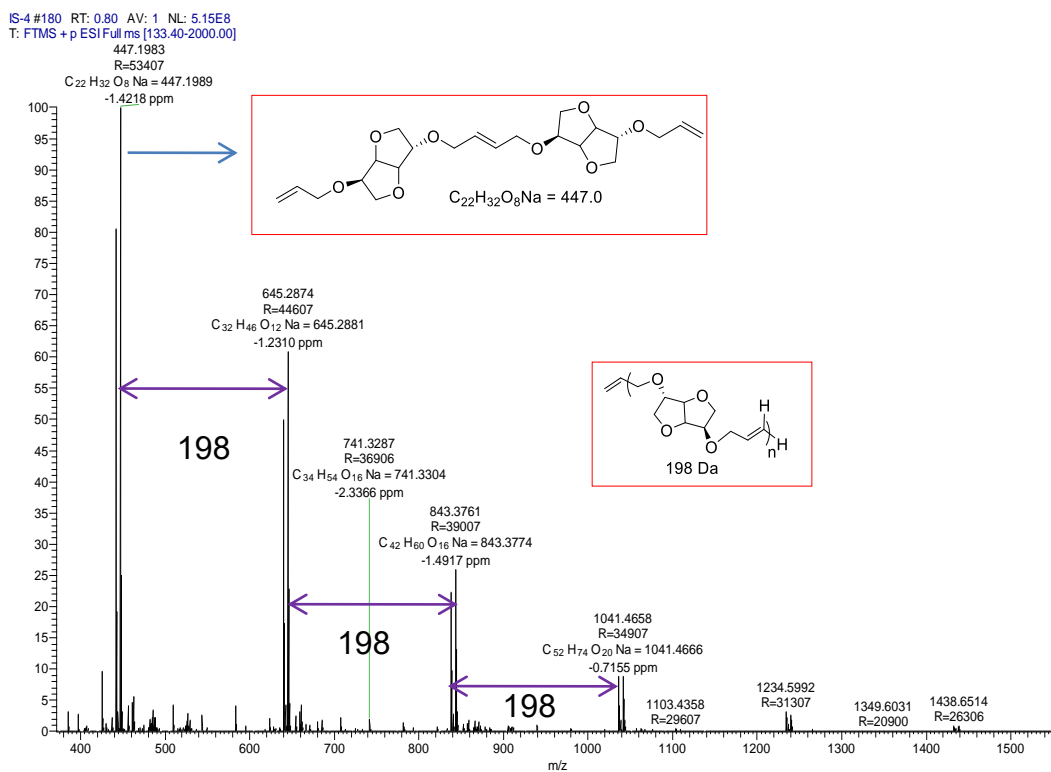


Figure 5.27. ESI-MS (+ve mode) spectrum of **P27b-1** $[M+Na]^+$ shows the 198 Da difference.

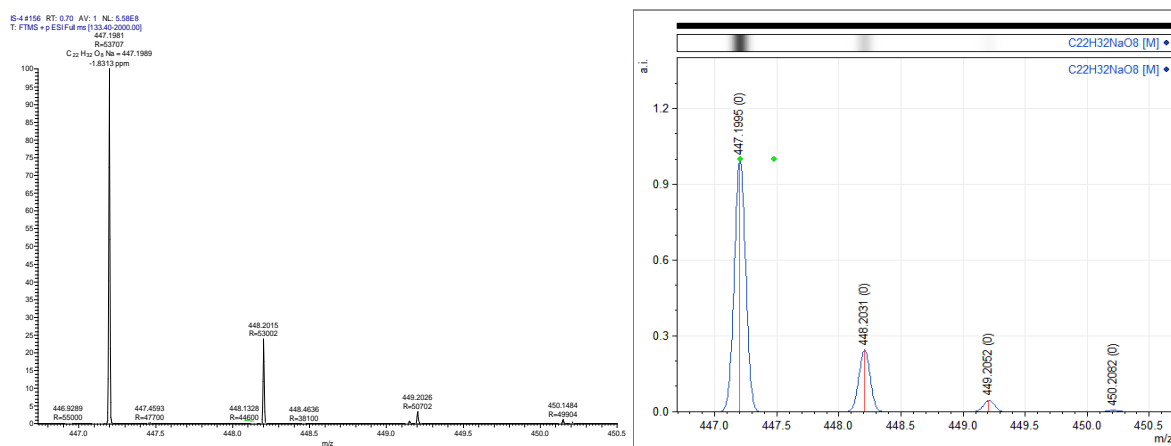


Figure 5.28. Expanded view of Figure 5.27 **P27b-1**(G-I) (left) and their simulated spectra (right) for comparison.

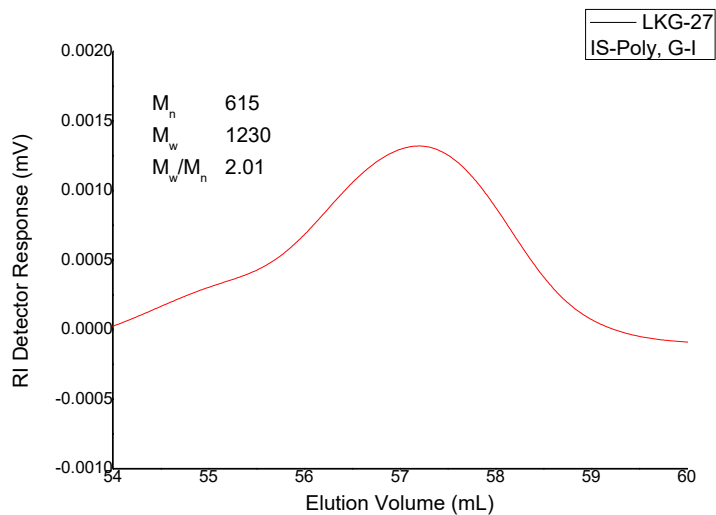


Figure 5.29. GPC chromatogram of **P27b-1 (G-I)** in chloroform at room temperature.

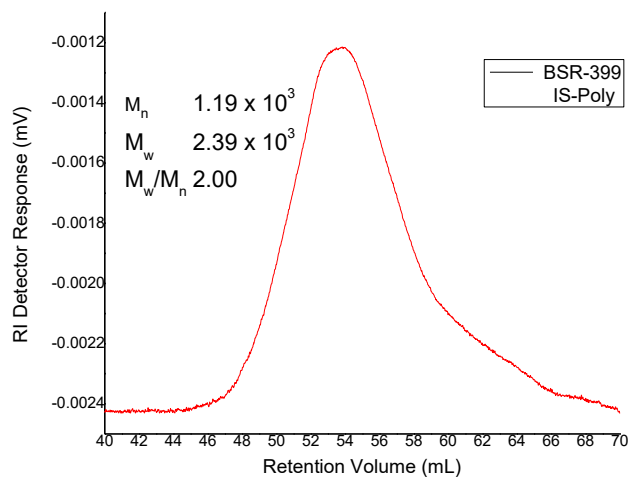


Figure 5.30. GPC chromatogram of **P27b-2(G-I)** with (2 mol% of benzoquinone) in chloroform at room temperature.

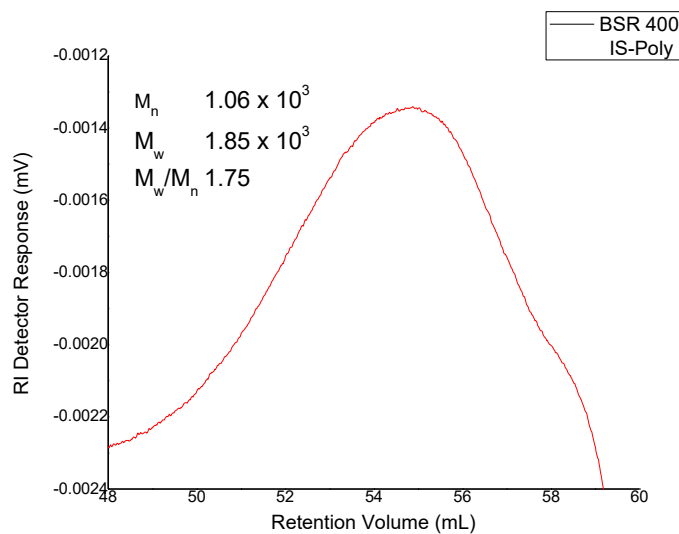


Figure 5.31. GPC chromatogram of **P27b-3(G-I)** with (two stage polymerization) in chloroform at room temperature.

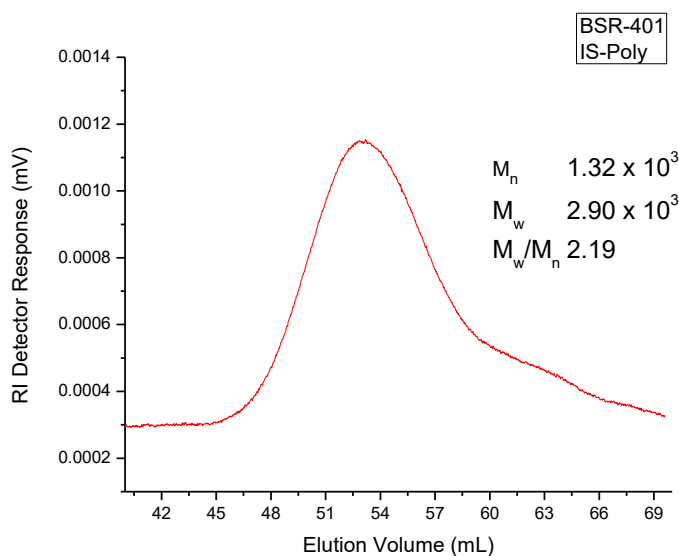


Figure 5.32. GPC chromatogram of **P27b-4 (G-I)** with (double amount of **G-I** catalyst and benzoquinone) in chloroform at room temperature.

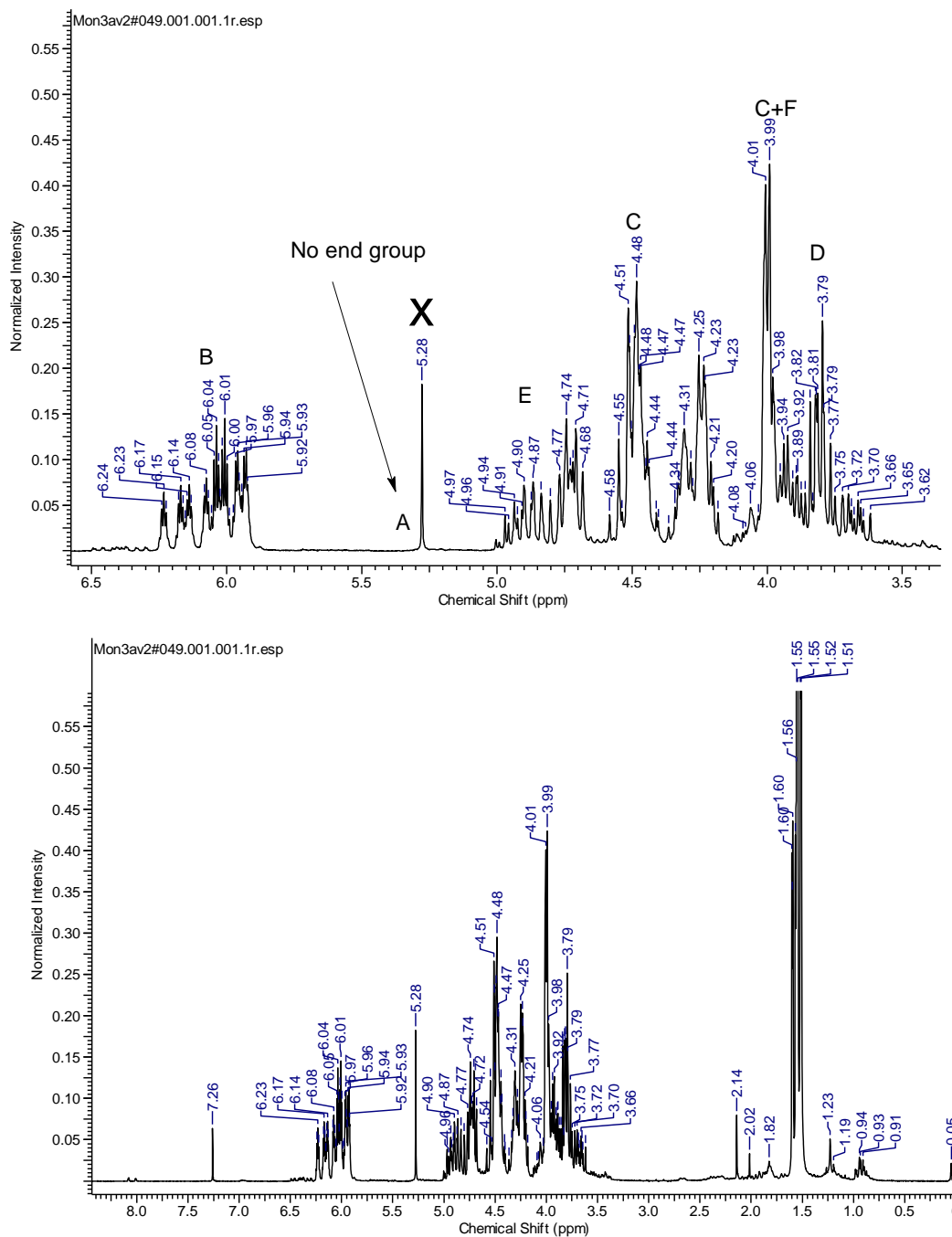


Figure 5.33. ^1H NMR spectrum of compound P27b-2 (with G-II) in CDCl_3 (bottom) and expanded view (top).

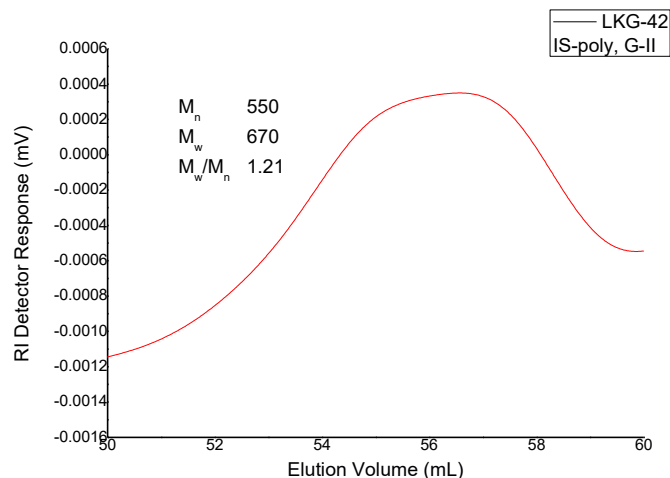
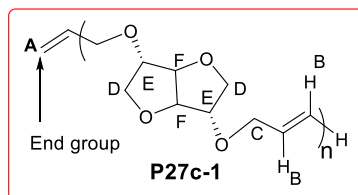


Figure 5.34. GPC chromatogram of **P27b-5 (G-II)** in chloroform at room temperature.

5.4.7. ADMET Polymerization of Isiodide-di(ether-ene) to **P27c-1-P27c-2**:

In a 10 ml Schlenk tube 0.447 g (1.97 mmol) of isiodide-di(ether-ene) was accurately weighed and the Schlenk was evacuated for one hour at room temperature to remove traces of air. To this was added 1 mol% (0.016 g, 1.97×10^{-5} mol) Grubbs 1st generation catalyst under the positive flow of argon. Polymerization was started at 60 °C and over a period of 1 hour the polymerization temperature was brought to 100 °C with slight vacuum in every 3-5 min to remove the by-product (ethylene). Finally, the polymerization was continued for next 7 hours at 100 °C under constant vacuum to obtain viscous material. The polymerization was quenched with ethyl vinyl ether and the resultant material was dissolved in chloroform. Attempts to precipitate this material from ice-cold methanol failed and a clear solution was obtained. The solvent was evaporated on rotary evaporator to get the viscous material (0.29 gm, 74.3 %). Similar polymerization protocol was followed for Grubbs-IInd generation catalyst.

P27c-1



¹H NMR (200 MHz, CDCl₃, 298 K) δ = 6.16 - 5.63 (m, 115H_B), 5.26-5.20 (m, 4H_A), 4.89-4.39 (m, 236H_E), 4.24-3.37 (m, 629H_{F+C+D}). ¹³C NMR (125 MHz, CDCl₃, 298 K) δ = 144.2-143.1 (s, vinyl gr. II-O-CH=CH-CH₃), 134.1 (s, C_B), 117.2 (s, C_A), 103.7-101.4 (s, vinyl gr. II-O-CH=CH-CH₃),

85.4-85.3 (s, C_E), 82.9-82.1 (s, C_F), 72.3-72.1 (s, C_C), 69.2, (s, C_D), 12.5 (s, vinyl gr. II-O-CH=CH-CH₃).

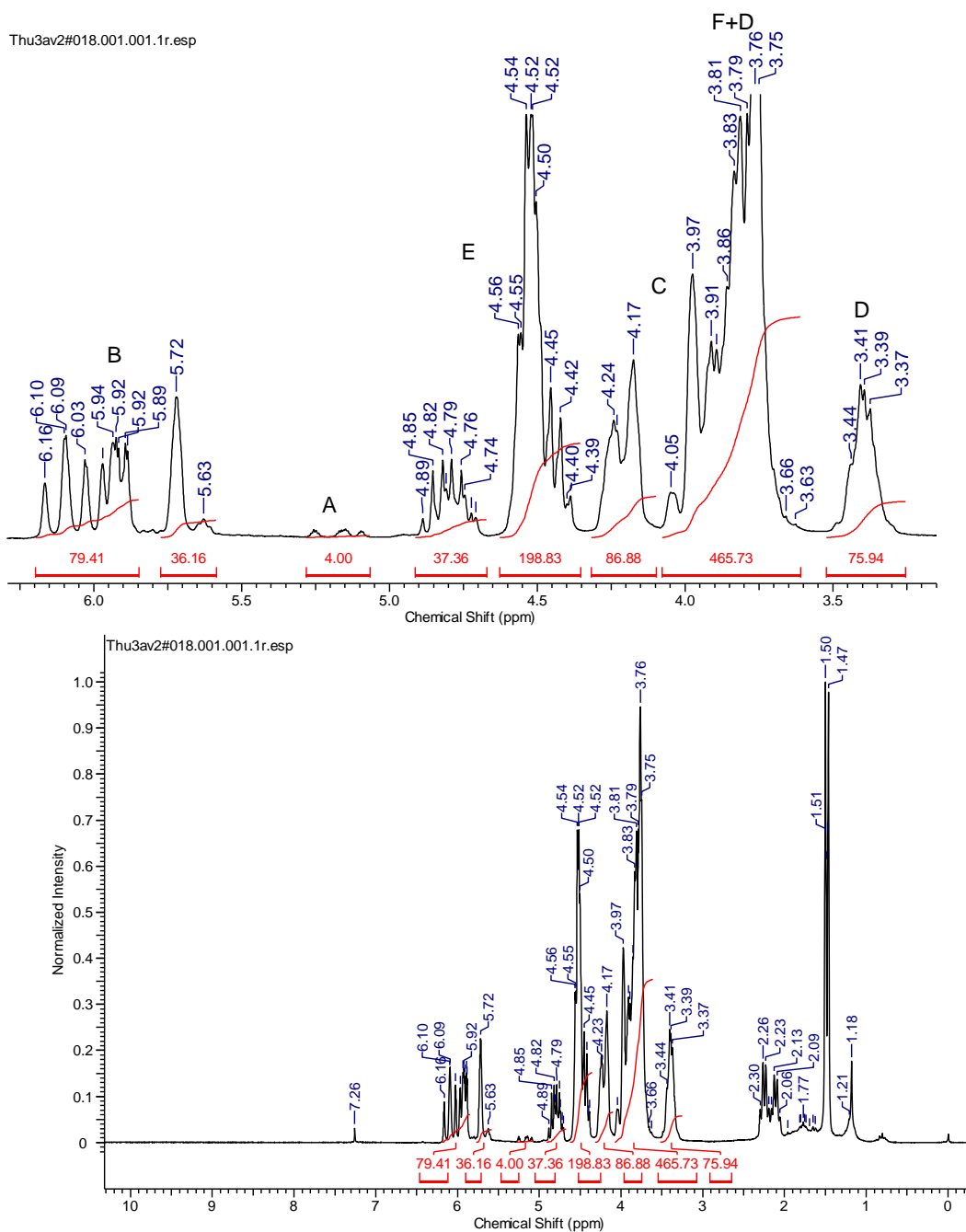


Figure 5.35. ¹H NMR spectrum of compound **P27c-1** (with G-I) in CDCl₃ (bottom) and expanded view (top) (200 MHz at 298 K).

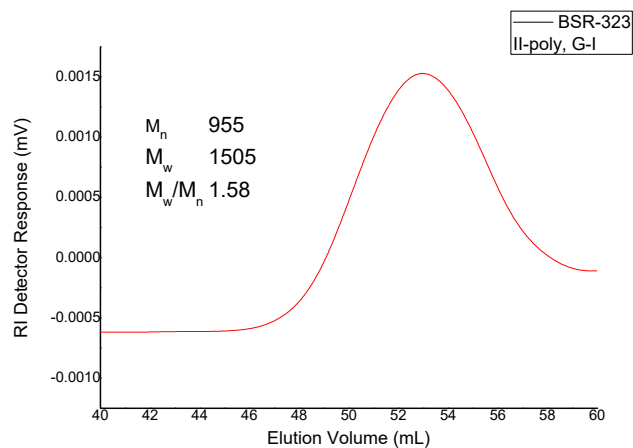


Figure 5.38. GPC chromatogram of **P27c-1(G-I)** in chloroform at room temperature.

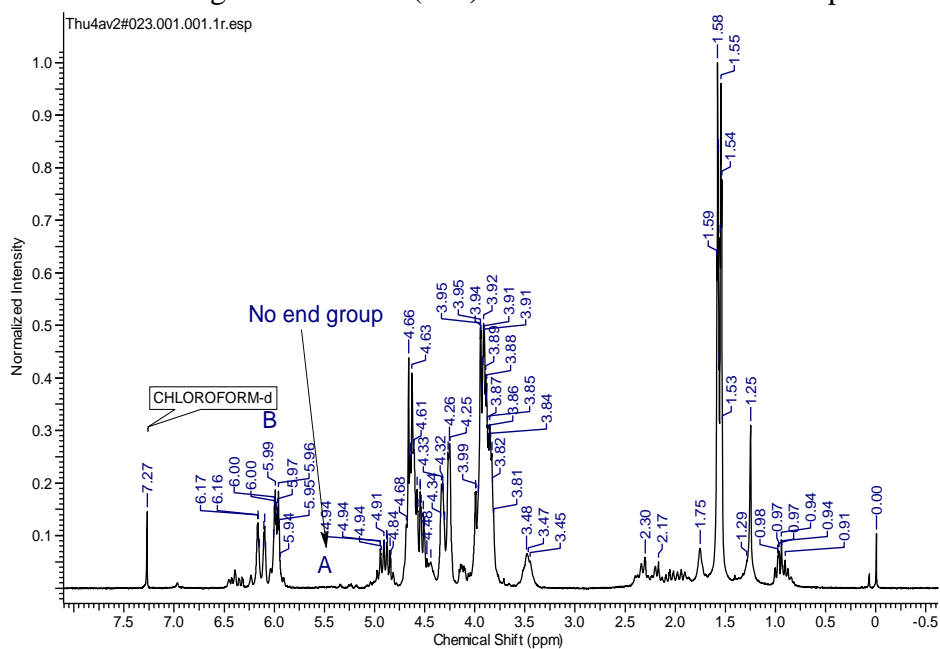


Figure 5.39. ^1H NMR spectrum of compound **P27c-2 (with G-II)** in CDCl_3 (bottom) and expanded view (top) (200 MHz at 298 K).

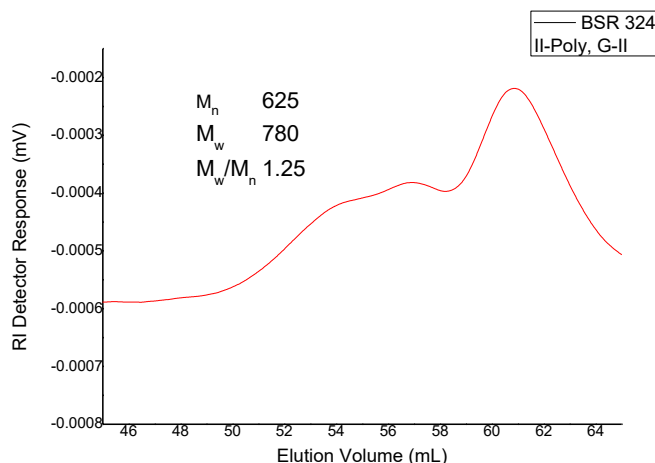


Figure 5.40. GPC chromatogram of **P27c-2(G-II)** in chloroform at room temperature.

5.5. Molecular Weight Determination by NMR Spectroscopy³⁶

ADMET polymerization experiments were performed and the exact chemical shift of the end groups was established (in this case $=\text{CH}_2$ see **Figure 5.35**). Thus, it was established that the peak attributed to the $=\text{CH}_2$ end group appears at around 5.03-5.26 ppm and in some cases, the signals were absent (**Figure 5.33** and **5.39**). An example of the molecular weight calculation for **P27c-1** is given below. The total number of backbone protons was added together (980). Then the total number of backbone protons was divided by the number of protons in a single repeat unit of the polymer (i.e. 14). So, $980/14 = 70$. The number of repeat units (70) is multiplied by 198 (where 198 is the molecular weight of the repeating unit). Hence, $70 \times 198 = 13800$ g/mol (last two digits rounded) (see **Figure 5.35**).

5.6. Conclusions:

A single step synthesis of isomannide di(ether-ene) **6a**, isosorbide di(ether-ene) **6b** and isoidide di(ether-ene) **6c** has been successfully demonstrated. The renewable diene-monomers were isolated in good to excellent yields after column chromatography. The formation of isohexide-di(ether-ene)s is confirmed by ^1H NMR spectroscopy which indicated a characteristic signal at around 3.91-4.04 ppm, arising from methylene protons ($-\text{OCH}_2$); a multiplet at around 4.9-5.35 ppm originating from terminal allylic ($=\text{CH}_2$) protons and another multiplet at around 5.69-6.01 ppm that can be assigned to allylic CH ($=\text{CH}-$) protons. The ^{13}C NMR of isohexide-di(ether-ene)s shows a characteristic resonance in the range of 71.2-73.1 ppm that can be attributed to methylene carbon ($-\text{OCH}_2$). ADMET polymerization of these dienes **6a-c** using Grubbs first

generation and second generation catalyst was attempted. Under the optimized polymerization conditions, poly-iso-hexide-di(ether-ene)s were obtained as highly viscous liquids. Grubbs 1st generation catalysts performed better as compared to Grubbs 2nd generation catalysts in majority of the cases and produced polymers with low molecular weights. Reduced intensity of the terminal olefinic protons in the range of 5.0-5.35 ppm in ¹H NMR suggests the formation of anticipated ADMET polymers **P27a-1-P27c-2**.

The NMR findings were corroborated by MALDI-ToF-MS spectrum, which revealed a mass difference of 198 Da between the two peaks that exactly corresponds to the mass of the polymer repeat unit. The molecular structure of **P27a-1-P27c-2** was fully established using a combination of 1-2D NMR spectroscopy, MALDI-ToF-MS, and GPC analysis. End group analysis of the polymers **P27a-1-P27c-2** by proton NMR revealed molecular weight in the range of 800-13800 g/mol, whereas GPC investigation shows the molecular weight in the range of 600-2900 g/mol. Addition of benzoquinone and two stage polymerization of **6b** yielded **P27b-1-P27b-5** with slightly higher molecular weight. Thus, the analysis of the poly(ether-ene)s suggests that low molecular weight polymer could be obtained under the experimental conditions.

Chapter-6

Summary and Outlook

6.1. Summary:

In recent years, utilization of renewable resources has become a key focus area of research activity for both academia and industry. The consumption of crude oil based chemicals will be increase in the near future with steadily increasing population. Considering these bottle-necks finding alternative sources to meet future needs is of almost importance. In this regard, the exploitation of biomass is crucial for upcoming production technologies. Specifically, cellulose is one of the foremost constituents of biomass (approximately, 35–50%) in addition to lignin and hemicellulose. Utilization of cellulose based chemicals as a renewable resource is of great interest at it can potentially avoid competition with food. The depolymerization reaction of cellulose to glucose by acid hydrolysis is being intensely investigated. Glucose and mannose are the main constituent platform chemicals for further chemical modification and functionalization. A class of compounds of high importance in this context is isosorbide, isomannide and isoidide (synthesized from isomannide by inversion of configuration) **Figure 6.1**.

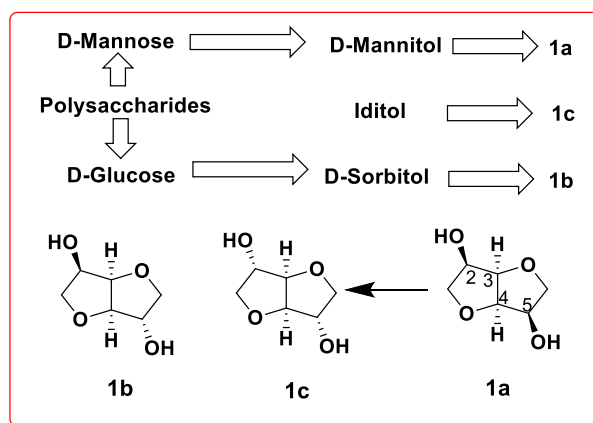
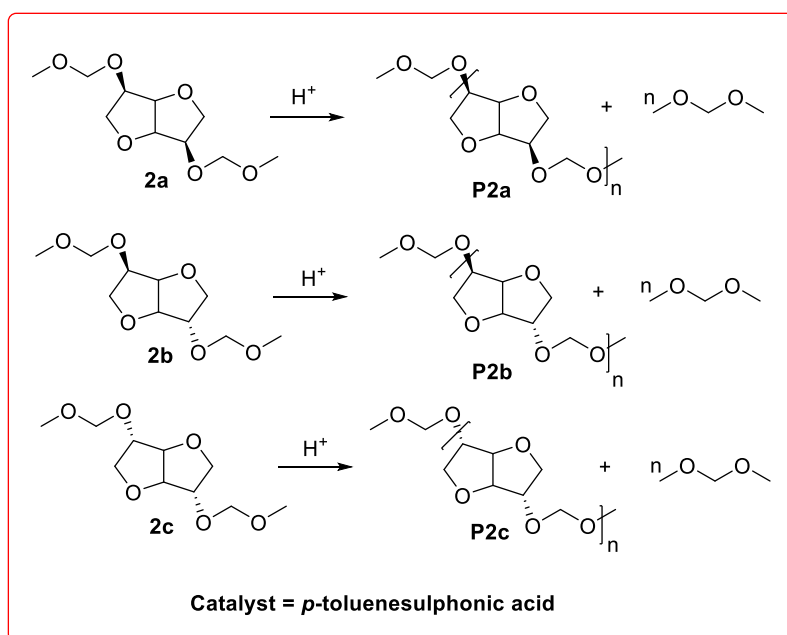


Figure 6.1. Representative synthesis of isohexides (top) and stereo-isomeric forms of isohexides (bottom), isomannide (**1a**), isosorbide (**1b**) and isoidide (**1c**).

These sugar-based isohexides are rigid, chiral and non-toxic and find multiple applications in polycondensates. Since these isohexides are bifunctional (having two-hydroxyl groups) researchers utilized them for direct polymerization at high temperature. However, high temperature polymerization of isohexides led to dark tar like polymers with low molecular weight. In this regard, Daan and co-workers developed a one carbon extension protocol and synthesized various biobased polymers. Apart from renewable origin, degradability is another requirement for the development of sustainable material. Polymeric degradation mainly depends on the nature of functional group present in repeating unit (monomer).

Literature suggests that acetal linkage degrades under mild acidic conditions. In our attempts to prepare polyacetals we have developed a single step synthetic protocol for the synthesis of isohexide-diacetals. These renewable building blocks, the diacetals **2a-c** were subjected to condensation polymerization. Acid catalyzed polycondensation of **2a-c** under mild conditions produced the corresponding polyacetals (**P2a-c**) as white solids (with molecular weights in the range of 3200 to 27600 g mol⁻¹) in good yields (**Scheme 6.1**). Mild polymerization conditions and color-free polymers suggest enhanced reactivity (due to one atom extension) of the new monomers compared to their parent isohexides.



Scheme 6.1. Acetal metathesis polymerization of the isohexide-diacetals to polyacetals **P2a-c**.

The identity of the resultant polymers was established after rigorous characterization. MALDI-ToF-MS revealed a repeat unit of 158 Da which exactly matches with the polyacetal repeat unit molecular weight, whereas 1D and 2D NMR experiments suggest that the stereochemistry of the monomer is retained in the polymer. The rigid polyacetals displayed higher melting temperatures compared to their linear analogues C5-C6-polyacetals. Having known that polyacetals are sensitive to acid catalyzed hydrolytic cleavage we set out to evaluate the rate of degradation of **P2a-c** in mild acidic media. The highest molecular weight polyacetal (**P2b-2**) was chosen as the most relevant representative for degradation investigations. Isosorbide-polyacetals (**P2b-2**) was stable towards practical washing (D₂O) and rinsing conditions. NMR investigations indicate that the polyacetals degrade in slightly acidic media. Time resolved GPC analysis of the

acid treated polymer revealed a decrease in the molecular weight of the polymer with time (**Figure 6.2**), further supporting the NMR findings.

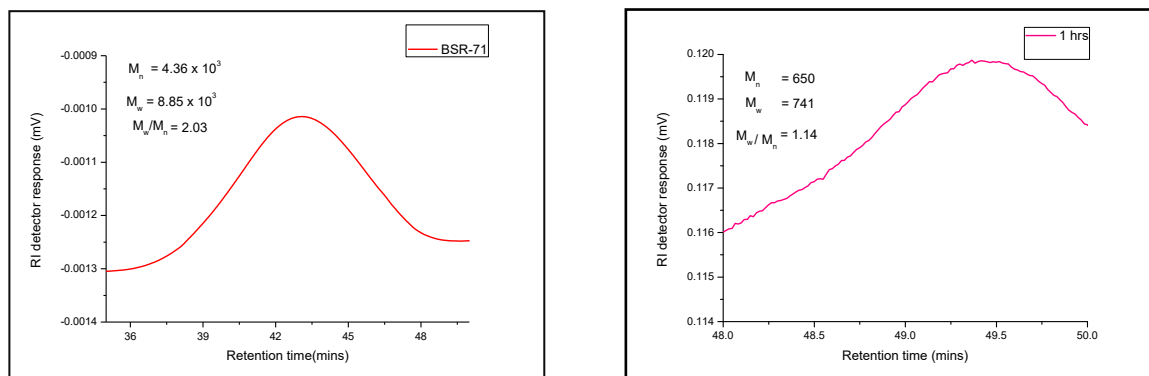
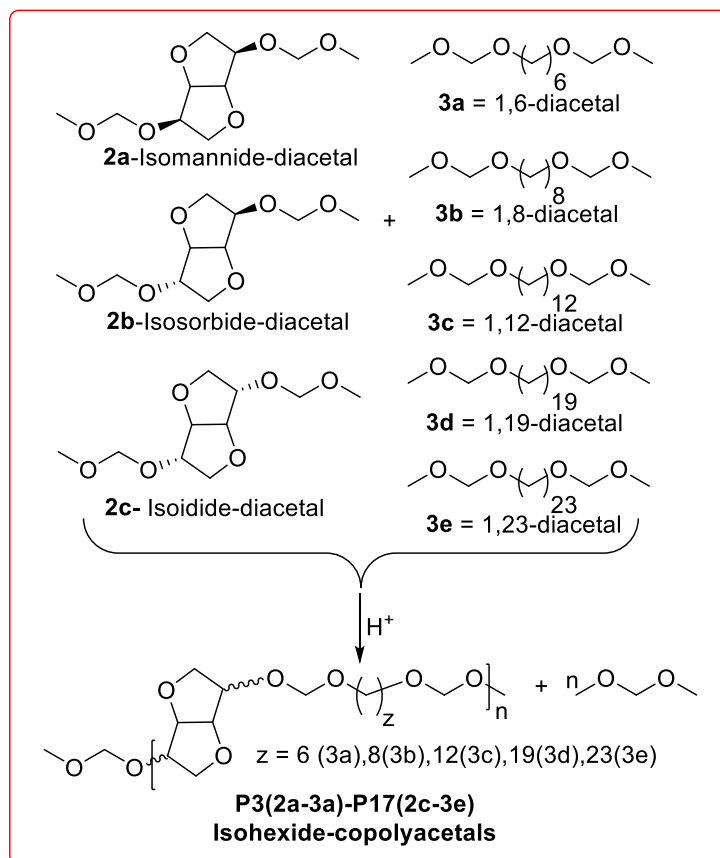


Figure 6.2. Time resolved GPC curve of **P2b-1** (left) and GPC curve after acidic degradation (right), in chloroform, against a PS standard.

It has been observed that the rate of degradation of these polyacetals is very fast. This is due to the hydrophilic nature of isohexide-polyacetals. To address this issue, we synthesized renewable copolyacetals by incorporating the long chain diacetals (hydrophobic) into the isohexide-diacetals (hydrophilic). First, the synthesis of plant oil based long chain-diacetals were carried out using methanesulfonic acid. Furthermore, acid catalyzed Acetal Metathesis CoPolymerization (AMCP) of isohexide-diacetals with linear, plant oil-derived long-chain diacetals was carried out to afford a small library of 15 new copolyacetals (**Scheme 6.2**).

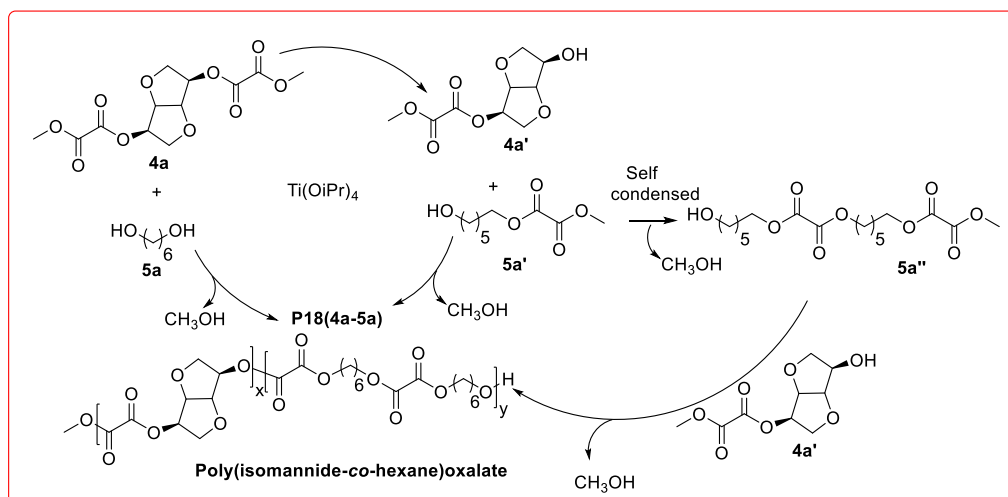


Scheme 6.2. Synthesis of copolyacetals **P3(2a-3a)-P17(2c-3e)** by AMCP.

Reduced intensity of the methoxy-protons and corresponding carbon indicated formation of desired copolyacetals. The proton NMR findings were corroborated by 2D NMR (NOESY, HSQC & HMBC), which established the correlation between the isohexide-segment and the linear aliphatic segment. Furthermore, ^1H NMR result indicates that the stereochemistry of the isohexide-diacetals **2a-c** is most likely retained during the copolymerization. Typically, the T_m of the copolyacetals was lower than the parent isohexide-polyacetals. This is partly due to the incorporation of flexible aliphatic segments in the parent isohexide-polyacetals. The copolyacetals **P10(2b-3c)**, **P15(2c-3c)**, **P16(2c-3d)**, **P17(2c-3e)** displayed a single melting transition indicating the presence of either perfectly alternating copolymer or one type of crystal form in the copolymers. It was observed that with an increasing carbon chain length of long chain diacetals (**2a-e**) the melting temperature of resultant copolyacetals increases. The copolyacetals were found to be thermally stable up to 325 °C. TGA analysis revealed that the copolyacetals derived from long-chain diacetals are more stable compared to the copolyacetals derived from short-chain diacetals. The biocompatibility of the copolyacetals was determined by subjecting the copolyacetal

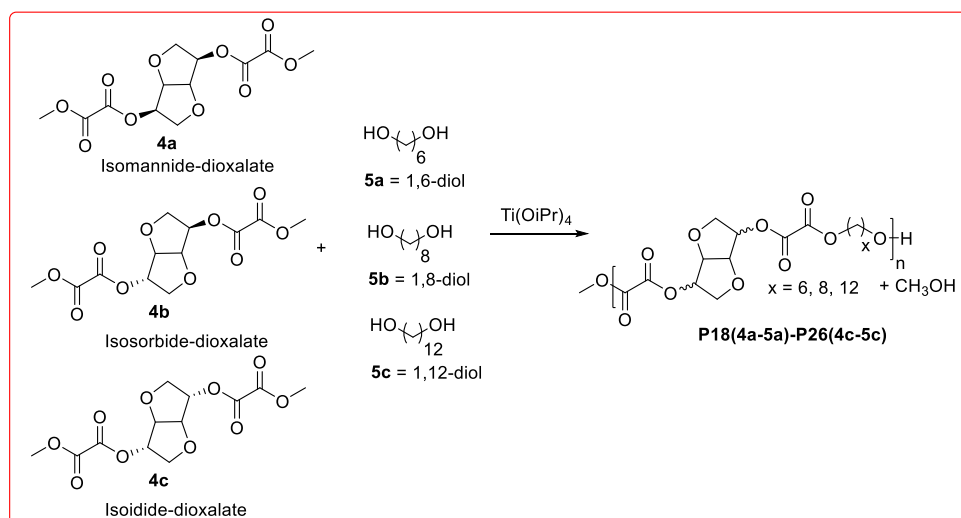
to various types of degradation. Acid induced degradation of copolyacetals was tracked by GPC (every 20 minutes), which revealed increasing degradation of copolyacetals over time. Thus, the time resolved molecular weight degradation investigations using GPC indicated slower degradation for long-chain copolyacetals as compared to their short-chain counterparts. Unlike the parent isohexide-polyacetals, hydrolytic degradation investigations revealed that the copolyacetals are relatively stable in acidic media over a period of 15 days with only 30% weight loss in 9M HCl solution. Thus, the rate of degradation of the copolyacetals was found to be much slower than the parent isohexide-polyacetal homopolymers. The reduced rate of degradation can be attributed to incorporation of hydrophobic long chain segments in the copolyacetals. In-situ degradation investigation (based on 1-2D NMR) suggested formation of formates, hemiacetals and diols as degradation products. This was further corroborated by column chromatographic isolation of the parent diols. These findings imply that the properties of the copolyacetals can be tuned to suit a particular application. Thus, the present strategy provides an additional handle to control the rate of degradation by choosing the right combination of isohexide-diacetal and linear-diacetal monomers.

Polyoxalates are known to degrade in aqueous hydrolytic conditions. Along the same line, we have developed sugar based polyoxalates and studied their degradation behavior under acidic conditions. Initially, the synthesis of sugar-derived isohexide-dioxalates has been established. The identity of isohexide-dioxalates (**4a-c**) was unambiguously ascertained using a combination of 1-2D NMR, mass spectroscopy and analytical methods. The synthetic utility of these sugar derived dioxalates was examined in condensation polymerization. Condensing isohexide-dioxalates (**4a-c**) with aliphatic renewable diols (**5a-c**) in presence of Lewis acid catalyst led to the production of poly(isohexide-*co*-alkane)oxalates. Quite surprisingly, the proton NMR of the polyoxalate **P18(4a-5a)** revealed a 2:1 ratio of 1,6-hexanediol (**5a**) and isomannide-dioxalate (**4a**) in the polymer backbone. This intriguing reactivity was found to be an outcome of cross metathesis between the two monomers **4a** and **5a**. Based on direct and indirect evidence, and control experiments, an alternative polymerization mechanism is proposed. In addition, identification and isolation of intermediate **5a'**[2-(2-methoxyacetoxy)ethyl 2-(2-hydroxyethoxy)-2-(λ 3-oxydanylidene)acetate] and **4a'** (3R, 6R)-6-hydroxyhexahydrofuro[3,2-b]-furan-3-yl methyl oxalate justified the 2:1 ratio of **5a:4a** observed in poly(isomannide-*co*-hexane)oxalate **P18(4a-5a)** Scheme 6.3. Thereafter, polymerization conditions were optimized to obtain high



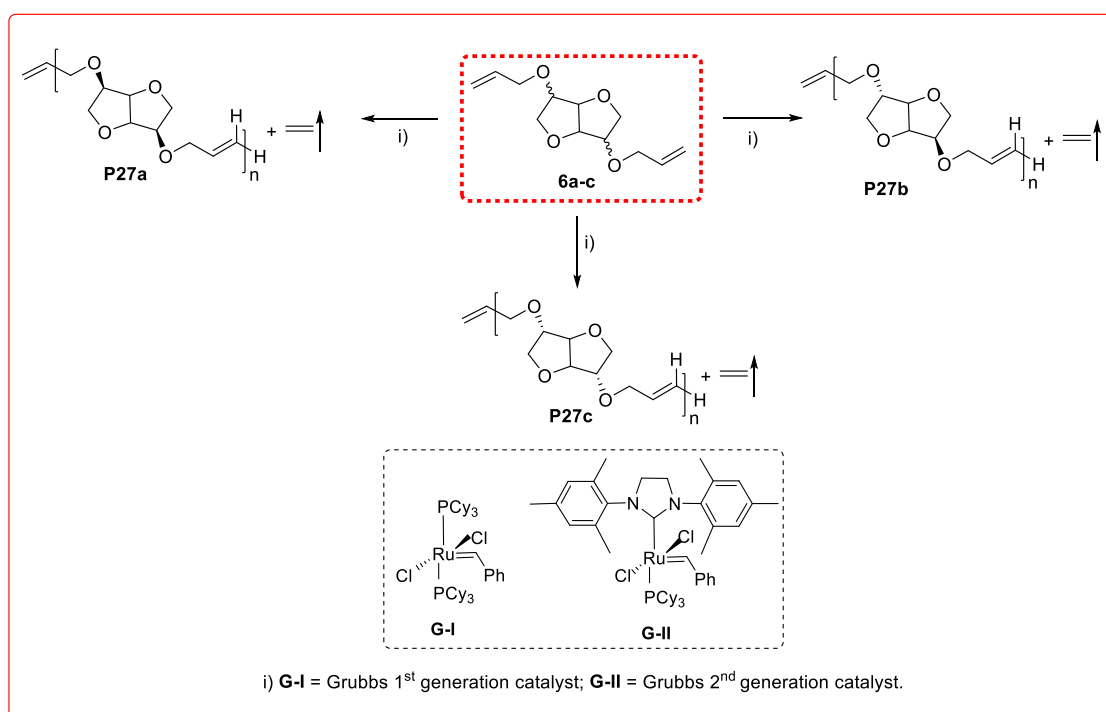
Scheme 6.3. Proposed mechanism for the formation of poly(isomannide-*co*-hexane)oxalate.

molecular weight polyoxalates **P18(4a-5a)-P26(4c-5c)** **Scheme 6.4.** The existence of polyoxalates was unambiguously ascertained using a combination of spectroscopic and analytical methods. GPC analysis of these polymers revealed molecular weights in the range 14000–68000 g/mol. In an attempt to demonstrate direct application of aforementioned polymers, transparent films were casted and their mechanical properties indicated formation of soft films. Solid and solution state degradation investigations established that polyoxalates are amenable to degradation over extended period of time. Thus, utilization of renewable feed-stocks to prepare chiral building blocks and commercially attractive sustainable polyoxalates has been demonstrated for the first time.



Scheme 6.4. Synthesis of poly(isohexide-*co*-alkane) oxalates.

Acyclic Diene Metathesis Polymerization is a well-known technique for the preparation of a broad range of polymeric architectures, including linear polymers, block-copolymers from telechelics and polymers with a definite branching density. Utilization of sugar based isohexides to make polymerization grade diene monomers is largely missing in the literature. Here we have synthesized sugar based isohexide di(ether-ene)s following the single step synthetic protocol. ADMET polymerization of these dienes **6a-c** using Grubbs first generation and second generation catalyst was attempted. Under the optimized polymerization conditions, poly-isohexide-di(ether-ene)s were obtained as highly viscous liquids. Grubbs 1st generation catalysts performed better as compared to Grubbs 2nd generation catalysts in majority of the cases and produced polymers with low molecular weights. Reduced intensity of the terminal olefinic protons in the range of 5.0-5.35 ppm in ¹H NMR suggests the formation of anticipated ADMET polymers **P27a-1-P27c-2** Scheme 6.5.



Scheme 6.5. ADMET polymerization of isohexide-di(ether-ene) to polyethers.

The NMR findings were corroborated by MALDI-ToF-MS spectrum, which revealed a mass difference of 198 Da between the two peaks that exactly corresponds to the mass of the polymer repeat unit. The molecular structure of **P27a-1-P27c-2** was fully established using a combination of 1-2D NMR spectroscopy, MALDI-ToF-MS, and GPC analysis. End group analysis of the polymers **P27a-1-P27c-2** by proton NMR revealed molecular weight in the range

of 800-13800 g/mol, whereas GPC investigation shows the molecular weight in the range of 600-2900 g/mol. Addition of benzoquinone and two stage polymerization of **6b** yielded **P27b-1-P27b-5** with slightly higher molecular weight. Thus, the analysis of the poly(ether-ene)s suggests that low molecular weight polymer could be obtained under the experimental conditions.

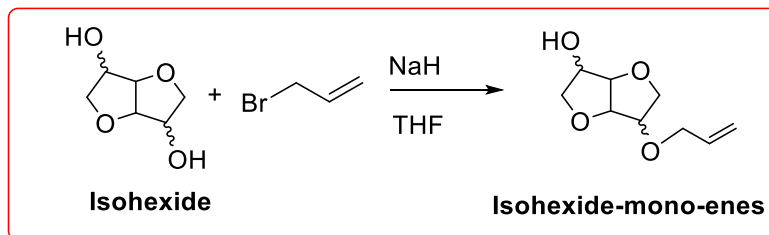
6.2. Outlook:

Although significant advancement is made in the field of isohexide and plat oil based polymers, these current polymers are not competent enough to replace crude oil based polymers. This is because of the properties and molecular weight of fossil based polymers are far better than these polymers. Secondly, the cost of the renewable monomers (sugar and plant oil based) is also high compared to cheap ethylene. One hand we have renewable and degradable polymers but we have to compromise with properties and price. On the other hand, polyethylene has excellent properties for all sort of applications but at the same time we have to compromise on degradation (it takes around 400 years to degrade completely). For the sustainable future the polymer should meet the following criteria,

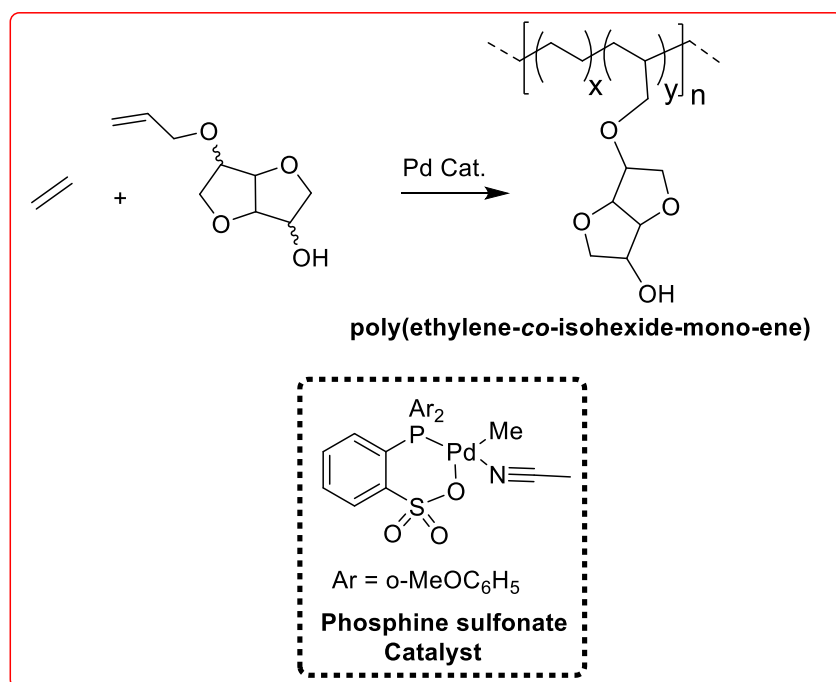
- a) The monomer should be easily accessible and cost of the monomers should be competitive.
- b) Polymerization method should be economically viable and should deliver high molecular weight polymers without comprising the properties.
- c) The resultant polymer should degrade in reasonable time after end use.

With these above criteria the instant solution for society would be the synthesis of new modified-copolymers. The composition of copolymer should be the ethylene and functional olefin (e.g. isohexide-based mono-enes). The rationale behind proposing these copolymers is to achieve right balance between hydrophobicity and hydrophilicity in the polymers. With this hypothesis if one can insert the isohexide-mono-enes monomer into the main polyethylene backbone, it will induce hydrophilicity in the resultant polymer and thus increase its availability for biodegradation by microorganisms. During biodegradation the polymer might convert to its monomers, followed by the mineralization of the monomers.

The isohexide-mono-enes can be synthesized treating isohexides with K_2CO_3 followed by addition of allyl bromide (**Scheme 6.6**). Synthesized isohexide-mono-enes monomers can be copolymerized with ethylene in presence of palladium phosphine-sulfonate catalyst to obtain the new copolymers (**Scheme 6.7**). Synthesized polymers can be thoroughly characterized and tested for various degradations.



Scheme 6.6. Synthesis of isohexide-mono-enes.



Scheme 6.7. Copolymerization of ethylene with isohexide-mono-ene.